Some Studies on Modifications of Low Dimensional Systems under the Application of Periodic Driving

THESIS

Submitted in partial fulfillment
of the requirements for the degree of

DOCTOR OF PHILOSOPHY

by

Tridev A Mishra
ID No. 2012PHXF0004P

Under the Supervision of

Dr. Tapomoy Guha Sarkar

and
Co-supervision of

Dr. Jayendra N. Bandyopadhyay

BITS Pilani
Pilani | Dubai | Goa | Hyderabad

BIRLA INSTITUTE OF TECHNOLOGY & SCIENCE, PILANI

2017

BIRLA INSTITUTE OF TECHNOLOGY & SCIENCE PILANI-333031 (RAJASTHAN) INDIA

CERTIFICATE

This is to certify that the work reported in the Ph.D. thesis entitled **"Some Studies on Modifications of Low Dimensional Systems under the Application of Periodic Driving"**, submitted by **Tridev A Mishra**, ID.No. **2012PHXF0004P** at Physics Department, BITS-Pilani, Pilani Campus for the award of the degree of Doctor of Philosophy (Ph.D.), is a bonafide record of his original work carried out under our supervision. This work has not been submitted elsewhere for any other degree or diploma.

Signature of the Supervisor

.....

Dr. Tapomoy Guha Sarkar

Assistant Professor,
Department of Physics,
BITS-Pilani, Pilani Campus

Date: .....

Signature of the Co-supervisor

.....

Dr. J. N. Bandyopadhyay

Assistant Professor,
Department of Physics,
BITS-Pilani, Pilani Campus

Date: .....

Abstract

The study of low dimensional systems has been significantly enriched by the novel behaviors observed when these systems are studied in the presence of periodic driving or non-trivial geometry. These have offered a means of modifying the gauge couplings in such systems which may, in certain cases, result in the breaking of key symmetries, thereby opening up new avenues of investigation. The role played by the development of optical lattices of cold atoms in the experimental validation of such phenomena has been influential. In this thesis we consider the effects of periodic driving on Hall systems both of the square lattice and Graphene types. Begining with a relatively straight forward study of the Landau-Fock-Darwin confinement of a spinless charged particle on a space with a conical disclination defect. Where we show the non-local effects of defects in the metric on the specturm and thermal properties of the system. We proceed to examine the lattice problem of driving the Aubry-André-Hamiltonian with a high frequency periodic magnetic field and study the modifications to the nature of the metal-insulator transition in the system. This is followed by a study of the Haldane model, essentially Graphene in tight binding form with complex valued next-nearest neighbour interactions, under a periodic sequence of delta function kicks. The emphasis being on the changes to the band topology under kicking. Finally, we discuss a 'Floquet Engineering' scheme to simulate curved Graphene in a cold atom setup using a specific periodic drive.

Acknowledgements

Human interactions are, arguably, by far the most complex out of all known to exist between objects animate or inanimate. Just like a pair of particles interacting via a field, we as people, cannot help but influence and be influenced at the same time. The evolution of my Ph.D has been no less of a many body interacting system the ground state for which, still eludes my grasp. But like any aspiring physicist worth his/her salt, I shall meticulously try to list out all influences and forces exerted by those around me that equilibriated what could so easily have turned chaotic and catastrophic. Yet being the stumbling, overzealous beginner that I am, I shall nonetheless err and omit for which I apologize to those overlooked. Bear with me for I am, physicist notwithstanding, a human first.

Central to the whole endeavour of course, have been my supervisor, Dr. Tapomoy Guha Sarkar and co-supervisor Dr. Jayendra Nath Bandyopadhyay. Their influence, far beyond anything that merits a perturbative treatment, can hardly be expressed in words. Thanks to them I learned the art of simultaneously carrying out research and grasping the rudiments of the subject. That physics has to be grabbed by its neck and not by its tail if one hoped to make anything of it. They forced me out of my comfort zone, time and again confronting me with research problems just beyond my reach, and in the process taught me how to grow. Most importantly, though I call them my supervisors, for want of better nomenclature, they actually stood beside me throughout, reposing in me a faith I was challenged to live up to. Learning physics from them was therefore an experience par excellence.

I owe a debt of gratitude to the faculty of the Department of Physics, the DRC, the various HODs through my tenure, especially my DAC members Dr. Biswanath Layek and Dr. Niladri Sarkar, for constant encouragement, valuable advice and

adminisitrative assistance. I wish to thank my DAC members for also devoting valuable time to assess the progress of my work and for reviewing and refining this thesis. It goes without saying that my doctoral work would not have been possible without the smooth functioning of the various mechanisms of the institute for which I am grateful to the Vice-Chancellor, the Director, Deans and Associate Deans of various divisions of the Birla Institute of Technology and Science, Pilani. Special thanks to the Chief Warden, SWD and the Unit Chief Estate management, Dr. Anshuman, for providing comfortable accomodations on campus; Prof. S. K. Verma (Dean, ARD) and Prof. Hemant Jadhav (Associate Dean, ARD) for counsel on and help with various official formalities. The non-teaching staff of the Physics department, Shrikant ji, Rajeev ji and Kundan ji deserve plaudits for efficiently handling any and all official matters. Same goes for Raghuveer ji and Mahipal ji over at ARD.

If the measure of a man is by the company he keeps then I fall short by yards. For my friends have revealed to me what I never thought myself capable of. Sourav, Varun, Bajaj, Shubham and Vipul, you guys lead me down this road so you better see me through to the end of it. Seniors/Colleagues but friends most importantly, Hiren, Surender, Mohit Bhai, Ashish, Ashok, Ravi, Amar, Balaji, Babaji, Captain, Ashis, Mohanty Bhai, Sachin, Mandeep, Arun, Keerti, Monika and others who I cannot mention for want of space, who anchored me to reality and kept me afloat on good humour and friendly banter when the undertow of turbulent Ph.D life got just a bit too strong for me to handle alone. Offering a helping hand when I needed it most. Rajath and Anurag, it was a pleasure working with you guys thanks for letting me reproduce our collaborative work in this thesis.

And of course, I cannot imagine repaying the love and support of my parents and little sister, without which none of this would have been possible.

Tridev Mishra

Preface

About the thesis The thesis considers certain specific low dimensional systems such as the Landau level problem in a disk geometry i.e. Landau-Fock-Darwin confinement, the square lattice in a perpendicular magnetic field as the 1-D Harper/ Aubry-André-Harper Hamiltonian, cold atom Graphene analogues and the Haldane model of Landau levels without a magnetic field, under the influence of background curvature or application of periodic driving schemes. The central technique to analyze driven systems being Floquet theory, which is used to obtain an effective time independent Hamiltonian to some approximation from a perturbation series. Aspects such as localization- delocalization transitions and conductance quantization are visited in the presence of driving. In cases where band topology is of interest the formalism for computing Chern numbers is used.

To the reader

The topics discussed in this thesis fall under the broad purview of theoretical condensed matter physics. Those actively engaged in this area are likely to peruse it with relative ease, especially those associated with the subdomains of driven quantum systems and Quantum Hall phenomena. Nevertheless, a general background of graduate level quantum, statistical and solid-state physics should suffice to grasp the core ideas discussed here. With its unusually large appendices, an effort has been made to make the thesis as self-contained as possible.

Thesis outline

This thesis comprises of six chapters and three appendices. The first chapter is an introduction followed by chapters (2-5) which discuss the

main body of research work that has been carried out. Here is a brief overview of the thesis' organization.

- **Chapter 1** Introduces specific aspects of low dimensional systems and driven quantum systems as they pertain to our studies and puts them in the context of the current research initiative in this area.
- **Chapter 2** elaborates the thermal properties of a charged spin-less particle in a Landau-Fock-Darwin potential in a background metric with conical disclination defect.
- In **Chapter 3** we study a metal-insulator phase transition in a magnetic-field driven Aubry-André-Harper Hamiltonian.
- **Chapter 4** looks at Floquet topological phase transitions in a Haldane model with periodic kicking.
- In **Chapter 5** we discuss a Floquet engineering technique to simulate curved Graphene in an optical lattice of ultra cold atoms.
- **Chapter 6** on Conclusions and Future Scope detailing a discussion of the conclusions drawn and future problems of interest.
- **Appendix A** provides a detailed introduction and discussion on certain basic aspects of the problem of spinless, tight binding electrons on a square lattice in a magnetic field.
- **Appendix B** is a step by step review of Floquet theory and its application to the study of time periodic quantum systems, introducing and deriving basic results and terminology.
- Finally, **Appendix C** provides a whirlwind tour of an interesting kinematical formulation of the geometric phase and its use in calculating topological inavriants of the Chern variety.

Contents

List of Figures

Nomenclature

Symbols

e	Magnitude of electronic charge
c	Speed of light
h	Planck's constant
l_B	Magnetic length
H_{L}	Landau level Hamiltonian in Landau gauge
H_{LD}	Landau-Fock-Darwin Hamiltonian
ω_p	Fock-Darwin oscillator/confinement frequency
ω_c	Cyclotron frequency
$\delta^{(2)}(\rho)$	2-D Dirac delta function
$g_{\mu\nu}$	Metric tensor
κ	Conical defect/kink parameter
k_B	Boltzmann's constant
$\mathcal{Z}$	Canonical partition function
U	Internal energy

C_{v}	Specific heat capacity
F	Helmholtz free energy
S	Entropy
E_{nm}	Landau-Fock-Darwin spectrum with disclination effect
$H(t), \mathcal{H}(t)$	Periodic time dependent Hamiltonian
$H_0, \widehat{H}_0$	Time independent Hamiltonian
$V(t), \widehat{V}(t)$	Periodic time dependent potential
$\widehat{V}_0$	Time constant Fourier coefficient of $\widehat{V}(t)$ or $V(t)$
$\widehat{V}_n$	n^{th}-order Fourier coefficient of $\widehat{V}(t)$ or $V(t)$
H_{eff}	Effective time independent Hamiltonian
$\widehat{H}^{(n)}$	n^{th}-order correction in expansion of H_{eff}
$\alpha(t)$	Time dependent magnetic flux quantum
α_0	Irrational flux quantum
V_0	Lattice on-site modulating potential
H_{eff}	Time-independent Effective Hamiltonian
$U(t_i, t_f), \mathbf{U}(t_f; t_i)$	Unitary time evolution operator
$\mathcal{J}_j$	j^{th}-order Bessel function
L	Size of 1-D lattice
D_2	Fractal dimension
$k, \mathbf{k}$	Wavevector/pseudomomentum in 1 and 2-D

k_x, k_y	$\hat{x}$ and $\hat{y}$ components of $\mathbf{k}$
$\sigma^x, \sigma^y, \sigma^z$	Pauli spin matrices
σ_{xy}	Transverse Hall conductance
a	Lattice constant
$H(\mathbf{k})$	Reciprocal space Hamiltonian
M	Sublattice staggering energy
t_1, t_2	Nearest and next-nearest neighbour hopping energies (Haldane model)
$E^{\mathrm{H}}_{\pm}(\mathbf{k})$	Haldane model spectrum
$\alpha_x, \alpha_y, \alpha_z$	$\hat{x}$, $\hat{y}$ and $\hat{z}$ components of pseudospin kicking
$\mathcal{H}_Z(\mathbf{k})$	Reciprocal space $\hat{z}$-kicked Haldane Hamiltonian
$\epsilon_Z(\mathbf{k})$	$\hat{z}$-kicked Haldane spectrum
$\mathcal{C}$	Chern number
$\mathcal{F}_{k_x,k_y}$	Berry curvature over Brillouin zone torus
Ω_j, Ω_N	j or N-point Bargmann invariant
$\rho(\mathbf{x}), \rho_\psi$	Pure state density matrix
$\Lambda(x, y)$	position dependence of metric conformal factor
$\Gamma_\mu(x)$	Spin connection term
e^i_ν	Veilbein
E^α_i	Inverse veilbein

$\Gamma^{\alpha}_{\mu\nu}$	Christoffel connection coefficients
$s^{\lambda\nu}$	Generators of spinorial transformations in curved space
$\gamma^{\mu}(x)$	Dirac gamma matrices
$\mathcal{P}_4$	4-phase pulse sequence
$K(x,y)$	Gauss curvature
$G(z,\mathbf{r},\mathbf{r}')$	Non-interacting Green's function
$\rho(\epsilon,\mathbf{r})$	Local density of states
$\Psi^{\dagger}_{k,j}, \Psi_{k,j}$	Fermionic creation and annihilation operators
$V_o(x,y)$	Continuous periodic potential
$\mathcal{V}_o$	constant modulating strength of $V_o(x,y)$
$\mathbf{R}_{nm}$	Bravais lattice vector
δ_{nm}	Kronecker delta
$\mathcal{H}$	Continuum Aubry André Harper (AAH) Hamiltonian
$\widetilde{W}_{nm}$	hopping matrix elements of AAH Hamiltonian
$\mathcal{T}$	pure lattice translation operator
$\widetilde{\mathcal{T}}$	magnetic translation operator
$\widetilde{\mathcal{T}}'_x, \widetilde{\mathcal{T}}'_y$	Commuting magnetic translations along magnetic unit cell sides
$\psi^{n}_{k_x,k_y}(x,y)$	Magnetic Bloch-band wavefunctions
$u^{n}_{k_x,k_y}(x,y)$	Generalized magnetic Bloch functions

$b^\dagger_{n,m}, b_{n,m}$	Real space creation and annihilation operators on square lattice
$b^\dagger_{k_x,k_y}, b_{k_x,k_y}$	Reciprocal space creation and annihilation operators
$\theta^x_{nm}, \theta^y_{nm}$	$\hat{x}$ and $\hat{y}$ translation phases
$\lvert\mathbf{k}\rangle \equiv \lvert k_x, k_y\rangle$	Reciprocal space basis kets
$\mathcal{W}(t)$	Time dependent Wronskian
b_α	Characteristic multipliers
q_α	Characteristic exponents
q'_α	Real characteristic exponents/quasienergies
$\mathbf{Q}'$	Diagonal matrix of real characteristic exponents
$\mathbf{\Phi}(t)$	Unitary Floquet solution matrix
$\mathbf{P}'(t)$	Periodic unitary component of $\mathbf{\Phi}(t)$
$\Phi_{\alpha\beta}(t)$	Matrix elements of $\mathbf{\Phi}(t)$
$P'_{\alpha\beta}(t)$	Matrix elements of $\boldsymbol{P}'(t)$
$\mathcal{H}_{\alpha\beta}(t)$	Matrix elements of $\mathcal{H}(t)$
$\Phi^n_{\alpha\beta}$	Fourier coefficients of $\Phi_{\alpha\beta}(t)$
$\mathcal{H}^n_{\alpha\beta}$	Fourier coefficients of $\mathcal{H}_{\alpha\beta}(t)$
$\mathcal{H}_F$	Floquet Hamiltonian
$\mathbb{H}$	Hilbert space
$\mathbb{T}$	space of square integrable T-periodic functions

$\mathbb{F}$	Extended Floquet Hilbert space/ Sambe space
$\|\tau_{\alpha}\rangle$	Eigenket of $\mathcal{H}_F$
ϵ_{α}	Eigenvalue of $\mathcal{H}_F$
$\|\boldsymbol{\phi}_\beta(t)\rangle$	Floquet state
$\|\mathbf{p}'_\beta(t)\rangle$	Floquet mode
$\mathbf{Q}'_{t_0}$	Stroboscopic Floquet Hamiltonian
$\mathbf{M}(t_f, t_i)$	Micromotion operator
$\mathbf{Q}'_{t_0}$	Stroboscopic Floquet Hamiltonian
$\mathbf{U}$	photon-number translation invariant unitary oprator in $\mathbb{F}$
$\widehat{\mathbf{U}}(t)$	Periodic unitary operator in $\mathbb{H}$
$\mathcal{H}_F^{\mathrm{D}}$	Diagonalized Floquet Hamiltonian
$\mathbf{U}_F$	Unitary operator block-diagonalizing $\mathcal{H}_F$ in $\mathbb{H}$
$\widehat{F}(t)$	Hermitian kick operator
$\widehat{F}^{(n)}$	n^{th}-order correction to $\widehat{F}(t)$
$\hat{R}_\alpha$	Resolvent operator
P	Model space projection operator
Q	Orthogonal space projection operator
$\mathcal{P}$	Zero-photon sector projection operator in $\mathbb{F}$
$\mathcal{Q}$	Higher photon sector projection operator in $\mathbb{F}$
$\Omega(\epsilon), \Omega_{BW}$	Wave operator

H_{BW}	Brillouin-Wigner effective time independent Hamiltonian
$\mathcal{B}$	Set of unit vectors in $\mathbb{H}$
$\mathcal{N}$	Set of non-zero vectors in $\mathbb{H}$
$\boldsymbol{\mathcal{R}}$	Complex projective ray space
$\boldsymbol{\mathcal{C}}$	Continuous curve in $\mathcal{B}$
$\pi[\cdot]$	Projection operator onto $\boldsymbol{\mathcal{R}}$
C	Continuous curve in $\boldsymbol{\mathcal{R}}$
$\Theta_{\text{tot}}[C]$	Total phase
$\Theta_g[C]$	Geometric phase
$\Theta_{\text{dyn}}[C]$	Dynamical phase
$T_\psi\mathcal{B}$	Tangent space to $\mathcal{B}$
$V_\psi\mathcal{B}$	Vertical subspace of tangent space to $\mathcal{B}$
$H_\psi\mathcal{B}$	Horizontal subspace of tangent space to $\mathcal{B}$
A_ψ	1-form acting on $T_\psi\mathcal{B}$
g_{ab}	metric tensor on $\boldsymbol{\mathcal{R}}$
$\mathcal{F}_{ab}$	curvature 2-form on $\boldsymbol{\mathcal{R}}$

Acronyms

QHE	Quantum Hall Effect
AAH	Aubry-André Harper
IPR	Inverse Participation Ratio

H_{BW}	Brillouin-Wigner effective time independent Hamiltonian
$\mathcal{B}$	Set of unit vectors in $\mathbb{H}$
$\mathcal{N}$	Set of non-zero vectors in $\mathbb{H}$
$\boldsymbol{\mathcal{R}}$	Complex projective ray space
$\boldsymbol{\mathcal{C}}$	Continuous curve in $\mathcal{B}$
$\pi[\cdot]$	Projection operator onto $\boldsymbol{\mathcal{R}}$
C	Continuous curve in $\boldsymbol{\mathcal{R}}$
$\Theta_{\text{tot}}[C]$	Total phase
$\Theta_g[C]$	Geometric phase
$\Theta_{\text{dyn}}[C]$	Dynamical phase
$T_\psi\mathcal{B}$	Tangent space to $\mathcal{B}$
$V_\psi\mathcal{B}$	Vertical subspace of tangent space to $\mathcal{B}$
$H_\psi\mathcal{B}$	Horizontal subspace of tangent space to $\mathcal{B}$
A_ψ	1-form acting on $T_\psi\mathcal{B}$
g_{ab}	metric tensor on $\boldsymbol{\mathcal{R}}$
$\mathcal{F}_{ab}$	curvature 2-form on $\boldsymbol{\mathcal{R}}$

Acronyms

QHE	Quantum Hall Effect
AAH	Aubry-André Harper
IPR	Inverse Participation Ratio

QSHE	Quantum Spin Hall Effect
IQHE	Integer Quuantum Hall Effect
LDOS	Local Density of States
SOC	Spin Orbit Coupling
TDPT	Time Dependent Perturbation Theory
BW	Brillouin-Wigner

Chapter 1

Introduction

1.1 Aspects of Low Dimensional Systems

The physics of low dimensional systems, 0, 1 and 2-dimensional quantum structures, has been a promising and intense field of theoretical research for several decades now [1–4]. Prominent examples are 0-D quantum dots [5, 6], 1-D carbon nanotubes as quantum wires and 2-D planar Graphene [4, 7, 8]. The study of such systems has thrown open an entire domain of Mesoscopic and Nanoscale physics, which forms a major portion of present day condensed matter physics [9]. Interesting properties of such systems emerge when they are subjected to external fields, which could be time dependent or independent. For the most part, the early literature in the area regarded constant electric and magnetic fields to examine electronic and optical properties of these systems [10–14].

The study of low dimensional systems witnessed a turning point with the discovery of the Quantum Hall Effect (QHE) by Klitzing, Dorda and Pepper (1980). Prior to this, the subtle intricacies of the problem of Landau levels on a lattice had engaged pioneers like Peierls, Wannier, Luttinger and Kohn, in the decades following the development of quantum mechanics. The system was found to sustain a metal-insualtor transition, put forth by Aubry and André (1980), which highlighted

the significance of self-duality in the 1- dimensional effective Harper form of the Hamiltonian. QHE opened diversified perspectives on the problem where the works of Thouless, Haldane and others introduced notions of topology into the band theory of solids. An actual material lattice that could potentially realize such topological features remained a far fetched notion until the discovery of Graphene by Geim and Novoselov (2004). Introducing its own revolution in the domain, Graphene expanded the scope of condensed matter physics to include notions from quantum field theory, high energy physics and even cosmology while putting an end to long held skepticism about the existence of a perfectly 2-dimensional solid. Its relativistic low energy regime and the role of symmetries in protecting the massless fermionic excitations that describe the ground state, have, made Graphene a crucible for ideas from gauge theory, geometry and topology.

In the last two decades the study of light-matter interactions has led to the development of a versatile quantum simulator in the form of ultra cold atoms in an optical lattice. This has given a new direction to research in low dimensional systems by allowing their physics to be replicated in a highly tunable apparatus that has allowed a controlled examination of various phenomena. This has further led to the development of periodic driving techniques to simulate gauge field couplings in such systems and the domain of 'Floquet Engineerig'. Which aims to design effective static Hamiltonians with desired properties by driving a chosen system. The techniques of Floquet theory and their application to periodic quantum systems enable the analysis of such novel systems as Floquet topological insulators. Where one has the flexibility of modifying the topological nature of the bands in the system. In this chapter we shall introduce the studies we have performed in the context of the current trends that prevail in the domain of low dimensional systems and mesoscopic physics.

1.1.1 The Quantum Hall System and Landau Level Problem

A remarkable phenomenon to emerge from this milieu was the Quantum Hall Effect (QHE) from the experiments of Klitzing, Dorda and Pepper [12] which revealed robust integer quantization of the transverse Hall resistivity of an inversion layer at the interface of a semiconductor heterojunction. The appearance of perfect integers, which were revealed in the plateaus of the resistivity curve when plotted against the applied magnetic field, was shown to be resilient even in the presence of disorder and independent of the geometry of the sample. Theoretical explanations of the effect soon followed [15–19] and introduced entirely new areas of mathematics, such as topology, in the study of condensed matter systems. Though the effect was observed in what was effectively a 2-D gas of electrons Thouless et. al. [15] were able to derive the quantization by considering the electrons to be on a 2-D square lattice to which a strong magnetic field had been applied in a direction perpendicular to the plane of the lattice. They were able to show that the Kubo-Greenwood formula, from linear response theory, when used to calculate the transverse conductance gave values in integer multiples of e^2/h where e is the magnitude of electronic charge and h the Planck's constant. A result which follows from, as they showed, the similarity between the way the Kubo-Greenwood conductance is calculated and the calculation of a topological invariant called a Chern number for a manifold with a fibre bundle [17]. The tight binding model of electrons considered by Thouless et. al. is itself a rich system and exhibits a subtle interplay of the electron's interaction with a magnetic field as well as a periodic potential. The reader may take a look at Appendix A for a detailed exposition of this system. For a detailed development of topological notions from their origins in ideas of Berry's phase one may refer to Appendix C. It charts a path to the calculation of invariants like the Chern number through the slightly unconventional formalism of kinematical arguments and Bargmann invariants as introduced by Mukunda and Simon [20].

Another feature of this square lattice Hall effect Hamiltonian, that appears on its reduction to an effective 1-D tight binding model due to P. G. Harper [21], is that this effective version offers an exceptional instance of a metal-insulator transition in a 1-D system. This reduced Hamiltonian known as the Harper Hamiltonian. When the multiple of the flux quantum through each plaquette of the square lattice happens to be irrational, the reduced 1-D form of the Harper Hamiltonian, is found to belong to a class of almost periodic Schrödinger operators, vigorously studied by mathematicians, called the almost Mathieu operator [22–24]. The Harper Hamiltonian now shows a variation in the on-site energy term which is incommensurate with the corresponding 1-D lattice site, imparting to it quasicrytalline properties and making a reciprocal space construction a formidable challenge. This is a delicate pursuit since conventional notions of band structure and the Brillouin zone have to be abandoned and the validity of the plane wave basis set is called into question for a significant portion of the system's spectrum. The main physical interest in this particular variant of the model is the theoretically demonstrated metal-insulator transition, due to Aubry and André [25], which draws parallels with the famed Anderson localization-delocalization transition [26], a phenomenon otherwise shown to be restricted to 3-D systems [27]. These myriad contributions to the model's analysis have led to the Hamiltonian being dubbed the Aubry-André-Harper (AAH) Hamiltonian. A crucial feature of this model, which lends significant insight into both the rational and irrational cases, is its duality property. This is found to surface time and again in the study of the system with perhaps its most significant role being in arguing the existence of the metal-insulator transition and the appearance of extended states in this effective 1-D model.

An aspect of study regarding these systems that has recieved relatively little attention in the literature is the effect of making the magnetic field in the problem time dependent. It would be natural to expect that such a modification should have

a profound impact on the general phenomenon of the Hall effect and on the nature of the transition from localized (i.e insulating) to extended (i.e. metallic) behaviour of the wavefunctions. The dearth of such studies is, however, justified since making the magnetic field time dependent severly complicates the problem especially in the tight binding AAH formulation. Since the subband structure that results from the presence of the magnetic field is dependent on the flux quantum which, if it changes with time, would lead to a reciprocal space Hamiltonian of varying dimensions for the case of rational flux quanta. Thus making an analysis in the reciprocal space almost impossible. An important starting point is to regard the magnetic field as oscillating periodically with time, as such an assumption allows a simpler route to analyze the system using the tools of Floquet theory (see Appendix B). Some works have tried to look at this problem in the context of the Hall effect and topological phase transitions [28, 29]. In [28], the authors consider a continuum version of the Hall problem in the presence time-periodic electric and magnetic fields. Of these, the magnetic field is regarded as a driving force in a kind of 'heterodyne' or frequency mixing device that the system mimicks. A modified version of the Hall conductivity called the heterodyne Hall conductivity is derived and shown to have quantized values for certain parameter regimes. The bulk of the system, which is a 2-D plane of the rectangular Hall geometry, is shown to support a current with frequencies that are shifted in integer multiples of the driving frequency from the input electric field value. Various classical cyclotron orbits of the electron are considered in the presence of the time dependent magnetic field and special closed loops are identified, that arise for certain values of the cyclotron and driving frequencies, for which the effective electronic mass diverges.

The work in [29] treats a bosonic cold atom system in an optical lattice which is coupled to synthetic gauge fields. This, contrary to the previous example, is a lattice model where the coupling of the gauge field takes the form of the Peierls

modification to the nearest neighbour hopping terms in the form of complex phase factors, in a tight binding model. The authors also consider an on-site Hubbard like repulsive interaction. The key feature of interest in this work is the authors' attention to making the gauge field dynamic by introducing a site dependence in these complex phase factors. This they acheive by proposing the use of a density-dependent gauge field which is sensitive to the occupation numbers at various sites in the optical lattice and hence introduces the site dependence. They find that for weak on-site interactions and a dynamic gauge field the system shows a topological phase transition in its ground state which is absent for the static field case. This argues in favour of investigating topological properties of lattice models with $U(1)$ gauge symmetry where the gauge field is made time-dependent, despite the inherent difficulties involved in doing so. In Chapter 3 we discuss a method based on an effective time independent Hamiltonian for the AAH Hamiltonian with a time dependent magnetic field, as a possible way of circumventing these issues. Where an exact diagonalization may be used to obtain the spectrum of the new effective Hamiltonian under the approxiamtion of a large driving frequency. Though the focus of our attention here is on the metal-insulator transition in the system and not on its topological properties. And the question of topological properties of the 2-D square lattice in the presence of a time dependent magnetic field is still an unattended open one. The available formalisms of calculating Chern numbers especially of the Thouless et. al. variety fall short of this task and even the high frequency, time independent effective Hamiltonian schemes are of no avail. The only recourse could possibly be a full time dependent perturbation theory approach using the Dyson series but this too relies on the magnetic field behaving perturbatively and ultimately the issues of developing a suitable band/Brillouin zone description of the system and avoiding inter-band transitions may complicate matters to no end.

An interesting variation of the Hall effect problem or the general single particle

Landau level problem [30] is to consider the system on a surface or space with non-trivial background geometry. The behaviour of the Landau level wavefunctions and the specturm show interesting properties in such problems. The spherical, disk (Fock-Darwin) and torus geometries have been considered [31], even in the presence of Coulomb interations and, the magnetic field , for the torus geometry is observed to have certain allowed values such that an integer number of flux quanta intercept the sample. In the spherical case several advantages are obtained over the conventional planar geometry of the Landau level problem such as the degeneracy of the Landau levels becomes finite in this case and one can have the notion of a filled Landau level for a finite number of particles. As opposed to the rectangular planar geometry where the levels are infinitely degenerate. The sphere being a compact manifold without an edge the system is purely bulk in nature and this frees it from the complications of finite size and edge effects.

The disk geometry is of special interest since it finds experimental realization in the form of quantum dot systems and allows an exact solution. The model consists of a parabolic confining potential over the normal planar Landau level problem, in general known as a Fock-Darwin potential as they first introduced it the context of this problem [32]. In this geometry the electrons in a plane are further confined to a disk or dot like region and translational symmetry is absent in both directions. Thus the infinite degeneracy of the Landau levels in the normal case gets lifted and the spectrum now depends on the relative values of the oscillator quantum numbers and the angular momentum quantum numbers corresponding to the component of the angular momentum normal to the plane.

Thus, this has generated some interest in the study of the Landau level problem in the presence of a background space with some defect in its metric or just the consideration of electromagnetic interaction between charged particles in a non-trivial geometry [33–36]. The objective is to generally look at such features as the

spectrum and the density of states in the presence of the backgroud topological defect. It is seen in such cases that the degeneracy of the spectrum does get affected depending on the symmetry of the defect and further various physical quantities show the imprint of the background geometry. A fact that highlights the role of non-local quantities in the physics of the electrons, even though the Hamiltonian description is local and the local nature of the metric may be flat. In Chapter 2 we look at the Landau Fock Darwin problem in a background space which has a conical disclination defect. There we focus on obtaining the thermal properties of a single particle in this confined system and observe interesting correlations between the defect quantifying prameter and the temperature of the thermal bath in which the system is considered.

We now proceed to a discussion of another important 2-D system which has garnered monumental interest in the condensed matter physics domain, i.e. planar (mono layer) Graphene [4, 7, 13, 14]. First isolated by Andre Geim and Konstantin Novoselov [37], at the University of Manchester in 2004, for which they were awarded the 2010 Nobel Prize in Physics, this material has enamoured theoretical and experimental physicsts alike with its astounding properties. From being the perfect realization of a 2-D solid to having remarkably high thermal and electrical conductivities and being one of the strongest known materials yet surprisingly flexible, Graphene has found widespread applications. In the following section we shall consider some aspects of the material as are relevant to this thesis.

1.2 Graphene : Non-Trivial Geometry and Band Topology

An important and interesting feature concerns the low energy dispersion relation in Graphene which happens to be linear [7, 8, 38]. Since the lattice has a hexag-

onal structure viewed as the interpenetration of two triangular sublattices it has two inequivalent sites per unit cell and hence the single band tight binding model for Graphene gives two subbands. A valence band and a conduction band, thereby giving the Hamiltonian a 2×2 structure in reciprocal space and the wavefunctions permit a spinor representation at the high symmetry points in the Brillouin zone. A pair of such points are called the Dirac points at which the valence and conduction bands touch giving Graphene its semi-metallic nature. It is around these Dirac points that the dispersion relation is linear and permits a comaprison to the dispersion of a particle in relativistic quantum mechanics [39]. This allows a continuum description of the system at low energies by the relativistic $(2+1)$-dimensional Dirac equation. This is an aspect of Graphene that has attracted high energy physicists and even cosmologists as Graphene now offers a table top system to study a variety of physics ranging from quntum electrodynamics, where it exhibits phenomena such as Klein tunneling [40] to such cosmological phenomena as the Unruh effect [41]. The relativistic structure of the equation allows a field theoretic description where various effects can be incorporated as gauge field couplings to the Dirac equation to model the changes to the spectrum and various electronic properties. Several works in the literature follow this line of treatment [41–55]. The approach allows one to study the electronic properties of a Graphene sheet which is curved in a manner that this curvature may be described using some conformal metric. Then one has to write the $(2+1)$-D Dirac equation with this as the choice of spatial metric and from there obtain the Hamiltonian by breaking covariance and ensuring hermiticity in the resulting non-relativistic Hamiltonian description. A point to note is that the gaplessness at the Dirac points ensures that the low energy excitations are massless fermions and that one has to work with the massless Dirac equation in such a case [38]. In general for describing the effects in a curved geometry the massless Dirac equation has to be written in curved space and this requires the introduction of the

spin connection term in order to write the covariant derivative from the momentum operator and the veilbein formalism from general relativity to transform the Dirac gamma matrices.

Other interesting treatments that this formalism allows is the consideration of stresses or defects in the Graphene sheet within the formalism of gauge fields and curvature [43–45]. In fact it is even possible in cases to model the curvature effectively as a potential applied to the flat space Dirac equation. Experimentally such systems are difficult to realize flexibly in actual Graphene samples but the advent of optical lattices of ultra cold atoms have offered a quantum simulation tool to study these interesting effects. The hexagonal lattice and Graphene like analogues have been realized using cold atoms in a variety of contexts [56–65]. In this context there have been attempts to realize optical lattice setups that simulate curvature in a Graphene like lattice geometry to study relativistic electrodynamics in the presence of gravity. In Chapter 5 we offer another method of simulating a curved graphene system by methods derived from periodic driving of optical lattices and the newly emerging technique of 'Floquet Engineering'. We shall elaborate the features and scope of this method in the following section.

In the context of band topology Graphene has shown itself to be rich in topological features even though not exactly a bulk-insuator, with its semi-metallic, Dirac-like linear dispersion at low energies [66, 67]. Besides the Quantum Spin Hall Effect in the presence of strong spin-orbit coupling [68–71], the manifestation of Zak phase and edge states in Graphene ribbons has been studied [72], experimental validation of the QHE and Berry's phase for Graphene has been peformed and various topological features of the honeycomb lattice have been investigated in cold-atom and photonic-crystal setups [64, 65, 73–75]. In gapless Graphene the Chern number evaluates to zero and the system is topologically trivial in the bulk. This is so due to the fact that the Dirac points are stable and protected by the time reversal and

inversion symmetries. As long as these symmetries remain unbroken a gap may not be opened at the Dirac points [66, 76, 77]. Even the presence of perturbations that respects these discrete symmetries can only move the Fermi points but not create a gap [78]. The presence or absence of these symmetries is determined by the nature of the hopping terms in a tight binding model of Graphene and the point group symmetries of the hexagonal lattice. Thus time reversal is ensured by the hopping elements to the nearest neighbours being real and it is not sensitive to any asymmetry in the strengths of the hoppings to the three nearest neighbouring sites. Inversion symmetry on the other hand would require the hoppings to be symmetric under an inversion operation which may be peformed about any center of a hexagon in the lattice or at either of the sublattice points. Another manner in which this symmetry may break is through a staggering of the on-site energies at the two sublattice sites within a unit cell. Whenever any such symmetry is broken the gap at the Dirac point appears due to the introduction of a non-zero σ^z Pauli matrix term in the $SU(2)$ representation of the Hamiltonian in reciprocal space. This is known as the mass term since it gives the low energy Dirac fermions a mass and for a constant value is also at times referred to as a 'Semenoff' mass. In essence the time reversal and inversion symmetries impose constraints on the spectrum at each wavevector or pseudomomentum value such that this term disappears from the Hamiltonian and a gap does not arise. In such a case the calculation of the Berry curvature [79] around the two Dirac points gives singular 'vortex' like values and the integral of this curvature gives $+\pi$ and $-\pi$ which cancel over the Brillouin zone to give zero Chern number and hence trivial topology. It was Haldane who was the first to note the role of breaking symmetries to make a Graphene like hexagonal lattice topologically non-trivial [66]. He identified the need to break time reversal symmetry by making the hoppings to next nearest neighbours complex valued. Although done in the context of studying a parity anomaly in a lattice model that supported

relativistic fermionic excitations in $(2+1)$-D, the model later acquired significance as a prototype for a Chern insulator which could exhibit Hall quantization even in the absence of a magnetic field. In Chapter 4 we study the effects of periodic kicking on the topological properties of the Haldane model and exhibit a topological phase transition in the resulting system.

1.3 Floquet Engineering

A term of recent coinage but gaining rapid acceptance, Floquet Engineering signifies the set of methods or practices which make use of an appropriately chosen form of external driving or forcing, which could be either mechanical or electromagnetic in nature, to influence the properties of a substrate or target system Hamiltonian in such a way as to give rise to an effective time independent Hamiltonian for the driven system that mimics any desired static Hamiltonian [80–82]. The theoretical basis for this approach is provided by Floquet Theory, a well founded mathematical result that explains the structure of solutions for differential equations with periodic coefficients. Further the formalism may be extended to give rise to the idea of a time independent hermitian effective Hamiltonian, that describes the long time dynamics relative to a period of driving, and a unitary micromotion operator that accounts for the short term dynamics. The scheme relies on the availability of convergent expansions that allow the effective Hamiltonian and the micromotion to be calculated upto some degree of approximation. The usual way is to assume a high frequency limit in which these expansions can be treated perturbatively to various orders in the inverse of the frequency and thus provide leading order corrections to the expressions of the effective Hamiltonian and the micromotion. For a thoroughly detailed account of this method starting from the fundamentals of Floquet theory to the treatment of the Schrödinger equation with a periodic Hamiltonian and the development of the Floquet Hamiltonian in an extended Floquet Hilbert

space upto the idea of the effective Hamiltonian and high frequency perturbative approxiamtions to it, the reader is advised to refer to Appendix B.

The theoretical origins of the idea of an effective description of a system driven by a high frequency periodic force was initially formulated in the classical problem of the Kapitza pendulum and solved by Landau [83, 84] where it was observed that the fast oscillations behave like a potential for the slow moving part. Extension of these ideas to quantum dynamics has been performed by several workers [85–89] with the development of a new extended Floquet space description and the notions of quasienergies and Floquet states as an effective stationary state description of a periodic time dependent problem [90, 91]. The recent trend has been the development of various high frequency expansions that attempt to get rid of various spurious contributions arising in the Floquet Hamiltonian say from an initial phase dependence or the artefactual breaking of symmetry in the Floquet band structure of a driven system [80, 82, 92, 93].

The experimental basis for the application of Floquet Engineering methods has largely been provided by the rapid advances in the area of ultra cold atoms in optical lattices [94]. These have provided an experimantal tool box for simulating various many body effects [95] and condensed matter systems where periodic driving has played a significant role in simulating effective fields that generate effects analogous to those found in the presence of magnetic fields and spin-orbit couplings [96–103]. Significant progress has been made in the methods that allow the coupling of artificial gauge fields to the bosonic or fermionic optical lattices. Such fields may be both abelian or non-abelian [104–114]. Even in realizing such couplings the use of periodic driving is important as several techniques use periodic 'shaking' of the optical lattice to achieve this [101, 102, 115, 116].

Floquet engineering techniques have also been developed in conjunction with the emerging field of Topological Insualtors to open up a new domain of 'Floquet

Topological Insulators' which has enabled the creation and manipulation of a wide range of topological phases and edge state phenomena such as Majorana modes [117–131]. Imparting non-trivial topology to trivial systems with new emergent Floquet topological phase transitions [132–139]. This includes two types of schemes where the driving may either be applied as light irradiating a material substrate such as Graphene or the periodic driving of cold atom and photonic crystal setups. In the former case the noteworthy initial step was taken by Oka and Aoki [140] where they study the effects of driving Graphene using circularly polarized light leading to the breaking of time reversal symmetry and opening of gaps in the Floquet spectrum which make the system topological and give rise to a kind of photoinduced Hall effect. This has spearheaded several works which have used irradiated Graphene as the setting for studying the hierarchy of Floquet band gaps and resulting edge modes, realizing tunable Floquet topological insulators in driven Graphene and inducing topological phase transitions via the merging of Dirac points [140–149]. In the case of cold atom systems and photonic crystal setups the Floquet methods have enabled the study of topological phase transitions by allowing the fine tuning of various system parameters [150–158].

A popular means of periodic driving is the use of delta-function kicks, or a periodic train of delta functions, which has been widely studied in the contexts of quantum chaotic behavior, non-linear dynamics and localization-delocalization transitions, when applied to quantum top, rotor or Harper Hamiltonians [159–161]. This kind of kicking is also known to impart interesting topological properties in the form of new Floquet topological phases such as semi-metallic phases in Harper models [162], chiral edge modes in Quantum Hall systems [163], appearance of unexpected topological equivalence between spectrally distinct Hamiltonians [164] as well as generation of Majorana end modes in 1-D systems [165]. This has led to interest in studying Dirac systems especially Graphene, its nano-ribbons and other

hexagonal lattice models such as the Kitaev model under periodic driving or kicking. [166–168].

We shall like to make mention of the fact that the traditional classification schemes which have been found to apply to ordinary Topological Insulators [169–171] do not always apply identically to the effective static Floquet topological Hamiltonians for periodically driven systems. This is because the Floquet quasienergies and hence the Floquet bands for driven lattice systems have a periodic structure and can, in a reduced zone kind of depiction, be compactified to a circle. Thus if a static Hamiltonian has N subbands with $N-1$ gaps then for a similar Floquet subband structure, N subbands have N gaps. An additional gap, between the topmost and bottom band, results from a folding back of the spectrum in a reduced Brillouin zone like representation for the quasienergies. It is the gap closing transitions in this gap that give rise to anomalous edge state behaviours often seen in Floquet topological insulators. This necessitates the definition of new winding number invariants that correctly capture the bulk-edge correspondence in these systems. Several such invariants and various classification schemes have been suggested in the literature and presently form an ongoing research effort [172–180].

1.4 Organization of the Thesis *

The thesis contains a total of six chapters, including this introduction, and three appendices. Here, we would like to give a brief outline of each of these, besides the introduction,

- ***Chapter 2***: The thermal properties of a system, comprising of a spinless non-interacting charged particle in the presence of a constant external magnetic field and confined in a parabolic quantum well are studied. The focus has been

*Summaries of the chapters on published results are adapted from the abstracts of the respective publications.

on the effects of a topological defect, of the form of conical disclination, with regard to the thermodynamic properties of the system. The study shows an interplay between magnetic field, temperature and the degree of conicity by setting two scales for temperature corresponding to the frequency of the confining potential and the cyclotron frequency of external magnetic field. The defect parameter is found to affect the quantitative behaviour of the thermodynamic quantities. It plays a crucial role in the competition between the external magnetic field and temperature in fixing the values of the thermal response functions.

- ***Chapter 3***: We investigate a variant of the AAH model corresponding to a bosonic optical lattice of ultra cold atoms under an effective oscillatory magnetic field. In the limit of high frequency oscillation, the system maybe approximated by an effective time independent Hamiltonian. We have studied localization/delocalization transition exhibited by the effective Hamiltonian. The effective Hamiltonian is found to retain the tight binding tri-diagonal form in position space. In a striking contrast to the usual AAH model, this non-dual system shows an energy dependent mobility edge - a feature which is usually reminiscent of Hamiltonians with beyond the nearest neighbour hoppings in real space.

- ***Chapter 4***: We move from the AAH type systems to hexagonal lattices. We consider a periodically δ-kicked Haldane type Chern insulator with the kicking applied in the $\hat{z}$ direction. This is known to behave as an inversion symmetry breaking perturbation, since it introduces a time-dependent staggered sub-lattice potential. We study here the effects of such driving on the topological phase diagram of the original Haldane model of a Hall effect in the absence of a net magnetic field. The resultant Floquet band topology is again that of a Chern insulator with the driving parameters, frequency and

amplitude, influencing the inversion breaking mass M of the undriven Haldane model. A family of such, periodically related, 'Semenoff masses' is observed to occur which support a periodic repetition of Haldane like phase diagrams along the inversion breaking axis of the phase plots. Out of these it is possible to identify two inequivalent masses in the reduced zone scheme of the Floquet quasienergies, which form the centres of two inequivalent phase diagrams. Further, variation in the driving amplitude's magnitude alone is shown to effect the topological properties by linearly shifting the phase diagram of the driven model about the position of the undriven case. A phenomenon that allows the study of Floquet topological phase transitions in the system. Finally, we also discuss some issues regarding the modifications to Haldane's condition for preventing band overlaps at the Dirac point touchings in the Brillouin zone, in the presence of kicking.

- ***Chapter 5***: The low energy continuum limit of graphene is effectively known to be modeled using the Dirac equation in (2+1) dimensions. We consider the possibility of using a modulated high frequency periodic driving of a two-dimensional system (optical lattice) to simulate properties of rippled graphene. We suggest that the Dirac Hamiltonian in a curved background space can also be effectively simulated by a suitable driving scheme in an optical lattice. The time dependent system yields, in the approximate limit of high frequency pulsing, an effective time independent Hamiltonian that governs the time evolution, except for an initial and a final kick. We use a specific form of 4-phase pulsed forcing with suitably tuned choice of modulating operators to mimic the effects of curvature. The extent of curvature is found to be directly related to ω^{-1} the time period of the driving field at the leading order. We apply the method to engineer the effects of curved background space.

- ***Chapter 6***: The important results of the work carried out in the preceeding

chapters is briefly summarized and some future avenues of investigation are discussed.

- ***Appendix A***: In this appendix we discuss the problem of spinless electrons on a 2-D square lattice in a magnetic field perpendicular to the lattice plane. This is a compilation of results and discussions found in various places in the literature collected here for easy reference and book keeping. Detailed derivations of the effective 1-D AAH Hamiltonian are provided. The various gauge arguments involved in defining the magnetic translation group are highlighted. We also provide a detailed account of the reciprocal space picture of the problem and the self-dual nature of the AAH Hamiltonian. The use of duality arguments in diagonalizing the reciprocal space Hamiltonian is illustrated and the subband structure for the case of rational values of flux quanta motivated.

- ***Appendix B***: This appendix deals with the key results and formalism associated with Floquet theory adapted from relevant sources. Their application to the problem of the Schrödinger equation with a periodic in time Hamiltonian and the development of the extended Floquet Hilbert space picture. The distinctions between the Floquet Hamiltonian and the effective Hamiltonian are delineated and the relation between them discussed. Two high frequency, perturbative expansion schemes are derived and their use in approximating the effective Hamiltonian is shown.

- ***Appendix C***: Here we review a kinematical formalism, due to Mukunda and Simon [20], which captures the notion of the Berry or geometric phase and offers a means of deriving quantities like the Berry curvature that are essential to compute topological invariants, such as the Chern number, for periodic systems.

Chapter 2

Thermal Properties of a Particle Confined to a Parabolic Quantum Well in 2D Space with Conical Disclination*

2.1 Introduction

In recent decades, advances in nanotechnology, semiconductor device fabrication and micro-fabrication techniques have thrown open the rich field of two dimensional electron systems (2DES) [1–3]. There is a special focus on systems with confinement along all three spatial dimensions [5, 6, 11, 181]. Several experiments aimed at understanding the electronic [2] and optical properties [182, 183] of such systems, commonly referred to as quantum dot [5, 184], have been undertaken [10, 11, 185, 186]. In some of these experiments the quantum dots are exposed to magnetic fields

** **This chapter is adapted from the paper "Thermal Properties of a Particle Confined to a Parabolic Quantum Well in 2D Space with Conical Disclination" by Mishra, Guha Sarkar and Bandyopadhyay (2014).***

of varying strength and their response is studied in terms of electron transport and inter-band tunneling properties [10, 11, 187, 188].

A reasonable model to describe such non-relativistic quantum dot systems requires a parabolic quantum well as the confining potential [189]. However, theoretical exploration of such models is far from exhaustive and presents several potential situations for study. One such aspect is the response of a charged particle confined to a quantum well in an applied magnetic field [190] and constrained to a surface with non-trivial geometry. An often studied topological defect is a conical disclination [33, 191–194], which has been the focus of quantum mechanical problems in curved space [33–36] of the Landau level type [30]. Another dimension of investigation [189, 195–197] looks into the thermodynamic properties of confined systems of the Landau-Fock-Darwin [32] type in ordinary Euclidean space. These lines of examination can be brought to converge on the issue of thermodynamic behavior of single electron confined in the presence of a conical disclination, a situation which has the potency to reveal the physics of quantum dots with novel geometry. The presence of topological defects in the constraining surface is expected to affect the thermodynamic characteristics of such a system and their asymptotic behavior.

In this chapter we analyze the properties exhibited by a charged particle constrained on a surface with a defect of the nature of conical disclination. The system comprises of the particle subjected to a magnetic field, while it is trapped in a parabolic Fock-Darwin potential. The approach is, to first calculate the energy spectrum and then use the canonical partition function to uncover the thermodynamic properties of the system. We have used the Schrödinger equation to obtain the energy eigenspectrum. This is motivated by the fact that spectroscopic studies of electronic states of quantum dots (such as InSb quantum dot) indicate that a Schrödinger Hamiltonian with a Fock-Darwin confining potential gives reasonable agreement with experiments [11]. We introduce a conical disclination defect in such

systems through the Volterra process [193] (discussed in the next section). The approach here borrows an idea from gravity, whereby the defect appears as a modification of geometry of the underlying space. We also note that a similar approach maybe adopted for graphene [4, 7] like 2D systems. However, the spectrum there is linear at the band minima and thereby the Dirac Hamiltonian has to be adopted. We have studied the variations of the thermodynamic quantities of interest like internal energy, specific heat and entropy with magnetic field, temperature and *extent of the defect*. The asymptotic limits of these are checked for confirmation with expected results.

The chapter consists of five sections. Sec. 2.2 gives a brief introduction to the Landau level problem and its Fock Darwin variant. Sec. 2.3 is dedicated to developing the mathematical formalism. The defect is introduced as a modification of the metric from its otherwise Euclidean form. Beginning with a suitable choice of coordinates, the Hamiltonian of the system is constructed. The Schrödinger equation is then solved for this Hamiltonian to obtain the energy spectrum. This is followed by obtaining the various thermodynamic variables of the system using the canonical partition function. The expressions for these quantities are recast in terms of dimensionless parameters and their behavior is studied. The asymptotics are checked for consistency. In Sec. 2.4 we present the results of our study. Finally we conclude with a discussion and summary in the last section.

2.2 Landau Level Problem

The fundamental, quantum-mechanical problem of a 2-dimensional gas of electrons (spin ignored) in a magnetic field perpendicular to their plane of motion is referred to as the Landau level problem, after L. D. Landau who first provided its solution [30]. Here we briefly survey the essential features of this system. The Hamiltonian

for this is, in general, given by [31]

$$H = \frac{1}{2m}\left(\mathbf{p} - \frac{e}{c}\mathbf{A}(x,y)\right)^2 \tag{2.1}$$

where m is the electronic mass and e the magnitude of its charge, $\mathbf{p}$ its momentum and $\mathbf{A}(x,y)$ the position dependent vector potential giving rise to a constant magnetic field $\mathbf{B}$ in the $\hat{z}$ direction, $\mathbf{B} = B\hat{z}$. The problem is usually solved in a certain gauge choice. Two common choices are the Landau gauge $\mathbf{A} = -B(y,0,0)$ and the symmetric gauge $B/2(-y,x,0)$. One may be guided by the geometry of the problem to prefer one over the other but the essential physical results are independent of this choice.

In the Landau gauge the Hamiltonian takes the form

$$H_{\mathrm{L}} = \frac{1}{2m}(-i\hbar\partial_x + \frac{e}{c}By)^2 + \frac{1}{2m}(-i\hbar\partial_y)^2 \tag{2.2}$$

where through a set of transformations, and a wavefunction ansatz $\psi_{\mathrm{L}}(x,y) = e^{ik_x}\psi_{\mathrm{L}}y$, the quadratic term in the y coordinate becomes a harmonic oscillator potential with its frequency as the cyclotron frequency $\omega_c = eB/mc$. Thus the spectrum is given by that of a 1-D oscillator

$$\epsilon_n = \hbar\omega_c\left(n + \frac{1}{2}\right) \tag{2.3}$$

with the quantum number n denoting the Landau level. The wavefunction is given by

$$\psi_{\mathrm{L}}(x,y) = Ce^{ik_x}H_n(y + k_x l_B^2)e^{(y+k_x l_B^2)^2/2l_B^2} \tag{2.4}$$

where C is the normalization constant, H_n is the usual Hermite polynomial which enters as the quantum harmonic oscillator solution, and l_B is the characteristic *magnetic length* scale $l_B = \sqrt{\frac{\hbar c}{eB}}$. Given that the solution is a free particle in the x

coordinate the Landau levels have an infinite degeneracy labelled by k_x.

The Landau Fock-Darwin [32] problem is an extension of Hamiltonian in eq.(2.1) by the addition of a 2-D harmonic oscillator potential in the following way

$$H_{\rm LD} = \frac{1}{2m}\left(\mathbf{p} - \frac{e}{c}\mathbf{A}(x,y)\right)^2 + \frac{1}{2}m\omega_p^2(x^2+y^2) \tag{2.5}$$

where ω_p is the frequency of the confining potential. Due to the radial symmetry of the potential above, the symmetric gauge is the preferred gauge of choice while solving this problem. Details of which can be found in [31]. In the remaining portion of this chapter we shall be considering this system on a space with a defect in its metric and studying its spectrum and thermal-statistical properties.

2.3 Formalism

The topological defect being introduced in the current chapter is a conical disclination. This entails a two-dimensional (2D) conical space which is locally flat at all points except for the origin [34]. The construction of this space is to be visualized as the consequence of cutting out a sector with a certain apex angle called the *deficit angle*, from the ordinary 2D flat space and subsequently welding together the newly revealed edges [198]. The metric for such a space, in the usual polar coordinates (r,ϕ) is given by $g_{\mu\nu} = \text{diag}(1,\ r^2)$. However, it has to be kept in mind that ϕ here has an incomplete angular range $[0,\ 2\pi\kappa]$ with $\kappa \neq 1$. This, being a consequence of the surgical procedure performed previously. The parameter κ is a measure of the deficit angle. It quantifies the conicity of the surface and shall henceforth be referred to as the *kink parameter*. The kink here represents a singular deformity of the 2D conical surface at the origin. The metric described above can be expressed

in terms of the complete angular coordinate θ as follows

$$ds^2 = \kappa^{-2} d\rho^2 + \rho^2 d\theta^2. \tag{2.6}$$

where, θ varies in $[0, 2\pi]$. The transformation from plane polar coordinates to the new coordinate system, i.e. from $(r, \phi) \rightarrow (\rho, \theta)$ is achieved via the set of transformation equations

$$\rho = \kappa r \qquad \theta = \kappa^{-1}\phi. \tag{2.7}$$

The curvature is measured by the quantity

$$2\pi \frac{\kappa - 1}{\kappa} \delta^{(2)}(\rho),$$

where $\delta^{(2)}(\rho)$ is the Dirac delta function in two dimensions [36]. Hence, for $0 < \kappa < 1$ we have negative curvature and for $1 < \kappa < \infty$ the curvature at origin is positive. We note that the metric described here in the context of 2D condensed matter system also arises in the description of space-time around a cosmic string [199].

In the above described space we consider a charged spin-less quantum particle (for our purposes it has electronic mass and charge). This particle is subjected to a constant magnetic field $\mathbf{B}$ which is normal to the conical surface. The appropriate choice of magnetic vector potential that yields such a magnetic field is given in the symmetric gauge by

$$\mathbf{A}(\rho) = \frac{B\rho}{2\kappa} \hat{e}_\theta \tag{2.8}$$

where $B = |\mathbf{B}|$. This gives rise to the standard quantized single particle Landau level states [30].

In order to model the confinement of the particle within a small region on the surface, we subject the particle to a parabolic potential of the Fock-Darwin type

[32] given by

$$V(\rho) = \frac{1}{2} M \omega_p^2 \frac{\rho^2}{\kappa^2} \tag{2.9}$$

where M is the effective mass of the particle and ω_p is a measure of the steepness of the confinement. The appearance of the kink parameter indicates that the background space is conical. The choice of such a potential is motivated by symmetry considerations and its frequent appearance in the modeling of quantum dots with low occupancy [200].

The Hamiltonian for the particle of mass M, assumed to be carrying a negative charge of magnitude e under minimal electromagnetic coupling, is given in the cone space coordinates (ρ, θ) as

$$\begin{aligned} H = &-\frac{\hbar^2}{2M}\left[\frac{\kappa^2}{\rho}\frac{\partial}{\partial\rho}\left(\rho\frac{\partial}{\partial\rho}\right) + \frac{1}{\rho^2}\frac{\partial^2}{\partial\theta^2}\right] - \frac{i}{2}\frac{\hbar\omega_c}{\kappa^2}\frac{\partial}{\partial\theta} \\ &+ \frac{1}{8}M\omega_c^2\frac{\rho^2}{\kappa^4} + \frac{1}{2}M\omega_p^2\frac{\rho^2}{\kappa^2} \end{aligned} \tag{2.10}$$

where the parameter ω_c introduced here is the cyclotron frequency $\omega_c = eB/Mc$. Note the appearance of the kink parameter $\kappa \neq 1$ when one expresses the Hamiltonian in the cone space.

The general form of eigenfunctions for this Hamiltonian can be guessed from symmetry arguments. Separation of the Schrödinger equation into radial and angular components yields such a general form

$$\psi(\rho, \theta) = \frac{1}{\sqrt{2\pi}} e^{im\theta} R_{nm}(\rho) \tag{2.11}$$

The quantum numbers n and m are to be defined using the appropriate boundary conditions. Here, $R_{nm}(\rho)$ stands for the radial component of the wave function.

The condition on m is readily obtained by requiring ψ to be unique under a rotation of 2π, ie $\psi(\rho,\theta) = \psi(\rho,\theta+2\pi)$. This implies that m has to be an integer. The Schrödinger equation $H\psi_{nm} = E_{nm}\psi_{nm}$ yields the following equation for the radial wave function $R_{nm}(\rho)$.

$$\begin{aligned} &-\frac{\hbar^2}{2M}\left[\frac{\kappa^2}{\rho}\frac{\partial}{\partial\rho}\left(\rho\frac{\partial}{\partial\rho}R_{nm}(\rho)\right) - \frac{m^2}{\rho^2}R_{nm}(\rho)\right] \\ &+\left(\frac{1}{2}\frac{\hbar\omega_c m}{\kappa^2} + \frac{1}{8}M\omega_c^2\frac{\rho^2}{\kappa^4} + \frac{1}{2}M\omega_p^2\frac{\rho^2}{\kappa^2}\right)R_{nm}(\rho) \\ &= E_{nm}R_{nm}(\rho) \end{aligned} \tag{2.12}$$

The procedure to solve the above equation is through a set of standard transformations, which involves the introduction of a new parameter Ω with dimension of frequency. The parameter Ω is given by

$$\Omega = \sqrt{\omega_p^2 + \left(\frac{\omega_c}{2\kappa}\right)^2}. \tag{2.13}$$

Following the formalism in [33] eq. (2.12) can be transformed to a form which permits solution in terms of the confluent-hypergeometric function. Our primary interest lies in the energy levels which are given by

$$E_{nm} = \left(2n + 1 + \frac{|m|}{\kappa}\right)\hbar\Omega + \frac{m\hbar\omega_c}{2\kappa^2} \tag{2.14}$$

To solve the radial eigenvalue equation (2.12), we introduce $\zeta = \rho^2 M\Omega/\hbar$. This transformation yields the following equation

$$\zeta\frac{\partial^2 R(\zeta)}{\partial\zeta^2} + \frac{\partial R(\zeta)}{\partial\zeta} + \Xi(\zeta)R(\zeta) = 0 \tag{2.15}$$

where we have used

$$\Xi(\zeta) = \frac{\beta}{\kappa^2} - \frac{\zeta}{4\kappa^4} - \frac{m^2}{4\kappa^2\zeta} \quad \text{and} \quad \beta = \frac{1}{2}\left(\frac{E_{mn}}{\hbar\Omega} - \frac{\omega_c m}{2\kappa^2\Omega}\right).$$

Using variables $\zeta' = \zeta/\kappa^2$ and $m' = m/\kappa$ we have

$$\zeta' \frac{\partial^2 R(\zeta')}{\partial \zeta'^2} + \frac{\partial R(\zeta')}{\partial \zeta'} + \Xi'(\zeta') R(\zeta') = 0 \tag{2.16}$$

where the new function Ξ' is

$$\Xi'(\zeta') = \beta' - \frac{\zeta'}{4} - \frac{m'^2}{4\zeta'}, \quad \text{with} \quad \beta' = \frac{1}{2}\left(\frac{E_{mn}}{\hbar\Omega} - \frac{\omega_c m'}{2\kappa\Omega}\right).$$

Assuming $R(\zeta')$ to be of the form

$$R(\zeta') = e^{-\frac{\zeta'}{2}} \zeta'^{\frac{|m'|}{2}} Y(\zeta'),$$

the equation (B.58) reduces to

$$\begin{aligned} \zeta' \frac{\partial^2 Y}{\partial \zeta'^2} &+ (|m'|+1-\zeta') \frac{\partial Y}{\partial \zeta'} \\ &+ \left(\beta' - \frac{|m'|}{2} - \frac{1}{2}\right) Y = 0. \end{aligned} \tag{2.17}$$

The solution to this equation is given in terms of the confluent-hypergeometric function as

$$Y(\zeta') = F\left[-\left(\beta' - \frac{|m'|}{2} - \frac{1}{2}\right),\ |m'|+1;\ \zeta'\right] \tag{2.18}$$

The requirement of boundedness of $R(\zeta')$ as $\zeta' \to \infty$ is met if

$$\beta' - \frac{|m'|}{2} - \frac{1}{2} = n, \tag{2.19}$$

where n is a non-negative integer. From this boundary condition (after substituting

m/κ in place of m') the eigenenergies are given by

$$E_{nm} = \left(2n + 1 + \frac{|m|}{\kappa}\right)\hbar\Omega + \frac{m\hbar\omega_c}{2\kappa^2} \tag{2.20}$$

The eigenfunctions corresponding to these eigenvalues are obtained after imposing the requirement that for integral values of n, the confluent hypergeometric function reduces to Laguerre polynomials given as

$$L_n^{\alpha}(\zeta') = \frac{\Gamma(\alpha + n + 1)}{\Gamma(\alpha + 1)\, n!} F(-n,\ \alpha + 1;\ \zeta') \tag{2.21}$$

here $\Gamma(n) = (n-1)!$is the usual gamma function.Thus the eigenfunctions are of the form

$$R(\zeta) = Ce^{-\frac{\zeta}{2\kappa^2}} \left(\frac{\zeta}{\kappa^2}\right)^{\frac{|m|}{2\kappa}} L_n^{\frac{|m|}{\kappa}}(\zeta) \tag{2.22}$$

where C is the constant of normalization.The first term in the product represents a Gaussian in the variable ρ whose spread is now determined by the degree of disclination. The localization of the wave function is hence sensitive to κ and consequently all probability densities are affected by the degree of conicity.The appearance of $|m|/\kappa$ indicates the deficit/surplus of the polar angle quantified through κ.

2.3.1 Computation of Thermodynamic Quantities

If we consider the system to be at equilibrium with a heat bath at temperature T, the canonical partition function shall be given by

$$\mathcal{Z} = \sum_{n,m} e^{-\beta(2n+1)\hbar\Omega}\ \ e^{-\beta\left[\frac{|m|}{\kappa}\hbar\Omega + \frac{m\hbar\omega_c}{2\kappa^2}\right]}. \tag{2.23}$$

where $\beta = \frac{1}{k_B T}$ and k_B is the Boltzmann constant. The sum is over the discrete energy levels given in Eq. (2.14). Introducing dimensionless variables $\chi_1 = \frac{\hbar\Omega}{\kappa}$ and $\chi_2 = \frac{\hbar\omega_c}{2\kappa^2}$ the above expression maybe simplified to

$$\mathcal{Z} = \frac{\sinh \chi_1}{4 \sinh\left(\frac{\chi_1 + \chi_2}{2}\right) \sinh\left(\frac{\chi_1 - \chi_2}{2}\right) \sinh(\kappa\chi_1)}. \tag{2.24}$$

It is now possible to compute thermodynamic quantities from this expression of the partition function.

The internal energy U for the system is given by

$$\begin{aligned} U &= -\frac{\partial \ln \mathcal{Z}}{\partial \beta} \\ &= -\Bigg\{ \chi_1 \coth(\beta\chi_1) - \frac{\chi_1 + \chi_2}{2} \coth\beta\left(\frac{\chi_1 + \chi_2}{2}\right) \\ &\quad - \frac{\chi_1 - \chi_2}{2} \coth\beta\left(\frac{\chi_1 - \chi_2}{2}\right) - \chi_1\kappa \coth\beta\kappa\chi_1 \Bigg\} \end{aligned} \tag{2.25}$$

Similarly one can obtain the specific heat capacity C_v

$$\begin{aligned} C_\mathrm{v} &= k_B\beta^2 \frac{\partial^2 \ln \mathcal{Z}}{\partial \beta^2} \\ &= k_B\beta^2 \Bigg\{ \frac{(\chi_1 + \chi_2)^2}{4} \mathrm{csch}^2\beta \frac{(\chi_1 + \chi_2)}{2} + \chi_1^2\kappa^2 \mathrm{csch}^2\beta\kappa\chi_1 \\ &+ \frac{(\chi_1 - \chi_2)^2}{4} \mathrm{csch}^2\beta \frac{(\chi_1 - \chi_2)}{2} - {\chi_1}^2 \mathrm{csch}^2\beta\chi_1 \Bigg\}. \end{aligned} \tag{2.26}$$

The Helmholtz free energy $F = -\ln \mathcal{Z}/\beta$ may be used to calculate the entropy S as

$S = (U - F)/T$. This yields the following expression

$$\begin{aligned} S = \frac{1}{T}\Bigg\{ & -\chi_1 \coth(\beta\chi_1) + \frac{\chi_1+\chi_2}{2}\coth\left(\beta\,\frac{\chi_1+\chi_2}{2}\right) \\ & + \frac{\chi_1-\chi_2}{2}\coth\left(\beta\frac{\chi_1-\chi_2}{2}\right) + \chi_1\kappa\coth(\beta\kappa\chi_1)\Bigg\} \\ & + k_B\Bigg\{\ln\sinh(\beta\chi_1) - \ln\sinh\left(\beta\frac{\chi_1+\chi_2}{2}\right) \\ & - \ln\sinh\left(\beta\frac{\chi_1-\chi_2}{2}\right) - \ln\sinh(\beta\kappa\chi_1) - \ln 4\Bigg\} \end{aligned} \tag{2.27}$$

We shall now study the variation of these quantities with the external magnetic field B and temperature T. In order to facilitate this, it is helpful to choose certain special units which render the physical quantities U, $C_{\rm v}$ and S dimensionless. We introduce a parameter $\alpha = \omega_c/\omega_p$ to quantify the magnetic field strength in units of $M\omega_p c/e$ and $\xi = k_B T/\hbar\omega_p$ to represent temperature measured in units of $\hbar\omega_p/k_B$. We also introduce $\widetilde{\alpha} = \sqrt{1+\alpha^2/4\kappa^2}$ and $\alpha_\pm = \widetilde{\alpha} \pm \alpha/2\kappa$.

Using these new dimensionless parameters, we have the internal energy U, entropy S and specific heat $C_{\rm v}$ may be expressed as

Internal energy :

$$\frac{U}{\hbar\omega_p} = \frac{1}{\kappa}\Bigg\{-\widetilde{\alpha}\coth\left(\frac{\widetilde{\alpha}}{\xi\kappa}\right) + \frac{\alpha_+}{2}\coth\left(\frac{\alpha_+}{2\xi\kappa}\right) + \frac{\alpha_-}{2}\coth\left(\frac{\alpha_-}{2\xi\kappa}\right) + \widetilde{\alpha}\kappa\coth\left(\frac{\widetilde{\alpha}}{\xi}\right)\Bigg\} \tag{2.28}$$

Specific heat :

$$\frac{C_{\rm v}}{k_B} = \frac{\widetilde{\alpha}^2}{\xi^2}\mathrm{cosech}^2\left(\frac{\widetilde{\alpha}}{\xi}\right) + \frac{{\alpha_+}^2}{4\kappa^2\xi^2}\mathrm{cosech}^2\left(\frac{\alpha_+}{2\kappa\xi}\right) + \frac{{\alpha_-}^2}{4\kappa^2\xi^2}\mathrm{cosech}^2\left(\frac{\alpha_-}{2\kappa\xi}\right) - \frac{\widetilde{\alpha}^2}{\xi^2\kappa^2}\mathrm{cosech}^2\left(\frac{\widetilde{\alpha}}{\kappa\xi}\right) \tag{2.29}$$

Entropy :

$$\frac{S}{k_B} = \frac{1}{\xi\kappa}\left\{-\widetilde{\alpha}\coth\left(\frac{\widetilde{\alpha}}{\xi\kappa}\right) + \frac{\alpha_+}{2}\coth\left(\frac{\alpha_+}{2\xi\kappa}\right) + \frac{\alpha_-}{2}\coth\left(\frac{\alpha_-}{2\xi\kappa}\right) + \widetilde{\alpha}\kappa\coth\left(\frac{\widetilde{\alpha}}{\xi}\right)\right\} + \left\{\ln\sinh\left(\frac{\widetilde{\alpha}}{\xi\kappa}\right) - \ln\sinh\left(\frac{\alpha_+}{2\xi\kappa}\right) - \ln\sinh\left(\frac{\alpha_-}{2\xi\kappa}\right) - \ln\sinh\left(\frac{\widetilde{\alpha}}{\xi}\right) - \ln 4\right\}. \tag{2.30}$$

The asymptotic behaviour of the above expressions in the low temperature limit is instructive to look at. The internal energy U in the low temperature limit is given by $U \to \hbar\Omega$, where Ω is defined earlier in eq.(2.13). The low temperature asymptotic form ($\xi \to 0$) of entropy S is given by

$$S \approx \left(1 + \frac{\alpha_+}{\xi\kappa}\right) e^{\frac{-\alpha_+}{\xi\kappa}} + \left(1 + \frac{\alpha_-}{\xi\kappa}\right) e^{\frac{-\alpha_-}{\xi\kappa}} + \left(1 + \frac{2\widetilde{\alpha}}{\xi}\right) e^{\frac{-2\widetilde{\alpha}}{\xi}} - \left(1 + \frac{2\widetilde{\alpha}}{\xi\kappa}\right) e^{\frac{-2\widetilde{\alpha}}{\xi\kappa}} \tag{2.31}$$

The specific heat in the low temperature limit, is approximated by the following function of temperature.

$$C_{\rm v} \approx \frac{4\widetilde{\alpha}^2}{\xi^2} e^{\frac{-2\widetilde{\alpha}}{\xi}} + \frac{\alpha_+^2}{\xi^2\kappa^2} e^{\frac{-\alpha_+}{\xi\kappa}} + \frac{\alpha_-^2}{\xi^2\kappa^2} e^{\frac{-\alpha_-}{\xi\kappa}} - \frac{4\widetilde{\alpha}^2}{\xi^2\kappa^2} e^{\frac{-2\widetilde{\alpha}}{\xi\kappa}} \tag{2.32}$$

2.4 Results and Discussion

2.4.1 The Energy Spectrum

The Landau-Fock-Darwin energy spectrum is given by Eq. (2.14). Fig. (2.1) shows the variation of E_{nm} with the external magnetic field parameter α, for a few chosen values of the kink parameter $\kappa = 0.75, 1.0, 1.5$. The behaviour of the energy levels is different for positive and negative values of the quantum number m. The figure shows the variation of E_{nm} with α for $n = 1, 2$. In the upper panel we show the case when the integer m is assumed to take positive values 2, 3, 4 and 5 for each

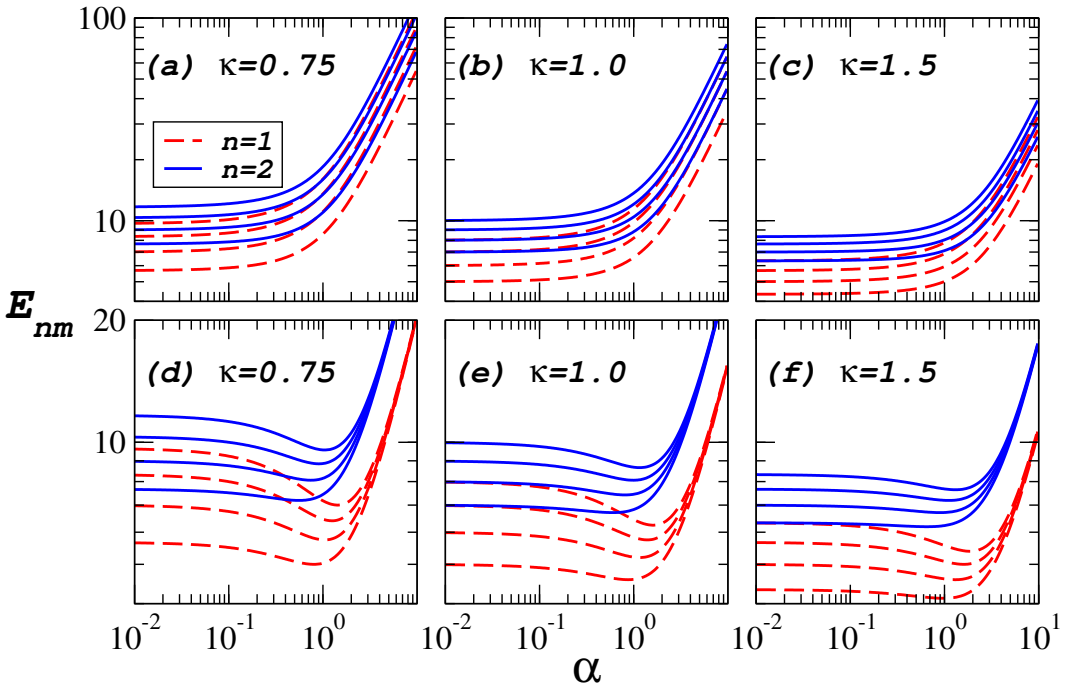

Figure 2.1: The low lying energies of the Landau-Fock-Darwin energy spectrum for various values of the kink parameter κ. The upper panel (a-c) shows the spectra for positive values of the quantum number $m = 2, 3, 4, 5$ (lower to the upper) and the lower panel (d-f) corresponds to negative values of $m = -2, -3, -4, -5$ with decreasing magnitude $|m|$ from upper to the lower curves.

n. The behaviour at very low magnetic field shows that E_{nm} is independent of α for $\alpha \lesssim 10^{-2}$. In this low magnetic field regime one finds the usual degeneracies of (n, m) pairs since $E_{nm} \approx (2n + 1 + |m|/\kappa)\hbar\omega_p$. In our case with $\kappa = 1.0$ this occurs, for example between (n, m) pairs like $[(2, 2), (1, 4)]$, $[(2, 3), (1, 5)]$ and $[(2, 4), (1, 6)]$. These degeneracies starts to get lifted when the external magnetic field is sufficiently high ($\alpha \approx 1$). At very high magnetic fields ($\omega_c >> \omega_p$) and for $m > 0$, we have $E \to [(2n + 1)/2\kappa + m/\kappa^2]\hbar\omega_c$ leading to new degeneracies. In the relatively high magnetic field region of $\alpha \approx 10$ one can readily observe that curves for all (n, m) are monotonically increasing with nearly fixed slopes. The transition between these extreme behaviours occurs in the intermediate field region of $\alpha \approx 1$. We note, that in the intermediate and large magnetic field regions the difference between the energy levels with the same value of n but different values of m is larger as compared to the

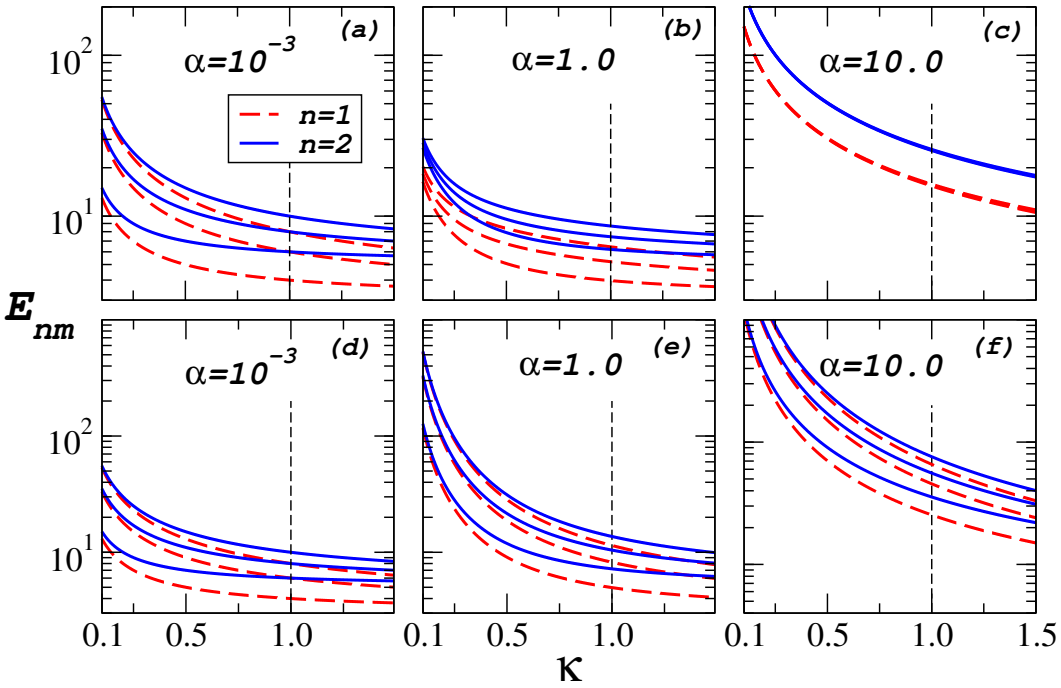

Figure 2.2: The first few levels of the Landau-Fock-Darwin energy spectrum as a function of the kink parameter κ. The upper panel corresponds to negative values of the quantum number $m = -1, -3, -5$. The lower panel shows the same for positive values of $m = 1, 3, 5$. Three magnetic field values are chosen with $\alpha = 10^{-3}, 1.0, 10.0$.

low field region. This is owing to the fact that ω_c is larger for higher magnetic fields. For example the level corresponding to $(1, 3)$ is higher than $(2, 2)$. The energy levels shift in magnitude for changing κ which implicitly affects the degeneracy pattern.

The figures in the lower panel 1(d)-1(f) shows the spectrum for negative m values. The low magnetic field behaviour is the same as for the positive m case. However at large magnetic fields the term $m\hbar\omega_c/2\kappa^2$ starts to play an important role and cancels the term $|m|\hbar\Omega/2\kappa$ in this regime. The spectrum becomes independent of m and only depends on n. The increase of E_{nm} is approximately linear with magnetic field α. The transition between the two regimes occurs again at $\alpha \approx 1$.

Figure 2.2 shows the variation of energy with the kink parameter κ for three different values of the applied magnetic field. Fig 2(a), (b) and (c) show the variation for negative m values ($m = -1, -3, -5$) corresponding to $n = 1, 2$. The curves show a monotonic decrease of E_{nm} with κ in all the three regimes of magnetic field α.

The value $\kappa = 1$ corresponds to the case with no topological defect. We note an asymmetry in the nature of variation of E_{nm} about this value of κ. The energy levels are a decreasing function of κ for both $\kappa \geq 1$ and $\kappa < 1$ showing that positive and negative deficit angles point towards fundamentally different physical situations. The expression for E_{nm} diverges as $\kappa \to 0$. This, however is of no real consequence since $\kappa = 0$ corresponds to an unphysical divergent curvature at the origin.

The vertical dotted line indicating the case without any defect ($\kappa = 1$) passes through the point of intersection of the energy levels. These points correspond to the degenerate energy levels at low magnetic field. The degeneracy of the (n, m) levels for $\kappa = 1$ are seen to get lifted for $\kappa \neq 1$ as the energy levels for different m vary differently with κ. In Fig. 2(c) the different m levels for a given n are degenerate and remain so, irrespective of κ. The figures 2(d)-2(f) show a similar variation for positive m values. Whereas the degeneracies at weak magnetic field (Fig. 2(d)) gets lifted for $\kappa \neq 1$ there are new degeneracies that are created at higher magnetic fields. This is seen in Fig. 2(e)-2(f) where non-degenerate energy levels at $\kappa = 1$ intersect each other at $\kappa \neq 1$ showing the emergence of accidental degeneracies that did not exist in the defect free theory.

2.4.2 Thermodynamic properties

The non-interacting spinless charged particles are assumed to be in equilibrium with a heat reservoir at temperature T. The starting point of the thermodynamic analysis is the evaluation of the partition function for the energy spectra given in Eq. (2.14). The Landau-Fock-Darwin Hamiltonian has two energy scales associated with the two frequencies ω_p (which fixes the strength of the parabolic confinement) and ω_c, the cyclotron frequency related to the external magnetic field. The relative strengths of these frequencies are expected to govern the equilibrium behaviour of the system. The thermodynamic properties of interest, depend on the temperature ξ and

external magnetic field α, expressed in our chosen convenient energy unit $\hbar\omega_p$. The parameters in the Hamiltonian $(\omega_p, \omega_c, \kappa)$ have a crucial interplay in determining the responses of the system. The $\kappa = 1$ case with no defects has been studied in earlier works [189, 195–197]. It is important to note that for $\kappa = 1$, the limiting behaviour of the system for $\omega_p \to 0$ (or equivalently $\omega_c >> \omega_p$) and $\omega_c \to 0$ are entirely different and describe two completely distinct physical situations. The former describes a pure Landau problem of a free particle without any confinement, whereas the latter describes a particle in a two dimensional parabolic well without a coupling to an external magnetic field. The $\omega_p \to 0$ limit has a pure quantum mechanical Landau-level spectra of a one-dimensional oscillator and has the degeneracy that depends on the size of the system. The energy spectra for the case $\omega_c \to 0$ mimics that of a 2D oscillator. The translational symmetry of the pure Landau level situation is lost completely in the other extreme limit of a pure confinement problem. The general Landau-Fock-Darwin solution interpolates between these extreme cases. In the presence of $\kappa \neq 1$ the same qualitative features are expected. However, the role of κ needs to be explored and is subsequently discussed in this chapter.

We follow the Gibbs formalism to compute thermodynamic quantities like free energy, entropy and specific heat. In this approach, the thermodynamic response functions are obtained as derivatives of the partition function. The canonical partition function (see Eq. 2.23) is obtained for the Hamiltonian in Eq. (2.10). In the final form, this partition function (see Eq. (2.24)) is seen to diverge in the limit $\omega_c >> \omega_p$ (or $\alpha >> 1$) since, χ_1 and χ_2 are equal in this limit. This singularity of the partition function, when the confinement strength is vanishingly small, has been addressed in [195–197] and maybe regularized by putting certain cutoffs to the smallest value that ω_p can take. This cutoff depends on the temperature and the degeneracy of the pure Landau level. The thermodynamic quantities like F, U, S and $C_{\rm v}$ however, manifest no such singularity. Figure 4.5 shows the variation of $C_{\rm v}$

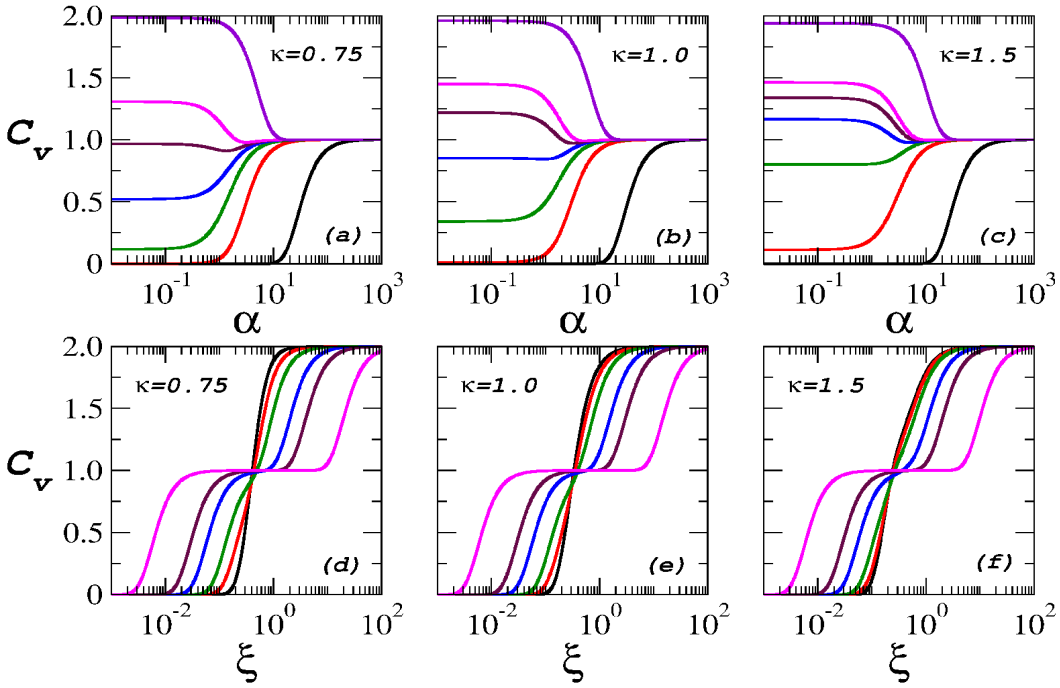

Figure 2.3: The $C_{\rm v}$ shown here is in units of k_B. The upper panel shows the variation of $C_{\rm v}$ with magnetic field for various values of temperature $\xi = 0.01, 0.1, 0.2, 0.3, 0.4, 0.5, 2.0$ (curves from lower to upper). At high magnetic fields $C_{\rm v}$ attains the value 1.0 as the spectrum reduces to the free Landau levels with no confinement. The high temperature value of $C_{\rm v}$ for moderate to low magnetic fields is 2 as the confinement term dominates at these regimes. The Lower panel shows the variation of $C_{\rm v}$ with temperature for $\alpha = 0.001, 1.0, 2.0, 5.0, 10.0, 50.0$ (left to right in the upper right corner of the figures). Here again the plateau in $C_{\rm v}$ is seen for the high magnetic fields and only at high temperatures $C_{\rm v}$ attains the value 2.0.

with magnetic field α and temperature ξ for different values of the kink parameter κ. The variation of $C_{\rm v}$ with α shows that for weak external magnetic field and low temperatures $C_{\rm v}$ asymptotically approaches *zero*. However, in this weak α regime, at high temperatures $C_{\rm v} \to 2k_B$ asymptotically. This is in consonance with the equipartition principle. The low α end behaves like a 2D oscillator (hence the factor 2). In the high magnetic field regime (α large), $C_{\rm v}$ saturates to k_B. This region corresponds to the pure Landau level with the energy spectrum of an 1D oscillator. The qualitative features are similar when $\kappa \neq 1$. However, we see that changing κ from 0.75 to 1.5 continuously, leads to a shift of the curves from the lower end towards the upper. This can be qualitatively ascribed to the fact that κ appears

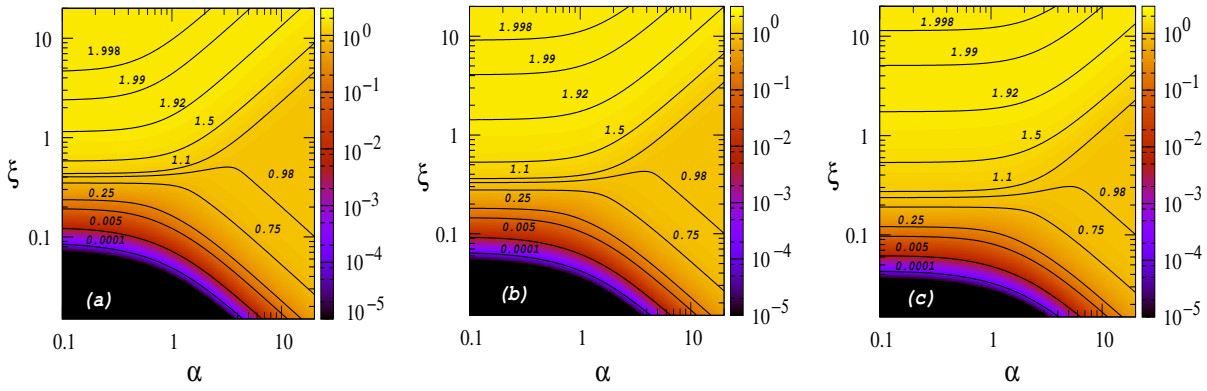

Figure 2.4: The contour map for specific heat $C_{\rm v}$ in the (ξ, α) phase plane, for three values of the kink parameter (a) $\kappa = 0.75$, (b) $\kappa = 1.0$, (c) $\kappa = 1.5$.

as a multiplicative factor to ξ in the expression for $C_{\rm v}$ and a change of κ roughly amounts to a recalibration of the temperature scale.

The variation of $C_{\rm v}$ with temperature ξ is shown in the lower panel of Fig. 4.5. When the value of α is small, the rise of $C_{\rm v}$ with temperature is steep, and in a very small temperature range, $C_{\rm v}$ rises from zero to a stable value of $2k_B$. Beyond the transition temperature, $C_{\rm v}$ remains flat at this value. In this situation the system is essentially dominated by the parabolic confining potential and the physics of the Landau levels is missing. The situation is considerably different when α is large. Here the effect of confinement is weak and $C_{\rm v}$ attains a plateau like level when temperature is increased. The value of $C_{\rm v}$ remains constant at k_B for a range of temperatures after which it rises to $2k_B$ only at high values of ξ. The formation of the plateau can be ascribed to the dominance of the Landau 1D oscillator spectrum at high magnetic fields as opposed to the 2D oscillator spectrum of the parabolic well when the magnetic field is weak. The extent of the plateau region is found to be sensitive to κ. We shall discuss this κ dependence later. Figure 2.4 shows the contour map of $C_{\rm v}$ in the (α, ξ) plane. At very low temperatures, $C_{\rm v} \to 0$ except, when the external magnetic field is large. The lower left corner of the (α, ξ) plane corresponds to this phase where $C_{\rm v}$ is small. Increasing the temperature at small values of α leads to a monotonic increase of $C_{\rm v}$ to its saturated value of $2k_B$ (upper

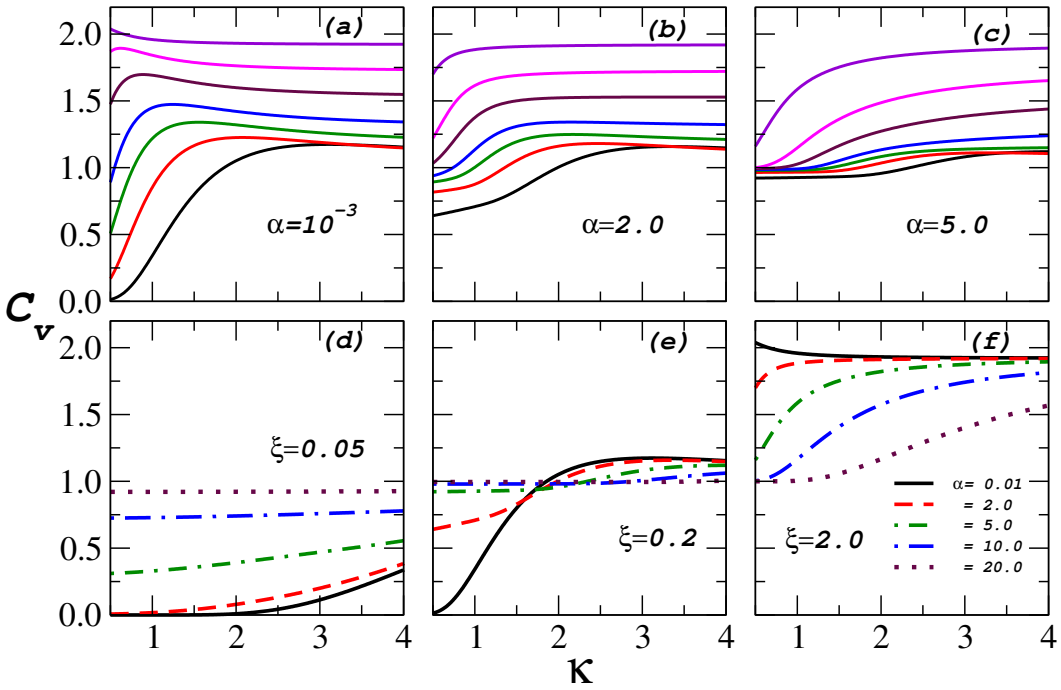

Figure 2.5: The dependence of $C_{\rm v}$ on the kink parameter κ for different values of external magnetic field α and temperature ξ. For the upper panel $\xi = 2.0, 1.0, 0.7, 0.5, 0.4, 0.3, 0.2$ (top to bottom).

left corner of the phase diagram). At such low values of α there is hardly any Landau coupling to the magnetic field. The Landau plateau occurs at large α when the energy spectrum approaches the Landau levels. This is the forked region of the contour map, where, for a considerable range of intermediate temperatures the value of $C_{\rm v}$ remains at the k_B level, and only increases to $2k_B$ at still higher temperatures (this is not seen in the phase diagram and occurs for values of ξ even above the upper right corner). The extent of the forking region (plateau in $C_{\rm v}$ depends on the kink parameter. Infact, it is seen to decrease with increasing κ. This can be understood by noting that a changing κ can be equivalently seen as changing ξ with a fixed κ. The qualitative features of the phase diagram remain the same when κ is varied. However, there are quantitative changes which we shall discuss now.

Figure 2.5 shows the variation of $C_{\rm v}$ with κ. At high temperatures, $C_{\rm v}$ is not sensitive to κ unless the magnetic field α is also very high. This is seen in the figures 5(a)-(c). The specific heat is however very sensitive to κ at low temperatures.

Increasing κ can be equivalently interpreted as a scaling of α and this explains the plateau (characteristic of large α) when κ is large. At large α (figure 5(c)), all the low temperature curves cluster around the k_B level and stabilizes at the $2k_B$ level only for high temperatures. Figure 5(e) shows that there is a cross over of $C_{\rm v}$ at a certain value of κ. This implies that at some intermediate low temperatures $C_{\rm v}$ is not much sensitive to the changes in the magnetic field for certain values of κ. At higher temperatures, however, $C_{\rm v}$ saturates to $2k_B$. This growth is slower for the curves corresponding to large α values which tends to stay in the plateau region as compared to the case when α is small. Here, we see that κ essentially re-calibrates the temperature scale.

Figure 2.6 shows the behaviour of the entropy as a function of magnetic field and temperature. The competition between the variables ξ and α decides the degree of order in the system. We find that the asymptotic form of S in Eq. (2.31) is valid for a certain value of ξ that depends on the magnetic field and κ. This region of validity of this limiting form of entropy is shown by broken lines in Fig. 2.6 (a)-(c). The third law of thermodynamics is respected and we have $S \to 0$ as $\xi \to 0$. The growth of entropy from the low temperature ordered regime to the disordered state at high temperature, depends on the magnetic field. The growth is steeper for higher magnetic fields. However at very high temperatures the magnetic field dependence keeps decreasing. Figures 6 (d-f) shows the variation of entropy with magnetic field. At very high magnetic field there is a slowing down on the rate at which S increases. This feature is seen for a wide range of temperatures. The effect of κ here is clearly that of a scaling parameter that re-calibrates the temperature scale ξ.

2.5 Summary and Conclusion

In this chapter, we have carried out a study of the thermodynamic ramifications of a conical defect, in the context of Landau-Fock-Darwin problem. The competing

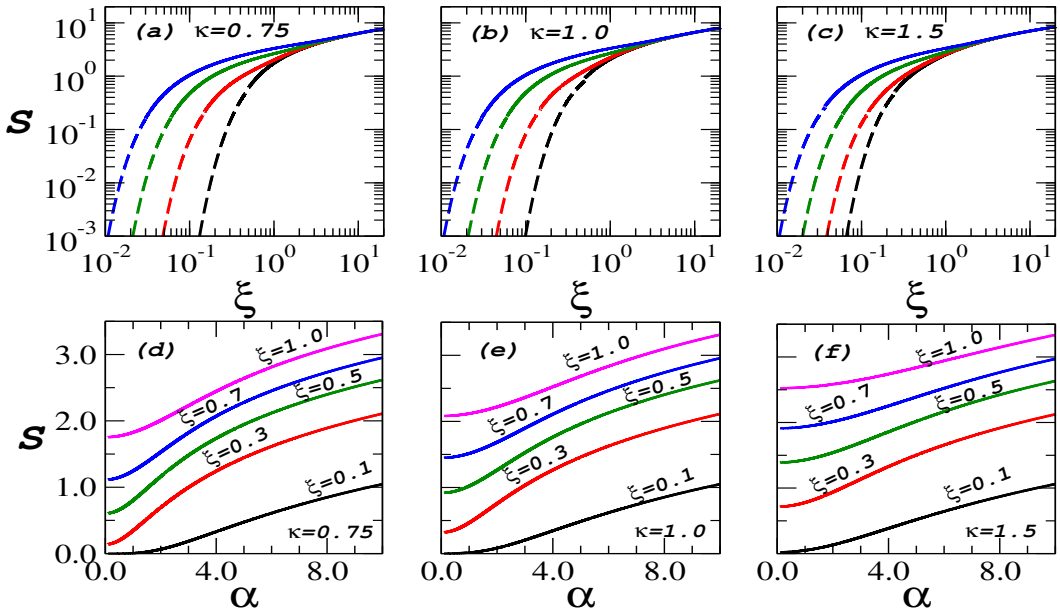

Figure 2.6: The upper panel (a-c) shows the variation of S with ξ for various values of α and κ with $\alpha = 10.0, 5.0, 2.0, 0.1$ (from left to right). The broken lines indicate the temperature range for validity of the low temperature asymptotic behaviour of S. The lower panel shows the α dependence of entropy for specific temperatures and κ.

behaviour of the temperature and magnetic field is noted, and how a change in the kink parameter influences this. The variation of quantities like specific heat and entropy with the kink parameter illustrates the physical effect of the disclination to be a sort of recalibration of the temperature scale. Also of note are the essential non trivialities inherent in the Landau-Fock-Darwin which are recovered here in the presence of the conical defect as is illustrated by the step in the specific heat curve at high magnetic fields, which reflects the interpolation of the behaviour between a 1D and a 2D oscillator.

We conclude by noting that it is possible to extend this analysis to further studies which could incorporate discrete lattice structure and interactions in the presence of this class of topological defects. In the following chapter we shall indeed move to a lattice description of the Landau level problem and study the effects of making the magnetic field a rapidly oscillating function of time. Though no non-trivial geometry is introduced we shall see that the driving suffices to modify the

localization-delocalization behaviour of the electronic wavefunctions from what is usually observed in this system.

Chapter 3

Phase transition in a Aubry-André system with rapidly oscillating magnetic field*

3.1 Introduction

Proceeding from a continuum description of the Landau level problem as a confined 2-D gas of spinless electrons in the previous chapter, we now move to another significant version which incorporates the effects of a discrete square lattice. Appendix A discusses the effects of this choice in great detail as far as the case of rational flux quanta is concerned, where a energy band description is permitted. In the current chapter we shall consider the physics of the system in the presence of irrational flux quanta that give rise to anomalous spectral properties and , of chief interest to us, a metal-insulator transition with a modualtion of the on-site lattice potential in the effective 1-D Aubry-André-Harper form of the Hamiltonian. To see how one goes from a square lattice to this 1-D form in the tight binding, nearest-neigbor approx-

* ***This chapter is adapted from the paper "Phase transition in a Aubry-André system with rapidly oscillating magnetic field" by Mishra, Sashidhara, Guha Sarkar and Bandyopadhyay (2016).***

iamtion one is referred to Appendix A. Here we shall study some aspects of the changes to the metal-insulator transition that are observed on making the irrational flux quantum a high frequency, periodic function of time.

Ever since its proposal by Anderson [26], localization, and transitions between localized and extended states, have been studied in a variety of systems [201]. Extensive analysis has been undertaken to understand various aspects of metal-insulator transitions, localization as well as existence of mobility edges in quasi-periodic or disordered 1D lattices using scaling and renormalization techniques [202–209]. A system which has served as a rich prototype for such studies is the Hamiltonian, originally due to Harper [21], and investigated for phase transitions by Aubry and André [25].

An important feature of the Harper Hamiltonian is the existence of a metal-insulator transition [25] reminiscent of Anderson transition. However, a notable difference is the absence of an energy dependent mobility edge separating the localized and extended states, which is a distinguishing feature of the Anderson transition in 3D. The Aubry-André-Harper (AAH) Hamiltonian exhibits a sharp, duality driven, transition at a unique critical value of the lattice modulation strength for all energies [22–24, 210]. An ensuing trend in recent works has been to develop variations on the model which manifest a Anderson-transition like mobility edge [211–214].

The quest is legitimized further by the substantial progress made by the cold atom community in reproducing complex condensed matter phenomena including Anderson localization [215, 216].

The experimental investigation of localization in 1D systems, especially of the quasiperiodic/incommensurate crystalline variety has witnessed a sustained interest ever since such lattices could be realized using ultra cold atoms,in a bichromatic optical potential, or photonic quasicrystals [216–223]. These studies have ranged from direct experimental demonstration [216, 218, 224–227] to numerical calculations

[219–221] with accompanying proposals for observing the appearance of localized phases and the Metal to Insulator or superfluid to Mott insulator transition (in the presence of interactions). Here, the control on the degree of commensurability has helped to identify the point of transition which, in the AAH model is the self duality induced critical point [223]. The Hofstadter variant and the AAH model in a 2D optical lattice have also been successfully realized [113, 114], in the context of simulating homogeneous magnetic fields in optical lattices. The effects of periodic driving on localization phenomena in 1D disordered systems as a possible means of weakening localization and arriving at extended or non local states has shown encouraging results [228, 229]. Similar pursuits in AAH systems with a view to analyzing diffusive transport behaviour and wavepacket dynamics in the presence of driving, have been promising in terms of appearance of delocalized states [230–232].

The technique of 'shaking' of ultracold atoms in optical lattices has risen to prominence as a flexible means of generating new effective Hamiltonians which may replicate the effects of disorder, curvature, stresses and strains, and several other phenomena as synthetic gauge fields both abelian or non abelian [102, 217, 233, 234]. Some recent studies in driven cold atom setups have looked at induced resonant couplings between localized states thereby making them extended [235] or at localization through incommensurate periodic kicks to an optical lattice [236]. In these models, the phase transition instead of being driven by disorder, is a consequence of deliberate incommensurate periodicity. Demonstration of this behaviour has also been sought in a phase space analysis of the transition [237–239].

However, conspicuous by their absence have been works which look at the AAH model with a rapidly oscillating magnetic field, using the extensive tunability of cold atom setups. The existing study of AAH systems assumes the magnetic field to be static in time. If the magnetic field is periodic, then one may find a perturbative solution in the limit of high frequency driving. We address this neglected aspect by

employing a formalism based on Floquet analysis to obtain an approximate effective time independent Hamiltonian for the system [80, 81, 86–89]. A pertinent enquiry about the effective system would be to look for a metal to insulator phase transition with an energy dependent mobility edge.

In this chapter, we consider a high frequency, sinusoidal effective magnetic field which couples minimally to the AAH Hamiltonian. The effective Hamiltonian is obtained for this system and its localization characteristics are compared with the usual self-dual AAH model in real and Fourier space. An energy dependent mobility edge has already been studied in the context of an AAH Hamiltonian with an exponentially decaying strength of hopping parameters (beyond nearest neighbor coupling) [211–213]. We explore the possibility of a similar mobility edge in our physically motivated effective Hamiltonian with only nearest neighbor hopping. The non self-dual nature of our model is analysed and some general features are investigated.In the section on Discussions, we attempt to reconcile our findings for the specific case with generic features of such non-dual models thereby putting the results in perspective. Finally, we discuss some possible experimental techniques that could be adapted to realize a version of the model presented here. Here, we highlight the difficulties involved in doing so and compare our model to some other driven cold atom AAH models in the literature.

3.2 Formalism

Recent successes in synthesizing tunable, possibly time-dependent, artificial gauge fields for systems of ultra cold neutral atoms in optical lattices [101, 240, 241] has opened a gateway to the strong field regime required for Hofstadter like systems [242]. The system to be studied here may also be realized as an incommensurate superposition of two 1D optical lattices [223], with the laser beams for one of them undergoing a time-dependent frequency modulation. This shall be discussed in detail

later, under Experimental Aspects.

We consider a tight binding Hamiltonian with nearest neighbor coupling that can be expressed as a time dependent Aubry-André-Harper Hamiltonian of the form $H(t) = H_0 + V(t)$, where

$$\begin{aligned} H_0 =& \sum_n |n\rangle\langle n+1| + |n\rangle\langle n-1| \\ V(t) =& V_0 \sum_n \cos[2\pi\alpha_0 n \cos(\omega t) + \theta]\, |n\rangle\langle n|. \end{aligned} \tag{3.1}$$

The summation here runs over all lattice sites. The time-dependent parameter $\alpha(t) = \alpha_0 \cos(\omega t)$ denotes the flux quanta per unit cell. An irrational value of α_0 shall render the on-site potential to be quasi-periodic. The harmonic time dependence of $\alpha(t)$ owes its origin to a time dependent magnetic field $\mathbf{B} = B_0 \cos(\omega t)\hat{\mathbf{z}}$. The other parameter θ is an arbitrary phase. The $|n\rangle$'s are the Wannier states pinned to the lattice sites which are used as the basis for representing the Hamiltonian and V_0 denotes the strength of the on-site potential. The time dependence in the argument of the cosine modulation of the on-site potential is different from usual time dependent AAH models where it is in the overall magnitude of the on-site potential. The periodic time-dependent operator $V(t)$ can be expanded in a Fourier series as

$$V(t) = \widehat{V}_0 + \sum_{1 \le j < \infty} \widehat{V}_j e^{ij\omega t} + \sum_{1 \le j < \infty} \widehat{V}_{-j} e^{-ij\omega t}. \tag{3.2}$$

In order to obtain the effective time independent Hamiltonian one writes the time evolution operator as

$$U(t_i, t_f) = e^{-i\hat{F}(t_f)} e^{-iH_{\text{eff}}(t_f - t_i)} e^{i\hat{F}(t_i)}, \tag{3.3}$$

where, one introduces a time dependent Hermitian operator $\hat{F}$. The idea is to push all the time dependence to the initial and final "kick" terms and render the main

time evolution to be dictated by a time independent Hamiltonian. The systematic formalism yields in the limit of large ω the following perturbative expansion for the effective time independent Hamiltonian given by [80]

$$\begin{aligned} H_{\text{eff}} &= H_0 + \widehat{V}_0 + \frac{1}{\omega}\sum_{j=1}^{\infty}\frac{1}{j}[\widehat{V}_j, \widehat{V}_{-j}] \\ &+ \frac{1}{2\omega^2}\sum_{j=1}^{\infty}\frac{1}{j^2}\left(\left[[\widehat{V}_j, H_0], \widehat{V}_{-j}\right] + h.c.\right) + \mathcal{O}(\omega^{-3}), \end{aligned} \tag{3.4}$$

where, ω^{-1} is the small perturbation parameter, and the series is truncated at $\mathcal{O}(\omega^{-2})$. In order to find the effective approximate Hamiltonian representing our system in the large ω limit, one needs to compute the Fourier coefficients in Eq.(3.2). This is done by using the following commonly valid expansions [243]

$$\begin{aligned} \cos(r\cos x) &= \mathcal{J}_0(r) + 2\sum_{p=1}^{\infty}(-1)^p \mathcal{J}_{2p}(r)\cos(2px) \\ \sin(r\cos x) &= 2\sum_{p=1}^{\infty}(-1)^{p-1}\mathcal{J}_{2p-1}(r)\cos[(2p-1)x], \end{aligned} \tag{3.5}$$

where, $\mathcal{J}_n(r)$'s are Bessel functions of order n. The Fourier coefficients of $V(t)$ may be obtained by inverting Eq.(3.2) using these expansions. We obtain

$$\begin{aligned} \widehat{V}_j &= (-1)^{\frac{j}{2}} V_0 \cos\theta \sum_n \mathcal{J}_j(2\pi\alpha_0 n)\,|n\rangle\langle n|; \quad j = \pm 2, 4, 6... \\ \widehat{V}_j &= (-1)^{\frac{j+1}{2}} V_0 \sin\theta \sum_n \mathcal{J}_j(2\pi\alpha_0 n)\,|n\rangle\langle n|; \quad j = \pm 1, 3, 5... \\ \widehat{V}_0 &= V_0 \cos\theta \sum_n \mathcal{J}_0(2\pi\alpha_0 n)\,|n\rangle\langle n|. \end{aligned} \tag{3.6}$$

We find that $[\widehat{V}_j, \widehat{V}_{-j}] = 0$ owing to the symmetric nature of the Fourier coefficients (for real V). Therefore the $\mathcal{O}(\omega^{-1})$ correction to the effective Hamiltonian vanishes and the first non-trivial correction is at $\mathcal{O}(\omega^{-2})$. The $\mathcal{O}(\omega^{-2})$ term of the effec-

tive Hamiltonian would require the commutator bracket $\left[[\widehat{V}_j, H_0], \widehat{V}_{-j}\right]$, which on evaluation yields

$$\left[[\widehat{V}_j, H_0], \widehat{V}_{-j}\right] = \begin{cases} \sum_n -V_0^2 \cos^2\theta \Big[\Big(\mathcal{J}_j[2\pi\alpha_0(n+1)] - \mathcal{J}_j(2\pi\alpha_0 n)\Big)^2 |n\rangle\langle n+1| \\ \qquad + \Big(\mathcal{J}_j[2\pi\alpha_0(n-1)] - \mathcal{J}_j(2\pi\alpha_0 n)\Big)^2 |n\rangle\langle n-1|\Big] \\ \qquad \text{if } j = \pm 2, 4, 6... \\ \sum_n -V_0^2 \sin^2\theta \Big[\Big(\mathcal{J}_j[2\pi\alpha_0(n+1)] - \mathcal{J}_j(2\pi\alpha_0 n)\Big)^2 |n\rangle\langle n+1| \\ \qquad + \Big(\mathcal{J}_j[2\pi\alpha_0(n-1)] - \mathcal{J}_j(2\pi\alpha_0 n)\Big)^2 |n\rangle\langle n-1|\Big] \\ \qquad \text{if } j = \pm 1, 3, 5... \end{cases} \tag{3.7}$$

Using the above expression in Eq. (3.4) we obtain the effective Hamiltonian, H_{eff}, for our system. We find that up to $\mathcal{O}(\omega^{-2})$, the effective Hamiltonian yields a nearest neighbor tight binding model with a zeroth order Bessel function modulating the site energies, and higher order Bessel functions make their appearance in the hopping terms. There have been works which have looked at inhomogenities in the hopping of the AAH model, arising not from driving but from the choice of next nearest neigbour hoppings in the corresponding 2D quantum hall model[244–247]. However, these models consider situations where the off-diagonal modulations are quasiperiodic through incommensurate modifications of cosine kind of terms. In our case above, the incommensurability is embedded in higher order Bessel functions, thereby variations in hopping strength are far more erratic and with signatures bordering on those of disorder. This is expected to have ramifications for the localization/extended behaviour of the eigenstates. This has been discussed in the next section and illustrated through localization phase plots.

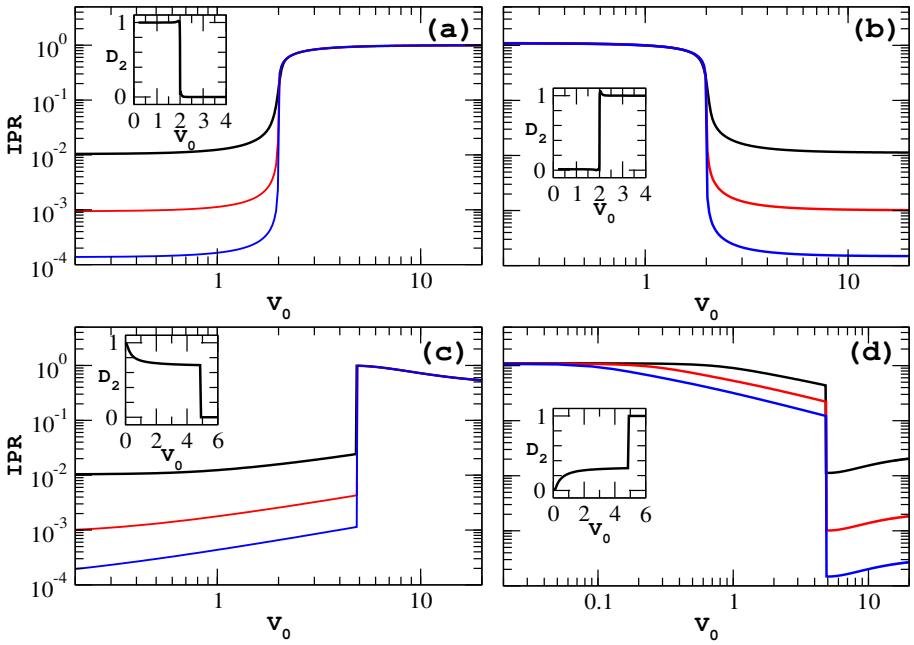

Figure 3.1: (Upper Panel)The metal to insulator transition of the AAH Hamiltonian for the lowest order eigenstate. Plot (a) shows the IPR versus V_0 in real space for $L = 144, 1597$ and 10946 (top to bottom). The inset shows the variation of D_2 with V_0 which also exhibits a transition. Plot (b) exhibits the mirror behaviour in the dual space. (Lower Panel) The transition seen in the IPR versus V_0 curve for the H_{eff}. Plots (c) and (d) are the real and dual space plots for the lowest state with phase $\theta = 0$.

3.3 Results

The simple AAH model has a well studied transition from localized (insulating) to delocalized (metallic) phase which occurs at a critical value $V_0 = 2$. To quantify the localization property we use the inverse participation ratio (IPR) defined as $\text{IPR} = \sum_{n=1}^{L} |a_n|^4 / \left(\sum_{n=1}^{L} |a_n|^2 \right)^2$ where a_n's are the expansion coefficients of the energy eigenstates in a local discrete site basis and L the number of lattice sites [248–250]. The IPR takes a value in the range 1 to $1/L$ with 1 indicating a perfectly localized state and $1/L$ for completely extended states. Figure 3.1(a) shows the transition in the real space IPR for the lowest order eigenstate with choice of irrational α_0 as inverse of the golden mean $(\sqrt{5} - 1)/2$ and $L = 144, 1597$ and 10946 . The inset in this plot indicates variation in the magnitude of the quantity $|D_2|$ with V_0,

where IPR $\propto L^{-D_2}$. For a given V_0, D_2 is obtained by fitting a linear regression line between $\log \mathrm{IPR}$ and $\log L$ and thereby obtaining the slope. The regression fitting is done using several values of L, taken to be large Fibonacci numbers. In all the plots discussed here the transitions depicted are for some finite choice of system size and hence not exactly 'step' changes but ramp up or down over some finite range of V_0 values. Further, the references to such transitions as abrupt or occuring at a critical value have to be interpreted within such numerical constraints. D_2 values shows an abrupt transition from 1 to 0 at the critical value irrespective of lattice size. This establishes the transition to be a integral feature of the model even in the thermodynamic limit of infinite lattice size and the critical point is protected in this limit. In order to switch to states in the Fourier domain, i.e, $|m\rangle$'s from the position space kets $|n\rangle$ we use the transformation

$$|m\rangle = \frac{1}{\sqrt{L}} \sum_n \exp(-i2\pi m\alpha_0 n)|n\rangle. \tag{3.8}$$

This enables one to write the AAH Hamiltonian in Fourier space and compute the IPR in this space. Figure 3.1(b) shows the transition in Fourier space for a set of parameters identical to those in plot (a). Here, again the characteristic transition occurs at the critical point $V_0 = 2$ and the curves in plot (a) are a mirror reflection of the curves in plot (b) about $V_0 = 2$. This is due to the exactly self dual nature of the AAH Hamiltonian. Thus, an extended regime in real space implies a localized one in Fourier space and vice versa. The inset for D_2 in Fourier space accordingly mirrors its real space counterpart.

In the case of our effective model, the IPR for the lowest order eigenstate exhibits a similar trend, as shown in Fig.3.1(c). The transition in this case for this state occurs at a new critical value $V_0 \approx 4.6$, all parameters being kept the same as in former plots. Another distinguishing feature of this transition for the driven case is the manner in which the IPR values approach the critical value and depart from

it, relative to the behaviour in the standard AAH model. In the extended regime, instead of the perfectly flat value of IPR ≈ 0, a slow positive gradient is observed indicating weak localization that progressively gets stronger until a sharp surge occurs at the critical point. Even beyond the transition there is a fall in the IPR due to the still imperfect nature of the localization. This unique behavior can be partially attributed to the non self-dual nature of the effective Hamiltonian which shall be discussed later. D_2, in the inset, continues to retain its scale invariant attributes and manifests the imprint of the transition. The difference, from the simple AAH model, lies in the fall in its value from 1 to a lower plateau before the transition. An indication of the existence of a parameter regime where the state is neither purely localized nor extended but a sort of composite. This is due to the unusual behavior of the wavefunction in the case of α_0 being a Liouville irrational number whereby, for some lattice modulations, no finite localization length may be found over which the state could be said to appreciably decay [22, 210]. Plot (d) which shows the Fourier space IPR for our model exhibits reciprocal behavior of the kind seen in the simple AAH model but with the major difference that plots (c) and (d) are not mirror reflected about the same critical value. This deviation is expected on grounds of the non self dual nature of our system's Hamiltonian. In Fourier space, D_2 analogously is not an exact mirror image of its real space version but all other qualitative characteristics remain the same. There are features in the driven system's Fourier space IPR which stand in contrast from the AAH model, as seen in plots (b) and (d) of Fig.3.1. Most notably, the driven model shows a discrimination between the different lengths as the curves in plot (d) transition from localized to extended regimes at different rates. This is not the case in the ordinary AAH model, where all lengths transition together, as seen in plot (b). This difference is an indicator of non-nearest neighbor couplings in our dual space effective Hamiltonian and the accompanying anomalous behavior of the wavefunctions in a

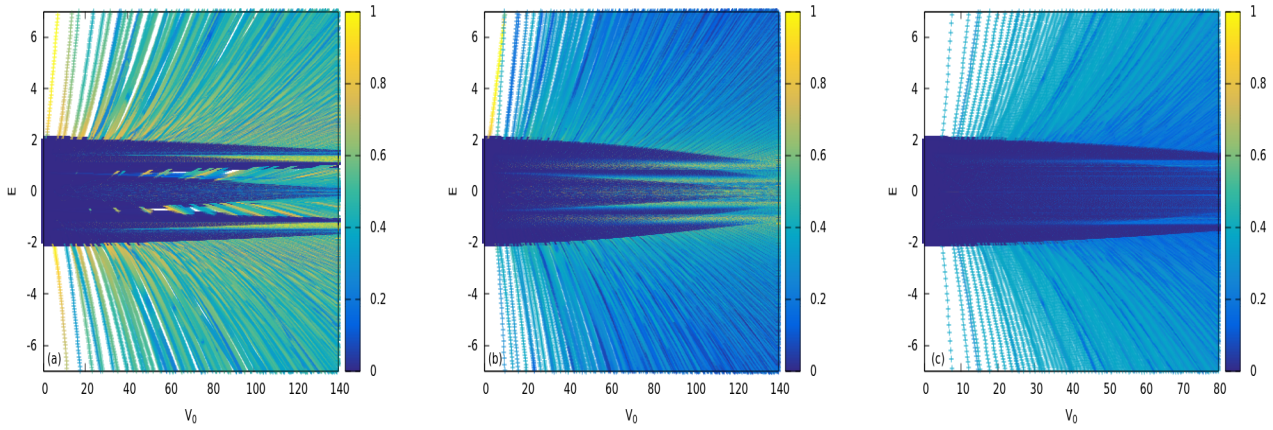

Figure 3.2: The localization phase diagram with IPR in the (E,V_0) phase plane, for lattice size $L = 4181$ three values of the variable θ (a) $\theta = 0$, (b) $\theta = \pi/4$, (c) $\theta = \pi/2$.

certain parameter range.

In order to understand how the properties of the transition are related to the normal modes of the effective driven system, we look at the localization phase diagram, i.e. the variation of IPR with V_0 and the low energy region of the spectrum at each V_0 . Figure 3.2 shows the IPR in the $V_0 - E$ plane. We consider three such plots for values of the phase, $\theta = 0$, $\theta = \pi/4$ and $\theta = \pi/2$ in Eq.(3.1) and lattice size $L = 4181$. The nature of the variation of IPR reveals a sharp energy dependent mobility edge for our model. The portion of the energy spectrum for which the IPR variation has been illustrated is chosen to clearly indicate the appearance of localized states . The choice of values for the phase is intended to isolate and compare the relative effects of the modified onsite term and the site dependent hopping terms. In all three plots the sector corresponding to low V_0 values and near to $E = 0$ shows a dense region of extended states which, (see eq.(3.1)), reflects the bare hopping structure.

The features in the these phase diagrams owe their origin to the relative dominance of different terms the driven effective Hamiltonian for a given θ. The anisotropy of the zero-order Bessel modulated on-site energy adds impurity/disorder like effects

on top of the inherent quasiperiodicity of the model. The fall off of this on-site energy with lattice sites diminishes the actual system size to a reduced one. The modified hopping strengths are also site dependent and vary in an oscillatory manner, with a damping with increasing site index. When the onsite potential damps out, the hopping terms from H_0 survive. This is expected to contribute to an increase in the IPR as the behaviour tends to one of a lattice with disorder. These factors collectively influence the spectral spread and density alongwith the loclalized/delocalized behaviour of the various eigenstates.

Plot 3.2 (a), for $\theta = 0$, depicts the appearance of quasi-localized states (yellow fringes) at the boundaries of the extended (deep blue) region. As V_0 increases, the dense region of extended states near $E = 0$ begins to manifest traces of localization in IPR values, introducing the mobility edges. This can be noted from the bifurcations of the phase boundary that begin to show up in with increasing V_0 with localized eigenstates piercing into portions of the spectrum which at lower V_0 were dominated by extended states. For higher energy the IPR values vary primarily between critical and extended behaviours. This is notably absent in the plots for $\theta = \pi/4$ and $\theta = \pi/2$ where critical behaviour is hardly observed and that too in a very narrow region around the phase boundary. The wider gapping in the eigenvalues as compared to the other two cases can be accorded to the overall stronger influence of the on-site term as compared to the hoppings.

Plot (b), for $\theta = \pi/4$, includes the effects of all the terms of the effective Hamiltonian. The appearance of localized states around $E = 0$ takes place as before. However, there is a notable lack of appearance of well localized states in the higher energy regions as compared to plot (a). This indicates a closer competetion between the on-site and hopping terms of the driven model. The significant localization effects, hence mobility edges, appear distinctly in a band around $E = 0$ and that too at higher V_0. This may be accounted for by the fact that for $\theta = \pi/4$ both the sine

and cosine modulations are present in the modified hopping (see eq.(3.7)), unlike the previous $\theta = 0$ case. Apart from contributing to the predominance of extended states in most of the spectrum, this more influential hopping part also makes the spectrum relatively less gapped.

Plot (c), for $\theta = \pi/2$ has been specifically shown to illustrate how the hopping terms in the driven AAH model behave in the absence of any on-site term. For this choice of θ the $\widehat{V}_0$ in eq.(3.6) goes to zero. As expected in the presence of just the hopping, the IPR values show an extended behaviour everywhere in the phase plot. However, one can still note a phase boundary differentiating the region of the purely extended states from somewhat less extended ones. The appearance and nature of the bifurcations in the boundary of this dense part of the phase plot with changing V_0, indicates the qualitative effects of the inhomogeneities in the hopping terms. Looking at plots (a) (b) and (c) it is clear that the role of the modulated onsite has the effect of enhancing the localization of states as well as creating a sharper mobility edge.

This indicates that the driven model shows a strong sensitivity to the phase θ in terms of the localizaton behaviour and the appearance of mobility edges. The number of these edges, as can be seen, is more for the $\theta = \pi/4$ case and is almost absent in the phase plot for $\theta = \pi/2$. A recent work [251], looks at a topological classification of AAH models with cosine modulated hoppings which differ by a phase factor from the onsite modulation. This helps to realize topologically distinct families of AAH Hamiltonians with the possibility of topological phase transitions between the different classes via a modification of the lattice modulations. Similar behaviour would be interesting to study in our driven context.

3.4 Discussion

In order to qualitatively analyze some of our results we consider a simplified model comprising of a trivial constant hopping term and an on-site potential T which is aperiodic or quasi-periodic. The Schrödinger equation is given by

$$a_{n+1} + a_{n-1} + \Lambda T(\alpha_0 n + \phi) a_n = E a_n \tag{3.9}$$

where, Λ is the strength of on-site energy and E are the energy eigenvalues. One can go to the dual space for the above system by defining an expansion, as follows

$$a_n = \frac{e^{ikn}}{\sqrt{L}} \sum_m \tilde{a}_m e^{i\, m(\alpha_0 n + \phi)} \tag{3.10}$$

where, the $\tilde{a}_m$'s are the dual space amplitudes, and k is a wave vector from the Bloch wave expansion ansatz. This allows T to be expressed as

$$T(\alpha_0 n + \phi) = \frac{1}{\sqrt{L}} \sum_{\acute{m}} \mathcal{T}_{\acute{m}} e^{i\, \acute{m}(\alpha_0 n + \phi)}. \tag{3.11}$$

Equations (3.10) and (3.11) yield an on-site term in the dual space from the the hopping terms of Eq.(3.9) as

$$a_{n-1} + a_{n+1} = \frac{e^{ikn}}{\sqrt{L}} \sum_m \tilde{a}_m e^{i\, m(\alpha_0 n + \phi)} \cos(\alpha_0 m + k) \tag{3.12}$$

with a cosine modulation of the on-site energy (as seen in the Aubry and André model). Interestingly, the real space on-site energy term transforms as

$$\Lambda T(\alpha_0 n + \phi) a_n = \frac{\Lambda e^{ikn}}{L} \sum_{\acute{m}} \sum_m \mathcal{T}_{\acute{m}} \tilde{a}_m e^{i\,(m + \acute{m})(\alpha_0 n + \phi)}. \tag{3.13}$$

The RHS can be slightly rearranged to give

$$\begin{aligned}\frac{\Lambda e^{ikn}}{L}\sum_{\acute{m}\neq\pm1}\sum_{m}\mathcal{T}_{\acute{m}}\tilde{a}_{m+\acute{m}}e^{i\,m(\alpha_0 n+\phi)}+\\ \frac{\Lambda e^{ikn}}{L}\sum_{m}(\mathcal{T}_1\tilde{a}_{m-1}+\mathcal{T}_{-1}\tilde{a}_{m+1})e^{i\,m(\alpha_0 n+\phi)}\end{aligned} \tag{3.14}$$

In the above form, the second term clearly indicates the apparent nearest neighbor hopping terms in the dual space whose strength is modulated by the Fourier components of T. It is the first term in the above expression which explicitly breaks the exact duality. The form of $\mathcal{T}_{\acute{m}}$ determines the extent to which different m values in the dual space are coupled. It is well known that for decaying oscillatory functions like Sinc and Bessel function of the zeroth order $\mathcal{T}_{\acute{m}}$ is a rectangular function, with possibly a $\acute{m}$ dependent modulation, symmetric about the origin. Thus, in our case, we expect a truncation effect in dual space which restricts the range of couplings. This deviation from exact duality is expected to have some impact on the probability of an "analytic accident" along the lines of [25]. The appearance of localized states (real eigenfunctions) happens when there are superpositions of counter-propagating plane waves with wave vectors of near-commensurate magnitude. This would mean, in our model, some harmonics from the expansion of T shall scatter the wave with wave vector k by an amount commensurate with $2n\pi$. This has to be considered together with the fact that for a rational approximation of α_0 as a ratio of two large successive Fibonacci numbers, the true momentum(Fourier) space eigenvalues κ are related to m as $\kappa = mF_{i-1}\mathrm{mod}F_i$, where F_{i-1} and F_i are successive Fibonacci numbers [204, 237]. Thus, what appear to be close neighbors in m could possibly be well separated in the actual wave vector space. Further, the range of m values that shall remain coupled in the dual space will be dictated by the extent of T in the real lattice for example the first zero in the Bessel function. The set of m's which conspires with a given k value to yield a localized state shall be dictated by V_0 and

$E(k)$. This explains the energy dependent mobility edge in Fig.3.2.

In the dual space, where k acts as a phase (see Eq.(3.12)), a state localized at few m values could be shifted by large amounts for a small change in k. This allows for the interpretation that a small change in ϕ could in effect cause a state localized around some lattice site to localize about a far off site. In terms of symmetry, the absence of translational invariance in Euclidean space of quasi-periodic structures with two incommensurate periodicities can be restored in an extended space using the ϕ dimension [252, 253]. This effect of ϕ on localization properties leads to the differences between the three plots in Fig.3.2.

3.5 Experimental Aspects

The experimental realization of our system may be achieved in several different ways, with ease and feasibility of implementation being the guiding criteria in the choice of method. We will explore two options here, from recent literature, which seem more or less promising. One way is to begin with a 2D optical lattice and then proceed in the manner described in some recent realizations of the Harper-Hofstadter Hamiltonian [113, 114]. The notion of simulating a synthetic magnetic field by means of generating effective flux per plaquette of the lattice is a generic feature. However, the true appeal of these methods compared to others for generating artificial magnetic fields for ultracold neutral alkali metal atoms in optical lattices, is the absence of coupling between different hyperfine states of the atoms. It is possible therefore to proceed with a single internal state and far detuned lasers to achieve homogeneous magnetic fields by a laser assisted hopping process. A pair of far detuned Raman lasers is employed, while tunneling in a particular direction is obstructed by means of a gradient/ ramp in the site energies using gravity or magnetic fields, to restore resonant tunneling between sites. The AAH Hamiltonian is obtained in a time independent effective way by averaging over the high frequency

terms and the hopping energy is modified by a complex position dependent phase.

We suggest using Raman lasers of frequencies close to those of the optical lattice, as prescibed by the authors, and to use the tunability of the flux per plaquette α_0 offered by such choice, to set it to an irrational value by adjusting the angle between the Raman beams. Introducing the time dependence is admittedly tricky. This is due to the fact that the static Harper Hamiltonian in the above technique is itself achieved by time averaging and we need it to have a further residual time dependence. For this one would have to vary α_0 periodically by say, modifying the angle between the Raman lasers periodically with time together with simultaneous time modulations of the detunings and the gradients in a fashion that the overall effect is of a periodic change that is of a rate slower than the oscillations to be averaged over while resonant tunneling occurs, but fast enough to remain detuned from the energy gap between the ground and excited bloch bands of the trapped atoms in the lattice potential. This yeilds a time scale which survives the first averaging and gives one a time dependent AAH Hamiltonian effectively being driven by an oscillating magnetic field. There are some obstacles to be overcome here such as arranging the time dependent detunings and the angular variation of the Raman lasers so as to vary α_0 sinusoidally as a function of time effectively, since there is a good chance of getting high frequency noisy components that have to be averaged over. Another issue is that 'the scheme does no realize the simple Landau gauge for a magnetic field'. We use this gauge in our analysis but the results, essentially the nature and existence of the Metal-insualtor transition, are independent of any such choice through the gauge freedom embodied in the choice of θ in the AAH Hamiltonian[25]. The analysis then would be modified only upto a gauge transformation. It would indeed be interesting if the method could be modified to include the Landau gauge.

On account of the multiple time dependent modulations in the realization just

discussed, heating and spontaneous photonic emission processes are a legitimate source of concern. We would like to outline another approach using a quasiperiodic 1D optical lattice which may have better characteristics as regards dissipative processes. Here we suggest using the bichromatic 1D optical lattice realization of the AAH model as described in [223] and suitably modifying it to implement our model. Essentially, a bichromatic optical lattice setup is one with a pair of superposed standing waves wherein one provides the tight binding structure to the Hamiltonian and the other, a weak secondary perturbing potential which, through adjustable non-commensurability of its wavelength with that of the first, offers a quasiperiodic/pseudorandom potential for the ultracold gas of atoms even to the extent of mimicking quasidisorder in the lattice [216]. The two standing waves have wavelengths in the ratio of two consecutive Fibonacci numbers. This helps to realize a workable notion of incommensurability in a finite lattice system by tending the value of the α_0 to near the inverse of the golden mean. As suggested in [223] this is the key requirement for the observation of a transition from extended to localized states i.e. to keep a large number of lattice sites in a single period of the on-site potential for finite systems.

The next step is to systematically introduce the driving. This is done by introducing a time dependence in the ratio of the wavelengths of the two standing wave lattices. More precisely, to do this we suggest generating the two standing waves using beam splitting and retro reflection by mirrors. If now the reflecting mirror corresponding to the primary tight binding lattice is shaken according to a protocol which mimics a sinusoidal drive say, by mounting it on a piezoelectric motor, it should be in principle possible to generate a sinusoidal time dependence in the irrational flux term. It would be preferable to use actuators that move the mirrors so as to produce acceleration effects on the lattice such that one may achieve time dependent Doppler shifts in the frequency and hence wavelengths of the station-

ary waves (where one averages over the fast oscillations in the amplitudes to get the hopping terms) which could be controlled in a sinusoidal fashion. This may be technically demanding under the present capabilities of shaking in optical lattice systems but is definitely worth exploring as a powerful instrument for studying effective Hamiltonians in a new time dependent regime.

In the two approaches highlighted above, the respective works [113] and [223] provide a clear map between the parameters of the simulated model and the experimental parameters such as laser intensities, recoil energies of the trapped neutral atoms and the energy gap between the ground state and lowest excited bloch band in the lattice. This mapping translates readily to the formalism of calculating the effective Hamiltonian. For instance in the case of the bichromatic construction the mapping of the continuous optical potential to a tight binding picture has been carried out in [223] using a set of local Wannier basis states. As per this construction our time dependent model, see eq.(3.1) would have V_0 to be a ratio of product of the height of the weak perturbing lattice with the time dependent ratio of the wavelengths of the two standing waves and an integral term, to the hopping element of the primary optical lattice. The term α_0 is just the ratio of the wavelengths of the two standing waves, made time dependent by shaking, which are two consecutive Fibonacci numbers. From the expressions in eqs. (3.6) and (3.7) it can be readily seen how the experimental parameters enter into the modified on-site and nearest neigbour hopping energy terms of the high frequency effective static Hamiltonian for the driven system.

Thus the relation between parameters of the setup and the derived model Hamiltonian can be traced in a straightforward manner. It is true that this manner of constructing the system will make the strength of the on-site modulation (or its ratio with the hopping energy) also a sinusoidal function of time but this is not expected to alter the system's features studied here in any significant way. We propose

studying this more general form of time dependence, with the strength of the on-site to off site energy also taken to be a function of time alongside the periodicity in α_0, as a future line of work.

Briefly, we would like to survey how our work contrasts with other early and recent work, which has emphasized periodic driving through additional potentials [235] and shaking [217] in AAH systems. In [217], shaking introduces a time dependent phase in the cosine term of the on-site energy. This phase is seperate from the incommensurate position dependence. The effect is a renormalization of the hopping energy so as to make it a function of the driving amplitude. This enables one to tune across the metal-isulator transition by varying the amplitude of the driving. Whereas in our system the driving is provided through an oscillatory effective magnetic field which manifests itself through the periodicity in α_0, hence present in the incommensurate position dependent term.

This is again different from [235] which employs a driving that is a weak space quasiperiodic and time periodic perturbation onto the AAH system modeled as a quasiperiodic optical lattice. Here, the driving is a weak perturbation to the original AAH Hamiltonian. In our case, however, the manner in which the AAH model is driven is non-perturbative by its very nature. An oscillating magnetic field, even of small amplitude, is in no way a weak perturbation and cannot be treated as such, it has to be looked upon in the Floquet picture of periodic time dependent Hamiltonians. The high frequency nature of the driving permits a Floquet theoretic treatment of a slightly analytical variety through the high frequency expansion available for the Floquet Hamiltonian. Only here, in the parameter $1/\omega$, is one allowed to use a perturbative treatment. This is formally different from [235] in that our modifications significantly alter the AAH model for which there is limited analytical footing in the high frequency regime. It would do well to regard the newly obtained static effective Hamiltonian as an independent system in its own right, with features that

are not to be expected in the undriven or weakly driven AAH models. This in fact merits looking into, as it would not be unjustified to anticipate exotic modifications to the traditional AAH Metal Insulator transition under these circumstances.

Also worth noting are the differences between the model in [235] and our system from a reciprocal space point of view. While our model is also non self dual it has an exact 1D structure with couplings that are beyond the nearest neighbour. In [235], the dual Hamiltonian is not exactly 1D and the extended states appear due to resonant couplings of localized states that are driving induced. This differs considerably from the mechanism (discussed in the previous section)that causes localization/delocalization behaviour in our driven system. In fact, the non self duality of our model sets it apart even from undriven variations on the AAH model (with mobility edges) which are self dual by construction [211–214], irrespective of the real space couplings being nearest neighbour or beyond it.

3.6 Conclusion

In this chapter we have studied the Aubry- André-Harper problem with an oscillatory magnetic field in the promising cold atom- optical lattice scenario. The problem is significantly simplified by going into an effective Hamiltonian which approximately represents the system in the limit of high frequency magnetic field. We find that this effective Hamiltonian is non-self dual, and though it exhibits a metal-insulator transition, it differs from the classic Aubry-André model in the emergence of an energy dependent mobility edge. The nearest-neighbor coupling form of the effective Hamiltonian yields this feature which is commonly observed in disordered 3D systems or Aubry-André like models with hoppings extending beyond the nearest neighbor.

The other significant phenomenon besides the onset of a metal-insulator in lattice systems of dimensions less than 3, in the presence of a magnetic field, is the

emergence of quantized values for the Hall conductance and topological properties in the band structure. We shall proceed in the next chapter to consider these features in a protoypical hexagonal lattice system, initially conjectured by Haldane and which has since become plausible given the discovery of Graphene. This system is a well known example of a Chern insulator and has the interesting property that it can exhibit Landau levels in the absence of a magnetic field. We shall see how the application of a periodic kicking scheme modifies the topology in such a system.

Chapter 4

Floquet topological phase transitions in a kicked Haldane-Chern insulator*

Topology and notions intrinsic to it were introduced into the band theory of solids through the work of Thouless, Halperin and others [15–19] while theoretically exploring the remarkable phenomenon of the Integer Quantum Hall Effect (IQHE) [12, 254]. Many such exotic features were predicted and identified for other associated phenomena, which went beyond conventional time-reversal symmetry breaking, such as the Quantum Spin Hall Effect (QSHE), in graphene and other topological materials [68–71].Experimentally, this has sparked off a flurry of activity directed towards the synthesis of materials and nano structures which exhibit such novel features [255–260]. As such shaping the field of 'Topological Insulators'. From a theoretical perspective, the broad objective has been to achieve a comprehensive classification scheme for these insulators [169–171].

Graphene, beyond its much touted mechanical and transport properties [4, 13,

**This chapter is adapted from the pre-print "Floquet topological phase transitions in a kicked Haldane-Chern insulator" by Mishra, Pallaprolu, Guha Sarkar and Bandyopadhyay arXiv: 1709.08354 (2017).*

14], has shown itself to be rich in topological features [67, 72] and various topological aspects of the honeycomb lattice have been investigated in cold-atom and photonic-crystal setups [64, 65, 73–75]. Studies of graphene irradiated or periodically driven by circularly polarized light have revealed rich topological textures beyond those seen in the undriven case [140–149]. An entire sub-domain of "Floquet Topological Insulators"[261] has emerged as a result, which has offered unprecedented control and freedom to engineer new topological phases and edge state(in some cases Majorana modes) behaviors [117–119, 121, 123, 124, 126–139] as well as a knob to study topological phase transitions in cold-atom or photonic crystal setups [150–152, 155–158]. The theoretical classification of Floquet topological insulators and the identification of valid topological invariants that correctly characterize the bulk-edge correspondence for these systems is an on-going effort [172–174, 176–180].

Of late, the use of delta-function kicks has also been shown to impart interesting topological properties in the form of new Floquet topological phases such as semi-metallic phases in Harper models [162], chiral edge modes in Quantum Hall systems [163], appearance of unexpected topological equivalence between spectrally distinct Hamiltonians [164] as well as generation of Majorana end modes in 1-D systems [165]. This has led to interest in studying Dirac systems especially graphene, its nano-ribbons and other hexagonal lattice models such as the Kitaev model under periodic driving or kicking [166, 168, 262]. In this chapter we shall be considering a form of kicking which is found to introduce a Semenoff like mass, hence no topological nontivialities (in the absence of time reversal symmetry breaking) in the spectrum of planar Graphene but, shows some promise as far as manipulating the topology of Haldane-like Chern insulators is concerned.

The recent success in realizing the Haldane model experimentally [65] within the framework of ultracold atoms in optical lattices has opened a doorway to engineering various kinds of Chern insulators, using the paradigm of shaken optical lattices and

the Floquet formalism, and studying topological transitions in them [156, 158, 263]. These realizations offer an appreciable degree of tunability and provide an encouraging platform for the study of Haldane systems under periodic driving. We consider these setups as possible avenues for realizing the kind of delta-kicked Haldane model which is the centrepiece of our study. Beyond the cold atom setups, an interesting recent experiment [149] drives graphene itself using ultrafast, short-duration low frequency laser pulses of circularly polarized light which open local gaps in the Floquet quasienergies of the irradiated graphene. This procedure hints at the creation of local Haldane like band structures but their topological classification has issues that need to be addressed. A more viable candidate for an actual material realization of the Haldane model is presented in [264] where, a honeycomb lattice, specifically Silicene, with out-of-plane staggering of sublattice sites, effectively realizes Haldane's prescription of a staggered magnetic field upon being subjected to an in-plane magnetic field which could be made very weak. Other interesting proposals exist, that realize Chern insulators either using electron correlations at low dimensions, in say double perovskite heterostructures [265], or the notion of in-plane magnetic fields, such as in perovskite monolayers [266] and laterally patterned p-type semiconductor heterostructures with low-symmetry interfaces [267]. The proposal in [264], along with the suggestions in [168] that outline methods to implement a kicking using hexagonal boron nitride over graphene [268–270], provide the broad experimental context in which our system has some hope of being realized. This motivates our academic interest in the study undertaken here.

In this chapter, we begin with an overview of various features of the Haldane model, broadly describing its spectral and topological aspects in Sec.4.1. This is followed by the description and analysis of our choice of a kicked Haldane model in Sec.4.1.2 and a brief introduction to the computation of the Chern topological invariant in Sec.4.2. A detailed exposition of the various properties and behaviour of

the kicked model is provided in the Sec.4.3, on results and discussion. We see that, the kicking scheme incorporates itself into the effective Hamiltonian in a way that it provides a means of manipulating the inversion symmetry breaking parameter of the Haldane model which is essentially the staggered off-set to the on-site energies at the two closest neighboring sites of the two interpenetrating triangular sublattices A and B. This and various other aspects are discussed therein, followed by a conclusion comparing our work to related studies.

4.1 The Kicked Haldane Model

4.1.1 The Undriven Haldane Model

The Haldane model [66] is a perfectly 2-dimensional Quantum Hall insulator with the unique property of exhibiting Quantum Hall behavior in the absence of any net magnetic field through any of its unit cells. It is one of the most elementary realizations of a Chern insulator as its band topology, under certain conditions, can be shown to belong to a non-trivial first Chern class. The way Haldane envisioned it was as a 2-D hexagonal lattice of atoms, much as is the case in Graphene, with a single tight binding orbital at each of the two lattice sites within a unit cell. These are the two distinct sites belonging to the A and B triangular sublattices as shown in Fig. (4.1) by filled and hollow points respectively. Normally, such a lattice shows a semimettalic band structure which is well known from Graphene. However, to realize an insulator, the degeneracies at the Dirac points in the 2-D Brillouin zone need to be lifted by breaking the inversion and time-reversal symmetries in the system. In the Haldane model these are broken to ensure Quantum Hall behaviour. The inversion symmetry is broken by giving an off-set to the on-site energies at the two inequivalent nearest neigbour sites A and B by an amount $-M$ and $+M$ respectively. Breaking inversion symmetry opens a gap at the band touchings in the Brillouin zone and

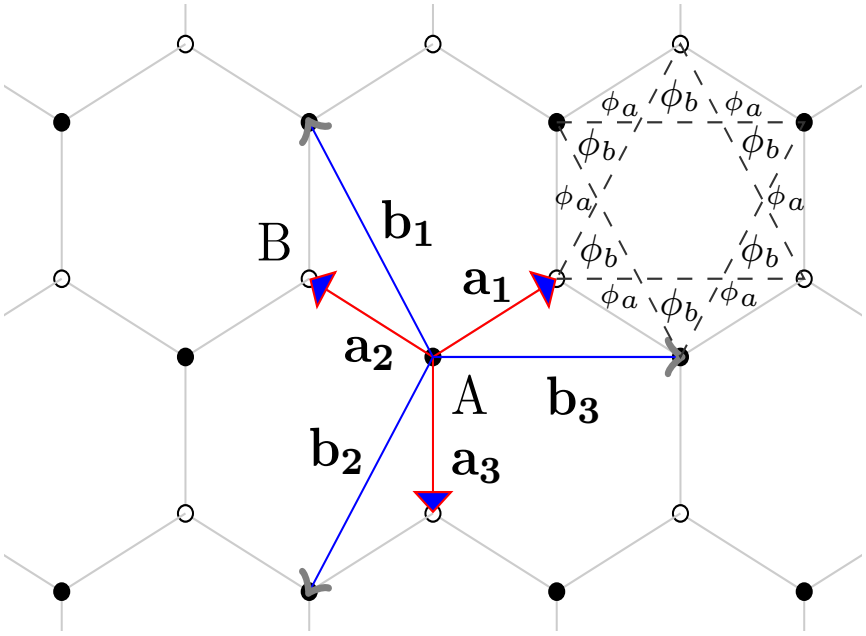

Figure 4.1: Schematic illustrating the honeycomb lattice with vectors to the nearest and next nearest neighbors of an A sublattice site. A flux configuration, where ϕ_a and ϕ_b are fluxes through the triangles that bound each of the labelled regions, is also shown which can make the next to nearest neigbour hoppings phase dependent with zero net flux in the hexagon i.e. $(\phi_a + \phi_b) = 0$.

makes the system a semiconductor/normal insulator. In order to get a topological insulator it is further required to break time-reversal symmetry which is done here by making the hoppings to the next to nearest-neighbor sites complex valued as, $t_2 e^{\pm i\phi}$, t_2 being real. The nearest neigbour hoppings t_1 on the other hand remain real valued. An ingenous choice of magnetic field helps to ensure this by making the overall magnetic flux through any of the hexagons (unit cells) of the lattice zero and hence realizes a globally vanishing magnetic field while at the same time breaking time-reversal symmetry. Though this does require the local existence of a spatially periodic magnetic field everywhere, perpendicularly applied to the lattice plane, following the periodicity of the lattice. Giving rise to a flux arrangement that collectively disappears over a unit cell. One such choice is illustrated in Fig. (4.1), where the condition $(\phi_a + \phi_b) = 0$ fulfills this requirement. Several such choices

are permitted by gauge freedom and since traveling along the sides of any hexagon encloses zero flux the t_1 hoppings acquire no phase contribution. The hopping term t_2 for the next to nearest neigbour sites acquires phases in hops around triangular cells which enclose non-zero flux. For the case in Fig. (4.1) this phase ϕ comes out to be $2\pi(2\phi_a + \phi_b)/\phi_0$ expressed in units of the flux quantum ϕ_0.

The need to break time-reversal invariance arises from the familiar requirement encountered in the IQHE [12, 15, 16, 254] that for the transverse conductance σ_{xy} to show quantized non-zero values time-reversal invariance must be absent in the system as otherwise σ_{xy} is an odd function and amounts to zero. It is the behavior of the gap that opens at the Dirac points also called the mass term from the low energy, (2+1)-D relativistic linearization approximation, that crucially determines the existence of the Hall conductance. In the presence of just broken inversion symmetry this mass term (M) is a Semenoff mass which has the same sign at both Dirac points and yeilds $\sigma_{xy} = 0$ which follows from the definition for the Chern invariant, in this case. However if time reversal invariance is absent the mass term (ϕ dependent) has opposite signs at these points and leads to a non-zero σ_{xy}.When both parameters M and ϕ are zero the bands touch at points in the Brillouin zone called Dirac points owing to the linear dispersion in the vicinity of these degenracies. These are high symmetry points in the Brillouin zone in addition to the band centre. In this situation the system is semi-metallic and allows a two-dimensional representation at these high symmetry points. When the symmetry breaking parameters take on other combinations of values the system is found to belong to insulating regions with the Chern number $\mathcal{C}$, for the valence band (lower band with the Fermi energy in the gap at zero temperature) taking values $\pm 1, 0$ depending on the relative strengths of the two parameters. These regions of different conductance values $\sigma_{xy} = \mathcal{C}e^2/h$ are seperated by a boundary where the gap closes at either one of the Dirac points in the Brillouin zone. These touchings are the transition band configurations where $\mathcal{C}$

's for the two bands can rearrange themselves by assuming values that add up to zero thereby ensuring the standard requirement that the total band bundle remains topologically trivial [17]. These and other properties of the model follow from its Hamiltonian and the linear approximation to it at the band touchings. We now take a closer look at this Hamiltonian which will serve as the target system for the intended driving scheme.

The two dimensional Haldane Hamiltonian in reciprocal space, as obtained from its real space tight binding form is

$$\begin{aligned} H(\mathbf{k}) =& 2\mathbf{I}t_2\cos\phi\sum_i\cos(\mathbf{b_i}\cdot\mathbf{k}) + t_1\left[\sum_i\{\sigma^x\cos(\mathbf{a_i}\cdot\mathbf{k}) + \sigma^y\sin(\mathbf{a_i}\cdot\mathbf{k})\}\right] \\ &+ \sigma^z\left[M - 2t_2\sin(\phi)\sum_i\sin(\mathbf{b_i}\cdot\mathbf{k})\right] \end{aligned} \tag{4.1}$$

Here, the quasi-momentum $\mathbf{k}$ is a good quantum number since the choice of magnetic field preserves the original translation symmetry of the lattice, $\mathbf{I}$ is the 2×2 identity element and σ^x, σ^y and σ^z are the Pauli matrices. From Fig.(4.1) the vectors $\mathbf{a_1} \equiv \left(\frac{\sqrt{3}a}{2}, \frac{a}{2}\right)$, $\mathbf{a_2} \equiv \left(\frac{-\sqrt{3}a}{2}, \frac{a}{2}\right)$ and $\mathbf{a_3} \equiv (0, -1)$ are the vectors from an A sublattice site to the nearest neighboring B sublattice sites. The a stands for the length of the bond joining nearby A and B sites. This choice is a matter of convention here and is defined by these vectors forming a closed right handed system with the cross product of any two in increasing sequence of the indices being aligned out of the plane in the direction of positive $\hat{z}$. While, as seen in the same figure, the vectors to the next nearest neigbour sites are chosen as $\mathbf{b_1} = \mathbf{a_2} - \mathbf{a_3}$, $\mathbf{b_2} = \mathbf{a_3} - \mathbf{a_1}$ and $\mathbf{b_3} = \mathbf{a_1} - \mathbf{a_2}$. Thus the summation index in the above Hamiltonian extends over these three possibilities for both kinds of vectors. The reciprocal space lattice for this system is also hexagonal and therefore first Brillouin zone (FBZ) is a hexagon with band touchings occuring at the zone corners. The FBZ comprises

of two inequivalent band touchings or Dirac points $\mathbf{K}$ and $\mathbf{K'}$. It is possible to rearrange this hexagonal FBZ into an equivalent rhomboidal one by shifting regions of the former by reciprocal lattice vectors. Within this description the Dirac points lie inside the FBZ and are given by $\mathbf{K} = \left(\frac{2\pi}{3\sqrt{3}a}, \frac{2\pi}{3a}\right)$ and $\mathbf{K'} = \left(\frac{4\pi}{3\sqrt{3}a}, 0\right)$. The two band energy dispersion that follows from the above Hamiltonian is

$$E^{\mathrm{H}}_{\pm}(\mathbf{k}) = 2t_2\cos(\phi)\left[2\cos\left(\frac{3ak_y}{2}\right)\cos\left(\frac{\sqrt{3}ak_x}{2}\right) + \cos(\sqrt{3}ak_x)\right] \pm \Bigg\{t_1^2\left[2\cos\left(\frac{ak_y}{2}\right)\right.$$
$$\left.\times\cos\left(\frac{\sqrt{3}ak_x}{2}\right) + \cos(k_y)\right]^2 + t_1^2\left[2\sin\left(\frac{ak_y}{2}\right)\cos\left(\frac{\sqrt{3}ak_x}{2}\right) - \sin(k_y)\right]^2$$
$$+ \left[M - 2t_2\sin(\phi)\times\left(-2\cos\left(\frac{3ak_y}{2}\right)\sin\left(\frac{\sqrt{3}ak_x}{2}\right) + \sin(\sqrt{3}ak_x)\right)\right]^2\Bigg\}^{\frac{1}{2}} \qquad (4.2)$$

On substituting the coordinates for either of the Dirac points $\mathbf{K}$ or $\mathbf{K'}$ in the above expression one gets $M - 3\sqrt{3}t_2\sin(\phi)$ and $M + 3\sqrt{3}t_2\sin(\phi)$ respectively. From this we arrive at the condition for the bands to touch at these points as $M = 3\sqrt{3}\nu t_2\sin(\phi)$ where $\nu = \pm 1$ depending on the particular Dirac point under consideration. Touching at both points occurs only when both inversion and time-reversal are present i.e both M and $t_2\sin(\phi)$ are zero. The touchings at individual Dirac points occur in Haldane's Chern number phase diagram at the transition boundaries where $\mathcal{C}$ undergoes a discrete step in its value.

An important condition included by Haldane in his description of the model is the constraint on the relative strengths of the hopping parameters given by $|t_2/t_1| < 1/3$ that ensures that the bands of the model do not overlap. This is useful for a clear observation of the band touchings in any physical realization of the model as it ensures that the upper and lower bands are always well seperated by a gap unless they touch with the energies at these touchings being extremal points or maximas if one considers the lower band. We will discuss this condition in the context of

kicking later on to see how it gets modified for the kicked system and also ascertain how it may be used to define a magnitude scale for the strength of the driving. Now, we move on to the model of interest in the present chapter which is the Haldane Hamiltonian under kicking.

4.1.2 Driven Haldane Model

The choice of driving the Haldane model using a periodic train of delta function kicks allows an exact Floquet treatment of the stroboscopic kind without recourse to a high frequency approximation of the kind used in [132, 271]. Central to such approaches, and the marked rise of interest in Floquet topological insulators, is the possibility of having a controllable parameter whose variation helps to tune the system from a normal to a topologocal insulator, or through different topological phases. Thus a system may be designed where, by sweeping an experimentally controllable parameter across a prescribed range of values, one could transition the total Chern number of the filled bands of the system between trivial and non-trivial values. Much like the different quantized conductance values assumed by the system in the IQHE when the magnetic field is swept adiabatically. The added advantage driving has to offer here, is that it achieves all this in relatively simpler, non-interacting effective static Hamiltonians. Since, in general, topological charaterisitics are robust features of a system and are unaffected by perturbations to a large extent, having systems which do show transitions from normal to topological insulators (and vice-versa) in a discrete manner is of considerable interest. This is so because interesting properties of the valence band Bloch functions are known to occur at the transitions such as, lack of a maximally localized Wannier representation in the Chern insulating phase and anomalous localization behaviour of the wavefunctions [272, 273]. Thus the transitions merit some attention in various systems where they can be realized in a manner which permits a simpler analytical/numerical approach to their study.

Our kicked model belongs to this category of systems.

Prior to expressing the Hamiltonian in the presence of kicking it would be useful to adopt some notation to denote terms in Eqs. (4.1) and (4.2). The structure of the Hamiltonian in Eq.(4.1) is of the general form $H(\mathbf{k}) = h_0(\mathbf{k})\mathbf{I} + \mathbf{h}(\mathbf{k}) \cdot \boldsymbol{\sigma}$, where $\boldsymbol{\sigma} = (\sigma^x, \sigma^y, \sigma^z)$ is the vector of Pauli matrices and

$$h_0(\mathbf{k}) = 2t_2 \cos(\phi) \left[2\cos\left(\frac{3ak_y}{2}\right) \cos\left(\frac{\sqrt{3}ak_x}{2}\right) + \cos(\sqrt{3}ak_x) \right].$$

The $\mathbf{h}(\mathbf{k})$ here, is the vector $[t_1 L(\mathbf{k}), t_1 F(\mathbf{k}), M - 2t_2 \sin(\phi) N(\mathbf{k})]$ with

$$L(\mathbf{k}) = 2\cos\left(\frac{ak_y}{2}\right) \cos\left(\frac{\sqrt{3}ak_x}{2}\right) + \cos(k_y)$$

$$F(\mathbf{k}) = 2\sin\left(\frac{ak_y}{2}\right) \cos\left(\frac{\sqrt{3}ak_x}{2}\right) - \sin(k_y)$$

$$N(\mathbf{k}) = -2\cos\left(\frac{3ak_y}{2}\right) \sin\left(\frac{\sqrt{3}ak_x}{2}\right) + \sin(\sqrt{3}ak_x)$$

.

It follows that

$$|\mathbf{h}(\mathbf{k})| = \sqrt{t_1^2 L^2(\mathbf{k}) + t_1^2 F^2(\mathbf{k}) + (M - 2t_2 \sin(\phi) N(\mathbf{k}))^2}.$$

The driving scheme is chosen to be a train of delta function kicks which are seperated by fixed time interval T. Such a scheme was introduced in the context of driving a hexagonal lattice, in particular graphene, as a platform for synthesizing novel dispersion relations and wave packet dynamics [168]. Here we propose using a kicking which is applied as the following perturbing term to the Hamiltonian

$$\mathcal{H}_{kick,\mathbf{k}}(t) = (\alpha_x \sigma^x + \alpha_y \sigma^y + \alpha_z \sigma^z) \sum_{m=-\infty}^{m=\infty} \delta(t - mT) \tag{4.3}$$

and represents a general 2×2 kicking protocol with the $SU(2)$ pseudo-spin structure

of the 2-dimensional Haldane Hamiltonian. The α_x, α_y and α_z stand for kicking amplitudes in the respective directions. Since we are consistently expressing the Hamiltonian and the perturbation to it in **k**-space, the kicking is applied uniformly to every unit cell of the lattice to have the reciprocal space representation of the above form. The dynamics of the system over a period T, under such a perturbation, are governed by an evolution operator $U_{XYZ} = U_{kick}U_{static} = e^{-i\boldsymbol{\alpha}.\boldsymbol{\sigma}}e^{-iH(\mathbf{k})T}$ where, $U_{XYZ} = e^{-i\mathcal{H}_{XYZ}(\mathbf{k})T}$ with $\mathcal{H}_{XYZ}(\mathbf{k})$ as the Floquet Hamiltonian and, $\boldsymbol{\alpha}$ and $\boldsymbol{\sigma}$ are $(\alpha_x, \alpha_y, \alpha_z)$ and $(\sigma^x, \sigma^y, \sigma^z)$ respectively. Using the algebra of Pauli matrices and some standard results associated with them, it is possible (as illustrated in [168]) to obtain the exact form of $\mathcal{H}_{XYZ}(\mathbf{k})$. In particular, we are interested in a kicking scheme where $\alpha_z \neq 0$ while $\alpha_x = \alpha_y = 0$ and henceforth assume these parameter values in the perturbing Hamiltonian in eq.(4.3). Thus we are interested in the $\hat{z}$-kicked Haldane model whose Hamiltonian we denote $\mathcal{H}_Z(\mathbf{k})$ which is obtained from $\mathcal{H}_{XYZ}(\mathbf{k})$ by putting in the requisite conditions. The calculation of $\mathcal{H}_{XYZ}(\mathbf{k})$ in the manner outlined in [168] will involve considering only the vector $\mathbf{h}(\mathbf{k})$ projected along the Pauli matrices. The diagonal part due to h_0 remains unmodified and finally shows up in the expression for $\mathcal{H}_Z(\mathbf{k})$ which is again of the structure $h_0(\mathbf{k})\mathbf{I} + \epsilon_z(\mathbf{k})\mathbf{h}'(\mathbf{k}) \cdot \boldsymbol{\sigma}$. The vector $\mathbf{h}'(\mathbf{k})$ is represented by components $(h'_x(\mathbf{k}), h'_y(\mathbf{k}), h'_z(\mathbf{k}))$ which are

$$h'_x(\mathbf{k}) = \frac{1}{\sin(T\epsilon_z)}\left[\frac{-t_1 L(\mathbf{k})}{|\mathbf{h}(\mathbf{k})|}\sin(T|\mathbf{h}(\mathbf{k})|)\cos(\alpha_z) + \mathrm{sgn}(\alpha_z)\frac{t_1 F(\mathbf{k})}{|\mathbf{h}(\mathbf{k})|}\sin(\alpha_z)\sin(T|\mathbf{h}(\mathbf{k})|)\right]$$

$$h'_y(\mathbf{k}) = \frac{1}{\sin(T\epsilon_z)}\left[\frac{-t_1 F(\mathbf{k})}{|\mathbf{h}(\mathbf{k})|}\sin(T|\mathbf{h}(\mathbf{k})|)\cos(\alpha_z) - \mathrm{sgn}(\alpha_z)\frac{t_1 L(\mathbf{k})}{|\mathbf{h}(\mathbf{k})|}\sin(\alpha_z)\sin(T|\mathbf{h}(\mathbf{k})|)\right] \tag{4.4}$$

$$h'_z(\mathbf{k}) = \frac{1}{\sin(T\epsilon_z)}\left[-\mathrm{sgn}(\alpha_z)\sin(\alpha_z)\cos(T|\mathbf{h}(\mathbf{k})|) - \frac{M - 2t_2\sin(\phi)N(\mathbf{k})}{|\mathbf{h}(\mathbf{k})|}\sin(T|\mathbf{h}(\mathbf{k})|)\cos(\alpha_z)\right]$$

The energy eigenvalues of $\mathcal{H}_Z(\mathbf{k})$, i.e the $\hat{z}$-kicked Haldane model, without the offset due to the $h_0(\mathbf{k})\mathbf{I}$ term of the undriven Haldane model, denoted by ϵ_z, is given by

$$\epsilon_z(\mathbf{k}) = \pm\frac{1}{T}\cos^{-1}\left[\cos(\alpha_z)\cos(T|\mathbf{h}(\mathbf{k})|) - \frac{\mathrm{sgn}(\alpha_z)}{|\mathbf{h}(\mathbf{k})|}(M - 2t_2\sin(\phi)N(\mathbf{k}))\sin(\alpha_z)\sin(T|\mathbf{h}(\mathbf{k})|)\right] \tag{4.5}$$

and $\mathrm{sgn}(\alpha_z)$ in both the equations above is the sign of α_z function.

This completes a description of the model Hamiltonian we are interested in. We now give a brief overview of the mathematical formalism that shall be used to compute the topological invariant for this model.

4.2 Computing the Chern Invariant and Hall conductance

The Chern invariant or Chern number for 2-D systems is the topological invariant that captures and quantifies the topological non-trivialities associated with the bands of a periodic system. The general definition involves treating the Bloch functions of the filled bands in any solid as defining a principal fibre bundle over the FBZ which is a torus. The Chern invariant is then calculated for any given band as the integral of the Berry curvature, which may be obtained from the Berry connection defined on this bundle over the FBZ [15, 79, 274]. This integral may be written in the following manner

$$\mathcal{C} = \int_{\mathrm{BZ}} \mathcal{F}_{k_x,k_y}(\mathbf{k})dk_x \wedge dk_y \tag{4.6}$$

where $\mathcal{F}_{k_x,k_y}$ is an antisymmetric tensor denoting a curvature 2-form, the Berry curvature or field. Haldane's work [66] suggests a simplified route to calculating the

Chern number for the various topological phases by an effective linearization of the spectrum at a Dirac point where the gap is like a mass term and coefficient of the σ^z matrix in the linearized Hamiltonian around this point. The total Chern number for the lower band is then given by the signs of the masses at the two inequivalent Dirac points in the FBZ as

$$\mathcal{C} = \frac{1}{2} \sum_{\nu=\pm 1} \nu \ \mathrm{sgn}(m_\nu), \tag{4.7}$$

where m_ν is the mass term at the corresponding Dirac point indexed by ν. Both the expressions are demonstrably equivalent and one can in principle derive eq.(4.7) from eq.(4.6). In our calculations we use both methods to develop the Chern number phase diagram in the presence of driving. The integration is performed numerically to validate the Hall conductivity quantization expected from the second definition.

We intend here to give a brief overview of the mathematical formalism adopted by us to compute the Berry curvature required in the above integral. This formalism is based on the concept of Bargmann invariants, first developed by V Bargmann, and later adapted to calculating differential geometric quantities on fibre bundles by Simon and Mukunda [20, 275, 276]. It essentially involves the use of $U(1)$ invariant pure state density matrices $\rho = |\psi\rangle\langle\psi|$ denote physical states or rays in a complex projective ray space. Then, the Bargmann invariants, are products of these density matrices, $\rho_1\rho_2\cdots\rho_j$ with the j states forming the vertices of a j-sided polygon in ray space. In more explicit terms a Bargmann invariant of order j for a set of as many normalized states $|\psi_j\rangle$ such that $\langle\psi_j|\psi_{j+1}\rangle \neq 0$, is

$$\Omega_j(\psi_1, \cdots, \psi_j) = \langle\psi_1|\psi_2\rangle\langle\psi_2|\psi_3\rangle\cdots\langle\psi_{j-1}|\psi_j\rangle\langle\psi_j|\psi_1\rangle \tag{4.8}$$

The phase of the Bargmann invariant in Eq.(C.2) is obtained as,

$$\mathcal{F}_{\alpha\beta}(\mathbf{x}) = \frac{1}{2i}\mathrm{Tr}(\rho(\mathbf{x})[\partial_\alpha\rho(\mathbf{x}), \partial_\beta\rho(\mathbf{x})]) \tag{4.9}$$

i.e. the Berry curvature. The $\mathbf{x} = (x_1, x_2, \cdots, x_{2N-2})$ denotes coordinates of points in ray space under some suitable parametrization, ray space being $2N-2$-dimensional for an N-level quantum system. In the case of lattice systems and Bloch functions these coordinates are $\mathbf{k}$-space coordinates $(k_x, k_y, \cdots)$. The indices α and βrun over the ray space dimensions. It is interesting to note that one can recover the customary expression for the Berry curvature, over the Brillouin zone, for 2×2 systems with translational invariance of the kind $H(\mathbf{k}) = \boldsymbol{\sigma}.\hat{n}(\mathbf{k})$, which is in general given by $\boldsymbol{\Omega}(\mathbf{k}) = \frac{1}{2|\hat{n}(\mathbf{k})|^3}\hat{n}(\mathbf{k}).[\partial_{k_x}\hat{n}(\mathbf{k}) \times \partial_{k_y}\hat{n}(\mathbf{k})]$ upon making the substitution $\rho(\mathbf{k}) = \frac{1}{2}(1 + \boldsymbol{\sigma}.\hat{n}(\mathbf{k}))$ in Eq.(4.9), $\mathbf{k}$ serving the role of $\mathbf{x}$. This is drawn from a general analogy to the spin-$\frac{1}{2}$ Bloch sphere construction for 2-level systems with Dirac structure. We use Eq.(4.9) with the same analogy for our $\hat{z}$-kicked Haldane Hamiltonian $\mathcal{H}_Z(\mathbf{k})$.

4.3 Results and Discussion

We shall now take up the discussion on (1) the range of driving parameters and their effects on the band structure, (2) effects of periodic kicking on the topological properties of the Haldane model and (3) the modification to Haldane's overlap criterion due to kicking.

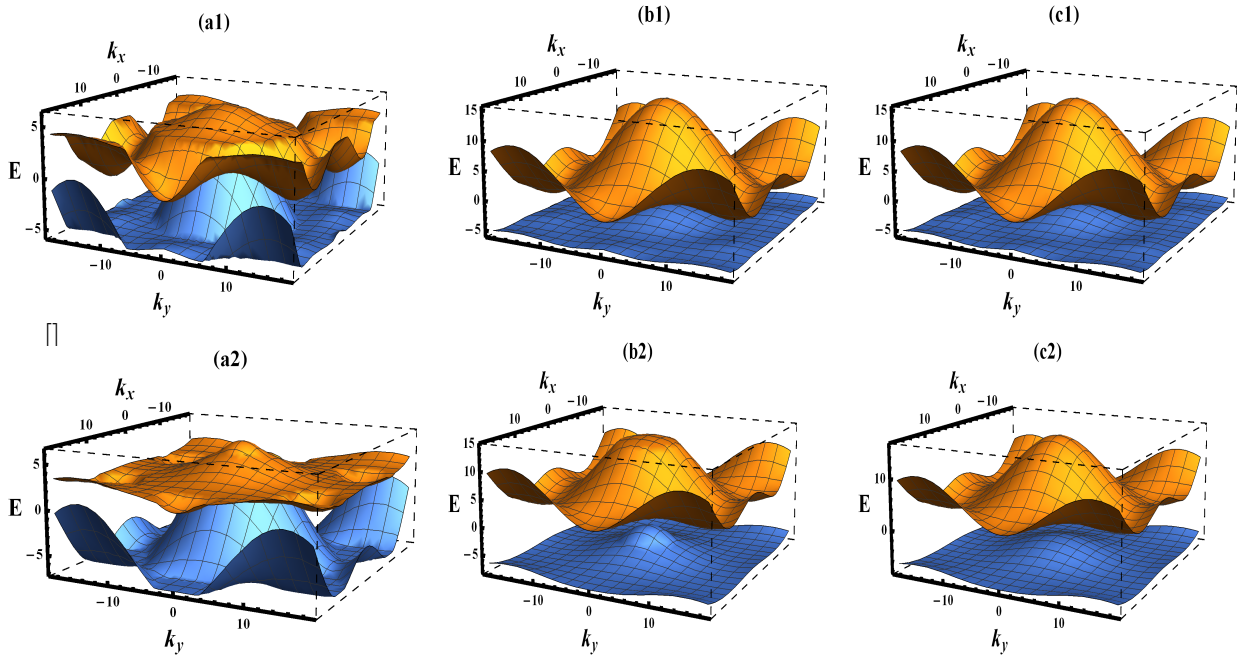

Figure 4.2: The plots of the spectrum, i.e. zero photon sector Floquet bands, for the driven Haldane model as seen for different driving frequencies. We consider a driving period of the form $T = 1/vt_1$ where $v = 0.5, 1$ and 2. The fixed parameters for all plots are $\phi = 0$, $t_1 = 3, t_2 = 1$ and $\alpha_z \approx 0$. Plots (a1) and (a2) are for $v = 0.5$ and $M = 2$ and 4 respectively. In these we note that, for zero driving amplitude, the band structure is very much different from that of the undriven case. At this low frequency the distortions are due to overlaps with Floquet sidebands. Plots (b1) and (b2) are for $v = 1$ and M values 2 and 5 respectively. Here, the choice of frequency works for the lower M value without any higher band interference but for the larger M, sideband overlaps occur. This is seen from the near flat truncation of the conductance band peak and the bump at the centre of the valence band in plot (b2). Plots (c1) and (c2) are for $v = 2$ and M values 2 and 5 respectively. They clearly indicate that this choice of frequency preserves the features of the Haldane spectrum when the driving is taken to zero.

4.3.1 Range of Driving Parameters and Effects on Band structure

The Floquet Hamitlonian we have calculated is obtained stroboscopically in an exact manner. Hence, there is in principle no restriction on the chosen driving frequency. However, there are still bounds as to how low one can go. The behavior of the band structure of the driven model requires this lower limit to be set by the convergence of the spectrum of the driven model to the undriven Haldane spectrum in the limit of $\alpha_z \to 0$ (i.e. taking the driving to zero). We observe that one can go to a driving frequency of the order of energy $\approx t_1$, if the undriven Haldane model, has parameter values $t_2 = 1$ and $t_1 = 3$. This choice of parameters satisfies the overlap prevention requirement.

To put this lower limit in perspective we note when $M = 0$ and $t_2 \sin(\phi) = 0$, the bandwidth of the Haldane model is $\approx 6t_1$ and hence one can work with a frequency up to this order. In this situation neither inversion nor time-reversal are violated and the system allows bands to touch at both Dirac points in the FBZ. The presence of M alters the bandwidth but is of no substantial influence if considered smaller than the nearest neighbor hoppings t_1.

For larger $M > 3.5$, there are overlaps of the ground state Floquet bands with the Floquet sidebands for driving period $\approx 1/t_1$. In this case it is observed that an upper limit to the driving period $T = 1/2t_1$ resolves this issue for all M choices. The issue with larger M s in the $1/t_1$ limit case can be resolved at non-zero driving amplitudes which remove the overlap to the sidebands but this does not hold true when one goes all the way down to zero driving amplitude. Thereby by making $1/2t_1$ the more favourable choice of upper limit for the period. These features are illustrated in Fig.4.2.

So, in a driving scheme based on periodic kicking we are able to free the analysis of the constraint of limiting the driving to high frequencies and instead go to com-

paratively lower values. This feature is absent in the schemes involving continuous drives, such as circularly polarized light, that require the photons of the driving radiation to be of energies larger than the bandwidth [132].

This brings us to the question of how the amplitude of driving influences the features of the driven system. We restrict ourselves to a discussion of how the driving amplitude affects the band structure for a fixed choice of the hopping energies and at some particular choice of M and ϕ. As already mentioned, the driving accentuates the inversion symmetry breaking and the gap that opens in the spectrum increases as the amplitude is increased. There are however effects on the band curvature. It is known that the kicking when applied to graphene leads to flat band structures at driving amplitudes of the magnitude $\alpha_z = \pi/2$ [168]. In the Haldane model one of the crucial differences in the band structure from that of ordinary graphene is the absence of particle hole symmetry due to the next nearest neighbor hoppings governed by t_2. A feature loosely understood in terms of the greater number of B sites than A sites in any finite bounded version of the system. Thus, for this model, when the amplitude of kicking is similarly increased, the band structure does not become completely flat, especially for the valence band. The conduction band does show nearly perfect flatness when the hopping energies are in the ratio satisfying $|t_2/t_1| < 1/3$.

The choice of ϕ here is kept fixed at 0 and M could be non-zero but within the range that shows topological behavior in the undriven case, i.e $[-3\sqrt{3}, 3\sqrt{3}]$. Though one may be cautioned that even in going upto this magnitude of driving the undriven overlap condition begins to break down in favor of a newer one hinted at earlier, but the signatures of flatness can be observed to occur well before this threshold is reached. In going beyond the $\alpha_z = \pm\pi/2$ limit the band structure is found to invert its curvature and as one proceeds to increase the driving to $\alpha_z = \pi$ the conduction and valence exchange their structure from what is seen near zero

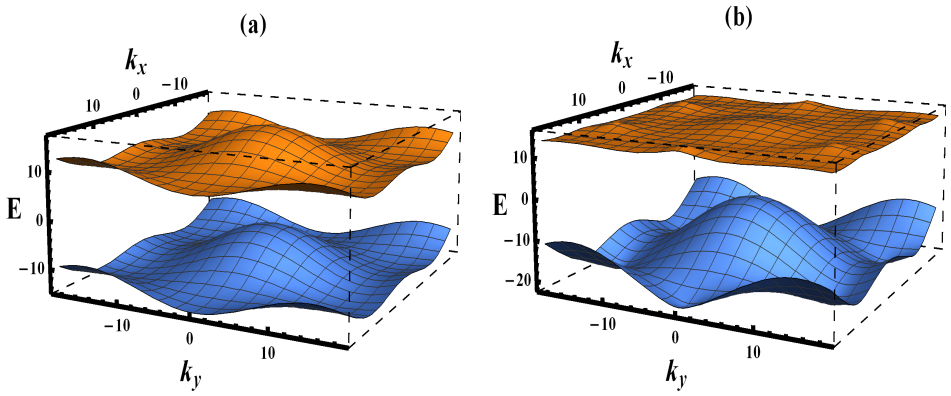

Figure 4.3: These plots indicate the behavior of the Floquet spectrum at relatively large driving amplitudes for the fixed parameters $\phi = 0$, $t_1 = 3$ and $t_2 = 1$. Plot (a) is for $\alpha_z = \pi/2$ and $M = 2$. It shows the appearance of the tendency to flatness in the band structure especially in the conduction band. Changing the M value does affect this behavior but the flatness can be found to occur at a suitable corresponding α_z value. Plot (b) is for $\alpha_z = \pi$ and $M = 0$. We see that the conduction and valence bands have completely exchanged their structures from the undriven case. Important to note that the conduction band now shows almost complete flatness with slight bumps at the Dirac point locations which touch with the minima of the valence band when one accounts for the folding of the Floquet quasienergies. Toplogically this has the effect of exactly exchanging the Chern numbers for the bands from the undriven case. This is discussed in detail in Sec.4.3.2.

driving. The interplay of the magnitude of M and α_z is found to effect the degree of flatness of the bands, especially the conduction band. These features are illustrated in Fig.4.3. We will see that due to the periodicity in the mass term stemming from the nature of the kicking, changing the magnitude of the driving causes the system to undergo transition in and out of topological phases in a periodic manner. In order to observe the full array of non-trivial topological behavior it suffices to work in the driving amplitude range of $\alpha_z \in [-(2n+1)\pi/2, (2n+1)\pi/2]$ and further within this range, the original condition to avoid overlap of bands when touchings occur i.e. $|t_2/t_1| < 1/3$ is valid almost within $\alpha_z \in [-1, 1]$. This range is sufficient to observe the competition between M and the driving in terms of influencing the topological phase, for a fixed choice of hoppings satisfying the above criterion.

However, to maintain sufficient generality in our discussion we will look at topo-

logical behaviour at large driving amplitudes and the new overlap condition that comes into play in these regimes. A point to note here is that though we fix hopping values while discussing the topological properties at large drivings thereby falling out of the criterion to avoid overlap of bands at these large driving amplitudes, this effect may be ignored so far as knowledge of the topological phases is concerned. If one is indeed interested in a realization of the driven model at high amplitude kicking and in observing the band touchings in the spectra an adjustment in the choice of hoppings, especially t_2, is necessary. Speaking in these terms necessarily assumes that one is working with a system where such parameters as the hopping energies and the site energies are free to be controlled and varied, this seems possible only in optical lattice setups where lattice depths and occupation densities of the ultracold atoms can be manipulated.

4.3.2 Topological features of the kicked model

4.3.2.1 Analytical Deductions

We now come to a discussion of the topological properties of the driven Haldane model. Here, we analyze the effects of periodic kicking on the Chern number phase diagram originally obtained by Haldane for the Hamiltonian in eq.(4.1) [66]. After the manner of the analysis presented there, we look at the mass term of our driven model, which is the coefficient of the σ^z matrix in 2D systems, for the various topological phases the system could exhibit. Thus we make use of the definition for obtaining the Chern number $\mathcal{C}$ given in eq.(4.7). To apply this we consider $\epsilon_z(\mathbf{k})h'_z(\mathbf{k})$ from eq.(4.4), which is the coefficient of σ^z in the driven Haldane Hamiltonian. The technique requires one to consider the gap at the Dirac points $\mathbf{K}$ and $\mathbf{K'}$, hence look a the sign of $h'_z(\mathbf{k})$ in the vicinity of these points. On doing so $\mathcal{C}$ is given by the

expression

$$\mathcal{C} = \frac{1}{2}\sum_{\nu=\pm 1} \nu \mathrm{sgn}\left[\frac{\epsilon_z(\mathbf{k})}{\sin(\gamma_\nu)}\Big(-\mathrm{sgn}(\alpha_z)\sin(\alpha_z)\cos(T|M-3\sqrt{3}\nu t_2\sin(\phi)|)\right.$$
$$\left. -\,\mathrm{sgn}(M-3\sqrt{3}\nu t_2\sin(\phi))\sin(T|M-3\sqrt{3}\nu t_2\sin(\phi)|)\cos(\alpha_z)\Big)\right] \quad (4.10)$$

where,

$$\gamma_\nu = \cos^{-1}\Big[\cos(\alpha_z)\cos(T|M-3\sqrt{3}\nu t_2\sin(\phi)|) - \mathrm{sgn}(\alpha_z)\mathrm{sgn}(M-3\sqrt{3}\nu t_2\sin(\phi))$$
$$\times \sin(\alpha_z)\sin(T|M-3\sqrt{3}\nu t_2\sin(\phi)|)\Big] \quad (4.11)$$

The denominator in the above expression for $\mathcal{C}$ goes to zero for certain values of the driving (α_z, T) and the Haldane model parameters (M, ϕ, t_1, t_2). Out of these the hopping parameters will usually be considered to be fixed for a given realization of the model. Here, we are interested in the general conditions that can be deduced from the form of the Chern number and the behavior of the mass term at the Dirac points under various choices of the driving and model parameters.

Thus the condition for the denominator to go to zero, the mass terms to vanish, and hence Berry curvature to diverge at either of the Dirac points, is given by $\gamma_\nu = n\pi$, with $n = 0, \pm 1, 2, 3\ldots$. This essentially reduces to the condition $\cos(|\alpha_z| + T\left(M - 3\sqrt{3}\nu t_2 \sin\phi\right)) = \pm 1$ which implies $|\alpha_z| + T\left(M - 3\sqrt{3}\nu t_2 \sin\phi\right) = n\pi$. The numerator of the expression for $\mathcal{C}$ (see eq.(4.10)), apart from the $\epsilon_z(\mathbf{k})$ term which does not play a role in determining the sign of the term (at the locations for the two Dirac points once one has chosen the valence band for calculating $\mathcal{C}$), go to zero for $\sin(|\alpha_z| + T\left(M - 3\sqrt{3}\nu t_2 \sin\phi\right) = 0$. The appearance of the indeterminate $0/0$ form which seems to occur is regulated in a limiting manner, by the presence of the $\epsilon_z(\mathbf{k})$ in the numerator. Thus what we have obtained is the condition for the bands to touch at either one of the Dirac points depending on the value of ν (± 1)

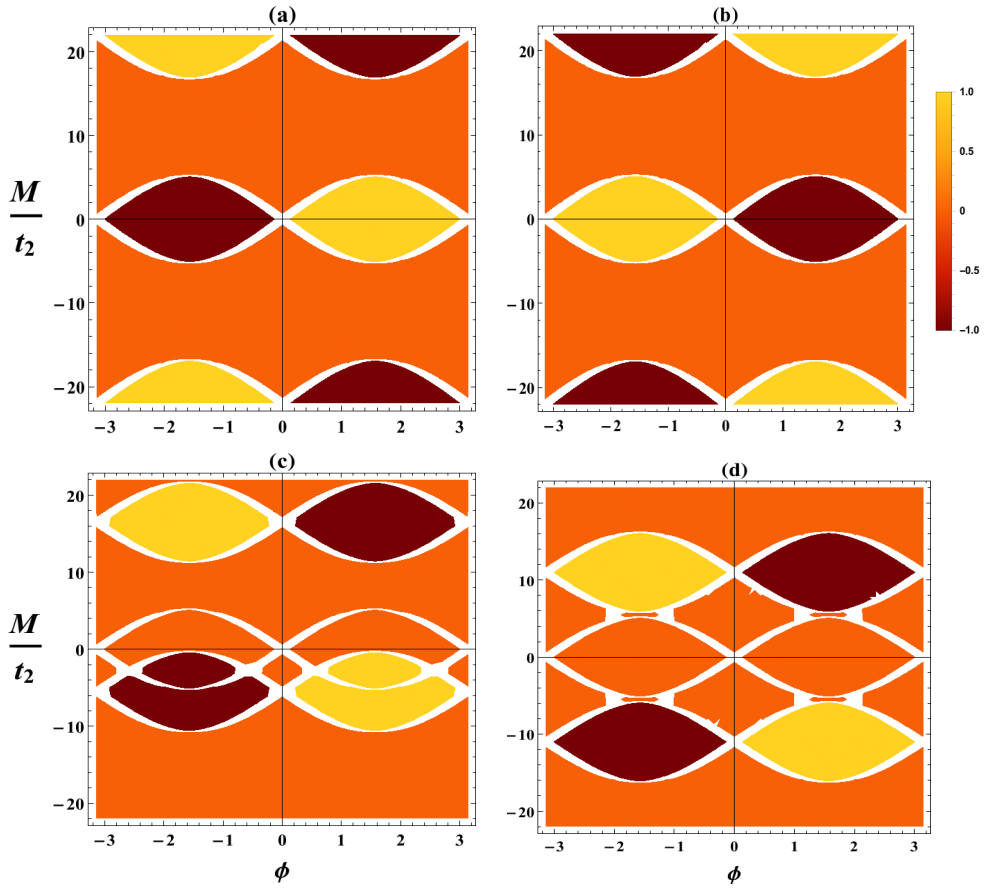

Figure 4.4: Plots of the Chern number in the M/t_2 and ϕ plane for different α_z values. The plots (a),(b),(c) and (d) are for α_z values $0, \pi, \pi/4$ and $\pi/2$ respectively. The darkest regions indicate a Chern number of -1, the lightest ones 1 and the intermediate shade is for 0 Chern numbers. The choice of undriven Haldane model hoppings, for these plots, is fixed at $t_1 = 3.5$ and $t_2 = 1$. The driving period is taken to be $T = \frac{1}{2t_1}$.

in the equation $|\alpha_z| + T\left(M - 3\sqrt{3}\nu t_2 \sin\phi\right) = n\pi$. This is the modified condition for the boundary sinusoids which enclose the topologically non-trivial phases in the case of the Haldane model under kicking.

A couple of features become apparent from this condition. We observe, that the periodic kicking has the effect of modifying the inversion breaking parameter M to $M - \frac{(n\pi - |\alpha_z|)}{T}$ which depends on the driving parameters α_z and T. Thus for different values of n, there is a specific set of values for (M, α_z, T) which would satisfy phase boundary conditions similar to the conditions satisfied by the Chern number in the

Haldane model. In this case we have a periodic recurrence of the phase diagram plotted between M/t_2 and ϕ along the M/t_2 axis, as manifested in repeated copies of the original Chern diagram for the undriven model on moving along this axis. Thus, the broad topological behavior of the undriven model is preserved in the driven model but now extends to newer regions of M values for a fixed choice of t_2. The system under driving begins to explore a larger space of parameters in terms of the occurrence of topological phases. Another feature that comes across is that the new condition for the phase boundaries depends on the magnitude of the driving $|\alpha_z|$ and is independent of its sign. In fact, the modification to the inversion breaking factor is such that it depends on the ratio α_z/T which encapsulates the complete effect of the driving. The appearance of the ratio indicates that the amplitude of the driving can be made to scale with the frequency in a linear fashion to obtain a class of driven models with identical topological behavior. There is even the possibility of choosing the amplitude of the kicking to gradually increase, in a linear fashion with time, on a scale adiabatic in comparison to the driving, so as to be effectively regarded as constant over several driving periods. With this one may realize a linear-in-time variation of the inversion breaking term and hence travel from a topologically non-trivial to a topologically trivial phase. This could be of use in schemes looking to quench Chern insulators across a topological phase boundary with a normal insulator to study various properties of dynamical topological phase transitions at the quantum critical point[277].

The effect of increasing the driving amplitude from zero (in either positive or negative sense), i.e. the undriven situation, is to shift the Haldane Chern number phases (pair of lobes due to the intersecting sinusoidal phase boundaries) vertically downwards, from their undriven position, along the M/t_2 axis. This effect applies to all the periodic copies of the phase diagram along this axis. Let M' be used to denote the new effective inversion breaking parameter in the presence of driving. Thus what

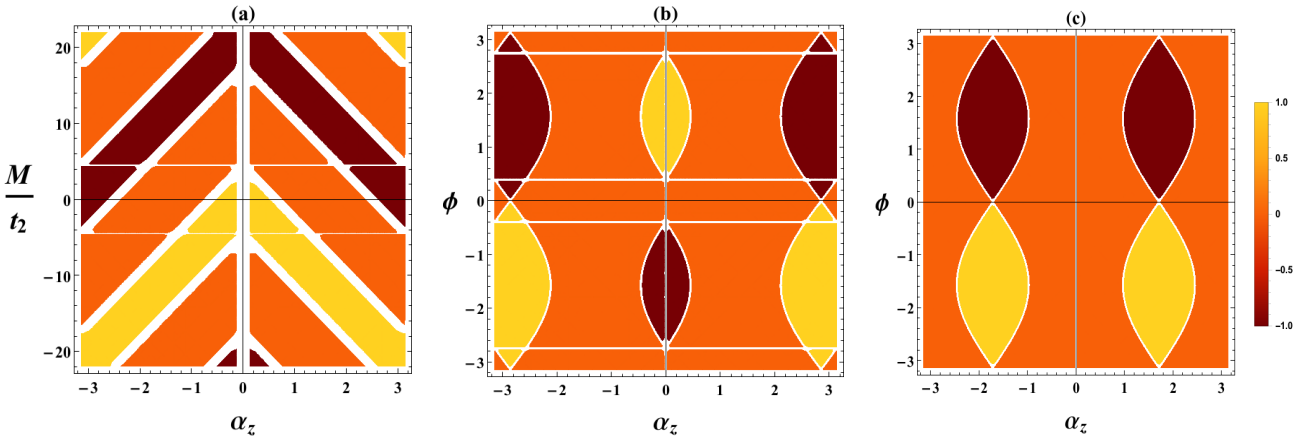

Figure 4.5: Various sectional views that indicate how the topological phase diagram varies with change in driving amplitude keeping one symmetry breaking parameter fixed and varying the other. Plot (a) indicates such variation for a fixed $\phi = \pi/3$ and illustrates the linear variation of the phases for different M/t_2 as α_z is changed. One notes the sharp turn the phases take at $\alpha_z = 0$, a clear consequence of the dependence of the phases on the driving magnitude $|\alpha_z|$. Plots (b) and (c) illustrate phase regions for varying ϕ and α_z, with M/t_2 choices fixed at 2 and 10 respectively. The Chern number convention for the shaded regions is the same as that for Fig.4.4.

we are effectively witnessing is a renormalization of the 'Semenoff mass' component M in the Haldane mass. In the undriven case there was a unique inversion breaking site energy M with the phase diagram center at $(M = 0, \phi = 0)$. This then had corresponded to a graphene like semi-metallic band structure with touchings at both Dirac points. In the driven model this admits multiple values as seen from $M' \equiv M - \frac{(n\pi - |\alpha_z|)}{T}$ and hence multiple semi-metallic centres $M - \frac{(n\pi - |\alpha_z|)}{T} = 0, \phi = 0.$ for the different n and α_z values. The n values define a set of several 'Semenoff Masses' at a give non-zero kicking all of which are valid choices around which topological phases can manifest. There is now a multiplicity of possible undriven Semenoff mass choices M which yield $M' = 0$. The period of driving T, which we fix with a specific t_1, decides the separation between the centres for a given driving. Thus the zero driving case does not collapse to a single M value topological phase structure (the original Haldane model) but still shows a multitude of such phase diagrams which may be regarded as a consequence of the folding or periodicity in Floquet

quasienergies. This hints that the topological phase diagrams repeat identically at a separation of $2\pi/T$ in the M values which is exactly the width of a quasienergy Brillouin zone.

Varying the driving α_z on the other hand, for a fixed choice of n and M, is a more physically plausible and interesting as that would take a chosen undriven model (M, ϕ) through a topological transition.This is very much like quantum Hall plateau transitions with adibatically varying magnetic field. An interesting feature that shows up is that for a given kicking amplitude at M values $\frac{(n\pi - |\alpha_z|)}{T}$, for different n say, 0 and 1 the Chern number phases are reflected about the $\phi = 0$ line in the phase diagram. This is of more significance when one varies the driving amplitude α_z to the relatively high regime of π or $-\pi$. Then the Semenoff mass M' post driving is equal to the undriven one M for $n = 1$ which is clear from the relation. So the Chern number phase diagram with its phases reflected about $\phi = 0$ now occupies the region of the phase diagram where earlier the undriven Haldane Chern number diagram was valid and thus in this extreme driving condition the topological phases undergo an exact inversion. This indicated that even an inversion breaking taken to a certain extreme may alter the band topology of a Chern insulator atleast in the presence of driving. However, physically there are issues with such large kicking amplitudes some of which have been discussed earlier.

Again one has to exercise some caution here, on account of the folding of the quasienergies. There is always the possibility of band touchings which occur at the extreme ends of the spectrum (quasienergy Brillouin zone boundaries), besides the conventional ones at the middle of the spectrum which occur in the undriven and driven cases. This could cause the Chern numbers to invert for the two bands. Indeed, what we see here is that, the inversion in phases is due to these band touchings at the $\pm\pi/T$ limits of the folded spectrum and hence the gap closing at the edges of the quasienergy Brillouin zone. These arguments sit well with the previous

discussion of the appearance of flat band behavior in the conduction band as driving amplitude is increased. As it starts to acquire the curvature characteristics which are present in the valence band in case of zero driving. Thereby an exact reversal of structure occurs between the valence and conduction bands and the Chern numbers flip due to this new closing opening transition. The band structure is shown in Fig. 4.3(b).

4.3.2.2 Evidence from Phase Diagrams

To illustrate the various aspects of the topological phase diagram for the driven Haldane model we refer Fig.(4.4). These figures are for parameter values $t_1 = 3.5$ and $t_2 = 1$ that satisfy the band overlap prevention condition. Again, we caution that variation to this condition in the presence of driving which has been hinted on several earlier occasions and so t_2 has to be changed beyond a certain driving amplitude regime but here this is ignored as the broad topological behavior is unaffected by this. The driving period is fixed at $T = \frac{1}{2t_1}$. This choice, as stated earlier, ensures that the limits of the Floquet quasienergy Brillouin zone remain beyond the bandwidth of the undriven model and thus manifests in the phase diagrams as avoided overlaps between the different replicas of the intersecting sinusoids that are seen one below the other in Fig.(4.4). Other previously discussed features that become apparent include, for instance, one can look at the the plots in Fig.(4.4) (a) and (b) which are for $\alpha_z = 0$ and $\alpha_z = \pi$ respectively and note that when the driving is taken to such extremes the band topology inversion spoken of earlier occurs. Additionally, though α_z is zero for the plot (a) and one does indeed see the undriven Haldane model phase diagram around the $(M = 0, \phi = 0)$ centre, there are still copies of similar non-trivial topological phases along the M/t_2 axis which are absent in the original Haldane model. This indicates that the stroboscopic Floquet Hamiltonian does not converge to the unperturbed Hamiltonian simply by taking the driving amplitude

to zero. One also has to take the limit of the driving period becoming very small and ideally going to zero. It is in this limit that one recovers the undriven model and this is true for the phases in plot (a) of fig.(4.4) as the other topological phase regions will get pushed out to infinity and one obtains Haldane's original phase diagram. An observation that is consistent with the fact that, in the limit of driving frequencies being infinitely large, one is precisely left with the undriven Hamiltonian as the exact description of the system. This is so as the separation between two pairs of intersecting sinusoids that delineate two topological phase regions is decided by the corresponding driving renormalized Semenoff masses and the difference between these masses can be seen to depend on the driving frequency. Thus one can easily see that the effect of varying the driving frequency, say decreasing it in our model, would be to bring the adjacent topological regions, enclosed between their respective pair of sinusoids, nearer to one another. Eventually, for the lower driving frequency limit , of which we have spoken earlier, the Haldane-like topological phase diagram copies are close enough for the sinusoids of adjacent diagrams to just touch each other. Going lower in the frequency would take one into the forbidden limit where these non-trivial regions begin to overlap.

Further, if one looks at plots (c) and (d) of fig.(4.4) we see that at the corresponding driving amplitudes of $\alpha_z = \pi/4$ and $\pi/2$ respectively have the effect of shifting the topological phases away from the parameter regions which were topologically non-trivial in the undriven situation. Thus in plot (c) one can clearly see the new topolgical region shifted with respect to the phase boundary for the undriven model, which is the pair of sinusoids intersecting at the origin in the phase plane. In particular the upper half of the region enclosed between the undriven model's phase boundaries is now topologically trivial. Thus the driving, as it is increased, shifts the phases in a linear fashion. One may consider some choice of undriven model parameters M and ϕ for which the system is in a topological phase and after

a certain magnitude of driving the model enters a topologically trivial phase. Thus the change in the driving amplitude can, as discussed earlier, bring a plateau transition in the Chern number. This effect is more pronounced in plot (d), where, the entire parameter range which was topological in the undriven case is now trivial and hence the driving does offer a path to transition the model between non-zero and zero Chern numbers and is hence a medium to study the normal to Chern insulator transition in such simple non-interacting systems.

Fig.(4.5) illustrates the topological phases of the kicked model when looked at from different cross-sectional views of the solid three dimensional structure that would result if the various phase plots for the α_z values , such as those in fig.(4.4), were stacked in proper sequence, one above the other, along an out of plane α_z axis. In this figure, all the parameter values that need specification to obtain the plots therein, are chosen to be the same as those used for fig.(4.4). Plot (a) in the figure depicts the behaviour of the topological regions for a ϕ value fixed at $\pi/3$ and, M/t_2 and α_z being varied. The linear variation of the phases in this picture reveals the linear shift in the sinusoidal lobes seen in the plots of fig.(4.4), with change in driving. Additionally, the sharp turn in slope, as if a reflection, of these linear phase regions, which are basically tubes with sinusoidal cross-sections, at $\alpha_z = 0$ is indicative of the driving depnedence being purely on the magnitude i.e. $|\alpha_z|$. Once this picture is established it becomes easier to interpret the other two plots (b) and (c), which show the $\phi - \alpha_z$ phase plane for M/t_2 values 2 and 10 respectively. Since a constant M/t_2 can be understood as a plane that slices a kind of Pan flute structure of the tubes of intersecting sinusoids. Thus on the plane one expects to get the projections of the tubes that are cut and this naturally depends on where one chooses to slice. So, where such flutes of different inclination meet, which is at the turning point i.e. $\alpha_z = 0$ or, if one considers the full periodicity, $n\pi$, they form an intersecting sinusoidal edge. If the slice is chosen that it cuts above or below

the exact centre of this ridge i.e. $M \neq 0$ then the projection on the corresponding $\phi - \alpha_z$ plane will have a pair of non-touching sinusoids at the centre. This is what shows up in the middle of plot (b). Of course the slice may be so chosen that it lies outside this intersecting sinusoid edge in which case it will cut the nearest sloping flute tubes and result in a projection with touching sinusoids, as is the case in plot (c). Due to the inherent periodicity in the phase diagram structure, as one goes through a complete period of the M/t_2 choices, the projections begin to show the undelying periodicity.

4.3.3 Modifications to Haldane's overlap criterion due to kicking

This broadly concludes our discussion of the topological features of the kicked Haldane model. We now turn our attention to the issue of avoiding band overlap in the presence of driving, a concern which has been repeatedly expressed at various points in the above discussion under different contexts. The prime consideration is to have the bands touch in a way that the spectrum allows these touchings to be detected without ambiguity. This imposes a relation on the hopping parameters. As the relative magnitude of t_1 and t_2 has the effect of influencing the degree of particle-hole symmetry breaking in the system, and hence, the nature of the touchings. Along lines similar to the arguments for Haldane's criterion we obtain the following condition that needs to be satisfied

$$\begin{aligned} 9t_2 < \cos^{-1}\left[\cos(\alpha_z)\cos\left(T\sqrt{9t_1^2+M^2}\right) - \frac{M\sin(\alpha_z)\sin(T\sqrt{9t_1^2+M^2})}{\sqrt{9t_1^2+M^2}}\right] \\ - \cos^{-1}\left[\cos(\alpha_z)\cos(T|M|) - \mathrm{sgn}(M)\sin(\alpha_z)\sin(T|M|)\right] \end{aligned} \tag{4.12}$$

In the above inequality one notes that a condition is imposed on the suitable values for t_2 once t_1 has been chosen. This is accompanied with the effects of

driving also having a role to play in the determination of this value. Both the driving amplitude α_z and the driving period T appear in the above expression. Since we have already done so in our earlier analysis T can be taken to dependen in an appropriate way on the nearest neigbour hoppings t_1. The M can be written in terms of the driving amplitude using the previously derived expressions for the new Semenoff masses M' depending on which n-th order semi-metallic center one is looking at to observe the band touchings, by putting that particular choice of M' to zero or $n\pi$. Thus the condition can be reduced to depend solely on α_z and t_1. Another feature of this condition is that unlike the ordinary one given by Haldane which has a simpler reciprocal relationship between the two hopping energies, the above relation is not easily invertible to a case where one fixes t_1 and calculates the condition on t_2. In the context of varying α_z for a fixed n in the choice of M' or changing n for fixed α_z the variation in the choice of t_2 will have the effect of altering the boundary sinusoids of the corresponding phase diagrams in the parameter space. Thus if one were to rigorously enforce this condition, which we have ignored for now in the phase diagrams in fig.(4.4) where t_2 is fixed at unity, we would observe a flattening or broadening of the pair of intersecting sinusoids. This follows from the fact that changing t_2 say in the diagram of a given α_z for different M and hence n values would rescale the vertical axis of the diagram. We would like to point out that adjusting t_2 is a freedom available only in certain realizations, as mentioned earlier, hence, if one is interested in driving the system across a topological transition it would be reasonable to do so in the previously suggested range of $\alpha_z \in [-1, 1]$. Since within this domain the ordinary haldane condition is a workable choice and one need not be concerned too much about the effects of driving in this regard.

4.4 Conclusion

We consider a $\hat{z}$-kicked Haldane model and examine the topological properties of this system. The effects of driving on the topological phase diagram of Haldane's originally proposed model are illustrated. We find that, besides introducing a periodicity in the phase diagram where the Haldane phase diagram is repeated at regular intervals along the inversion breaking axis M/t_2, a signature of the periodicity of the Floquet quasienergy spectrum, the driving magnitude is solely responsible for a linear shift in the topological phases of the driven model relative to their undriven counterparts. This suggests the use of this driven model to study Floquet topological phase transitions.

This is different from the optically driven Haldane models of [132, 271] where the tunable parameter toys with the time-reversal symmetry breaking by modifying those terms of the effective Hamiltonian which depend on the phase of the complex valued next-nearest neigbour hoppings of the undriven Haldane model. Although the overall effect is to still traverse between topological and non-topological regions of the Haldane Chern number phase plot as drawn against the symmetry breaking parameters, yet this is brought about in a different manner. To be precise this distinction becomes fully apparent when one considers the effective Hamiltonian post-driving in the vicinity of a Dirac point which of course would be usually gapped in the given case. Also, the driving at sufficiently large amplitudes causes a modification of the band overlap avoidance criterion as originally suggested by Haldane in his model.

Finally, we would like to mention that this kicking scheme could be also applied to the Kane-Mele model for spin orbit coupling in hexagonal lattices [70, 71] to study the effect of driving on the Z_2 topological index which characterizes the topology in such QSHE systems. This is proposed as a future work that we intend to undertake.

Chapter 5

Floquet analysis of pulsed Dirac systems: A way to simulate rippled graphene*

5.1 Introduction

The previous chapter considered modifications to topological aspects of the band structure in the hexagonal lattice of the Haldane model under a periodic kicking scheme. We now proceed to illustrate the use of Floquet engineering techniques to modify the geometry of a hexagonal lattice system such as an optical lattice realization of Graphene. We propose the use of a periodic pulsing sequence that would replicate the physics of a curved or rippled Graphene sheet by introducing curvature as a gauge field in the low energy continuum Dirac equation description of Graphene. The study builds on the established progress in the simulation of condensed matter systems in optical lattices of ultracold atoms.

Quantum systems subjected to high-frequency periodic driving have become a

*This chapter is adapted from the paper "Floquet analysis of pulsed Dirac systems: A way to simulate rippled graphene" by Mishra, Guha Sarkar and Bandyopadhyay (2015).

prominent feature of quantum simulation studies [95, 240]. These studies are mostly aimed at modelling various unique condensed-matter systems [278, 279]. Floquet theory and its applications have been extensively studied [280]. Field induced driving [111], or that generated through mechanical straining, for instance, in graphene [43–47] have demonstrated their ability to create novel gauge structures and modify the energy spectra. Such driving schemes have hence become increasingly popular in cold atom and ion-trap systems as a means of implementing effective potentials that could simulate magnetic fields or spin-orbit couplings [96–103]. The theoretical formalism underlying these driven quantum systems relies on a time dependent forcing that synthesizes an effective approximate time independent Hamiltonian [85–91, 281]. A recent trend in these investigations has been inclined towards looking at a variety of driving schemes to explore potentially interesting Hamiltonians [80].

In much of the last decade two areas have witnessed rapid progress, namely, the physics of graphene with its applications [4] and ultra cold atoms in optical lattices [94]. Interest in the former is driven by the realization of a perfectly flat two-dimensional (2D) system and the unique physics observed in the material due to its relativistic dispersion relation [8, 38, 282]. Optical lattices, on the other hand, has offered an indispensable simulator for realizing many-body condensed matter phenomena and noting their response to a highly controllable variation of system parameters. This has motivated a significant advancement in the efforts to simulate graphene like systems in optical lattice [56–65]. Graphene systems have been studied in the presence of time dependent potentials [283, 284]. Further graphene is noted to show exotic properties, either under mechanical strain, curvature or possessing defects such as dislocations [41–55]. These studies often use a continuum model of Dirac fermions in curved (2+1) dimensions in the limit of low energy excitations. This has also been investigated in the cold atom/optical lattice setup with the objective of studying relativistic electrodynamics in the presence of gravity [285].

The experimental realization of such systems has presented technical difficulties arising from the spin-like and position dependent nature of the nearest-neighbor hopping amplitude in their Fermi-Hubbard Hamiltonian. The essential requirement is the coupling of an artificial non-abelian gauge field to the ultra cold fermionic atoms in the optical lattice (near half-filling) giving rise to the appropriate effective dynamics [104–112].

A key ingredient of all such simulations involves the generation of artificial gauge fields in optical lattices through periodic driving or 'shaking' [101, 102, 115, 116]. We propose the use of a certain driving scheme to obtain an effective curved graphene model in the optical lattice setup. The key distinction of our proposed scheme from similar works [285] is our use of pulse sequences with suitably chosen modulating operators, as described in [80], to generate the effects of smooth driving. This is suggested as an alternate scheme to circumvent difficulties arising from the complicated form of the effective tunneling parameter in conventional treatments. An added advantage of this method is the easy correspondence afforded by it between the continuum and the lattice using a suitable map relating the operators in the two pictures.

In this chapter, we outline a scheme for the generation of an approximate effective Hamiltonian using periodic time dependent forcing on a fermionic 2D optical lattice having the Bloch band topology of flat graphene such that the resulting static effective system mimics the features of a curved background. To compare with the Dirac equation in curved (2+1) dimensional background we consider a metric with a conformally flat spatial part. The Dirac equation in this curved background is cast in a Hamiltonian form to allow easy comparison with the lattice Hamiltonian in the continuum limit. The effects of background curvature are noted. We have found an effective approximate time-independent Hamiltonian which is obtained from a specific high frequency time-periodic driving of the flat space Dirac Hamiltonian. This

effective Hamiltonian is found to be identical to the Dirac Hamiltonian in curved space at the leading order.

We also note the direct correspondence between the nature and the periodicity of the driving to the form and the extent of curvature. The modification of the electronic properties, specifically Local Density of States (LDOS) is studied in low energy regimes near the Fermi points.

5.2 Formalism

5.2.1 Massless Dirac Equation in curved (2+1) D space

We consider the effects of curvature of the background space on the massless Dirac equation. The curved space Dirac Hamiltonian is believed to govern the quasi-particle (i.e., the massless Dirac fermion) dynamics in the continuum limit of the low energy approximation for graphene sheets with curvature. In the subsequent sections, we shall elaborate upon our intent to replicate such systems in the framework of optical lattice simulation.

The Dirac equation in (2+1) dimensional space-time has been studied in various contexts and has a well defined formalism [286–294]. This section provides a brief overview of this as relevant to the problem studied in this chapter. We consider a (2+1) dimensional space-time as the backdrop for our analysis. We choose a space-time metric of the form

$$ds^2 = dt^2 - e^{-2\Lambda(x,y)}(dx^2 + dy^2). \tag{5.1}$$

where t represents the time coordinate, x and y are the spatial isothermal Cartesian coordinates, and $e^{-2\Lambda(x,y)}$ denotes the conformal factor. We note here that the two-dimensional spatial part of this metric diag $(1, -e^{-2\Lambda(x,y)}, -e^{-2\Lambda(x,y)})$ is completely

general in representing two-dimensional curved surfaces. This metric has been used in the context of studying Dirac equation coupled to curved space-time [295] with a distribution of defects, for instance, in the case of corrugated graphene sheets [43–45].

In order to write the curved space Dirac equation we make use of the vielbein or triad formalism in $(2+1)$ D space [296]. This is required to appropriately write special relativistic equations, originally formulated in a flat spacetime, in curved spacetime. The idea is to write all quantities and hence the equations in locally inertial frames i.e Lorentz frames at each point of the curved spacetime manifold. Veilbeins help to transform vectors, tensors and spinors between the local Lorentz coordinates and the global curved spacetime coordinates. The veilbeins $e^a_\nu(x)$ are defined by the way they relate the local flat Mikowskian metric to the global metric of curved spacetime,

$$g_{\mu\nu}(x) = e^a_\mu(x) e^b_\nu(x) \eta_{ab} \tag{5.2}$$

and hence, the vielbein field can be interpreted as the square root of the metric. While going from flat to curved spacetime the general approach involves replacing Lorentz tensors by quantities that transform like tensors under general coordinate transformations, η_{ab} by $g_{\mu\nu}$, and the ordinary derivative by the covariant derivative. For the case of invariance under Lorentz transformations this method suffices with the covariant derivative containing the affine connection, whose components are given by the Christoffel connection coefficients $\Gamma^\alpha_{\nu\mu}$, as an addition to the ordinary derivative. This gives the correct change to a vector under parallel transport over any Riemannian manifold. However the case of invariance under spinorial transformations requires the introduction of the vielbein field and the covariant derivative in this case has what is called as the spin connection term included in its definition. This is required to correctly account for the change in spinors as they are translated in the presence of gravity. In the following paragraphs we illustrate the use of this

formalism for the purpose of writing the curved space Dirac equation.

The Dirac equation in curved space-time takes the form

$$i\gamma^{\mu}(x)(\partial_{\mu} + \Gamma_{\mu}(x))\psi = 0 \tag{5.3}$$

The spin connection term, $\Gamma_{\mu}(x)$, is given by [295]

$$\Gamma_{\mu}(x) = g_{\lambda\alpha}(e^{i}_{\nu,\mu}E^{\alpha}_{i} - \Gamma^{\alpha}_{\nu\mu})s^{\lambda\nu} + a_{\mu}\mathcal{I} \tag{5.4}$$

where e^{i}_{ν} and E^{α}_{i} denote the usual vielbeins and their inverses respectively, $\Gamma^{\alpha}_{\nu\mu}$ are the Christoffel connection coefficients and $s^{\lambda\nu}$ are the generators of spinor transformation in curved space-time. This expression illustrates the indeterminacy of the connection term to upto a constant a_{μ}. Hence Γ_{μ} has an arbitrary trace [295]. This offers a gauge freedom which can be exploited depending on the nature of the problem. We take the standard choice for Γ_{μ} as

$$\Gamma_{\mu}(x) = \frac{1}{2}g_{\lambda\alpha}(e^{i}_{\nu,\mu}E^{\alpha}_{i} - \Gamma^{\alpha}_{\nu\mu})s^{\lambda\nu} \tag{5.5}$$

with,

$$s^{\lambda\nu}(x) = \frac{1}{2}[\gamma^{\lambda}(x), \gamma^{\nu}(x)]. \tag{5.6}$$

The γ matrices with curved space-time indices are related to the usual Dirac matrices in flat space by $\gamma^{\mu}(x) = E^{\mu}_{i}(x)\gamma^{i}$. We choose the following representation using the Pauli matrices for the γ^{i}s

$$\gamma^{0} = \sigma^{z} \quad \gamma^{1} = i\sigma^{y} \quad \gamma^{2} = -i\sigma^{x}. \tag{5.7}$$

In our choice of representation, σ^{z} is diagonal and σ^{y} is complex.

The spin connection components, for our metric [see Eq.(5.1)], are given as

$$\Gamma_1(x) = \frac{i}{2}\frac{\partial\Lambda(x,y)}{\partial y}\sigma^z,\ \Gamma_2(x) = -\frac{i}{2}\frac{\partial\Lambda(x,y)}{\partial x}\sigma^z. \tag{5.8}$$

The massless Dirac equation in curved (2+1) space-time, can hence be written as

$$\begin{aligned}\Bigg[i\sigma^z\frac{\partial}{\partial t} - e^{\Lambda(x,y)}\left(\sigma^y\frac{\partial}{\partial x} - \sigma^x\frac{\partial}{\partial y}\right)\\ + \frac{e^{\Lambda(x,y)}}{2}\left(\frac{\partial\Lambda(x,y)}{\partial y}\sigma^x - \frac{\partial\Lambda(x,y)}{\partial x}\sigma^y\right)\Bigg]\psi = 0,\end{aligned} \tag{5.9}$$

where we have used eqns. (5.3) and (5.5). This equation can be recast in an explicitly Hamiltonian form by breaking the manifestly covariant form as

$$i\frac{\partial\psi}{\partial t} = e^{\Lambda(x,y)}\left[-i\sigma^j\partial_j - \frac{i}{2}\left(\frac{\partial\Lambda(x,y)}{\partial y}\sigma^y + \frac{\partial\Lambda(x,y)}{\partial x}\sigma^x\right)\right]\psi. \tag{5.10}$$

The entire operator acting on ψ in the RHS of the above equation may be interpreted as the Dirac Hamiltonian in curved space. This Hamiltonian is required to be synthesized using the driven optical lattice. As will be shown later it is possible to formulate a driving scheme which does exactly this. In the following section we discuss a procedure for obtaining an effective time-independent Hamiltonian for periodically driven systems. This shall find appropriate implementation in optical lattices.

5.2.2 Periodic Pulsing and Effective Hamiltonians

In the study of quantum systems having periodic time dependent Hamiltonians [90, 91], a special category is devoted to the class of systems where the system is subjected to high frequency periodic forcing [85]. The theoretical treatment of such systems has its roots in the study of similar classical systems [83, 84]. The literature suggests various routes to arrive at an effective time-independent Hamiltonian [86–

89]. The traditional practice of using the Cambell-Baker-Hausdorff (CBH) expansion or Trotter expansion to study Floquet systems has certain inherent defects [87, 281]. A recent approach [80], inspired by [87], forms the basis of our formalism. It uses the idea of engineering effective Hamiltonians by applying carefully selected periodic driving schemes to quantum systems, geared towards generating desired effective static systems.

To start with, we consider a time-periodic Hamiltonian $H(t)$ that can be written as

$$H(t) = H_0 + V(t), \tag{5.11}$$

where H_0 is time independent and $V(t)$ is the periodic time dependent part such that $V(t+T) = V(t)$. The periodic time-dependent operator $V(t)$ can be expanded in a Fourier series as

$$V(t) = \widehat{V}_0 + \sum_{1\leq n<\infty} \widehat{V}_n e^{in\omega t} + \sum_{1\leq n<\infty} \widehat{V}_{-n} e^{-in\omega t}. \tag{5.12}$$

In order to obtain the effective time independent Hamiltonian one writes the time evolution operator as

$$U(t_i, t_f) = e^{-i\widehat{F}(t_f)} e^{-iH_{\text{eff}}(t_f - t_i)} e^{i\widehat{F}(t_i)}, \tag{5.13}$$

where, one introduces a time dependent Hermitian operator $\widehat{F}$. The idea is to push all the time dependence to the initial and final "kick" terms and render the main time evolution to be dictated by a time independent Hamiltonian. The systematic formalism (see appendix) yields the following expression for the effective Hamilto-

nian [80]

$$H_{\text{eff}} = H_0 + \widehat{V}_0 + \frac{1}{\omega}\sum_{n=1}^{\infty}\frac{1}{n}[\widehat{V}_n, \widehat{V}_{-n}] + \frac{1}{2\omega^2}\sum_{n=1}^{\infty}\frac{1}{n^2}\left(\left[[\widehat{V}_n, H_0], \widehat{V}_{-n}\right] + h.c.\right) + \mathcal{O}(\omega^{-3}). \tag{5.14}$$

The correction terms that appear in the effective Hamiltonian depend on the commutator of the Fourier coefficients $\widehat{V}_n$ with each other and with the unperturbed Hamiltonian H_0. It is worth noting, that, for potentials which have time-reversal symmetry ($V(t) = V(-t)$) Eq. (5.12) imposes restrictions on the coefficients so that the commutator $[\widehat{V}_n, \widehat{V}_{-n}]$ vanishes. For such potentials the leading order correction is $\mathcal{O}(\omega^{-2})$. The appearance of the $\mathcal{O}(\omega^{-1})$ term with a non-zero coefficient is a feature of potentials with dependence on momentum operators in addition to position and time. Time reversal symmetry is broken in these cases. Several possible choices for such potentials are worked out in [80]. Our choice of driving potential, discussed in the latter portion of this chapter, falls into this category. This serves as a helpful reminder of the occasional deviations from the intuitively expected $\mathcal{O}(\omega^{-2})$ leading order correction in the effective Hamiltonian, which is expected for potentials with time reversal symmetry.

We shall now focus on a specific kind of forcing potential. The driving potential $V(t)$ shall be considered to be a sequence of pulses that repeat periodically. The choice of the number of phases in a given pulse sequence dictates the form of the effective Hamiltonian. This offers a wide variety of possibilities up to a given order ω^{-1} in the perturbation expansion.

Let us consider a general N-phase pulse sequence, with period T, of the form

$$V(t) = \sum_{r=1}^{N} f_r(t) V_r \tag{5.15}$$

where f_r denotes a square profile such that

$$f_r(t) = \begin{cases} 1, & (r-1)T/N \leq t \leq rT/N, \\ 0, & \text{elsewhere.} \end{cases} \tag{5.16}$$

Here, V_r are arbitrary operators that are free to be chosen as per ones requirement. Each phase lasts for a duration of T/N. We also impose the condition $\sum_{r=1}^{N} V_r = 0$.

The time-dependent Hamiltonian for such a choice of driving is then

$$H(t) = H_0 + \sum_{r=1}^{N} f_r(t) V_r. \tag{5.17}$$

Using the Fourier series expansion this can be written as

$$H(t) = H_0 + \sum_{n \neq 0} \widehat{V}_n e^{in\omega t}, \tag{5.18}$$

where

$$\widehat{V}_n = \frac{1}{2\pi i} \sum_{r=1}^{N} \frac{1}{n} e^{-2\pi i n r/N} (e^{2\pi i n/N} - 1) V_r. \tag{5.19}$$

It is possible to use Eq.(5.14) at this stage to obtain a generic expression for the time-independent effective Hamiltonian for the kind of driving given in Eq. (5.15) (refer Eq. (30) in [80]).

Given the flexibility of choosing the number of phases and also the modulating operators, a wide variety of effective Hamiltonians can be generated. The next section deals with one such choice that enables us to design the required gauge field to simulate the physics of curved graphene in optical lattices. The usefulness of such a pulsing scheme is demonstrated by showing its equivalence to an optical lattice shaken/modulated by a smooth driving.

The modulation scheme used in standard optical lattices does not consist of such pulsing and instead uses smooth driving. The effective Hamiltonian obtained for

smoothly modulated optical lattices carries an imprint of the modulation frequency through the renormalized hopping term (which is a function of ω). On Taylor expanding the hopping parameter as a series in ω^{-1}, this effective Hamiltonian matches with the one obtained by a pulsing scheme at the leading orders [80].

5.2.3 Simulating rippled graphene: Optical Lattice Scheme

As mentioned previously, the use of fermionic optical lattices to simulate Dirac cones and massless Dirac fermions is well established. In such a system the application of a time-dependent sinusoidal modulation can be used to obtain novel gauge effects in an artificial time-averaged manner. The possibility of doing this using the method discussed in the previous section is elaborated here.

Among the wide range of choices that do exist, our problem lends itself rather neatly to a 4-phase pulse sequence with modulation of the Hamiltonian given by

$$\mathcal{P}_4 : \{H_0 + A, H_0 + B, H_0 - A, H_0 - B\} \tag{5.20}$$

This compares to Eq.(5.15) for $N = 4$ with $V_1 = -V_3 = A$ and $V_2 = -V_4 = B$, where A and B are suitable operators. As discussed in the last section, this is equivalent to a smooth driving of the form

$$V(t) = A\cos(\omega t) + B\sin(\omega t). \tag{5.21}$$

This choice of the time-dependent potential yields the following effective Hamiltonian [80]

$$\begin{aligned} H_{\text{eff}} = H_0 + \frac{i}{2\omega}[A, B] + \\ \frac{1}{4\omega^2}\left([[A, H_0], A] + [[B, H_0], B]\right) + \mathcal{O}(1/\omega^3) \end{aligned} \tag{5.22}$$

It is significant in our context to note that the expression for H_{eff} has both first order and second order terms in ω with the appropriate commutator brackets. The freedom in the choice of A and B allows us to engineer the desired effective Hamiltonian.

The periodic driving scheme has a small parameter ω^{-1}, the time-period of forcing. It is our contention that it is possible to use the formalism of generating effective approximate Hamiltonians, through a choice of suitable operators A and B as mentioned in Eq.(5.20), to reproduce a Dirac Hamiltonian in curved space. This would involve choosing an appropriate pulsing scheme.

We note that the low energy limit of a continuum approximation of graphene, as simulated in the lattice, has the Hamiltonian of the form [4]

$$H_{\mathrm{G}} = -iv_F\sigma^j\partial_j \tag{5.23}$$

in units of $\hbar$, where v_F is the Fermi velocity and $\partial_j = (\partial_x, \partial_y)$ is the gradient operator in 2-dimensions. We shall subsequently work in units where $v_F = 1$. This motivates us to consider the primary Hamiltonian in our analysis as $-i\sigma^j\partial_j$. The discussion here solely employs the continuum formalism for the operators and the mapping to the second quantized forms for the operators and the Hamiltonians are only introduced later in the section on results and discussion.

Let us consider a driving scheme with $H_0 = -i\sigma^j\partial_j$, the Dirac Hamiltonian in flat space and choose the operators A and B of the form

$$A = \sigma^j\alpha_j \qquad B = \sigma^k\beta_k \tag{5.24}$$

where, $\alpha_j = [i\partial_y, -i\partial_x, 0]$ and $\beta_k = [0, 0, -f(x, y)]$. With this choice, Eq.(5.22)

yields an approximate effective Hamiltonian H_{eff} up to order ω^{-1} given by

$$\begin{aligned} H_{\text{eff}} = \frac{1}{2}\left[-i\left(1+\frac{f(x,y)}{\omega}\right)\sigma^j\partial_j\right] \\ -\frac{1}{2}\left[i\sigma^j\partial_j\left(1+\frac{f(x,y)}{\omega}\right)\right] \end{aligned} \tag{5.25}$$

For large ω this is a good approximation. The term of $\mathcal{O}(\omega^{-2})$ is significantly suppressed and manifests as non-trivial couplings and maybe ignored for our present analysis. With a substitution

$$e^{\Lambda(x,y)} = \left(1+\frac{f(x,y)}{\omega}\right)$$

we have

$$H_{\text{eff}} = \frac{1}{2}[-ie^{\Lambda(x,y)}\sigma^j\partial_j - i\sigma^j\partial_j\ e^{\Lambda(x,y)}] \tag{5.26}$$

such that the entire expression is in terms of $\Lambda(x,y)$ instead of $f(x,y)$. The Hamiltonian in Eq.(5.26) can be further simplified and explicitly written as follows

$$H_{\text{eff}} = e^{\Lambda(x,y)}\left[-i\sigma^j\partial_j - \frac{i}{2}\left(\frac{\partial\Lambda(x,y)}{\partial y}\sigma^y + \frac{\partial\Lambda(x,y)}{\partial x}\sigma^x\right)\right] \tag{5.27}$$

We seek to map this effective time-independent Hamiltonian that is obtained from the original time-dependent Hamiltonian to the Dirac Hamiltonian in curved space. The function $\Lambda(x,y)$ appearing here is expected to be mapped to the metric in some fashion in the equivalent curved space description.

Comparing Eq.(5.27) and Eq.(5.10) we establish the correspondence between the periodically driven effective system and a curved space description. The function $\Lambda(x,y)$ that depends on the periodic driving scheme is now seen to appear in the conformal factor of the metric in the curved space picture. A quantity of geometrical

interest describing 2D curved surface is the Gauss curvature $K(x, y)$ given by

$$K(x, y) = e^{2\Lambda}\nabla^2(\Lambda) \tag{5.28}$$

This scalar function has complete information about the curved 2-D surface. Since $\Lambda = \ln\left(1 + \frac{f(x,y)}{\omega}\right)$ depends on the driving scheme f and driving frequency ω, the curvature shall depend on these directly. It is hence possible to reproduce the effects of curvature ($K \neq 0$) by suitably manipulating the driving scheme. This completes the mapping between the two equivalent pictures.

In order to confirm that our model suitably mimics the properties of curved graphene, it is required that some physical quantity associated with it be computed and obtained experimentally. We regard the Local density of states (LDOS) to be a suitable candidate. In the following we briefly recapitulate its significance and prescribe a method for determining it theoretically.

The LDOS is a quantity of interest in the study of electronic and transport properties of various condensed matter systems. It offers information regarding the spatial variation in the density of states over a region, arising out of local disturbances, that can be verified experimentally using scanning tunneling microscopy (STM) techniques. It is therefore a physically relevant parameter for our study. Our analysis suggests that the electronic properties for a periodically driven graphene like optical lattice system, describable by a Dirac Hamiltonian, shall be the same as one expects for the same system in a curved background without any periodic forcing. To compute the LDOS [297] one first needs to calculate the Green's function for the system, for the case of non-interacting electrons, as follows.

$$G(z, \mathbf{r}, \mathbf{r}') = \sum_n \frac{\psi_n(\mathbf{r})\psi_n^*(\mathbf{r}')}{(z - E_n)} \tag{5.29}$$

where, z denotes a complex energy variable, ψ_n are energy eigenstates in coordinate

representation, E_n represents the energy eigenspectrum and the sum ranges over the n eigenvalues of energy. The expression for the LDOS is given as

$$\rho(\epsilon, \mathbf{r}) = -\frac{1}{\pi} Im \sum_n \frac{|\psi(\mathbf{r})|^2}{(\epsilon + i\delta - E_n)} \tag{5.30}$$

which may be written as

$$\text{LDOS} = \rho(\epsilon, \mathbf{r}) = -\frac{1}{\pi} Im[G(\epsilon + i\delta, \mathbf{r}, \mathbf{r}')] \tag{5.31}$$

We shall compute the LDOS numerically using the spectrum of the Hamiltonian in Eq. (5.27) and compare it with the flat space case where $\Lambda = 0$.

5.3 Results and Discussion

The study of alterations to the electronic properties of graphene sheets as a result of deformation, curvature, defects or impurities focuses chiefly on the modifications to the LDOS or the appearance of a gap at the Fermi points [46, 48, 49, 282, 298–303]. These works discuss the possibility of opening a band gap in graphene at the Dirac point, which is known to be topologically protected by inversion and time reversal symmetries [66, 76, 77]. The presence of perturbations that respects these discrete symmetries can only move the Fermi points but not create a gap [78]. A hybridization of the Fermi points with opposite topological charge (winding number) allows a subsequent opening of gap [304].

In our present analysis we attempt to examine the effect on the LDOS for graphene-like optical lattice under a periodic driving. The approach has similar motivations to earlier studies on LDOS in rippled graphene [48, 49]. The principal difference being that our system does not involve taking a graphene sheet with any curvature or defects but imparting curved-graphene properties to an optical lattice

via pulsing. The choice of the driving scheme function $f(x, y)$ that maps to the conformal factor in the metric is taken as

$$f(x, y) = x^2 + y^2. \tag{5.32}$$

This choice of the driving scheme is used to compute the curvature according to Eq. (5.28) and yields a constant Gaussian curvature $K(x, y) = \frac{4}{\omega}$. Thus the curvature turns out to be inversely proportional to the driving frequency ω. Hence, with our high frequency driving scheme (high frequency is a necessary condition required for the convergence of the perturbation series in Eq.(B.55)(see Appendix B, section B.4.2.1) we are able to model a small positive constant curvature.

The deep significance behind the similarity between the Dirac Hamiltonian in curved space and the effective time independent Hamiltonian needs to be addressed. This can be understood by acknowledging that the effects of both curvature and driving find expression through the unifying formalism of effective gauge fields. In the case of a rippled graphene sheet [48, 49, 51–54] it has been well established that the effect of curvature manifests in the curved space Dirac equation through an artificial magnetic vector potential giving rise to a pseudo- magnetic field. This is a reinterpretation of the contribution coming from the spin connection and the curved space gamma matrices, which characterize the changes to the ordinary flat space derivatives (giving the correct form of the covariant derivatives in curved space). The modification gets carried over into the lattice picture through a phase factor that modulates the hopping term (Peierls phase). This is the usual way to couple a gauge field to a tight binding Hamiltonian.

It is also a matter of fact that periodic driving can indeed replicate gauge structures [80]. A landmark approach [101] maybe used to simulate complex valued hopping parameters with a tunable value for the Peierls phase in the effective time independent lattice Hamiltonian. Thus a scheme for simulating a vector poten-

tial that amounts to a finite pseudo-magnetic flux through a 2D lattice is available. Mathematically, the slow part of the eigen states of the Floquet Hamiltonian $-i\hbar\frac{\partial}{\partial t} + H$ are the object of study in the time independent picture. The use of a unitary gauge transformation $e^{iF(t)}$ (see appendix B Sec.B.4.2.1) to map the states of the system to a projective space where the evolution of the system is governed by a time independent H_{eff}, essentially involves a transformation of the time evolution operator in a manner similar to the transformation of the momentum operator (i.e. the operator for translation) in the presence of a minimally coupled gauge field. The equation Eq.(B.54), in appendix B Sec.B.4.2.1, is very similar to a gauge transformation. Thus, from a differential geometric point of view, the periodic driving defines its own connection due to which arises a holonomy in the line bundle over the projective space of rays of the Hilbert space [305]. In this manner a gauge invariant time dependent phase appears as corrections to the quasi-energies of the system over time periods large compared to that of the high frequency periodic driving.

It is possible to write down the operators A and B of the driving in the conventional second quantized notation. To do so we adopt a convention in which the fermionic optical lattice Hamiltonian reads

$$H_0 = J\sum_{\langle k,j\rangle} \Psi^\dagger_{k+1,j}\sigma^x\Psi_{k,j} + \Psi^\dagger_{k,j+1}\sigma^y\Psi_{k,j} - h.c. + H_{\text{on-site}} \tag{5.33}$$

where, J is the plain hopping parameter, a the lattice spacing, $\Psi^\dagger_{k,j} = (\hat{a}^\dagger_{k,j}, \hat{b}^\dagger_{k,j})$ creates a particle at the site (ka, ja) in some spin state. The operators $\hat{a}_{k,j}$ and $\hat{b}_{k,j}$ stand for the two triangular sub-lattices of the optical lattice. The operators A and B in this convention, for the choice of $f(x, y)$ in Eq. (5.32), becomes

$$\begin{aligned} A &= -\frac{i}{2a}\sum_{\langle k,j\rangle} \Psi^\dagger_{k,j+1}\sigma^x\Psi_{k,j} - \Psi^\dagger_{k+1,j}\sigma^y\Psi_{k,j} - h.c. \\ B &= -\sigma^z\frac{a^2}{2}\sum_{\langle k,j\rangle} k^2\Psi^\dagger_{k+1,j}\sigma^x\Psi_{k,j} + j^2\Psi^\dagger_{k,j+1}\sigma^y\Psi_{k,j} + h.c. \end{aligned} \tag{5.34}$$

In the above expressions, we make use of the following map between continuum operators and those on the lattice as [80]

$$\begin{aligned} -i\sigma^x\partial_x &\equiv \frac{i}{2a}\sum_{\langle k,j\rangle}\Psi^\dagger_{k+1,j}\sigma^y\Psi_{k,j} - h.c. \\ -i\sigma^y\partial_y &\equiv \frac{i}{2a}\sum_{\langle k,j\rangle}\Psi^\dagger_{k,j+1}\sigma^x\Psi_{k,j} - h.c. \end{aligned} \tag{5.35}$$

and

$$x^2 + y^2 \equiv \frac{a^2}{2}\sum_{\langle k,j\rangle} k^2\Psi^\dagger_{k+1,j}\sigma^x\Psi_{k,j} + j^2\Psi^\dagger_{k,j+1}\sigma^y\Psi_{k,j} + h.c. \tag{5.36}$$

The mapping between the continuum operators and their lattice counterparts enables the actual possibility of simulation of the Hamiltonian on the lattice.

The issue of experimentally realizing the system as described above is contingent on successful implementation of the lattice operators A and B, followed by a design of the driving which would ultimately yield the desired effective Hamiltonian in the time independent approximation. This has to be approached in an incremental fashion. The operators A and B are themselves constructed from operators for position and momentum in a 2D, fermionic optical lattice. Experimental realization of these operators uses pulsed directional hoppings i.e. time dependent modulation of tunneling [96] by varying the laser intensity in a certain direction. However, in our case the 2×2 character of the Hamiltonian is also to be accounted for. This requires a periodic drive capable of imparting such features.

A scheme, recently suggested, in an effort to simulate spin-orbit coupling (SOC) through periodically driving a tight-binding lattice of neutral ultra-cold atoms [306] may enable this. This uses a spin-dependent periodic driving force, achieved through a time periodic magnetic field coupled to opposite spin states, to generate complex valued tunneling parameters. There is an additional radio frequency coupling between adjacent spin states. The cumulative effect when viewed from the perspective

of a time independent effective Hamiltonian is that of an optical lattice with a spin-dependent renormalization of the hopping term. This technique is accompanied with the added advantage of generating a site dependent phase associated with the terms of the Hamiltonian which are associated with tunneling between adjacent sites (this being an essential feature of our Hamiltonian). It must be noted here that this work [306] deals with a 1D lattice, whereas we require the scheme to be adapted for the 2D case.

The procedure, upto this point, manages to realize the operators A and B in a time averaged manner. In order to further set up our curved space Hamiltonian we have to resort to alternating between the two operators in the manner of the 4-phase pulse sequence discussed in Sec. 5.2.3. Thus another layer of time averaging will be required to arrive at our desired Hamiltonian. The pulsing may be devised such that during the phase when A is supposed to act we use a combination of laser tuned tunneling and radio frequency tuning and for B just the SOC modelling technique be used. The need to work with multiple time scales is apparent here and one is required to average through these to get at the desired Hamiltonian over a prolonged duration. The issues related to cooling and the spontaneous emission of photons are claimed to be partially overcome in the SOC modelling technique discussed above as compared to near-resonant Raman laser coupling schemes. However, periodic driving does create excitations in the system which may lead to spontaneous emission. This is influenced by the driving frequency, lattice modulation and interactions between particles (see references in [306]). The experimental viability of sustaining multiple time scales in the system to obtain the desired dynamics over a reasonable duration of time without undue heating and excitations has to be further looked into and is beyond the scope of the study in this chapter.

It also remains to be seen how the approach suggested above compares with the purely spatial techniques elaborated in [285]. One of these is to use the magnetic

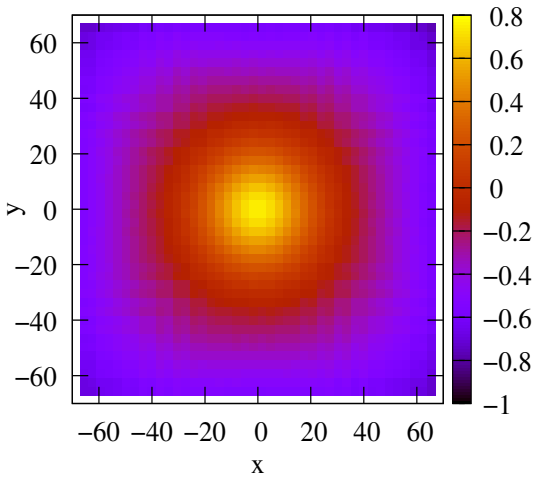

Figure 5.1: Correction to the LDOS given by $\frac{\rho}{\rho_o} - 1$ with ρ being the LDOS for pulsed graphene and ρ_o that for ordinary graphene.

field induced Zeeman splitting of the hyperfine levels and design the system as a bichromatic spin-independent super-lattice. The fermi gas of atoms used can be made to populate various sublevels and transition between them via laser induced tunneling. The spatially dependent nature of the tunneling is ensured by making the Raman laser detunings hence Zeeman splittings spatially dependent. This method however, besides its inherent technical complexity, has to contend with issues of stability and the lifetime of atomic excitations owing to spontaneous emission of photons. An alternative method, also put forward in the same work, considers using the waist spread of laser beams to generate tunneling terms. Here the variation of the laser intensity over the dimensions of the lattice created spatially dependent hopping terms. The drawback of this method is the restriction to only a Gaussian variation of the tunneling operators and no control over this feature can be exerted. This significantly limits the freedom of realizing various metrics for the curved space Hamiltonian.

We investigate the nature of the LDOS for the Hamiltonian in Eq. (5.27) and look for the imprint of spatial curvature in its behavior. The LDOS computations are performed for the choice of the driving scheme given in Eq. (5.32). The expressions

in Eq. (5.29) and Eq. (5.31) are evaluated numerically to estimate the LDOS. The Fig. C.1 shows the modification to the LDOS for our system over that of normal graphene in flat space. The figure shows the quantity $(\rho/\rho_0) - 1$ plotted in the color contour map against the spatial coordinates x and y. As seen in the figure, a large positive correction is centered at the reference origin indicating maximum increase in the number of available states per unit energy. This is a clear indication that electronic properties are significantly altered in our system. An 80% correction is observed at the maxima for our choice of driving frequency which yields a ω^{-1} of ~ 0.01. We note that a similar behavior of the LDOS has also been observed in the study of graphene in curved space with positive curvature [51–54].

5.4 Conclusion

We conclude by noting that the use of periodic forcing to generate the effects of curved space on 2D quantum systems has a far reaching influence in theoretical studies and technological applications. The traditional Floquet analysis of periodically driven systems uses the CBH/Trotter expansion to find the effective static Hamiltonians. We use an alternative perturbative formulation using a pulsed driving scheme and find an effective approximate Hamiltonian. We show that the driving scheme can be chosen to simulate tunable geometric properties of curved space. The massless Dirac equation and Hamiltonian in curved space, that model electronic behavior in curved graphene, are derived for a conformal metric. The same is shown to be obtained in a periodically driven fermionic optical lattice having chosen the appropriate modulating operators. We go on to analyze the geometrical and physical features of the system, namely, the Gauss curvature and LDOS. These are computed for a particular choice of metric and deviations from the unperturbed system are noted. This opens up the possibility of synthesis of new systems in quantum simulators and the study of their physical properties.

Appendix A

The Aubry-André-Harper Model

A.1 Introduction

The physical model essentially comprises of spin-less non-relativistic electrons, free to move on a 2-dimensional square lattice under a tight-binding approximation with a spatially uniform magnetic field applied perpendicular to the lattice plane. In a way it may be regarded as the continuum Landau level problem, of electrons in a plane subjected to a perpendicular constant magnetic field, formulated on a lattice. This is an old classic problem with a rich history, dating back to the very beginings of quantum mechanics. The Peierls-Onsager substitution and the introduction of the effective Hamiltonian [21, 307–310] for Bloch electrons in a magnetic field were some of the initial proposals towards its solution. However, for the longest time the problem has eluded capture in a complete analytical picture [311–316]. Though, substantial progress has been made in making it more amenable to numerical approaches [242, 317], the accuracy and validity of the Peierls substitution and consequent calculations of the diamagnetism of strongly bound electrons on the lattice have been questioned time and again [312, 318–321]. Nonetheless, the Peierls substitution has been proven to be remarkably resilient and has given a profound insight in situations where a single-band approximation is valid and no field-induced

inter-band transitions occur. Interest in the model intensified when it was found to harbour certain remarkable and unexpected phenomena of a subtle nature. These include predominantly, the experimental discovery of the QHE [12] and the theoretical prediction of a metal-insulator transition [25]. Such fascinating features of this innocuous looking system are underpinned by anomalous properties of its spectrum which, as a function of the magnetic field strength, shows an intricate butterfly-like fractal structure in certain field regimes [242, 315]. An explanation for the metal-insulator transition may be obtained from the spectral features of the system at certain field values, however, the quantized values of the Hall conductance are more profoundly encoded in non-trivial topological aspects of the band structure.

The key parameter in the system, as shall be discussed in detail later in this appendix, is the flux of the magnetic field through an individual plaquette of the square lattice, in units of the flux quantum, denoted by α. The interesting behaviour of the spectrum shows up at high values of the magnetic field, of the order of thousands of tesla. The nature of the dependence of α on the field B and the lattice constant a (order of angstroms) necessitates this for a reasonable range of its values, say α approaching unity. The structure of α may be interpreted, according to Hofstadter [242], as a ratio of two inherent scales or periodicities of the system. These are, the period associated with an electron in a Bloch state of wavevector $2\pi\hbar/a$ and the period of a cyclotron orbit due to the field i.e. eB/mc, where m is the electron's mass and e its charge. It would be instructive to regard these as competing energy scales in the system, which in the case of length scales is prescribed by the lattice constant a and the magnetic length $l_B = \sqrt{c\hbar/eB}$ appearing in the Landau level problem, under the applied magnetic field. This bears hints of the recursive, nested butterfly fractal that results when one looks at the energy eigenvalues as a function of α, since a trade-off between length scales is a signature of fractals. In a heuristic manner one may try to understand this as a sort of truce between the

solutions of two distinct problems, both vying to be the principal candidate for the ground state solution of the problem. They are, the Bloch waves for the electron in a periodic potential and the Landau levels for electrons in a plane with a magnetic field perpendicularly applied. Nature resolves the dilemma by weaving these two solutions together in an infinite hierarchy of level-splittings where both the band structure and the Landau levels have their degeneracies lifted to yeild the complex structure that one sees. Even the wavefunctions are versatile in that they show the full gamut of extended (Bloch-wave like), localized (cyclotron-orbit) or critical (multifractal) behaviour depending on the nature of α and the ratio of the on-site to hopping energies of the square lattice.

These aspects make the problem an inevitably complex one and to approach it on some firm analytical footing requires one to consider it in either one of two opposite asymptotic limits. At one end is the strong potential limit where the lattice periodic potential dominates. This limit justifies the tight-binding approximation and one proceeds to construct a set of generalized wavefunctions satisfying the Bloch conditions in the presence of the field. These wavefunctions are derived, as we shall see, by defining a group of operators that commute with the Hamiltonian in the presence of the magnetic field, called the magnetic translation operators. A more general approach however, is based on the use of a basis of site-localized atomic-orbital like functions to expand the state of the system. The electronic band structure of the 'zero field' case is now observed to split into finer subbands in the presence of relatively weak magnetic fields . The other extreme is the strong field regime where the periodic potential is treated as a weak perturbation to the harmonic-oscillator like Landau levels of almost free electrons, causing their degeneracies to lift by broadening and splitting into sublevels. Both these limits are important stepping stones to a fuller understanding of the problem but traditionally the tight-binding (and nearest-neigbour) single band approximation has recieved greater attention in the

literature. We shall also focus our attention on this limit as one can use it to derive both the metal-insulator transition and the quantized Hall conductance. It may be noted that both the limits yeild identical secular equations for the Schrödinger eigenvalue problem with B going to B^{-1} on going from one limit to the other[322].

In this appendix, we look at the strong potential limit of the problem for the two related but distinct physical situations of α being rational i.e. of p/q form, where p and q are relatively prime integers, and α being an irrational number. In the first case the spectrum is characterized by the existence of bands and hence allows a continuous spread of eigenvalues interspersed with gaps. This gap structure was the subject of Hofstadter's work [242] that led to the butterfly fractal. The case of irrational α on the other hand has a singular continuous spectrum where the 'bands' are elements of a Cantor set and exhibit scaling properties [204, 209]. In either case, the analysis of the system is assisted by an effective simplification of the Hamiltonian from a two dimensional to a one dimensional form as introduced by Harper [21] in his study of metallic diamagnetism. This shall also be our manner of treatment in the following sections. The case of rational α offers a route to the topological properties of the system which manifest themselves in the quantized values of the Hall conductance for the various bands in the spectrum. These 'quantum numbers' or integers are found to be associated with an integer valued topological invariant, the Chern number, which is defined for the fibre bundle of the eigenfunctions for the system on the 2-torus constituting the Brillouin zone in reciprocal space [15, 19, 274]. A broader account of the origins of non-trivial topology in the band structure of systems, starting from fundamental ideas of the geometric or Berry's phase, is offered in appendix C.

This and the other features, mentioned above, are elaborated in the following portion of the appendix. We begin with an explicit derivation of the discretized 1-D tight binding, nearest neighbor form i.e. the AAH Hamiltonian from the continuum

model. Once this has been firmly established, we move on to discussions of the rational α case.

A.2 2-D Continuum to the 1-D Discretized Hamiltonian

The discussion in this section borrows largely from a similar analysis in H. J. Stöckmann's *Quantum Chaos* [323]. It is revisited here solely for the purposes of ready-reference and to make the thesis reasonably self-contained.

The continuous real space Hamiltonian for AAH system may be written as follows

$$\mathcal{H} = \frac{1}{2m}\left(\mathbf{p} - \frac{e}{c}\mathbf{A}(x,y)\right)^2 + V_o(x,y) \tag{A.1}$$

where m and e are the electronic mass and charge. The effect of the magnetic field is incorporated via the Peierls-Onsager substitution by transforming the canonical free electron momentum as $\mathbf{p} \to \mathbf{p} - \frac{e}{c}\mathbf{A}(x,y)$, with $\mathbf{A}$ being the vector potential in some suitable gauge which results in a constant magnetic field $\mathbf{B} = \boldsymbol{\nabla} \times \mathbf{A} = B\hat{z}$ normal to the plane of the lattice. The scalar potential V_o models the two dimensional periodic lattice potential as seen by the electrons. In explicit terms it may be cast, for example, in the following harmonic fashion

$$V_o(x,y) = \mathcal{V}_o\left(\cos\frac{\pi x}{a}\sin\frac{\pi y}{a}\right)^n \tag{A.2}$$

where $\mathcal{V}_o$ is the strength of the lattice potential modulation, with n controlling the depth or steepness of the potential and a being the lattice constant. In order to obtain a finite-dimensional discretized version of the problem one needs to define a choice of basis for the Schrödinger eigenvalue problem for the Hamiltonian $\mathcal{H}$. A suitable choice can be made based on the standard approach to tight binding

calculations for the zero field case where the only effect to be accounted for is due to the periodic lattice potential $V_o(x, y)$. One begins by choosing a set of localized atomic orbitals called Wannier functions, which are peaked at the lattice sites and decay rapidly in amplitude away from them. In order to simplify matters we regard just a single valence orbital or Wannier function at each site denoted by $\phi(x, y)$. It follows that the Wannier function for an electron at a lattice site $\mathbf{R}_{nm}$, where $\mathbf{R}_{nm} = n\mathbf{a} + m\mathbf{b}$ is the Bravais lattice vector for the site indexed (n, m), is $\phi(x - na, y - ma)$ or in the Dirac ket formalism simply, $|n, m\rangle$. Let $\Psi(x, y)$ represent the state of an electron in the lattice which, as is well known, has to satisfy the Bloch criterion. Then the procedure is to expand $\Psi(x, y)$ in the basis of the $\phi(x, y)$'s which form a complete orthonormal set over the lattice sites, with $\langle n', m'|n, m\rangle = \delta_{n'n,m'm}$ or equivalently $\int_{-\infty}^{\infty}\int_{-\infty}^{\infty} \phi^*(x - n'a, y - m'a)\phi(x - na, y - ma)dxdy = \delta_{n'n,m'm}$, in the following manner

$$\Psi(x, y) = \sum_{n,m} c_{nm}\phi(x - na, y - ma) \tag{A.3}$$

The reader may be reminded here that the requirement of fulfilling the Bloch condition is met in the above construction by allowing the following for the expansion coefficients

$$c_{nm} \propto \frac{1}{\sqrt{N}} e^{i(k_x n + k_y m)}. \tag{A.4}$$

Where N is the total number of lattice sites and (k_x, k_y) an arbitrary vector in the Brillouin zone of the problem. This imparts the required periodicity with reciprocal lattice vectors in reciprocal space. Such an ansatz when supplied to the Hamiltonian without the magnetic field, $\mathcal{H}_o = \dfrac{\mathbf{p}^2}{2m} + V_o(x, y)$, in the the Schrödinger eigenvalue equation gives

$$\mathcal{H}_o\Psi(x, y) = E\Psi(x, y). \tag{A.5}$$

On a pedagogical sidenote, the unperturbed periodic potential problem has an exact solution in terms of the Bloch functions so this procedure may seem entirely

redundant. However, the Wannier functions are historically [309, 324] a construct derived from the Bloch functions which provide a basis of site-localized functions that prove useful in dealing with problems where perturbations are applied to the periodic potential situation. This was shown to be true when the perturbing fields in question are varying slowly enough for one to neglect contributions arising from different bands. For the purposes of our discussion here, they help to illustrate how tight binding Hamiltonians are constructed and prove their real worth when we come to the description of the electrons in a combination of the periodic potential and the magnetic field.

Now, in order to obtain a set of secular equations for the coefficients c_{nm}, we first take the expectation value of $\mathcal{H}_o$ in the eq.(A.5) with respect to Ψ. This yields a matrix representation for the system as

$$
\begin{aligned}
&\iint_{-\infty}^{\infty} \Psi^*(x,y)\mathcal{H}_o\Psi(x,y)dxdy = E\iint_{-\infty}^{\infty} \Psi^*(x,y)\Psi(x,y)dxdy \\
\Rightarrow &\iint_{-\infty}^{\infty} \sum_{k,l} c_{kl}^*\phi^*(x-ka,y-la)\mathcal{H}_o\sum_{n,m} c_{nm}\phi(x-na,y-ma)dxdy \\
&= E\iint_{-\infty}^{\infty} \sum_{k,l} c_{kl}^*\phi^*(x-ka,y-la)\sum_{n,m} c_{nm}\phi(x-na,y-ma)dxdy \\
\Rightarrow &\sum_{k,l}\sum_{n,m} c_{kl}^*c_{nm}\iint_{-\infty}^{\infty} \phi^*(x-ka,y-la)\mathcal{H}_o\phi(x-na,y-ma)dxdy \\
&= E\sum_{k,l}\sum_{n,m} c_{kl}^*c_{nm}\iint_{-\infty}^{\infty} \phi^*(x-ka,y-la)\phi(x-na,y-ma)dxdy \\
\Rightarrow &\sum_{k\neq n,\, l\neq m}\sum c_{kl}^*c_{nm}\iint_{-\infty}^{\infty} \phi^*(x-ka,y-la)\mathcal{H}_o\phi(x-na,y-ma)dxdy \\
&+\sum_{k=n,\, l=m}\sum c_{nm}^*c_{nm}\iint_{-\infty}^{\infty} \phi^*(x-na,y-ma)\mathcal{H}_o\phi(x-na,y-ma)dxdy \\
&= E\sum_{k,l}\sum_{n,m} c_{kl}^*c_{nm}\delta_{kn,lm}
\end{aligned}
\tag{A.6}
$$

This equation can be written more concisely by introducing some notation for the

space integrals of the form

$$E^0_{nm} = \iint_{-\infty}^{\infty} \phi^*(x-na, y-ma)\mathcal{H}_o\phi(x-na, y-ma)dxdy$$
$$W_{kl,nm} = \iint_{-\infty}^{\infty} \phi^*(x-ka, y-la)\mathcal{H}_o\phi(x-na, y-ma)dxdy \tag{A.7}$$

with these the matrix equation becomes

$$\sum_{k\neq n,\, l\neq m}\sum W_{kl,nm}c^*_{kl}c_{nm} + \sum_{n,m} c^*_{nm}c_{nm}E^0_{nm} = E\sum_{n,m} c^*_{nm}c_{nm}$$

Finally after an exchange of indices in the first summation on the left, interchanging k with n and l with m, and collecting the coefficients of c^*_{nm} on either side one gets the secular equation under tight-binding

$$\sum_{k\neq n,\, l\neq m}\sum W_{nm,kl}c_{kl} + c_{nm}E^0_{nm} = Ec_{nm} \tag{A.8}$$

Solving this system of equations for the coefficients c_{nm} ultimately gives the complete information regarding the state of the system. The eigenvalues of the matrix described here give the information on the spectrum i.e E values. This requires however, for one to specify certain values like E^0_{nm} and $W_{kl,nm}$, which are input parameters that characterize the system.

In the situations where a magnetic field is present i.e. for the Hamiltonian $\mathcal{H}$ in eq.(A.1), the procedure outlined above applies as such with certain modifications to the solution ansatz on account of the $\mathbf{A}(x, y)$ which modifies the canonical momenta. It is straightforward to see that in this case in general $\mathcal{H}$ does not have the periodicity with Bravais lattice vectors of $\mathcal{H}_o$. This results from the position dependence of $\mathbf{A}$ which does not possess such periodicity. A way around this is discussed later while considering the case of rational α. At present, to approach the tight binding form of the eigenvalue equation in the presence of a field, we consider a

gauge transformed version of the solution above, i.e. $\widetilde{\Psi} = \exp(-\frac{ie}{\hbar c}\int \mathbf{A}.\mathbf{dl})\Psi$. Such a $\widetilde{\Psi}$ is expected to be a solution for the system since the $U(1)$-gauge invariance of the Schrödinger equation implies that one is able to gauge away the effects of an $\mathbf{A}$ with such a transformation and hence, relating the solution in the absence of the field, Ψ to the one in its presence, $\widetilde{\Psi}$. This statement however, conceals a significant caveat concerning the fact that once the lattice translation periodicity is lost, the Bloch functions are no longer viable candidates for the solution to the problem, atleast not without some additional conditions. This implies that the gauge transformation argument cannot be directly applied to the Bloch functions as a whole unless one revises the periodicity. We shall see that this can be done in the case of rational α, by introducing the magnetic translation operators. While, in a completely independent approach, the transformation can be suitably applied to the set of localized position space basis functions that are free of the periodicity requirement. This basis is suited for developing the tight-binding and 1-D AAH Hamiltonian, when used for expanding the state of the system. The fact that Wannier functions give a precise convergence to Bloch functions when appropriately superposed justifies their use as an expansion basis for the lattice perturbed with a magnetic field. The concomitant issues of convergence and the phase modification that might assure this are mentioned later. As we shall find out, in the case of rational α, where a modified version of the lattice periodicity is found to exist, this expansion converges to a set of Bloch functions satisfying the more generalized periodicity criterion. In the case of irrational α however, the complete absence of the periodicity condition may result in a faliure of convergence in certain cases. The fact remains that, with this choice of a basis, one is already working with an approximation and the eigenvalues we arrive at finally will only be as good as our choice of basis. This is to be interpreted in the numerical/computational sense that, in the absence of knowledge regarding the energy eigenbasis of the system one is left with an off-diagonal symmetric Hermitian

matrix, tri-diagonal at best, and the problem becomes one of finding its eigenvalues.

The choice of the vector potential made here is $\mathbf{A}(x, y) = B(0, -x, 0)$, consistent with a constant $\mathbf{B}$ in the $\hat{z}$ direction. A Landau gauge choice of this form is analytically convenient and offers a simplified path to the reduced 1-D form of the problem. $\widetilde{\Psi}$ for such a potential is Ψ along with an additional phase acquired on travelling along the $\hat{y}$-direction, while none is collected on moving in the $\hat{x}$-direction. Thus, for a shift in the $\hat{y}$-direction by a lattice constant the phase change in $\widetilde{\Psi}$ amounts to $\frac{-2\pi i\alpha x}{a}$. Where,

$$\alpha = \frac{eBa^2}{hc}, \tag{A.9}$$

is the flux through a plaquette or unit cell of the square lattice in units of the flux quantum hc/e i.e the number of flux quanta. As mentioned earlier this could be a rational or an irrational number leading to distinct spectral behaviour in both cases. In the event that it is rational, it is customary to denote it in the form of a ratio of coprime integers as p/q. This fraction is usually used for the case when the periodic potential is considered to be strong with respect to the magnetic field(weak field). One begins with a single tight binding energy band and proceeds to study its splitting into subbands. This happens to be the case that interests us in this section. Alternatively, in the strong magnetic field limit when the periodic potential behaves like a perturbation, α is understood as the number of unit cells that intersect a single flux quantum and $\alpha = q/p$. The case where Landau levels form the primary structure that splits into finer bands. In both cases however, as long as α is rational, p/q denotes the number of flux quanta through each plaquette of the square lattice.

The construction of the solution ansatz for this gauge choice is done in a manner similar to the one in eq.(A.3), by expanding $\widetilde{\Psi}$ in the basis of the ϕ's but now with the gauge transformation applied to the localized Wannier states themselves

$$\widetilde{\Psi}(x, y) = \sum_{n,m} c_{nm} e^{-2\pi i m\alpha x/a} \phi(x - na, y - ma) \tag{A.10}$$

This choice of expansion has been used advantageously by Luttinger [309] in an early work to generalize a theorem due to Wannier [325], expanded upon by Slater [324], on the electron's energy eigenvalues in perturbed periodic potentials. This theorem was restricted to position dependent potentials while Luttinger sought to extend it to velocity-dependent perturbing potentials, which accompany the introduction of a magnetic field into the Hamiltonian via the Peierls substitution.

The theorem implies, that given $E_0(\mathbf{k})$ i.e. the energy eigenvalues in the unperturbed periodic potential, where $\mathbf{k}$ is the crystal momentum, the eigenvalues in the presence of a perturbing potential of the form $e\widetilde{V}(\mathbf{r})$, are given by the eigenvalue equation

$$[\widehat{E}_0 + e\widetilde{V}(\mathbf{r})]\psi = E\psi$$

where E and ψ are the eigenvalues and eigenstate of the perturbed system and $\widehat{E}_0 = E_0(-i\hbar\boldsymbol{\nabla})$ now is the same operator function of $-i\hbar\frac{\partial}{\partial x}$, $-i\hbar\frac{\partial}{\partial y}$ and $-i\hbar\frac{\partial}{\partial z}$ as it was of k_x, k_y and k_z . The validity of the theorem was shown for the case of a slowly varying potential $\widetilde{V}(\mathbf{r})$. Luttinger demonstrates how this theorem can be made to accomodate the case of a slowly varying magnetic field provided one considers the phase modified expansion for the system's state as in eq.(A.10) and assumes the Wannier functions, ϕ's, to be infinitely localized (an assumption which Luttinger shows has significant bearing on the gauge freedom arguments made previously). The eigenvalue equation to be solved in this case becomes

$$[\widehat{E}_0 + e\widetilde{V}(\mathbf{r})]\psi = E\psi \tag{A.11}$$

where $\widehat{E}_0 = E_0(-i\hbar\boldsymbol{\nabla} - \frac{e}{c}\mathbf{A})$. It is easily seen that the previous form of the eigenvalue expression has undergone a Peierls like modification. This is an important feature of Luttinger's result, accurate in so far as the approximations that yeild it hold well. It manages to extend the Peierls substitution from the Hamiltonian in position

space to the band energies E_0, which are a function of the crystal momentum $\mathbf{k}$, by making them depend on $\mathbf{A}$. Though derived in the presence of a position dependent perturbing potential $\widetilde{V}(\mathbf{r})$, the result holds independently of it. As a stronger or more generalized version of Peierls' result, this theorem is more sophisticated in the sense that it suggests a means of obtaining the spectrum in the presence of magnetic field perturbations using the known band structure of the translationally symmetric unperturbed problem. This assumes that the perturbations respect such a band structure by not giving rise to any interband transitions. In fact it would be precise to restate the result as the transformation of the band structure, $E_0(\mathbf{k}) \equiv E_0(\frac{\mathbf{p}}{\hbar}) \rightarrow E_0(\frac{\mathbf{p}-e\mathbf{A}/c}{\hbar})$. Since the $\boldsymbol{\nabla}$ operator in eq.(A.11) is a gradient operator with respect to the lattice sites and not over continuous space and it is just a position space operator representation of crystal momentum $\mathbf{k}$. Such a modification is also the basis of Harper's work on the problem [21] that initially arrived at a tri-diagonal, tight binding model under a single-band approximation, which is our objective also in this section.

An observation that may be made regarding the system in general, in the light of the above discussion on the lattice version of the Landau level problem, as well as in the continuous translational invariance case, concerns the modification of the commutation algebra of the position and momentum variables. The components of the mechanical momentum fail to commute with each other due to the appearance of the position dependent $\mathbf{A}$ as is familiar in the standard Landau level problem. In the case of a system with discrete translational invariance this feature surfaces in commutation properties of the components of the crystal momentum $\mathbf{k}$ as is apparent in the description of the theorem mentioned previously. The change of $\mathbf{k} \rightarrow \frac{1}{\hbar}(\mathbf{p} - \frac{e}{c}\mathbf{A})$ indicates that the wavevector, which initially constituted a good quantum number is now transformed into an operator thus giving the Hamiltonian matrix off-diagonal terms in reciprocal space. Thus the plane wave basis or conventional Bloch basis

ceases to offer an exact solution and the Fourier reciprocality between the discrete position set in real space and the reciprocal lattice vectors is not entirely sufficient to solve the matter. At first glance it appears as though both position and momentum space are now on an equal footing and neither is better off as an avenue to the solution of the problem. This is not entirely true though, since for the case of rational α, certain momentum space manipulations exist which exploit residual periodicity of the system to define a new subband structure and Brillouin zone with the Hamiltonian reduced to a finite dimensional symmetric tri-diagonal form. However, there is no denying that the presence of the vector potential through some particular choice of gauge fundamentally alters the clear seperation between position and momentum variables. Where earlier a straightforward Fourier relationship prevailed, now a particular direction in position/momentum space may acquire operator like features with respect to the other and become related to it by Fourier like transforms. These become inseparable now from gauge transformations. With a certain choice of coordinate basis amounting to a gauge choice and such transformations begin to fall under a special category of duality transformations. This, in a subtle manner amounts to the fact that what used to be representations in either position or momentum space with the respective components of each commuting amongst themselves, are no longer so. This is far more intricate now, in the sense that the introduction of a non-commuting algebra between the configuration space variables themselves, gives it its own canonical structure such that say, in position space itself both coordinates form a canonical pair. One may choose an effective representation of the problem in either one of them. This is well illustrated in the Landau gauge as we will note, where one may attribute a non-zero phase to a translation either in the $\hat{x}$ or $\hat{y}$ directions. These situations are related through a gauge transformation. For either of these one may obtain the 1-D effective Hamiltonian. These would in turn be related by dual transformations in position and reciprocal space. It then fol-

lows that there is a blurring of the distinction between the real space and reciprocal space representations of the Hamiltonian atleast in terms of notational appearance and mathematical structure. This gives rise to the powerful notion of duality in this system which forms the basis of several arguments about the band structure, existence of degeneracies and the occurance of a metal-insulator transition in the model.

Prior to proceeding further with the derivation of the effective 1-D tight binding nearest neigbour AAH Hamiltonian, it would be worthwhile to go over certain results in Luttinger's work [309] which offer some perspective on the remarks made about the gauge aspects in the choice of expansion in eq.(A.10). The argument proceeds in the following manner, since the presence of the magnetic field gives rise to terms of the form $\mathbf{A}\cdot\mathbf{p}$ in the Hamiltonian. Luttinger makes the case for an expansion of the state of the system in the Wannier basis of the kind in eq.(A.10). In a general fashion, without reference to a particular gauge choice, this may be written as

$$\widetilde{\Psi}(x,y)=\sum_{n,m}c_{nm}e^{\frac{ie}{\hbar c}\mathcal{G}_{nm}}\phi(x-na,y-ma) \tag{A.12}$$

where setting

$$\mathcal{G}_{nm}=\int_{\mathbf{R}_{nm}=(na,ma)}^{\mathbf{r}=(x,y)}\mathbf{A}(\bar{\mathbf{r}})d\bar{\mathbf{r}}, \tag{A.13}$$

which represents the integral of the vector potential along a straight line from the lattice site (n,m) to an arbitrary point in space (x,y), has the desired effect of eliminating the complicating $\mathbf{A}\cdot\mathbf{p}$ term, upto some approximation. As per the procedure adopted by Luttinger it is advisable to reparametrize the above integral in the form

$$\mathcal{G}_{nm}=\int_0^1(\mathbf{r}-\mathbf{R}_{nm})\cdot\mathbf{A}(\mathbf{R}_{nm}+\zeta(\mathbf{r}-\mathbf{R}_{nm}))d\zeta \tag{A.14}$$

where ζ is the new parameter, ranging in $[0,1]$ that parametrizes the line joining

$\mathbf{R}_{nm}$ and $\mathbf{r}$. This choice makes it convenient to express the gradient of $\mathcal{G}_{nm}$ which we shall need later. The effect of this phase modification becomes clearer on subjecting the $\widetilde{\Psi}$ to action under the continuum Hamiltonian $\mathcal{H}$ (see eq.(A.1)), as

$$\begin{aligned}\mathcal{H}\widetilde{\Psi}(x,y) &= \mathcal{H}\sum_{n,m} c_{nm} e^{\frac{ie}{\hbar c}\mathcal{G}_{nm}}\phi(x-na, y-ma) \\ &= \sum_{n,m} c_{nm}\left[\frac{1}{2m}(\mathbf{p}-\frac{e}{c}\mathbf{A})^2 + V_o\right] e^{\frac{ie}{\hbar c}\mathcal{G}_{nm}}\phi(x-na, y-ma) \qquad \text{(A.15)}\end{aligned}$$

If one cares to compare with Luttinger's original work they will note that the position dependent perturbation $e\widetilde{V}(\mathbf{r})$, which was discussed in the context of Wannier's theorem, has been dropped from the Hamiltonian for simplicity as all the arguments apply even in its absence. The non-trivial term required to be evaluated in the above expression is the action of $\frac{1}{2m}(\mathbf{p}-\frac{e}{c}\mathbf{A})^2$ on $e^{-\frac{ie}{\hbar c}\mathcal{G}_{nm}}\phi(x-na, y-ma)$, which proceeds as follows, where for the moment we drop the argument of ϕ for compact representation and call it simply ϕ_{nm},

$$\begin{aligned}&\frac{1}{2m}(\mathbf{p}-\frac{e}{c}\mathbf{A})^2 e^{\frac{ie}{\hbar c}\mathcal{G}_{nm}}\phi_{nm} \\ &= \frac{1}{2m}\left(-i\hbar\boldsymbol{\nabla}-\frac{e}{c}\mathbf{A}\right)\left(-i\hbar\boldsymbol{\nabla}-\frac{e}{c}\mathbf{A}\right)e^{\frac{ie}{\hbar c}\mathcal{G}_{nm}}\phi_{nm} \\ &= \frac{1}{2m}\left(-i\hbar\boldsymbol{\nabla}-\frac{e}{c}\mathbf{A}\right)\left(\frac{e}{c}(\boldsymbol{\nabla}\mathcal{G}_{nm})e^{\frac{ie}{\hbar c}\mathcal{G}_{nm}}\phi_{nm} - e^{\frac{ie}{\hbar c}\mathcal{G}_{nm}}i\hbar(\boldsymbol{\nabla}\phi_{nm})\right. \\ &\left.-\frac{e}{c}\mathbf{A}e^{\frac{ie}{\hbar c}\mathcal{G}_{nm}}\phi_{nm}\right) \\ &= \frac{1}{2m}\left[-\hbar^2\left(\frac{ie}{\hbar c}(\boldsymbol{\nabla}^2\mathcal{G}_{nm})e^{\frac{ie}{\hbar c}\mathcal{G}_{nm}}\phi_{nm} - \frac{e^2}{\hbar^2c^2}(\boldsymbol{\nabla}\mathcal{G}_{nm})^2 e^{\frac{ie}{\hbar c}\mathcal{G}_{nm}}\phi_{nm} + \right.\right. \\ &\left.\left.\frac{ie}{\hbar c}e^{\frac{ie}{\hbar c}\mathcal{G}_{nm}}(\boldsymbol{\nabla}\mathcal{G}_{nm})\cdot(\boldsymbol{\nabla}\phi_{nm})\right) - \hbar^2\left(\frac{ie}{\hbar c}(\boldsymbol{\nabla}\mathcal{G}_{nm})e^{\frac{ie}{\hbar c}\mathcal{G}_{nm}}(\boldsymbol{\nabla}\phi_{nm})\right.\right.\end{aligned}$$

$$
\begin{aligned}
&+ e^{\frac{ie}{\hbar c}\mathcal{G}_{nm}}(\boldsymbol{\nabla}^2\phi_{nm})\Big) + \frac{i\hbar e}{c}\Big((\boldsymbol{\nabla}\cdot\mathbf{A})e^{\frac{ie}{\hbar c}\mathcal{G}_{nm}}\phi_{nm} + \frac{ie}{\hbar c}\mathbf{A}\cdot(\boldsymbol{\nabla}\mathcal{G}_{nm})e^{\frac{ie}{\hbar c}\mathcal{G}_{nm}} \\
&\times \phi_{nm} + e^{\frac{ie}{\hbar c}\mathcal{G}_{nm}}\mathbf{A}\cdot(\boldsymbol{\nabla}\phi_{nm})\Big) - \frac{e}{c}\mathbf{A}\cdot(\boldsymbol{\nabla}\mathcal{G}_{nm})e^{\frac{ie}{\hbar c}\mathcal{G}_{nm}}\phi_{nm} \\
&+ \frac{i\hbar e}{c}e^{\frac{ie}{\hbar c}\mathcal{G}_{nm}}\mathbf{A}\cdot(\boldsymbol{\nabla}\phi_{nm}) + \frac{e^2}{c^2}\mathbf{A}^2e^{\frac{ie}{\hbar c}\mathcal{G}_{nm}}\phi_{nm}\Big] \\
&= e^{\frac{ie}{\hbar c}\mathcal{G}_{nm}}\frac{1}{2m}\Big[-\frac{ie\hbar}{c}(\boldsymbol{\nabla}^2\mathcal{G}_{nm}) + \frac{e^2}{c^2}(\boldsymbol{\nabla}\mathcal{G}_{nm})^2 - \frac{2ie\hbar}{c}(\boldsymbol{\nabla}\mathcal{G}_{nm})\cdot\boldsymbol{\nabla} \\
&- \hbar^2\boldsymbol{\nabla}^2 + \frac{ie\hbar}{c}(\boldsymbol{\nabla}\cdot\mathbf{A}) - \frac{2e^2}{c^2}\mathbf{A}\cdot(\boldsymbol{\nabla}\mathcal{G}_{nm}) + \frac{2i\hbar e}{c}\mathbf{A}\cdot\boldsymbol{\nabla} + \frac{e^2}{c^2}\mathbf{A}^2\Big]\phi_{nm} \qquad \text{(A.16)}
\end{aligned}
$$

The expression in parentheses in the final stage of the above simplification is identified as $\left[\mathbf{p} - \frac{e}{c}(\mathbf{A} - (\boldsymbol{\nabla}\mathcal{G}_{nm}))\right]^2$. It may be noted here that the operator $\boldsymbol{\nabla}$ is the gradient operator over continuous space variables and is used in the position space representation of $\mathbf{p}$, by $-i\hbar\boldsymbol{\nabla}$, as the generator of continuous translations. Thus, we can now rewrite eq.(A.15) in the following way

$$
\mathcal{H}\widetilde{\Psi}(x,y) = \sum_{n,m} c_{nm}e^{\frac{ie}{\hbar c}\mathcal{G}_{nm}}\left[\frac{1}{2m}\left\{\mathbf{p} - \frac{e}{c}(\mathbf{A} - (\boldsymbol{\nabla}\mathcal{G}_{nm}))\right\}^2 + V_o\right]\phi_{nm} \qquad \text{(A.17)}
$$

From the above expression it is apparent that the quantity $\boldsymbol{\nabla}\mathcal{G}_{nm}$ is well situated to compensate the influence of the gauge field $\mathbf{A}$ and an exact compensation will require certain approximations which shall be arrived at shortly. This is a crucial simplification afforded by the expansion in eq.(A.12) or, for a specific gauge choice, in eq.(A.10) that one is able to reduce to what is essentially an eigenvalue problem for the unperturbed periodic lattice, with Hamiltonian $\mathcal{H}_o$, atleast approximately. At first, however, one is required to evaluate $\boldsymbol{\nabla}\mathcal{G}_{nm}$ in a manner such that the final form of the Hamiltonian is hopefully a function of a gauge independent quantity allowing us to make the required physical approximations. In order to achieve this we use the parametrized version of $\mathcal{G}_{nm}$ in eq.(A.14), for which the gradient operation

yields

$$\boldsymbol{\nabla}\mathcal{G}_{nm} = \int_0^1 d\zeta \boldsymbol{\nabla}[(\mathbf{r}-\mathbf{R}_{nm})\cdot\mathbf{A}(\mathbf{R}_{nm}+\zeta(\mathbf{r}-\mathbf{R}_{nm}))]$$
$$= \int_0^1 d\zeta[((\mathbf{r}-\mathbf{R}_{nm})\cdot\boldsymbol{\nabla})\mathbf{A}(\mathbf{R}_{nm}+\zeta(\mathbf{r}-\mathbf{R}_{nm})) + (\mathbf{A}(\mathbf{R}_{nm}+\zeta(\mathbf{r}-\mathbf{R}_{nm}))\cdot\boldsymbol{\nabla})(\mathbf{r}-\mathbf{R}_{nm})$$
$$+ (\mathbf{r}-\mathbf{R}_{nm})\times\{\boldsymbol{\nabla}\times\mathbf{A}(\mathbf{R}_{nm}+\zeta(\mathbf{r}-\mathbf{R}_{nm}))\} + \mathbf{A}(\mathbf{R}_{nm}+\zeta(\mathbf{r}-\mathbf{R}_{nm}))\times(\boldsymbol{\nabla}\times(\mathbf{r}-\mathbf{R}_{nm}))] \tag{A.18}$$

This integral can be simplified by making use of the identities,
$\boldsymbol{\nabla}\times\mathbf{A}(\mathbf{R}_{nm}+\zeta(\mathbf{r}-\mathbf{R}_{nm})) = \zeta\mathbf{B}(\mathbf{R}_{nm}+\zeta(\mathbf{r}-\mathbf{R}_{nm}))$, $\boldsymbol{\nabla}\times\mathbf{r} = 0$ and $\mathbf{A}\cdot(\boldsymbol{\nabla}\mathbf{r}) = \mathbf{A}$.
This brings us to

$$\boldsymbol{\nabla}\mathcal{G}_{nm} = \int_0^1 d\zeta[((\mathbf{r}-\mathbf{R}_{nm})\cdot\boldsymbol{\nabla})\mathbf{A}(\mathbf{R}_{nm}+\zeta(\mathbf{r}-\mathbf{R}_{nm})) + \mathbf{A}(\mathbf{R}_{nm}+\zeta(\mathbf{r}-\mathbf{R}_{nm}))$$
$$+ (\mathbf{r}-\mathbf{R}_{nm})\times\zeta\mathbf{B}(\mathbf{R}_{nm}+\zeta(\mathbf{r}-\mathbf{R}_{nm}))] \tag{A.19}$$

The integration of the second term in the integrand i.e. $\int_0^1 d\zeta\mathbf{A}(\mathbf{R}_{nm}+\zeta(\mathbf{r}-\mathbf{R}_{nm}))$, can be shown to be equal to
$\mathbf{A}(\mathbf{R}_{nm}+\zeta(\mathbf{r}-\mathbf{R}_{nm}))-\int_0^1 d\zeta((\mathbf{r}-\mathbf{R}_{nm})\cdot\boldsymbol{\nabla})\mathbf{A}(\mathbf{R}_{nm}+\zeta(\mathbf{r}-\mathbf{R}_{nm}))$ on using integration by parts. This on being inserted into eq.(A.19) produces a cancellation with the first term in the integrand and one is left with

$$\boldsymbol{\nabla}\mathcal{G}_{nm} = \mathbf{A}(\mathbf{R}_{nm}+\zeta(\mathbf{r}-\mathbf{R}_{nm})) + \int_0^1 d\zeta(\mathbf{r}-\mathbf{R}_{nm})\times\zeta\mathbf{B}(\mathbf{R}_{nm}+\zeta(\mathbf{r}-\mathbf{R}_{nm})) \tag{A.20}$$

In this form, upon insertion into eq.(A.17), the explicit $\mathbf{A}$ dependence in the Hamiltonian operator is made to disappear completely and is replaced by the appearance of the gauge indepedent $\mathbf{B}$, as

$$\mathcal{H}\widetilde{\Psi}(x,y) = \sum_{n,m} c_{nm} e^{\frac{ie}{\hbar c}\mathcal{G}_{nm}} \left[\frac{1}{2m}\left\{\mathbf{p} - \frac{e}{c}(\int_0^1 d\zeta(\mathbf{r}-\mathbf{R}_{nm})\times\zeta\mathbf{B})\right\}^2 + V_o\right]\phi_{nm} \tag{A.21}$$

The appearance of the magnetic field $\mathbf{B}$ explicitly in the Hamiltonian enables one to clearly determine the kind of physical approximation that needs to be made in order to get rid of the gauge coupling term in the mechanical momentum. This prompts Luttinger to invoke a strong localization for the Wannier functions ϕ_{nm}, such that $\mathbf{r} \approx \mathbf{R}_{nm}$, under which the $\int_0^1 d\zeta(\mathbf{r} - \mathbf{R}_{nm}) \times \zeta\mathbf{B}$ term goes to zero. A consequence of the fact that, as the ϕ_{nm}'s tend to a Dirac delta distribution any space integrals containing them, such as the one above, and in general expectation values of quantities will have support only at exactly the lattice sites. Thus, effectively reducing the operative Hamiltonian in this case to simply the periodic lattice problem's $\mathcal{H}_o$. A sequence of steps from here on, accompanied at appropriate points by this approximation, leads to Luttinger's generalization of Wannier's theorem to magnetic field perturbations. The nature of the localization approximation, however, merits closer examination. The physical import of this is the requirement that the magnetic field be slowly varying over space and the truer this is the more accurately the assumption works for a given set of Wannier functions. A feature that can be viewed as a competing interplay between the rapidity of field variation and the spread of the Wannier functions in space, since under the approximation, an extremely slow field variation allows the localization constraint to apply less restrictively thereby allowing a finite, though small, spread in the Wannier functions, whereas for a fast varying field this condition has to be more stringently enforced. The surmise here is essentially that restrictions on the Wannier functions translate directly to constraints on the Bloch functions that give rise to them. Which, in turn, is tantamount to a certain choice of periodic potential(s) which may differ from the actual one defined for the lattice giving rise to errors in the approximation. Thus, it becomes apparent that, the strong localization argument by its very nature shifts the regime of examining the problem towards the strong periodic potential limit. Though in the author's own assessment any estimate of the errors involved in making this ap-

proximation and hence also the domain of validity of the theorem being proven, is extremely difficult to ascertain within this framework itself. Nonetheless, this does not prevent one from inferring the relationship between limiting the spread of a set of localized orbitals, being treated here as a basis, and achieving gauge field independence (upto a phase) in the set of secular equations representing the eigenvalue problem. Shown here to be a consequence of discretizing the system Hamiltonian by sampling position space only at the lattice sites as is the case when the Wannier functions are considered to be exactly localized. It is a remarkable feature of this line of reasoning that choosing to work in a convenient gauge for the problem can be cast as a localization/discretization condition once one chooses to examine it in a suitably selected basis of phase modified functions under the simplifying situation of slowly varying fields.

It, therefore, seems to follow from the strong localization limit discussed above that, the tight binding description with just nearest neigbour interactions taken into account serves to simplify the problem atleast under certain approximations. We now derive this 1-D form of the Hamiltonian in the following. Considering the space integrals of eq.(A.7) but now with an expansion of the kind in eq.(A.10), they become

$$\begin{aligned} E^0_{nm} &= \iint_{-\infty}^{\infty} \phi^*(x-na, y-ma)\mathcal{H}_o\phi(x-na, y-ma)dxdy \\ \widetilde{W}_{nm,kl} &= \iint_{-\infty}^{\infty} \phi^*(x-na, y-ma)e^{2\pi i(m-l)\alpha x/d}\mathcal{H}_o\phi(x-ka, y-la)dxdy \end{aligned} \quad \text{(A.22)}$$

The tight binding equations, see eq.(A.8), have now to be modified to account for this as

$$\sum_{k\neq n,\, l\neq m}\sum \widetilde{W}_{nm,kl}c_{kl} + c_{nm}E^0_{nm} = \widetilde{E}c_{nm} \quad \text{(A.23)}$$

where they represent the tight binding system in the presence of a magnetic field with the vector potential in the Landau gauge as chosen before and $\widetilde{E}$ denotes the

eigenvalues for the perturbed system. The above results are readily obtained by following the same steps as were employed for the case of the unperturbed lattice in eq.(A.6). The E^0_{nm} integral in eq.(A.22) denotes the on-site energy at a lattice site for the unperturbed Hamiltonian $\mathcal{H}_o$. Since this is a translationally invariant Hamiltonian, it is a constant for all sites that could be assumed to be zero without any loss of generality, as this would just be akin to a shift in the energy reference. Translational symmetry also permits us to write the integral $\widetilde{W}_{nm,kl}$ after a coordinate displacement by primitive lattice vectors, i.e $x \to x + ka$ and $y \to y + la$, and is now denoted by

$$\widetilde{W}_{nm,kl} = e^{2\pi i(m-l)\alpha k}\widetilde{W}_{n-k,m-l},$$

where

$$\widetilde{W}_{rs} = \iint_{-\infty}^{\infty} \phi^*(x - ra, y - sa)e^{2\pi i s\alpha x/d}\mathcal{H}_o\phi(x, y)dxdy$$

This modification helps to introduce a reference point in the lattice such that one can speak in terms of near and far neighbors with the differences $n - k$ and $m - l$ behaving as a set of neighborhood indices. Thus, the tight binding equation of eq.(A.23) after limiting the range of interactions to the nearest neigbors, becomes

$$\widetilde{W}_{10}(c_{n+1,m} + c_{n-1,m}) + \widetilde{W}_{01}(c_{n,m+1}e^{-i2\pi n\alpha} + c_{n,m-1}e^{i2\pi n\alpha}) = \widetilde{E}c_{nm} \tag{A.24}$$

Something that has been implicitly assumed here is that $\widetilde{W}_{01} = \widetilde{W}_{0-1}$ and $\widetilde{W}_{10} = \widetilde{W}_{-10}$, relationships that arise out of the known parities of atomic wavefunctions. Further, the coefficients in the above equation can be seen to be independent of the m index in a way that is not true for n. As mentioned previously in the context of nature of coefficients c_{nm} in relation to assuring conformity with Bloch conditions in the unperturbed case, the requirement $c_{nm} = e^{im\theta}c_n$ models the lattice periodicity which still holds in the $\hat{y}$-direction under the gauge choice. The θ here, is simply the Bloch phase acquired on translating the wavefunction by a primitive lattice vector

in the $\hat{y}$-direction where, the wavevector k_y corresponding to this shift relates to it as $\theta = k_y/a$. After incorporating these relations in eq.(A.24) the 1-D effective form of the tight-binding equation is obtained as

$$\widetilde{W}_{10}(c_{n+1} + c_{n-1}) + 2\widetilde{W}_{01}\cos(2\pi\alpha n + \theta) = \widetilde{E}c_n \tag{A.25}$$

this may be cast in the more familiar and customary form of the equation by dividing throughout by $\widetilde{W}_{10}$ and denoting $\widetilde{E}/\widetilde{W}_{10}$ by $\widetilde{E}^0$ and $2\widetilde{W}_{01}/\widetilde{W}_{10}$ by ζ,

$$c_{n+1} + c_{n-1} + \zeta\cos(2\pi\alpha n + \theta) = \widetilde{E}^0 c_n \tag{A.26}$$

This is the Harper equation for $\zeta = 2$ and is the general AAH 1-D tight-binding equation. The model is 1-D but with the special feature that the on-site energy is now periodically modulated with site i.e. $\zeta\cos(2\pi\alpha n + \theta)$. It is now possible to read off the 1-D AAH Hamiltonian from the tight-binding equation above and express it in the Dirac ket notation

$$H_0 = \sum_n |n\rangle\langle n+1| + |n\rangle\langle n-1| + \zeta\cos(2\pi\alpha n + \theta)|n\rangle\langle n| \tag{A.27}$$

Here the kets $|n\rangle$ are a choice of canonical basis such that if the c_n' s are regarded as the components of the column vector $|c\rangle$, then $c_n = \langle n|c\rangle$.

This concludes the derivation of the 1-D effective Hamiltonian for the problem of Landau levels on a lattice. It is interesting to note this particular limit of the problem with its tight-binding, nearest-neighbor description and the fields being assumed to vary slowly enough. Though it may seem that these are restrictive approximations they are, surprisingly, powerful enough to capture several important physical features of the system. So much so that the phenomenon of Hall conductance quantization [12], originally observed for a 2-D inversion layer of electrons at

the interface of a semiconductor heterostructure modelled as an electron gas was, in fact, first theoretically well justified for such a discretized lattice version of the problem [15]. Such instances adduce the usefulness of studying this model.

A.3 The case of rational α of the form p/q

Hofstadter was the first to point out that the Bloch electron problem in a magnetic field makes a spectral distinction between the two possibilities of rational or irrational values for the system parameter α [242]. He notes, besides the self-similar hierarchical nature of the magnetic energy levels or bands, that one should in principle be able to deduce the nature of the spectrum for the irrational case from what one sees for rational α. Since, as he argues, any physical system that distinguishes between the raional and irrational values of any of its parameters can do so only in a mathematical sense because were this distinction allowed to manifest in the physically observable properties of the system it would lead to their being everywhere discontinuous as one varied the parameter(s) over the real line. Indeed an algorithm that performs this deduction is also offered by him. This insight coupled with the fact that for rational α one is able to exploit certain periodicity conditions which permit a Bloch like analysis, makes it an important case to study.

In the previous section an effective 1-D Hamiltonian was worked out for the system of tightly bound electrons on a square lattice in a magnetic field. The approach used there made no recourse to symmetry arguments for defining the structure of solutions to the eigenvalue problem. However, when α is of the form p/q, a modified version of the lattice translation symmetry exists, that is, if one agrees to a redefinition of the lattice unit cell so as to enlarge it in such a way that it accomodates a single flux quantum of the normally incident magnetic field. This allows one to define a set of translation operators called the magnetic translation operators which commute with the Hamiltonian of the problem. We shall, in this section, lay out the

manner in which these operators are defined, derive the generalized Bloch functions that follow the revised periodicity criterion and generally illustrate how one may go about using the various features of this model to simplify the calculations required to obtain its spectrum and other observed properties. Another key difference is that the discussion in this section, unlike in the previous one, has no initial intent to arrive at an effective 1-D description, since, as we shall see, we begin with a Hamiltonian in the full 2-D picture. Although, it does so happen that one inevitably ends up with such a description simply on going to the reciprocal space picture of the system even when the position space Hamiltonian is 2-D.

A.3.1 The Continuum picture and generalized Bloch solutions

The discussion in this section is a coherent compilation of two of M. Kohmoto's pedagogical papers on the diamagnetism of lattice electrons [274, 326]. The choices of notation made here may, at times, reflect this provenance. Looking back at the position space continuum Hamiltonian for the problem, see eq.(A.1), certain general observations may be restated. The periodicity of the crystal potential V_o, such that, $V_o(x+a,y) = V_o(x,y+a) = V_o(x,y)$ does not automatically imply such periodicity for $\mathcal{H}$ which also depends on $\mathbf{A}(\mathbf{r})$. The position dependence of $\mathbf{A}$ is aperiodic for the currently considered case of a magnetic field constant over all space. Thus, as mentioned earlier, one has to refrain from a straight forward application of Bloch's theorem. We circumvented this difficulty in the previous section by selecting a site-localized basis of Wannier functions to expand the state of the system. Presently, we shall elaborate the alternative approach of magnetic translation operators that makes use of the rationality of α.

From the group theoretic approach to Bloch solutions for the Hamiltonian $\mathcal{H}_o$, of lattice electrons without the field, one is familiar with discrete translation operators.

An operator of this kind denoted by $\mathcal{T}$ translates any function of position space coordinates by some Bravais lattice vector $\mathbf{R}_{nm}$, depending on the choice made in its definition. This action on some general function $u(\mathbf{r})$ is given by

$$\mathcal{T}u(\mathbf{r}) = u(\mathbf{r} + \mathbf{R}_{nm}).$$

Where explicitly one may denote $\mathcal{T} = e^{-\frac{i}{\hbar}\mathbf{R}_{nm}\cdot\mathbf{p}}$. Such a $\mathcal{T}$ commutes with $\mathcal{H}_o$ and the Bloch functions turn out to be the eigenbasis that simultaneously diagonalizes $\mathcal{H}_o$ and $\mathcal{T}$. When $\mathcal{T}$ acts on $\mathcal{H}$, however, it effects the transformation $\mathbf{A}(\mathbf{r}) \rightarrow \mathbf{A}(\mathbf{r} + \mathbf{R}_{nm})$. Here in general $\mathbf{A}(\mathbf{r}) \neq \mathbf{A}(\mathbf{r} + \mathbf{R}_{nm})$. Thus in its present form $\mathcal{T}$ does not commute with $\mathcal{H}$ and this is where magnetic translation operators come into the picture. The objective is to construct a translation operator $\widetilde{\mathcal{T}}$ that commutes with $\mathcal{H}$, i.e. $[\widetilde{\mathcal{T}}, \mathcal{H}] = 0$, in a particular gauge. One is assisted in this task by the observation that for a uniform magnetic field, values of the vector potential at points seperated by Bravais lattice vectors can be related as

$$\mathbf{A}(\mathbf{r}) = \mathbf{A}(\mathbf{r} + \mathbf{R}_{nm}) + \boldsymbol{\nabla}\chi(\mathbf{r}) \tag{A.28}$$

where $\chi(\mathbf{r})$ is a scalar field. Thus, when the ordinary translation operator $\mathcal{T}$ is made to act on $\mathcal{H}$ we obtain

$$\begin{aligned}
\mathcal{T}\mathcal{H} &= \mathcal{T}\left[\frac{1}{2m}(\mathbf{p} - \frac{e}{c}\mathbf{A}(\mathbf{r}))^2 + V_o(\mathbf{r})\right] \\
&= \left[\frac{1}{2m}(\mathbf{p} - \frac{e}{c}\mathbf{A}(\mathbf{r} + \mathbf{R}_{nm}))^2 + V_o(\mathbf{r} + \mathbf{R}_{nm})\right]\mathcal{T} \\
&= \left[\frac{1}{2m}\left\{\mathbf{p} - \frac{e}{c}(\mathbf{A}(\mathbf{r}) - \boldsymbol{\nabla}\chi(\mathbf{r}))\right\}^2 + V_o(\mathbf{r})\right]\mathcal{T}
\end{aligned} \tag{A.29}$$

The modification in the gauge coupling term that results from this action reminds us of the modification which was found to occur as a result of the action of $\mathcal{H}$ on the transformed basis of Wannier functions in eq.(A.17). There the term $\left[\mathbf{p} - \frac{e}{c}(\mathbf{A} - (\boldsymbol{\nabla}\mathcal{G}_{nm}))\right]^2$

stemmed from the action of $\mathcal{H}$ on the exponential factor $e^{\frac{ie}{\hbar c}\mathcal{G}_{nm}}$. This suggests the use of such a phase factor in redefining the translation operator so as to compensate the additional $\boldsymbol{\nabla}\chi(\mathbf{r})$ that appears in the translated Hamiltonian and is the main cause for inadequacy of the conventional lattice translation operator $\mathcal{T}$. Let us consider the action of $\mathcal{H}$ on the term $e^{\frac{ie}{\hbar c}\chi(\mathbf{r})}$,

$$\begin{aligned}\mathcal{H}e^{\frac{ie}{\hbar c}\chi(\mathbf{r})} &= \left[\frac{1}{2m}(\mathbf{p}-\frac{e}{c}\mathbf{A}(\mathbf{r}))^2 + V_o(\mathbf{r})\right] e^{\frac{ie}{\hbar c}\chi(\mathbf{r})} \\ &= e^{\frac{ie}{\hbar c}\chi(\mathbf{r})}\left[\frac{1}{2m}\left\{\mathbf{p}-\frac{e}{c}(\mathbf{A}(\mathbf{r})-\boldsymbol{\nabla}\chi(\mathbf{r}))\right\}^2 + V_o(\mathbf{r})\right]\end{aligned}$$

and from eq.(A.29) we may write

$$\begin{aligned}\mathcal{H}e^{\frac{ie}{\hbar c}\chi(\mathbf{r})} &= e^{\frac{ie}{\hbar c}\chi(\mathbf{r})}\left[\frac{1}{2m}\left\{\mathbf{p}-\frac{e}{c}(\mathbf{A}(\mathbf{r})-\boldsymbol{\nabla}\chi(\mathbf{r}))\right\}^2 + V_o(\mathbf{r})\right]\mathcal{T}\,\mathcal{T}^{-1} \\ &= e^{\frac{ie}{\hbar c}\chi(\mathbf{r})}\mathcal{T}\left[\frac{1}{2m}(\mathbf{p}-\frac{e}{c}\mathbf{A}(\mathbf{r}))^2 + V_o(\mathbf{r})\right]\mathcal{T}^{-1} \\ &= e^{\frac{ie}{\hbar c}\chi(\mathbf{r})}\mathcal{T}\;\mathcal{H}\;\mathcal{T}^{-1} \\ \Rightarrow \mathcal{H}e^{\frac{ie}{\hbar c}\chi(\mathbf{r})}\mathcal{T} &= e^{\frac{ie}{\hbar c}\chi(\mathbf{r})}\mathcal{T}\;\mathcal{H}\end{aligned}$$

If now one were to define $\widetilde{\mathcal{T}} = e^{\frac{ie}{\hbar c}\chi(\mathbf{r})}\mathcal{T}$ the desired magnetic translation operator results which commutes with $\mathcal{H}$. A more rigorous analysis that derives such operators can be found in [327]. From the above sequence of steps the crux of the reasoning applied to solve the problem seems to rest on how one chooses $\mathcal{G}_{nm}$, in Luttinger's approach, or what we have now as $\chi(\mathbf{r})$. While in the previous section the choice of $\mathcal{G}_{nm}$ in eqs.(A.13) and (A.14) was motivated by the possibility of compensating the vector potential term in $\mathcal{H}$, arguments for which were offered in a retrospective manner once it became clear how the transformation affected the Hamiltonian. The structure of $\chi(\mathbf{r})$ is similar but derives from the condition in eq.(A.28). In the end both are essentially the same and one is just shifting from a passive to an active view of the transformation so to speak. Since in the previous section we chose to apply a

gauge transfrormation to a discrete basis and study the action of the Hamiltonian of the system on the state expanded in this basis. While in the present section the emphasis has shifted to actively transforming the Hamiltonian and determining those translatory transformations that leave the Hamiltonian invariant. The object as always is to reduce the problem to an eigenvalue equation for which solutions are known which in this case is the periodic potential problem of lattice electrons without the field.

Another feature that will help to connect the current treatment with Luttinger's presented previously is that, choosing to work with discrete translation operators blends nicely with the strong localization constraints that were mentioned while trying to eliminate gauge dependence. As the result in both cases is the discretization of the system which happens to be germane to its solution. This discretization in the previous section mapped the problem to the zero field case and in the present context of translation operators will be seen to have a similar effect by allowing the construction of a lattice of magnetic cells which can be treated as a new periodic lattice with just the unit cells having multiple sites compared to the original square lattice. A convergence of the two approaches therefore, becomes easier to imagine in this limit. With this understanding we might use some more of the machinery made available in [309] to write down $\widetilde{\mathcal{T}}$ in a form that reinforces the Peierls substitution. To do this we use the association between $\chi(\mathbf{r})$ and a difference version of $\mathcal{G}_{nm}$ i.e. $\mathcal{G}_{n-n',m-m'}$ which in the parametrized notation of eq.(A.14) can be expressed as

$$\chi(\mathbf{r}) = \mathcal{G}_{n-n',m-m'} = \int_0^1 (\mathbf{r}-(\mathbf{R}_{nm}-\mathbf{R}_{n'm'}))\cdot\mathbf{A}(\mathbf{R}_{nm}-\mathbf{R}_{n'm'}+\zeta[\mathbf{r}-\{\mathbf{R}_{nm}-\mathbf{R}_{n'm'}\}])d\zeta \tag{A.30}$$

This is no different from $\mathcal{G}_{nm}$ in that just a reformulation of Bravais lattice vector for the reference site (n, m) is made in terms of a difference of lattice vectors. It works like the replacement $\mathbf{r} \to \mathbf{r} + \mathbf{R}_{n'm'}$ in the integral in eq.(A.14) so as to extend the

domain of integration in eq.(A.13) from the neighbourhood of a single lattice point to that around another lattice point. This in a clever manner helps to non-trivially enforce the localization criterion in a way that makes the phase depend only on discrete lattice sites. This can be seen by putting $\mathbf{r} = \mathbf{R}_{nm}$ in eq.(A.30) as

$$\begin{aligned}\mathcal{G}_{n-n',m-m'}(\mathbf{r} = \mathbf{R}_{nm}) &= \int_0^1 \mathbf{R}_{n'm'} \cdot \mathbf{A}(\mathbf{R}_{nm} - (1-\zeta)\mathbf{R}_{n'm'})d\zeta \\ &= \int_0^1 \mathbf{R}_{n'm'} \cdot \mathbf{A}(\mathbf{R}_{nm} - \zeta\mathbf{R}_{n'm'})d\zeta \end{aligned} \tag{A.31}$$

This structure of $\chi(\mathbf{r})$ is useful to us in proving an identity which helps to express $\widetilde{\mathcal{T}}$ in a compact manner that hints at a Peierls like modification of the canonical momentum in the definition of $\mathcal{T}$. Thus taking an ordinary translation operator to a magnetic translation one. The identity in question is that for the magnetic translation operator which is now

$$\widetilde{\mathcal{T}} = e^{\frac{ie}{\hbar c}\chi(\mathbf{r})}\mathcal{T} = \exp\left\{\frac{ie}{\hbar c}\int_0^1 \mathbf{R}_{n'm'} \cdot \mathbf{A}(\mathbf{R}_{nm} - \zeta\mathbf{R}_{n'm'})d\zeta\right\}\exp\{-\mathbf{R}_{n'm'} \cdot \boldsymbol{\nabla}\} \tag{A.32}$$

one is allowed to write

$$\widetilde{\mathcal{T}} = \exp\{-\mathbf{R}_{n'm'} \cdot [\boldsymbol{\nabla} - (ie/\hbar c)\mathbf{A}(\mathbf{R}_{nm})]\} = \exp\{(-i/\hbar)\mathbf{R}_{n'm'} \cdot [\mathbf{p} - (e/c)\mathbf{A}_{nm}]\} \tag{A.33}$$

To show that the right hand side of both the equations is indeed the same one can begin by proving the following result which is a continuum version of the identity i.e.

$$\exp\{-\mathbf{R} \cdot (\boldsymbol{\nabla} - (ie/\hbar c)\mathbf{A}(\mathbf{r}))\} = \exp\left\{\frac{ie}{\hbar c}\int_0^1 \mathbf{R} \cdot \mathbf{A}(\mathbf{r} - \zeta\mathbf{R})d\zeta\right\}\exp\{-\mathbf{R} \cdot \boldsymbol{\nabla}\} \tag{A.34}$$

A short proof (due to Luttinger) may be sketched as follows. Consider the operator

$$F(\eta) = \exp\left\{\frac{ie}{\hbar c}\int_0^\eta \mathbf{R}\cdot\mathbf{A}(\mathbf{r}-\zeta\mathbf{R})d\zeta\right\}\exp\{-\eta\mathbf{R}\cdot\boldsymbol{\nabla}\} \tag{A.35}$$

then,

$$\begin{aligned}\frac{dF}{d\eta} &= \frac{d}{d\eta}\left[\exp\left\{\frac{ie}{\hbar c}\int_0^\eta \mathbf{R}\cdot\mathbf{A}(\mathbf{r}-\zeta\mathbf{R})d\zeta\right\}\right]\exp\{-\eta\mathbf{R}\cdot\boldsymbol{\nabla}\} \\ &\quad + \exp\left\{\frac{ie}{\hbar c}\int_0^\eta \mathbf{R}\cdot\mathbf{A}(\mathbf{r}-\zeta\mathbf{R})d\zeta\right\}\frac{d}{d\eta}[\exp\{-\eta\mathbf{R}\cdot\boldsymbol{\nabla}\}] \\ &= \frac{ie}{\hbar c}\mathbf{R}\cdot\mathbf{A}(\mathbf{r}-\eta\mathbf{R})\exp\left\{\frac{ie}{\hbar c}\int_0^\eta \mathbf{R}\cdot\mathbf{A}(\mathbf{r}-\zeta\mathbf{R})d\zeta\right\}\exp\{-\eta\mathbf{R}\cdot\boldsymbol{\nabla}\} \\ &\quad + \exp\left\{\frac{ie}{\hbar c}\int_0^\eta \mathbf{R}\cdot\mathbf{A}(\mathbf{r}-\zeta\mathbf{R})d\zeta\right\}\exp\{-\eta\mathbf{R}\cdot\boldsymbol{\nabla}\}(-\mathbf{R}\cdot\boldsymbol{\nabla})\end{aligned}$$

In the first term on the RHS of the equation above it is possible to rearrange the $\frac{ie}{\hbar c}\mathbf{R}\cdot\mathbf{A}(\mathbf{r}-\eta\mathbf{R})\exp\{-\eta\mathbf{R}\cdot\boldsymbol{\nabla}\}$ portion as $\exp\{-\eta\mathbf{R}\cdot\boldsymbol{\nabla}\}\frac{ie}{\hbar c}\mathbf{R}\cdot\mathbf{A}(\mathbf{r})$ by recognizing that $\exp\{-\eta\mathbf{R}\cdot\boldsymbol{\nabla}\}$ is the displacement operator that shifts functions of position by an amount $\eta\mathbf{R}$. After doing so one is able to write

$$\frac{dF}{d\eta} = F(\eta)\left[-\mathbf{R}\cdot\boldsymbol{\nabla} + \frac{ie}{\hbar c}\mathbf{R}\cdot\mathbf{A}(\mathbf{r})\right] = F(\eta)\left[-\mathbf{R}\cdot\left(\boldsymbol{\nabla} - \frac{ie}{\hbar c}\mathbf{A}(\mathbf{r})\right)\right]$$

This is a differential equation in $F(\eta)$ and can be solved for it, yeilding upon integration

$$F(\eta) = \exp\{-\eta\mathbf{R}\cdot(\boldsymbol{\nabla} - (ie/\hbar c)\mathbf{A})\}$$

where the constant of integration is decided using $F(0) = 1$ as is required by its definition in eq.(A.35) and one can recover the identity by putting $\eta = 1$ in the above since the RHS above equates to that of eq.(A.35) thereby establishing the continuum version of the required relationship implied in eqs.(A.32) and (A.33). We have thus devised a means of representing the magnetic translation operator $\widetilde{\mathcal{T}}$ in a form that appears as a Peierls modification of the ordinary translation operator

$\mathcal{T}$. So for instance, if working in the symmetric gauge, $\widetilde{\mathcal{T}}$ becomes

$$\widetilde{\mathcal{T}} = \exp\left\{\frac{i}{\hbar}\mathbf{R}\cdot\left[\mathbf{p} + (e/c)\frac{\mathbf{r}\times\mathbf{B}}{2}\right]\right\} = \mathcal{T}\exp\left\{(ie/\hbar c)\frac{(\mathbf{B}\times\mathbf{R})\cdot\mathbf{r}}{2}\right\} \tag{A.36}$$

The above can be shown to commute with $\mathcal{H}$ in the symmetric gauge i.e. $\mathbf{A}(\mathbf{r}) = \frac{\mathbf{B}\times\mathbf{r}}{2}$. Though we have managed to fulfill the requirement of defining translation operators that commute with the Hamiltonian of lattice electrons in a magnetic field, one runs into the difficulty that translations along $\hat{x}$ and $\hat{y}$ directions no longer commute. Let us, for the purposes of all discussions here, assume that the primitve unit vectors of the square Bravais lattice that forms the scaffolding of our system, are aligned along the cardinal directions of the reference coordinate system. If we denote the operator for translations by a lattice constant, in the $\hat{x}$ direction, by $\widetilde{\mathcal{T}}_x$ and for those along $\hat{y}$ by $\widetilde{\mathcal{T}}_y$ then using eq.(A.36) one may write

$$\widetilde{\mathcal{T}}_x = \mathcal{T}_x\exp\left\{(ie/\hbar c)\frac{yBa}{2}\right\} \qquad \widetilde{\mathcal{T}}_y = \mathcal{T}_y\exp\left\{-(ie/\hbar c)\frac{xBa}{2}\right\} \tag{A.37}$$

where we have used $\mathbf{B} = B\hat{z}$, $\mathbf{r} = (x, y)$ and $\mathbf{R} = a\hat{x}$ or $a\hat{y}$ for $\widetilde{\mathcal{T}}_x$ and $\widetilde{\mathcal{T}}_y$ respectively, with a being the lattice constant as defined before. $\mathcal{T}_x$ and $\mathcal{T}_y$ are the ordinary translation operators for translating by a in the corresponding directions in the absence of the field. They naturally commute with each other. Now it is easy to show, using the above representations, that

$$\begin{aligned}\widetilde{\mathcal{T}}_x\widetilde{\mathcal{T}}_y &= e^{2\pi i\frac{eBa^2}{\hbar c}}\widetilde{\mathcal{T}}_y\widetilde{\mathcal{T}}_x \\ &= e^{2\pi i\alpha}\widetilde{\mathcal{T}}_y\widetilde{\mathcal{T}}_x\end{aligned} \tag{A.38}$$

We use eq.(A.9) to identify the term in the exponent as a function of the number of flux quanta crossing a single plaquette of the square lattice. The magnetic translation operators for directions orthogonal to each other lying in the plane per-

pendicular to the applied field do not commute upto the phase factor as shown above. If one is to take the traditional route of finding the eigenbasis that simultaneously diagonalizes $\mathcal{H}$ and $\widetilde{\mathcal{T}}$, as is the case with ordinary Bloch solutions, one is required to first resolve the non-commutativity just discussed. Since we are concerning ourselves with the case of rational α i.e. of the form p/q (p and q being relatively prime) it is possible to extract a subset of orthogonal magnetic translation operators that do commute with one another. A situation that arises when the condition $e^{2\pi i\alpha} = 1$ is met. This requires α to be an integer and is most trivially satisfied for $\alpha = p$ which is the case when a single unit cell of the square lattice is so chosen that it intersects p flux quantua of the magnetic field. Therefore an enlargement of the unit cell is called for with new Bravais lattice vectors to be defined, which form a subset of the original set of Bravais lattice vectors, as $\mathbf{R}'_{nm} = nqa\hat{x} + ma\hat{y}$. Such a redefinition is not unique in the sense that one could as easily have gone on to enlarge the unit cell to include q cells and it would have the same effect as far as ensuring commutativity is concerned. This is true atleast in the case of the symmetric gauge example treated here. If one were to go with a Landau gauge choice for the vector potential then one is forced to make a choice out of the two extensions. What it boils down to is, as we shall see, how the position dependent phase , determined by the gauge choice, gets allocated to shifting the wavefunction along the sides of the newly conceived magnetic unit cell. Though this may change the appearance of the resulting generalized Bloch functions, the essence of the physical situation lies in the number of flux quanta that cross the magnetic unit cell and this depends purely on the magnetic field strength. This quantum number, it will be seen, is a more fundamental constant of the problem and can be shown to be related to topological properties of the system.

Let the new, commuting translation operators be denoted by $\widetilde{\mathcal{T}}'$. These operators also commute with $\mathcal{H}$ by definition. Consider a function ψ which is a simultaneous

eigenfunction of both $\mathcal{H}$ and $\widetilde{\mathcal{T}}'$. It is possible now to use the arguments applicable to the $\mathcal{T}$'s for Bloch electrons governed by the pure lattice Hamiltonian $\mathcal{H}_o$, in the context of $\mathcal{H}$ and $\widetilde{\mathcal{T}}'$. Thus, using ideas from group theory and by the relations obtained from successive applications of translation operators one may arrive at the eigenvalue equations for the $\widetilde{\mathcal{T}}'$ s when made to act on ψ. To write these equations we note that $\widetilde{\mathcal{T}}'_x \equiv \widetilde{\mathcal{T}}_{x=qa}$ and $\widetilde{\mathcal{T}}'_y \equiv \widetilde{\mathcal{T}}_{y=a}$ provide the correspondence between translations along the new primitive unit cell sides and the older magnetic translation operators. Thus, expressing the action of unit translations $\widetilde{\mathcal{T}}'_x$ and $\widetilde{\mathcal{T}}'_y$ on ψ in this parlance gives us

$$\begin{aligned} \widetilde{\mathcal{T}}'_x\psi &= \widetilde{\mathcal{T}}_{x=qa}\psi = e^{ik_xqa}\psi \\ \widetilde{\mathcal{T}}'_y\psi &= \widetilde{\mathcal{T}}_{y=a}\psi = e^{ik_ya}\psi \end{aligned} \tag{A.39}$$

Where k_x and k_y are reciprocal-space coordinate variables that arise in a fashion similar to that in the derivation of Bloch solutions for the periodic lattice problem. The functions ψ here are the Bloch like solutions for the network of magnetic unit cells which form a periodic structure over the original square lattice. Since the primitive unit cell has undergone a redefinition this also manifests in the reciprocal space picture as a resizing of the Brillouin zone. So under the new periodicity conditions, $0 \leq k_x \leq 2\pi/qa$ and $0 \leq k_y \leq 2\pi/a$. ψ here, is the generalized Bloch function or magnetic Bloch function and can be written in a form similar to that of the ordinary Bloch functions by expicitly denoting the band index n and **k**-space coordinate dependence and resolving into the plane wave factor and the corresponding periodic modulating component as follows

$$\psi^{\mathrm{n}}_{k_x,k_y}(x,y) = e^{ik_xx+ik_yy}u^{\mathrm{n}}_{k_x,k_y}(x,y) \tag{A.40}$$

The band index n has a different interpretation from the simple periodic potential

case as in the presence of a magnetic field the bands undergo a splitting and reorganization. There are indications of this in the fact that the magnetic unit cell contains several sites as compared to the primitive unit cell of the square lattice and from a reciprocal space perspective, in the observation that the reconstituted first Brillouin zone (FBZ) of the lattice of magnetic cells is a fraction of the earlier Brillouin zone. We shall discuss aspects of the new band structure and its origins soon when we consider the tight binding picture. The functions $u^{\rm n}_{k_x,k_y}(x,y)$ are counterparts of the periodic real functions that are an essential component of Bloch solutions. In the case of ordinary Bloch solutions these functions follow the periodicity of the Bravais lattice exactly without the accumulation of any phase on translations by Bravais lattice vectors. However, in the presence of a magnetic field, and with a redefinition of the unit cell the properties of these functions are modified subject to the eigenvalue equations in eq.(A.39) and using eq.(A.37) can be shown to be

$$\begin{aligned}
\widetilde{\mathcal{T}}_{x=qa}\psi &= e^{ik_xqa}\psi \\
\Rightarrow \mathcal{T}_{x=qa}\exp\left\{(ie/\hbar c)\frac{yBqa}{2}\right\}\psi^{\rm n}_{k_x,k_y}(x,y) &= e^{ik_xqa}\psi^{\rm n}_{k_x,k_y}(x,y) \\
\Rightarrow \exp\left\{(ie/\hbar c)\frac{yBqa}{2}\right\}\mathcal{T}_{x=qa}e^{ik_xx+ik_yy}u^{\rm n}_{k_x,k_y}(x,y) &= e^{ik_xqa}e^{ik_xx+ik_yy}u^{\rm n}_{k_x,k_y}(x,y) \\
\Rightarrow e^{(ie/\hbar c)\frac{yBqa}{2}}e^{ik_xqa}e^{ik_xx+ik_yy}u^{\rm n}_{k_x,k_y}(x+qa,y) &= e^{ik_xqa}e^{ik_xx+ik_yy}u^{\rm n}_{k_x,k_y}(x,y) \\
\Rightarrow u^{\rm n}_{k_x,k_y}(x+qa,y) &= e^{-i\pi py/a}u^{\rm n}_{k_x,k_y}(x,y) \qquad \text{(A.41)}
\end{aligned}$$

Where we have used the fact that $e^{(ie/\hbar c)\frac{yBqa}{2}}$ can be written as $e^{-i\pi py/a}$ using $\alpha = \frac{eBa^2}{h} = p/q$, taking $c = 1$ units. In a similar way one can treat the second eigenvalue equation for the $\hat{y}$ translation and arrive at the following

$$u^{\rm n}_{k_x,k_y}(x,y+a) = e^{i\pi px/qa}u^{\rm n}_{k_x,k_y}(x,y)$$

Thus we observe that the translations of these functions along the edges of a mag-

netic unit cell i.e. in effect translating by the modified unit lattice vectors has the effect of accumulating a certain amount of phase. These are in fact the generalized Bloch functions satisfying the new periodicity criteria in the presence of the field. While for the simple Bravais lattice or periodic potential problem without the field these functions tend to be real, with the applicaton of the field this feature no longer necessarily holds. This is in part due to the phase constraints imposed in the equations above. In the evaluation made above the choice of the symmetric gauge is implicit. This brings us to comments made earlier on the role played by the gauge choice in the form and appearance of these phase factors. A different choice of gauge in which to write the vector potential would indeed alter the quantity of phase change accompanying individual translations. Therefore to extract a physically meaningful quantity one has to look at the overall phase change that the wavefunction undergoes on going around the magnetic unit cell in a full circuit. This amounts to $2\pi p$ which is gauge independent. In a general manner one could consider writing the $u^{\mathrm{n}}_{k_x,k_y}$' s in complex notation with magnitude and phase denoted explicitly as follows

$$u^{\mathrm{n}}_{k_x,k_y}(x,y) = |u^{\mathrm{n}}_{k_x,k_y}(x,y)|e^{i\vartheta_{k_x,k_y}(x,y)}$$

In this form it becomes easier to give a geometric interpretation for the flux quanta through a magnetic unit cell in terms of the total change in the phase of the complex phasor above. This can be thought of as a vector whose orientation is specified by $\vartheta_{k_x,k_y}(x,y)$ which itself is a function of position and hence the arrow representing the complex quantity above rotates accordingly. In case one is interested to quantify the number of complete rotations this oriented quantity makes as one traverses with the function on a closed path around the magnetic unit cell, it is possible to do so

with an integral of the form

$$p = -\frac{1}{2\pi}\int d\mathbf{s}\frac{\partial\vartheta_{k_x,k_y}(x,y)}{d\mathbf{s}} \tag{A.42}$$

Here, the integral is performed in a counterclockwise fashion with $d\mathbf{s}$ being the line element along the path of integration. An important fact to realize here is that the integration takes a gauge dependent quantity $\vartheta_{k_x,k_y}(x,y)$ to a gauge independent one, p. This is because accumulating the tangent to the phase function along the path in this manner is effectively a line integral of the vector potential around a loop and this through Stoke's theorem is related to the curl of the vector potential and hence the magnetic field. What one is actually computing here is a topological quantity which is independent of the choice of gauge potential. Kohmoto in [274] chooses to understand p as the number of zerores of the generalized Bloch function $u^{\mathrm{n}}_{k_x,k_y}(x,y)$ lying inside a magnetic unit cell. This is based on the view that going in a circle around a zero of the wavefunction either clockwise or anticlockwise contibutes a 1 or -1 to the integral above. As the arrow representing the function completes one full rotation on encircling a zero. Thus we can imagine a sort of epicyclical rotation of the arrow as the circuit around the magnetic cell is covered. And now there are multiple rotations (p in number) as several zeros coincide at the same point. These zeros are also called vortices and the associated topological number, p here, is called the vorticity.

This brings us as far as we can come with a continuum analysis, ignoring the topological details for now. In this framework it became possible to give a general definition of magnetic translation operators and identify a commuting subset of these which allows modified solutions of the Bloch variety to be defined. However, apart from the changes to the size of the Brillouin zone, so far no mentions of the band structure and the modifications to it in the presence of the field have been made. This is to be addressed in the following section where we shift to the tight binding

perspective.

A.3.2 Tight Binding and Band structure

The tight binding method within the single band limit has the advantage of providing the energy explicitly as an analytical function of $\mathbf{k}$ which describes a single band of the system, usually in a nearest neighbour approximation. This is true when one uses this technique in tandem with a knowledge of the exact energy eigenfunctions of the system. Such an approach leads to the following function for the energy band of the square lattice, as is familiar from fundamental solid state physics

$$E_0(\mathbf{k}) = 2E_0[\cos k_x a + \cos k_y a] \tag{A.43}$$

This function results on writing the eigenvalue problem for the square lattice with a nearest neigbor tight binding Hamiltonian for the lattice electrons and the eigenfunctions chosen to be plane waves satisfying the Bloch criterion. In section A.2 we derived a 1-dimensional tight binding nearest neighbour Hamiltonian for the system of electrons on a square lattice in a magnetic field. In the process we came across a glimpse of the 2-D tight binding Hamiltonian of the system that can be captured from eq.(A.24), where the secular equation of the corresponding eigenvalue problem is expressed. Since we are interested in aspects of the band structure it would help to see how such a Hamiltonian emerges from the eigenvalue function in eq.(A.43). This would require us to invoke the theorem due to Luttinger discussed in section A.2. Where we may recall that a transformation of the kind $\mathbf{k} \to \mathbf{k}' = \frac{1}{\hbar}(\mathbf{p} - \frac{e}{c}\mathbf{A})$, which promotes the $E_0(\mathbf{k})$ to an operator $\widehat{E}_0$ as discussed earlier, is called for. We return to to the Landau gauge choice $\mathbf{A}(x, y) = B(0, -x, 0)$ to maintain consistency with previously obtained expressions.

Under this transformation the following replacements have to be made $k_x \to$

$k'_x = -i\partial/\partial x$, $k_y \to k'_y = -i\partial/\partial y + eBx/\hbar c$ in the eigenvalue equation

$$\begin{aligned}
&\widehat{E}_0(\mathbf{k}')u(\mathbf{r}) = \widetilde{E}u(\mathbf{r}) \\
&2E_0[\cos k'_x a + \cos k'_y a]u(\mathbf{r}) = \widetilde{E}u(\mathbf{r}) \\
&2E_0\left[\cos\left(-ia\frac{\partial}{\partial x}\right) + \cos\left(-ia\frac{\partial}{\partial y} + \frac{eaBx}{c}\right)\right]u(\mathbf{r}) = \widetilde{E}u(\mathbf{r})
\end{aligned} \tag{A.44}$$

where $u(\mathbf{r})$ is chosen to denote the position dependent state function in reciprocal space basis. If in the above the cosines are written in the exponentaited notation of Fourier components and we use the fact that $\exp\{\pm a\partial_i\}$ with $i = x, y$ is just the generator of translations along coordinate directions by $\pm a$, the eigenvalue equation assumes the familiar tight binding form in position space

$$[u(x+a)+u(x-a)+e^{\frac{ie}{\hbar c}Bax}u(y+a)+e^{\frac{-ie}{\hbar c}Bax}u(y-a)] = \widetilde{E}/E_0 u(\mathbf{r}) = \widetilde{E}^0 u(x) \tag{A.45}$$

Substituting here $u(\mathbf{r}) = e^{ik_y y}u(x)$ gives us the 1D form that we had earlier derived

$$\begin{aligned}
u(x+a) + u(x-a) + 2\cos\left(\frac{eBax}{\hbar c} + k_y a\right)u(x) &= \widetilde{E}^0 u(x) \\
\Rightarrow u_{n+1} + u_{n-1} + 2\cos(2\pi\alpha n + k_y a)u_n &= \widetilde{E}^0 u_n
\end{aligned} \tag{A.46}$$

This, it is easy to see, is exactly the secular equation in eq.(A.26) with the minor exception that ζ is missing on account of the fact that we have taken the hopping energies to be identical along both coordinate directions in the square lattice. Also $\widetilde{E}^0$ here, which is basically $\widetilde{E}/E_0$, is in good agreement with its anologue in eq.(A.26). Along side this, the equivalence between θ and $k_y a$, soundly establishes the correspondence between the two equations.

The above exercise shows an alternate means of setting up the 1-D tight binding nearest neighbor Hamiltonian for the system which is firmly rooted in a 2-D reciprocal space single band formulation, hence quite different from the localized

basis technique of section A.2 . The brief description made here illustrates, facts earlier noted, that an important switch occurs when the magnetic field is turned on and originally real eigenvalues change to operators. An instance of the non-commutativity of **k**-space coordinates brought on by a modification of the energy band function in the spirit of Peierls' substitution as affirmed by Luttinger's extension to Wannier's theorem. A Hamiltonian defined with these non-commuting variables is hardly expected to be diagonal. So a diagonal $H(\mathbf{k})$, which is a feature of periodic lattice systems and what makes the reciprocal space such an appealing basis to solve the eigenvalue problem, is absent as can be seen from eq.(A.44).

This difficulty however, does not entirely rule out a **k**-space approach to the solution. Rather we shall see that, if approached in the right manner, one does achieve considerable simplification of the system of secular equations in this domain due to the favourable boundary conditions available here alongwith the deep duality properties of the system. In order to fully exploit this it is important to note that the eigenvalue problem in **k**-space and hence the Hamiltonian $H(\mathbf{k})$ are not restricted to a 2-D description of the kind in eq.(A.44). Which is more of a continuum variety in reciprocal space just as the Hamiltonian $\mathcal{H}$ of eq.(A.1) is in position space. This invites the consideration that one could in principle explore, just as was done for position space, the possibility of a 1-D description of $H(\mathbf{k})$. Thus, as it turns out, such a description greatly simplifies the problem when used in conjunction with the reciprocal space implications of the commuting magnetic translation operators in position space. The method that we shall use to obtain the Hamiltonian in this 1-D form needs some justification.

It is a remarkable feature of this model that, within the reciprocal space picture, a discretized 1-D tight binding like, nearest neighbour Hamiltonian can be obtained by pursuing much of the same reasoning that applies to the position space picture. In the vein of remarks made earlier the gauge field causes both the real and Fourier

domains to have the same formal structure and the duality of the model resides in this homogenity. What becomes apparent is that the gauge modified hoppings in real space translate to couplings between different wavevectors/crystal momenta in **k**-space. A consequence of using a localized basis in this space much like a Wannier basis on the sites in position space, except here the basis vectors are indexed continuously by the **k** values. By choosing to localize in reciprocal space it is implicit that one is adopting extended Bloch wave functions in position space of which the generalized variety of eq.(A.41) are a special case. Reasoning that serves us well for the case of rational α since working with such extended states is more in line with an energy band description. The couplings in reciprocal space yeild off-diagonal terms in the Fourier transformed Hamiltonian and the effort centers on trying to minimize these terms by choosing appropriate sets of **k** values that do not couple. As a result of this we obtain the 1-D Hamiltonian which is a symmetric tridiagonal matrix that offers the easiest path to the eigenvalues of the system. This can be thought of as the reciprocal space implication of the real space exercise of defining commuting magnetic translation operators. The Brillouin zone restructuring and reinterpretation that follows, yields the new band structure with finer subbands appearing.

At this point it proves useful to shift to a formalism that captures and illustrates the above features in the most economical fashion. For this purpose the notation of second quantized operators to write the translation operators the Hamiltonian is immensely helpful. We choose to abstract the 2-D nearest neighbour tight binding Hamiltonian form the eigenvalue equation in eq.(A.45) and model the translation and phase multiplication of the wavefunction $u(\mathbf{r})$ seen there using covariant translation operators. Note that these translation operators have no precedent in our discussions so far and do not originate in a continuum picture as was the case with the ones defined in the previous segment. They emerge rather from the discretized

tight binding model of the Hamiltonian and are defined only at the lattice points in space. However, an earlier expression that does come close may be found in the equations (A.32) and (A.33) where the discretization is enforced by the strong localization requirement. In the continuum discussion there these operators commute with the Hamiltonian $\mathcal{H}$ and strong localization is a useful simplification. If one goes to a tight binding picture though, these operators in terms of their non-commuting orthogonal $\hat{x}$ and $\hat{y}$ components enter into the structure of the Hamiltonian and hence fail to commute with it. Thus, whereas in the continuum case commuting with the Hamiltonian did not depend on the commutation of the translations along the orthogonal components, it does so in case of the discretized tight binding description. Here we shall make no reference to any particular gauge choice unlike in eq.(A.45). So shifts in the wavefunction along either primitive lattice vector of the square lattice may, most generally, acquire phase. The tight binding Hamiltonian thus, in an arbitrary $U(1)$ guage choice, is written as follows using these translation operators

$$H = -t(\widetilde{T}_x + \widetilde{T}_y) + \text{h.c.} \tag{A.47}$$

where, $\widetilde{T}_x = \sum_{n,m} b^\dagger_{n+1,m} b_{n,m} e^{i\theta^x_{nm}}$ and $\widetilde{T}_y = \sum_{n,m} b^\dagger_{n,m+1} b_{n,m} e^{i\theta^y_{nm}}$ are the translation operators for moving the electrons by a lattice constant in the $\hat{x}$ and $\hat{y}$ directions respectively, t being the corresponding hopping energy. The covariant translation operators are written in second quantized notation using the site-indexed creation and annihilation operators, $b^\dagger$ and b, respectively . The phases here are consistently given by $\theta^x_{nm} = \frac{e}{\hbar c} \int_n^{n+1} A_x dx$ and $\theta^y_{nm} = \frac{e}{\hbar c} \int_m^{m+1} A_y dy$, A_x and A_y being the x and y components of $\mathbf{A}$. These choices are a result of considering the summation to range over the nearest-neigbours of the given lattice site and so one need only integrate the vector potential over branches of the lattice connecting to these neighbouring sites. Since this is the most general depiction of the problem where moving along either branch of the square lattice contributes a phase to the electron's wavefunction. Once

again these translation operators suffer from the same non-commutativity issues that plagued their brethren. This can be illustrated by considering the successive action of translations in orthogonal directions on a site-localized state $|n,m\rangle = b^\dagger_{n,m}|0\rangle$ by flipping the ordering as follows

$$\begin{aligned}
\widetilde{T}_x\widetilde{T}_y|n,m\rangle &= \widetilde{T}_x b^\dagger_{n,m+1}e^{i\theta^y_{nm}}|0\rangle = e^{i(\theta^y_{nm}+\theta^x_{nm+1})}b^\dagger_{n+1,m+1}|0\rangle \\
\widetilde{T}_y\widetilde{T}_x|n,m\rangle &= \widetilde{T}_y b^\dagger_{n+1,m}e^{i\theta^x_{nm}}|0\rangle = e^{i(\theta^x_{nm}+\theta^y_{n+1m})}b^\dagger_{n+1,m+1}|0\rangle \\
\widetilde{T}_y\widetilde{T}_x|n,m\rangle &= e^{i2\pi\varphi_{nm}}\widetilde{T}_x\widetilde{T}_y|n,m\rangle
\end{aligned} \tag{A.48}$$

Here, we have a result similar to that in eq.(A.38) with $2\pi\varphi_{nm} = \theta^x_{nm} + \theta^y_{n+1m} - \theta^x_{nm+1} - \theta^y_{nm}$ which is exactly $\frac{2\pi e}{hc}\oint \mathbf{A}.d\mathbf{r}$ i.e. line integral of the vector potential around a cell of the square lattice, which follows from the way these phases have been defined. This makes the φ_{nm} equivalent to α in eq.(A.38) since the integral just evaluates to the flux of the magnetic field through an individual cell of the square lattice. As already understood, to move in the direction of a Bloch-like analysis, the task is to construct operators that commute with the Hamiltonian and amongst themselves, structural cues for doing which are taken from the form of the operators above. Something which can be achieved by defining magnetic translation operators in a spirit similar to that of the $\widetilde{\mathcal{T}}$'s derived earlier but this time in the second quantized formalism. To do this we consider

$$\widetilde{\mathcal{T}}_x = \sum_{n,m} b^\dagger_{n+1,m}b_{n,m}e^{i\chi^x_{nm}} \qquad \widetilde{\mathcal{T}}_y = \sum_{n,m} b^\dagger_{n,m+1}b_{n,m}e^{i\chi^y_{nm}}$$

We now determine the conditions on the phases χ^x_{nm} and χ^y_{nm} for the operators defined above to commute with the Hamiltonian in eq.(A.47). One of the commutation

relations that must be satisfied for this to happen is $[\widetilde{T}_x, \widetilde{\mathcal{T}}_x] = 0$ which implies

$$\begin{aligned}
[\widetilde{T}_x, \widetilde{\mathcal{T}}_x] &= \sum_{n,m} b^{\dagger}_{n+2,m} b_{n,m} e^{i(\chi^x_{nm} + \theta^x_{n+1m})} [e^{(\chi^x_{n+1m} + \theta^x_{nm} - \chi^x_{nm} - \theta^x_{n+1m})} - 1] = 0 \\
&\Rightarrow \chi^x_{n+1m} + \theta^x_{nm} - \chi^x_{nm} - \theta^x_{n+1m} = 0 \\
&\Rightarrow \Delta_x \chi^x_{nm} = \Delta_x \theta^x_{nm}
\end{aligned} \tag{A.49}$$

Similarly one could work out the remaining constraints from the commutators $[\widetilde{\mathcal{T}}_x, \widetilde{T}_y] = 0$, $[\widetilde{\mathcal{T}}_y, \widetilde{T}_x] = 0$ and $[\widetilde{\mathcal{T}}_y, \widetilde{T}_y] = 0$. They yeild $\Delta_y \chi^x_{nm} = \Delta_x \theta^y_{nm} = \Delta_y \theta^x_{nm} + 2\pi\varphi_{nm}$, $\Delta_x \chi^y_{nm} = \Delta_y \theta^x_{nm} = \Delta_x \theta^y_{nm} - 2\pi\varphi_{nm}$ and $\Delta_y \chi^y_{nm} = \Delta_y \theta^y_{nm}$ respectively. Solving these relations for χ^x_{nm} and χ^y_{nm} we obtain

$$\chi^x_{nm} = \theta^x_{nm} + 2\pi m \varphi_{nm} \qquad \chi^y_{nm} = \theta^y_{nm} + 2\pi n \varphi_{nm}$$

In this manner one is able to derive operators that commute with the Hamiltonian in eq.(A.47) but these operators still do not commute amongst themselves i.e. $[\widetilde{\mathcal{T}}_x, \widetilde{\mathcal{T}}_y] \neq 0$. This is a matter that has already been considered where we shifted from the $\widetilde{\mathcal{T}}$ to the $\widetilde{\mathcal{T}}'$ operators by arguing an enlargement of the unit cell. As was apparent there, this introduction of operators with an Abelian Lie algebra, is a gauge dependent procedure. We showed that for the Landau gauge the commuting subset of the magnetic translation operators is formed by $\widetilde{\mathcal{T}'}_x \equiv \widetilde{\mathcal{T}}_{x=qa} = \widetilde{\mathcal{T}}^q_x$ and $\widetilde{\mathcal{T}'}_y \equiv \widetilde{\mathcal{T}}_{y=a} = \widetilde{\mathcal{T}}_y$. This applies identically in the current formalism. A quick way to see this is that in eq.(A.38), where the commutation is off by a phase with α and φ_{nm} already shown to be identical, if one hits both sides of this equation with $\widetilde{\mathcal{T}}_x$ successively 'q' times for $\alpha = \varphi_{nm} = p/q$ then

$$\begin{aligned}
\widetilde{\mathcal{T}}^q_x \widetilde{\mathcal{T}}_y &= e^{i2\pi q \varphi_{nm}} \widetilde{\mathcal{T}}_y \widetilde{\mathcal{T}}^q_x \\
\widetilde{\mathcal{T}}^q_x \widetilde{\mathcal{T}}_y &= \widetilde{\mathcal{T}}_y \widetilde{\mathcal{T}}^q_x
\end{aligned} \tag{A.50}$$

With these operators one can find a set of good quantum numbers for the system that label the energies unambiguously. As can be surmised from the eigenvalue equations of eq.(A.39) these quantum numbers are the momentum space wavevectors like the ones known for lattice electrons without the field but, to be precise a subset of them. Note that, as stated formerly, this is because not all values of the original Brillouin zone serve as good quantum numbers, atleast not altogether at once, as will become clearer when we obtaint the Fourier transformed Hamiltonian $H(\mathbf{k})$. Only that subset of wavevectors or pseudomomenta is useful in this regard which corresponds to translations along the sides of the magnetic unit cell. As is dictated by the Abelian translation group obtained above that commutes with the Hamiltonian, the new Brillouin zone is defined within the limits $0 \leq k_x \leq 2\pi/qa$ and $0 \leq k_y \leq 2\pi/a$. If one looks back at the generalized Bloch functions of eq.(A.41) it is clear that it is the displacements along the sides of the magnetic unit cell that allow a certain set of continuous $\mathbf{k}$-space values to qualify as good quantum numbers. Even when this is true one sees that the functions $u^{\mathrm{n}}_{k_x,k_y}$ still do not have the exact periodicity seen in Bloch functions but have phases attached to their translations by magnetic cell vectors. Although one may in principle get rid of these by making certain choices for p and q and, most importantly, by imposing localization through fixing $x = qa$ and $y = a$ in the relations there. This reinforces what has been a recurrent theme in attempting to solve the problem of lattice electrons in a magnetic field by placing localization in the position space site-based functions as a foremost requirement to obtain a band like solution for the system. Under the present gauge choice only the $\hat{y}$ direction translations have phase contributions given by $\theta^y_{nm} = \frac{e}{\hbar c}\int_m^{m+1} A_y dy = \frac{e}{\hbar c} aBn(m+1-m) = 2\pi n\varphi_{nm}$. Therefore in the present formalism the operators in eq.(A.47) become $\widetilde{T}_x = \sum_{n,m} b^\dagger_{n+1,m} b_{n,m}$ which is just an ordinary translation as if the field were absent and $\widetilde{T}_y = \sum_{n,m} b^\dagger_{n,m+1} b_{n,m} e^{i2\pi n\varphi_{nm}}$ being appropriately covariantized.

With the knowledge of a commuting subset of magnetic translations and the

existence of corresponding momentum quantum numbers it is possible to use a description of the eigenstates indexed by these momenta to draw certain conclusions regarding the spectrum of the case being considered. For instance, consider a momentum space ket $|\mathbf{k}\rangle = |k_x, k_y\rangle$, which is a localized function of reciprocal space coordinates, as satisfying the requirements of being an eigenstate of the system. We have seen that the operators $\widetilde{\mathcal{T}}_x$ and $\widetilde{\mathcal{T}}_y$ commute with the Hamiltonian so a state $\widetilde{\mathcal{T}}_x|k_x, k_y\rangle$ is also an eigenstate of the system. Again, since $\widetilde{\mathcal{T}}_x$ and $\widetilde{\mathcal{T}}_y$ do not commute with each other it turns out that this state does not have the same set of quantum mumbers as $|k_x, k_y\rangle$. This can be seen with the help of the eigenvalue equations in eq.(A.39) where one is called on to replace ψ with $|\mathbf{k}\rangle$ to put them in the present notational context of states labelled by the crystal momenta. Their remaining structure is unchanged and one may use them to illustrate

$$\widetilde{\mathcal{T}}_y\widetilde{\mathcal{T}}_x|k_x, k_y\rangle = e^{-i2\pi\varphi_{nm}}\widetilde{\mathcal{T}}_x\widetilde{\mathcal{T}}_y|k_x, k_y\rangle = e^{i(k_y-2\pi\varphi_{nm})}\widetilde{\mathcal{T}}_x|k_x, k_y\rangle$$

where we have used the eigenvalue equation $\widetilde{\mathcal{T}}_y|\mathbf{k}\rangle = e^{ik_y}|\mathbf{k}\rangle$. Thus, the quantum numbers associated with the state $\widetilde{\mathcal{T}}_x|k_x, k_y\rangle$ are $(k_x, k_y - 2\pi\varphi_{nm})$ as opposed to those for the state $|k_x, k_y\rangle$ given by (k_x, k_y) although both the states have the same energy. The steps illustrated in the above equation may be repeated 'q' times by the application of $\widetilde{\mathcal{T}}_x$ and hence one can have 'q' distinct k_y values implying 'q' different quantum numbers corresponding to the same energy. The system therefore has a q-fold degeneracy in its spectrum when $\varphi_{nm} = p/q$ i.e rational and written as a ratio of coprime integers.

For a fuller understanding of the spectral properties and hence the band structure we need to shift to a complete momentum space description of the system. This is brought about by Fourier transforming the Hamiltonian H in eq.(A.47). Let us write the position space version of this Hamiltonian in the Landau gauge chosen

above. This happens to be

$$H = \sum_{n,m} -tb^{\dagger}_{n+1,m}b_{n,m} - tb^{\dagger}_{n,m+1}b_{n,m}e^{i2\pi n\varphi_{nm}} + \text{h.c.} \tag{A.51}$$

In order to obtain the Fourier transform of the above Hamiltonian denoted by $H(\mathbf{k})$ which is defined by the following transform integral

$$H = \frac{1}{(2\pi)^2}\int_{-\pi}^{\pi} dk_x \int_{-\pi}^{\pi} dk_y H(\mathbf{k}) \tag{A.52}$$

it becomes necessary to define first the Fourier transforms of the creation and annihilation operators as

$$\begin{aligned} b^{\dagger}_{n,m} &= \frac{1}{(2\pi)^2}\int_{-\pi}^{\pi} dk_x \int_{-\pi}^{\pi} dk_y e^{i(k_x n + k_y m)} b^{\dagger}_{k_x,k_y} \\ b_{n,m} &= \frac{1}{(2\pi)^2}\int_{-\pi}^{\pi} dk_x \int_{-\pi}^{\pi} dk_y e^{-i(k_x n + k_y m)} b_{k_x,k_y} \end{aligned} \tag{A.53}$$

Here, $b^{\dagger}_{k_x,k_y}$ and b_{k_x,k_y} are the momentum space creation and annihilation operators respectively. The $\mathbf{k}$-space coordinates, $-\pi \leq k_x \leq \pi$ and $-\pi \leq k_y \leq \pi$, are considered to be folded up into a 2-torus representing the FBZ of the square lattice such that $k_x \equiv k_x + 2\pi j$ and $k_y \equiv k_y + 2\pi l$, j and l being integers. Also from the manner in which the limits of the Brillouin zone have been defined we are working in units scaled such that the lattice constant a is taken to be unity. The idea is to substitute these expansions in the Hamiltonian above and arrange the resulting expression to enable comparison with eq.(A.52) such that $H(\mathbf{k})$ can be read off from there. On a slightly more pedantic note, an additional factor of $\sqrt{N}$, N being the number of sites in the square lattice for a finite system, is required in the denominator of the transform integrals to satisfy certain normalization requirements. It will also play a role in an identity that shall be used to simplify the expressions while computing $H(\mathbf{k})$ but since it gets cancelled on the whole and does not affect

the final result we may as well regard its presence as implicit. On substituting the above expansions in H we get for the $\hat{x}$ direction translation term $\sum_{n,m} -tb^{\dagger}_{n+1,m}b_{n,m}$ and its hermitian conjugate

$$
\begin{aligned}
&= -t\sum_{n,m}\frac{1}{(2\pi)^4}\int_{-\pi}^{\pi}dk_x\int_{-\pi}^{\pi}dk_y\int_{-\pi}^{\pi}dk'_x\int_{-\pi}^{\pi}dk'_y\Big\{b^{\dagger}_{k_x,k_y}e^{i[k_x(n+1)+k_ym]}b_{k'_x,k'_y}e^{-i[k'_xn+k'_ym]} \\
&\quad + b^{\dagger}_{k_x,k_y}e^{i[k_x(n-1)+k_ym]}b_{k'_x,k'_y}e^{-i[k'_xn+k'_ym]}\Big\} \\
&= -t\sum_{n,m}\frac{1}{(2\pi)^4}\int_{-\pi}^{\pi}dk_x\int_{-\pi}^{\pi}dk_y\int_{-\pi}^{\pi}dk'_x\int_{-\pi}^{\pi}dk'_y\Big\{b^{\dagger}_{k_x,k_y}b_{k'_x,k'_y}e^{ik_x}e^{i[(k_x-k'_x)n+(k_y-k'_y)m)]} \\
&\quad + b^{\dagger}_{k_x,k_y}b_{k'_x,k'_y}e^{-ik_x}e^{i[(k_x-k'_x)n+(k_y-k'_y)m)]}\Big\}
\end{aligned}
$$

At this point an identity for periodic systems that is helpful is $\sum_{\mathbf{R}_{nm}} e^{i\bar{\mathbf{k}}\cdot\mathbf{R}_{nm}} = N\delta_{\bar{\mathbf{k}},0}$ which holds for any Bravais lattice where N, as before, is the total number of sites, $\mathbf{R}_{nm}$ stands for any Bravais lattice vector and $\bar{\mathbf{k}}$ is any vector in the first Brillouin zone which is consistent with the Born-von Karman boundary conditions. For a proof one may refer to Appendix F of *Solid State Physics* by Aschcroft and Mermin. The reason this is helpful is that in the above expression one may harmlessly move the summation $\sum_{n,m}$ past the integrations and apply it on the exponential $e^{i[(k_x-k'_x)n+(k_y-k'_y)m)]}$ which yields the following application of the identity

$$\sum_{n,m} e^{i[(k_x-k'_x)n+(k_y-k'_y)m)]} = N\delta_{(k_x-k'_x,k_y-k'_y),0}$$

Note that using this relation will necessarily bring N into our expressions but, as mentioned before, cancels with the N that implicitly resides in the denominator with $(2\pi)^4$. Thus we may neglect it without loss of generality. We may now use this result to simplify the combination of integration and summation calculated earlier

to

$$\frac{1}{(2\pi)^4}\int_{-\pi}^{\pi}dk_x\int_{-\pi}^{\pi}dk_y\int_{-\pi}^{\pi}dk'_x\int_{-\pi}^{\pi}dk'_y\Big\{b^\dagger_{k_x,k_y}b_{k'_x,k'_y}e^{ik_x}\delta(k_x-k'_x)\delta(k_y-k'_y)$$
$$+\,b^\dagger_{k_x,k_y}b_{k'_x,k'_y}e^{-ik_x}\delta(k_x-k'_x)\delta(k_y-k'_y)\Big\}$$

where it is possible to use an identity known to be valid for Fourier integrals, $\frac{1}{(2\pi)^2}\int_{-\pi}^{\pi}dk'_x\int_{-\pi}^{\pi}dk'_y\delta(k_x-k'_x)\delta(k_y-k'_y)=1$, representing the integration of a 2-D Dirac distribution over a 2-torus and the fact that the ditribution samples any function of $\mathbf{k}$ being integrated with it at $k'_x=k_x$ and $k'_y=k_y$. With this one can immediately write

$$\begin{aligned}\sum_{n,m}-tb^\dagger_{n+1,m}b_{n,m}+\text{h.c.}&=-t\frac{1}{(2\pi)^2}\int_{-\pi}^{\pi}dk_x\int_{-\pi}^{\pi}dk_y b^\dagger_{k_x,k_y}b_{k_x,k_y}(e^{ik_x}+e^{-ik_x})\\&=\frac{1}{(2\pi)^2}\int_{-\pi}^{\pi}dk_x\int_{-\pi}^{\pi}dk_y[-2t\cos(k_x)b^\dagger_{k_x,k_y}b_{k_x,k_y}]\end{aligned}\tag{A.54}$$

A similar series of steps can be applied for the $\hat{y}$ direction translation term $\sum_{n,m}-tb^\dagger_{n,m+1}b_{n,m}e^{i2\pi n\varphi_{nm}}$ and its hermitian conjugate but this analysis is made slightly more interesting by the presence of the phase term. In this case we have

$$\begin{aligned}=&-t\sum_{n,m}\frac{1}{(2\pi)^4}\int_{-\pi}^{\pi}dk_x\int_{-\pi}^{\pi}dk_y\int_{-\pi}^{\pi}dk'_x\int_{-\pi}^{\pi}dk'_y\Big\{b^\dagger_{k_x,k_y}e^{i[k_xn+k_y(m+1)]}b_{k'_x,k'_y}e^{-i[k'_xn+k'_ym]}e^{i2\pi n\varphi_{nm}}\\&+b^\dagger_{k_x,k_y}e^{i[k_xn+k_y(m-1)]}b_{k'_x,k'_y}e^{-i[k'_xn+k'_ym]}e^{-i2\pi n\varphi_{nm}}\Big\}\\=&-t\sum_{n,m}\frac{1}{(2\pi)^4}\int_{-\pi}^{\pi}dk_x\int_{-\pi}^{\pi}dk_y\int_{-\pi}^{\pi}dk'_x\int_{-\pi}^{\pi}dk'_y\Big\{b^\dagger_{k_x,k_y}b_{k'_x,k'_y}e^{ik_y}e^{i[(k_x-k'_x+2\pi\varphi_{nm})n+(k_y-k'_y)m)]}\\&+b^\dagger_{k_x,k_y}b_{k'_x,k'_y}e^{-ik_y}e^{i[(k_x-k'_x-2\pi\varphi_{nm})n+(k_y-k'_y)m)]}\Big\}\end{aligned}$$

$$=\frac{1}{(2\pi)^4}\int_{-\pi}^{\pi}dk_x\int_{-\pi}^{\pi}dk_y\int_{-\pi}^{\pi}dk'_x\int_{-\pi}^{\pi}dk'_y\Big\{b^{\dagger}_{k_x,k_y}b_{k'_x,k'_y}e^{ik_y}\delta(k_x-k'_x+2\pi\varphi_{nm})\delta(k_y-k'_y)$$
$$+b^{\dagger}_{k_x,k_y}b_{k'_x,k'_y}e^{-ik_y}\delta(k_x-k'_x-2\pi\varphi_{nm})\delta(k_y-k'_y)\Big\}$$

Thus, finally we have

$$\sum_{n,m}-tb^{\dagger}_{n,m+1}b_{n,m}e^{i2\pi n\varphi_{nm}}+\text{h.c.}=\frac{1}{(2\pi)^2}\int_{-\pi}^{\pi}dk_x\int_{-\pi}^{\pi}dk_y-t[e^{-ik_y}b^{\dagger}_{k_x+2\pi\varphi_{nm},k_y}b_{k_x,k_y}$$
$$+e^{ik_y}b^{\dagger}_{k_x-2\pi\varphi_{nm},k_y}b_{k_x,k_y}] \tag{A.55}$$

So from the equations eq.(A.54) and eq.(A.55) whose sum gives the complete Hamiltonian one can compare to eq.(A.52) and it is possible to read off $H(\mathbf{k})$ as the following expression

$$H(\mathbf{k})=-2t\cos(k_x)b^{\dagger}_{k_x,k_y}b_{k_x,k_y}-t[e^{-ik_y}b^{\dagger}_{k_x+2\pi\varphi_{nm},k_y}b_{k_x,k_y}+e^{ik_y}b^{\dagger}_{k_x-2\pi\varphi_{nm},k_y}b_{k_x,k_y}] \tag{A.56}$$

From this structure of the Fourier transformed Hamiltonian a couple of things can be readily seen. Firstly, though the Hamiltonian is defined for a unique k_y value throughout, this is not true for the k_x value as it couples to $k_x+2\pi\varphi_{nm}$ and $k_x-2\pi\varphi_{nm}$ thereby leading to off-diagonal terms in the reciprocal space Hamiltonian. At this point we may recall the comments made earlier about how to simplify the structure of the Hamiltonian to such an extent in reciprocal space that the eigenvalue problem becomes reasonably solvable. In order to do so we must recognize that the Fourier variables as presently defined are inadequate to fulfill the role of good quantum numbers since they have been defined keeping the translational symmetry of the bare lattice, without the field, in mind. The presence of the field then makes itself felt in this picture through the couplings between the different k_x sectors, as mentioned before. To find a region of $\mathbf{k}$-space in which the momenta do not couple

becomes pivotal in obtaining a diagonal Hamiltonian in this space. This requires us to identify the correct translational symmetry in the presence of the field which, for the case of rational flux p/q, happens to be that of the magnetic unit cells introduced earlier. Since this implies a reduction in the Brillouin zone by a factor of q along the k_x component this diminished region of momentum space offers the useful quantum numbers with uncoupled momentum values. This we as may recollect from prior statements is is closely linked to the enlarged magnetic unit cell which is constructed by fusing q cells of the square lattice in accordance with the gauge choice. If we define the new variable k_x^0 within this new Brillouin zone sector and wish to write the Hamiltonian in eq.(A.56) in terms of it such that we now work with a diagonal $H(k_x^0, k_y)$ defined by $H = \frac{1}{(2\pi)^2}\int_{-\pi/q}^{\pi/q} dk_x^0 \int_{-\pi}^{\pi} dk_y H(k_x^0, k_y)$. It is required that we use the substitution $k_x = k_x^0 + 2\pi j\varphi_{nm}$ and write the Hamiltonian as a sum over j ranging from 1 to q to address all the k_x values in the FBZ of the bare square lattice. Thus, what has effectively occured, is that the original Brillouin zone has been split up into sectors within which the Fourier Hamiltonian is diagonal and all the far off couplings get resolved into simple couplings between states of the nearest neigbouring sectors in momentum space. To see this let us first write $H(k_x^0, k_y)$ following the definition outlined above

$$H(k_x^0, k_y) = \sum_{j=1}^{q}\Big\{-2t\cos(k_x^0 + 2\pi j\varphi_{nm})b^\dagger_{k_x^0+2\pi j\varphi_{nm},k_y} b_{k_x^0+2\pi j\varphi_{nm},k_y} \\ - t[e^{-ik_y} b^\dagger_{k_x^0+2\pi(j+1)\varphi_{nm},k_y} b_{k_x^0+2\pi j\varphi_{nm},k_y} + e^{ik_y} b^\dagger_{k_x^0+2\pi(j-1)\varphi_{nm},k_y} b_{k_x^0+2\pi j\varphi_{nm},k_y}]\Big\} \tag{A.57}$$

The seperation of the Brillouin zone into q sectors is necessary also, because for $\varphi_{nm} = p/q$ and $-\pi/q \leq k_x^0 \leq \pi/q$, to cover all the $k_x \in [-\pi, \pi]$ one uses the intervals $k_x^0 + 2\pi j\varphi_{nm} \in [-\pi/q + 2\pi j\varphi_{nm}, \pi/q + 2\pi j\varphi_{nm}]$ whose union is taken over $j = 1, \ldots, q$. Thus we have the original single band of the bare square lattice split

up into q subbands. In this way a reduced Brillouin zone of $-\pi/q \leq k_x^0 \leq \pi/q$ ensures that no distinct k_x^1 and k_x^2 belonging to this interval can ever be coupled by the Hamiltonian in eq.(A.57). Because if it were the case that these momenta are coupled then they have to satisfy $k_x^1 + 2\pi j_1 \varphi_{nm} = k_x^2 + 2\pi j_2 \varphi_{nm}$ which implies $k_x^1 - k_x^2 \geq 2\pi\varphi_{nm}$ but this cannot be true since $k_x^1 - k_x^2 = 2\pi/q$ at most. An interesting feature of the above Hamiltonian has to do with its periodicty in reciprocal space. From solid state physics in general it is well known that the FBZ uniquely determines the properties of a periodic system in a reduced zone scheme and that rest of the momentum space is related to the points in here by some combination of reciprocal lattice vectors. This shows up as a periodicity in the $H(\mathbf{k})$ as $H(\mathbf{k} + \mathbf{K}) = H(\mathbf{k})$, $\mathbf{K}$ being a reciprocal lattice vector. For the conventional Brillouin zone of the bare square lattice such a reciprocal lattice vector is $K_x = 2\pi$. However, for $H(k_x^0, k_y)$ one observes a considerably different periodicity since the Hamiltonian at $k_x^0 = 0$ repeats again at $k_x^0 = 2\pi\varphi_{nm}q$ i.e after a shift of $2\pi p$ and so is true for all the other momenta belonging to the reduced Brillouin zone in the presence of the field. Thus the new reciprocal lattice vector $2\pi p$ is p times the older one. This works as, though $H(k_x^0, k_y)$ couples momenta from k_x^0 to k_x values that are technically outside the FBZ of the bare lattice one can always reflect these intervals via a reciprocal lattice vector of the bare lattice to some set of adjacent intervals that cover $[-\pi, \pi]$. Thus the couplings that extend the dependence of the Hamiltonian to a region p times the FBZ of the original square lattice can be rolled into a region of width 2π by this method. This then effectively ensures that the Hamiltonian in $\mathbf{k}$-space repeats itself after cycling once through the q subbands and though this folding may have no otensible effect on the energies it does have an impact on the topological properties of the corresponding wavefunctions satisfying the generalized Bloch criteria as seen earlier.

A clearer way to see the q subband structure is by using this Hamiltonian in an

eigenvalue equation. We expect that since the k_y values do not couple at all the Hamiltonian has the possibility of an effective 1-D description, just as in position space but this time with the added advantage that the number of sites is limited to q. To see this let us write the eigenvalue equation in momentum space as

$$H(k_x^0, k_y)|\Psi_{\mathbf{k}}\rangle = E_{k_x^0,k_y}|\Psi_{\mathbf{k}}\rangle \tag{A.58}$$

The dimensionality of $H(k_x^0, k_y)$ may be inferred in some sense from the position space translationally symmetric modification of the simple unit cell to a q times bigger magnetic unit cell. This is akin to having multiple sites per unit cell and hence, if viewed generally from the perspective of such lattices, the wavefunction for such a unit cell is considered as a superposition of the contributing local orbitals at each site whose overlap gives the correct valence configuration of electrons as required for a tight binding description. This then gives a reciprocal space Hamiltonian of corresponding dimensionality, so for q sites the Hamiltonian is $q \times q$ dimensional for a given $\mathbf{k}$ value. Usually in the simplest case one is concerned with the same single orbital at each site which is also true here. In cases where multiple orbitals have to be considered at each site the reciprocal space Hamiltonian may have non zero off diagonal terms due to the Hamiltonian coupling distinct orbitals at the same $\mathbf{k}$ value. However, for $H(k_x^0, k_y)$ such terms arise within the same orbital for different $\mathbf{k}$ values hence ruling out an exact diagonal description in momentum space with energies characterized by unique pseudomomenta. So, as we shall see, one is at best able to reduce to a system of equations that couples neighbouring sets of otherwise uncoupled $\mathbf{k}$ values. These features of the reciprocal space Hamiltonian can be conveniently embedded in the above eiegnvalue equation by a basis which is the set of plane waves one from each of the q sectors and indexed by momenta which are coupled. Each of these q states can be thought of as the Fourier counterpart of corresponding position space orbitals at the q inequivalent sites when transformed

to momentum space using their periodicities with the appropriate lattice vectors. This slightly simplified picture is achieved if the state $|\Psi_{\mathbf{k}}\rangle$ is constructed as

$$|\Psi_{\mathbf{k}}\rangle = \sum_{j=1}^{q} \psi_j b^{\dagger}_{k_x^0+2\pi j\varphi_{nm},k_y}|0\rangle \tag{A.59}$$

where $|0\rangle$ denotes the vaccum state from which other occupied states of various energies may be obtained by the action of the creation operator as shown above. Thus, we see that in this form the state is a q component wavefunction for a given k_x^0 and k_y. In this choice of basis when one expresses $H(k_x^0, k_y)$ in the eigenvalue relation of eq.(A.58) with some additional simplifications such as the feature that $H(k_x^0, k_y)$ is diagonal in the annihilation operators. Thus their presence can be absorbed into the vaccum state as they may contribute at best as phases and not affect the eigenvalues. The creation operators on the other hand do involve couplings which as seen in the basis choice above can be used to generate states from the vaccum. This helps to translate these couplings to the coefficients ψ_j's of the various momentum sectors resulting in a nearest neighbour tight binding like description, for the eigenvalue eq.(A.58), as follows

$$-t[e^{-ik_y}\psi_{j-1} + e^{ik_y}\psi_{j+1}] - 2t\cos(k_x^0 + 2\pi j\varphi_{nm})\psi_j = E_{k_x^0,k_y}\psi_j \tag{A.60}$$

This sets up a set of secular equations that yeild q eigenvalues when $\varphi_{nm} = p/q$ by splitting a single band of the bare square lattice to q subands in the presence of the field. As can be seen this is again a Harper equation but now formulated in a complete momentum space description and with an additional boundary constraint on the coefficients given by $\psi_{j+q} = \psi_j$. At various points in our discussion so far, of the problem of Bloch electrons in a magnetic field, we have made mention of the duality property of this system. Any coordinate transformation in the presence of the magnetic field is tantamount to a gauge transformation. Also as the field causes

position space coordinate variables and reciprocal space variables to fail to commute amongst themselves the gauge/coordinate transformation within a particular representation also acquires a Fourier transformation like character. The duality manifests as an identical exchange of the variables in terms of how they occur in the expressions of various gauge independent functions of these variables when formulated in the interchangable gauge choices. This can be seen more explicitly if we choose to apply a transformation of the form

$$\psi_j = \sum_{l=1}^{q} e^{i2\pi\varphi_{nm}jl} g_l \tag{A.61}$$

to eq.(A.60). This yields the following

$$\begin{aligned}
&-t[e^{-ik_y}\sum_{l=1}^{q} e^{i2\pi\varphi_{nm}(j-1)l} g_l + e^{ik_y}\sum_{l=1}^{q} e^{i2\pi\varphi_{nm}(j+1)l} g_l] - 2t\cos(k_x^0 + 2\pi j\varphi_{nm})\sum_{l=1}^{q} e^{i2\pi\varphi_{nm}jl} g_l \\
&\quad = E_{k_x^0,k_y}\sum_{l=1}^{q} e^{i2\pi\varphi_{nm}jl} g_l \\
&\Rightarrow -t[\sum_{l=1}^{q} e^{i2\pi\varphi_{nm}jl}(e^{-i(2\pi\varphi_{nm}l+k_y)} + e^{i(2\pi\varphi_{nm}l+k_y)})g_l] - t(e^{i(k_x^0+2\pi\varphi_{nm}j)} + e^{-i(k_x^0+2\pi\varphi_{nm}j)}) \\
&\quad \times \sum_{l=1}^{q} e^{i2\pi\varphi_{nm}jl} g_l = E_{k_x^0,k_y}\sum_{l=1}^{q} e^{i2\pi\varphi_{nm}jl} g_l \\
&\Rightarrow -t[\sum_{l=1}^{q} 2\cos(k_y + 2\pi\varphi_{nm}l) e^{i2\pi\varphi_{nm}jl} g_l] - t[\sum_{l=1}^{q} e^{ik_x^0} e^{i2\pi\varphi_{nm}j(l+1)} g_l + \sum_{l=1}^{q} e^{-ik_x^0} e^{i2\pi\varphi_{nm}j(l-1)} g_l] \\
&\quad = E_{k_x^0,k_y}\sum_{l=1}^{q} e^{i2\pi\varphi_{nm}jl} g_l \\
&\Rightarrow -t[e^{-ik_x^0} g_{l-1} + e^{ik_x^0} g_{l+1}] - 2t\cos(k_y + 2\pi\varphi_{nm}l) g_l = E_{k_x^0,k_y} g_l
\end{aligned} \tag{A.62}$$

The final equation above is termed the dual of eq.(A.60) and we see that the transformation has exchanged k_x^0 and k_y between the two expressions. In obtaining it a symmetry transformation that has also been used is $k_x^0 \to -k_x^0$, since this leaves the spectrum unchanged as it has reflection symmetry about $k_x^0 = 0$. The duality

transformation as defined above affects this exchange without making any alterations to the definition of the magnetic unit cell, the newly defined Brillouin zone hence, essentially the band structure. Thus the duality transformation belongs to the class of unitary basis changing transformations that leave the physical aspects of the model unchanged. Now if one chose to begin with an alternate gauge choice right from the start with a non zero A_x instead of A_y in the Landau gauge it would lead to phases along translations in the $\hat{x}$ direction unlike what was the case earlier. In this gauge the eq.(A.60) comes out to be

$$-t[e^{-ik_x}g_{l-1} + e^{ik_x}g_{l+1}] - 2t\cos(k_y^0 + 2\pi\varphi_{nm}l)g_l = E_{k_x,k_y^0}g_l \tag{A.63}$$

We note that the above equation when compared with eq.(A.62) shows them to be identical except that in eq.(A.63) the range of the **k**-space variables comprising the Brillouin zone is $-\pi \leq k_x \leq \pi$ and $-\pi/q \leq k_y^0 \leq \pi/q$. This has exactly exchanged the ranges for k_x^0 and k_y in eq.(A.60). Since both the dual form of the secular equations in reciprocal space and the gauge transformed ones are identical in their formal structure and as they both have to give the same physical features of the model, this fact can be used to make certain comments about the spectrum and eigenvalues which would otherwise be quite difficult to deduce. One such property can be determined from the fact that in eq.(A.62) the spectrum $E_{k_x^0,k_y}$ has q subbands due to q coupled k_x sectors while in eq.(A.63) the subbands of E_{k_x,k_y^0} are due to couplings between q k_y sectors. So as $-\pi \leq k_y \leq \pi$ and $-\pi/q \leq k_y^0 \leq \pi/q$, $E_{k_x^0,k_y} = E_{k_x,k_y^0+\frac{2\pi n'}{q}}$, with $n' = 1,\ldots,q$ which means that the spectrum due to $E_{k_x^0,k_y}$ is q-fold degenerate. This can be thought of as say for a given k_x^0 or $k_x^0 + 2\pi j\varphi_{nm}$ belonging to its particular sector all k_y values belong to the same subband and further from the gauge transformed secular equations which give the splitting of the k_y into sectors of $k_y^0 + 2\pi n'\varphi_{nm}$ one knows that groups of such q coupled momenta from these sectors belong to the same energy value and hence the degeneracy must

exist.

Since we began with the objective of obtaining the best route to an efficient diagonalization of the momentum space Hamiltonian, there is a further simplification that can be made over the secular equation in eq.(A.60) that facilitates this aim. To do this we make the substitution $\psi_j = h_j e^{-ik_y j}$ in that equation. This gives us

$$-t[h_{j-1} + h_{j+1}] - 2t\cos(k_x^0 + 2\pi\varphi_{nm}j)h_j = E_{k_x^0,k_y}h_j \tag{A.64}$$

From its appearance it seems we have gotten rid of the k_y dependence but this is superficial since the boundary conditions still contain the dependence on it as $h_{j+q} = e^{ik_y q}h_j$. Yet the above set of secular equations offer a $q \times q$ tri-diagonal matrix with no $\mathbf{k}$ dependence on the diagonal and upper and lower diagonals which considerably simplifies the diagonalization. The only dependence on k_y is present at the upper right and lower left corners, this is to take into account the stated periodic boundary conditions. Thus the eigenvalues of the problem are obtained by diagonalizing the governing matrix $M(E, k_x^0, k_y)$ of the above secular equation which is done by solving the following determinant equation for its roots,

$$\begin{aligned}\mathrm{Det}(M(E,k_x^0,k_y)) &= \mathrm{Det}\begin{vmatrix} \nu_1 - E & -t & 0 & 0 & \cdots & -te^{-iqk_y} \\ -t & \nu_2 - E & -t & 0 & \cdots & 0 \\ \vdots & \vdots & \vdots & \ddots & \vdots & \vdots \\ 0 & \cdots & 0 & -t & \nu_{q-1} - E & -t \\ -te^{iqk_y} & 0 & \cdots & 0 & -t & \nu_q - E \end{vmatrix} \\ &= 0\end{aligned}$$

where, $\nu_j = -2t\cos(k_x^0 + 2\pi\varphi_{nm}j)$. The usual method is to solve for the eigenvalues numerically using routines for symmetric tri-diagonal matrices since the matix in the above determinant can be considered a sparse enough version of this kind with slight

offset due to the corner terms. Though this in general does not affect the quality of the numerically obtained eigenvalues much. There are certain gauge indepedent relations such as the charateristic polynomial from the above determinant whose dependence on k_x and k_y can be determined using duality arguments of the kind used to reason the degeneracy of the spectrum. We shall not enter into these details here. For these and other details the reader is advised to peruse the references mentioned earlier. This concludes our discussion of the spectrum of the AAH model in so far as it permits an analytical approach.

Appendix B

Floquet Theory and high frequency perturbative expansions

B.1 Introduction

In this appendix we shall consider the motivation and description of various aspects of Floquet theory as applied to the study of quantum systems with time-periodic Hamiltonians. Although this is merely a compilation of well known results and techniques belonging to this, by now, significant topic in the literature, it is hoped that collecting them here will provide a ready reference for their use in different portions of the thesis, making it to some degree self-contained. We will also look at some high frequency perturbative expansions for the time-independent Floquet Hamiltonian that have gained recent popularity in the literature, from their use in a wide range of applications that have come to be termed as 'Floquet engineering' [80–82].

The problem of the Schrödinger equation with a periodic in time Hamiltonian has been of considerable interest as a subset of the general time-dependent problem in quantum mechanics. Since, most applications involving time dependence arose in the

context of systems, of atoms or spins, interacting with oscillating electric and magnetic fields, consequently giving rise to spectral transitions [85, 86, 88, 90, 91, 328]. While looking at transitions in discrete quantum systems caused due to interactions with an oscillating field modelled as a classical harmonic sinusoid, Shirley [329], was led to compare the effectiveness of time-dependent perturbation theory (TDPT) techniques in determining the transition probabilities between various states of a system. He discusses, through the most elementary example, that of a two-level system, the various limitations of results obtained via the conventional time-dependent perturbation methods. These include the apparent violation of unitarity of the famous Fermi Golden rule for the transition probability rate at large times, obtained to a first order in perturbation. The ad hoc procedures required to avoid secular and singular terms in these probability amplitudes at resonance and the ineffectiveness of the theory in capturing multiple quantum transitions. Further, the method is burdened with the assumption of a weak field strength. To circumvent these, Shirley suggests making use of phase factoring methods, which take the form of a rotating frame/wave approximation, in the case of say a spin-$\frac{1}{2}$ system in a rotating magnetic field, and seperating the time dependent Hamiltonian into a constant part and one with a comparatively higher frequency time dependence. This higher frequency term is neglected in calculating the transition probabilities and one is able to obtain the same Lorentzian distribution or Rabi line for the transition probability as obtained from TDPT. Furthermore, this expression preserves unitarity and gives the correct form of the Golden rule for large times. This, in a very basic manner, demonstrates the advantages that a time independent approxiamtion has to offer given that one goes about formulating it correctly. Form this one draws the motivation for a more rigorous approach to obtaining a time-independent Hamiltonian for the driven system and Floquet theory enters as a viable formalism to achieve this objective. Essentially, the significant advantage offered by this framework is

the possibility of incorporating the effects of time-dependence to different frequency scales in a perturbative manner to improve the accuracy of the results, where the effects of including the ignored time dependent part begin to be felt. That too in a method that is, in most cases, analytically and computationally simpler than the alternative TDPT methods.

Shirley generalizes the analysis to systems with multiple quantum levels and suggests their reduction to two level systems, for the purpose of studying resonant transitions, via the use of degenerate time-independent perturbation theory, once the constant portion of the Hamiltonian has been seperated out. This finds use in the Floquet formalism as well, since the approach transforms a finite Hamiltonian for a time dependent interaction to an infinite dimensional time-idependent one. The perturbation theory allows to project to a subspace of dimensions equal to those of the undriven Hamiltonian, by accounting for the effects of interactions with the other excluded levels to various orders. As we shall see, the perodicity intrinsic to Floquet systems also helps to simplify the analysis of these systems. Therefore, a general structure for the theory has emerged, where the complete time evolution of the time-periodic system is modelled using a time independent effective Hamiltonian upto a micromotion governed by a periodic-in-time unitary operator. Thus the method concerns itself with employing various means to obtain the effective Hamiltonian, if not exactly, then at least to some reasonable appoximation. A high frequency limit facilitates the calculation of such a Hamiltonian and its concomitant micromotion operator by allowing the use of perturbative expansions that can compute both these operators upto higher orders of accuracy. Various such perturbative schemes have been used in the literature, each with its own merits and demerits [80, 82, 87, 92, 93].

Here, we shall begin by outlining and developing the rudimentary principles of Floquet theory and illustrate their application to the general problem of the time-periodic Schrödinger equation. The notions of the Floquet operator, quasienergies

and Floquet states shall be elucidated and we shall look at various formulations of the time-independent Floquet Hamiltonian and the micromotion operator. We shall also regard some of the more commonly used perturbative expansions in the high frequency driving regime. Along the way the construction of a Floquet Hilbert space becomes apparent [91], denoted by $\mathbb{H}\otimes\mathbb{T}$, which is a composite of the standard Hilbert space $\mathbb{H}$ of the time dependent quantum system and the space of periodic in time functions (with a given time period, say T), denoted by $\mathbb{T}$.

B.2 Basic Floquet Theory

In this section we shall give a brief overview of the various results and conditions associated with Floquet theory. These are all well established mathematically. This will provide the necessary background for applying the theory to the periodic Hamiltonian bearing Schrödinger equation. As regards the notation, all bold uppercase Roman letters denote matrices, lower case ones are vectors and greek indices are used to identify individual components of these matrices or vectors.

The theory addresses a system of differential equations of the form

$$\dot{\mathbf{z}} = \mathbf{A}(t)\mathbf{z} \tag{B.1}$$

where, $\mathbf{A}(t+T) = \mathbf{A}(t)$ is of size $N \times N$, periodic with period T, and $\mathbf{z}$ turns out to be of the form $e^{qt}\mathbf{p}(t)$. This is further known to satisfy the requirement that for the N values $q_1, q_2, \ldots, q_N$,

$$e^{q_1 T} e^{q_2 T} \cdots e^{q_N T} = \exp\left(\int_0^T \mathrm{Tr}(\mathbf{A}(t'))dt'\right). \tag{B.2}$$

We shall now proceed to justify these results using certain ideas from linear algebra and applying them to the theory of differential equations with periodic co-

efficients. Looking at eq.(B.1), one might express its N solutions as the vectors $\mathbf{z}_1(t), \mathbf{z}_2(t), \ldots, \mathbf{z}_N(t)$. From these it is possible to construct a matrix $\mathbf{Z}(t)$ of the form

$$\mathbf{Z}(t) = \left[\left[\mathbf{z}_1\right]\left[\mathbf{z}_2\right]\cdots\left[\mathbf{z}_N\right]\right] \tag{B.3}$$

thereby giving a $N \times N$ matrix whose columns are the N linearly independent solutions of the system of N simultaneous first order differential equations represented in matrix form in eq.(B.1). Such a solution matrix itself satisfies the differential equation $\dot{\mathbf{Z}} = \mathbf{AZ}$, with $\mathbf{Z}$ being called the fundamental matrix if it is non-singular. Which is usually the case since the $\mathbf{z}_1(t), \mathbf{z}_2(t), \ldots, \mathbf{z}_N(t)$ are linearly independent for all cases of interest. In the special case that a boundary condition is satisfied such that $\mathbf{Z}(t_0) = \mathbf{I}$, $\mathbf{I}$ being the identity element, $\mathbf{Z}$ is called the principal fundamental matrix. We shall see that it is this matrix which has a key role to play in the determination of the eigenvalues of the effective time independent Floquet Hamiltonian. Thus it is important to note that the fundamental matrix is decided by the system of differential equations that it satisfies and is characteristically associated to them.

Due to the linearity of the differential equations and hence the fact that any linear combination of the independent solutions should also be a solution of the system, it is of interest to observe that multiplying $\mathbf{Z}$ by a constant non-singular matrix again yeilds another fundamental matrix for the same system of equations. Hence for any constant, non-singular $\mathbf{C}$ a $\mathbf{Y}'(t) = \mathbf{Z}(t)\mathbf{C}$ is nothing but another solution matrix with its columns now being linear combinations of those of $\mathbf{Z}$. This makes $\mathbf{Y}'$ also a fundamental matrix. This may be regarded as a defining property of fundamental matrices. From what we have discussed so far, it would be good to keep in mind that this property of fundamental matrices of the system in eq.(B.1) is to be exploited in identifying the principal fundamental matrix for the Schrödinger equation with periodic coefficients. This, we shall see, plays a crucial role in determining the quasienergies of the driven system.

Another useful property of the solution matrix $\mathbf{Z}$ occurs when its determinant is the same as its Wronskian given by $\mathcal{W}(t)$. When this is true it can be shown that

$$\mathcal{W}(t) = \mathcal{W}(t_0)\exp\left(\int_{t_0}^{t} \mathrm{Tr}(\mathbf{A}(t'))dt'\right). \tag{B.4}$$

To see this, we can expand $\mathbf{Z}(t)$ in a Taylor series expansion about $t = t_0$ with $\Delta t = t - t_0$, and retain terms upto first order in Δt,

$$\begin{aligned}\mathbf{Z}(t) &= \mathbf{Z}(t_0) + \Delta t\ \dot{\mathbf{Z}}(t_0) + \mathcal{O}((\Delta t)^2) \\ &= [\mathbf{I} + \Delta t\ \mathbf{A}(t_0)]\,\mathbf{Z}(t_0) + \mathcal{O}((\Delta t)^2)\end{aligned}$$

Using the above linearized approximation, it follows that the determinant of $\mathbf{Z}(t)$, and from the assumption made earlier, the Wronskian can be written as

$$\begin{aligned}\det(\mathbf{Z}(t)) &= \det[\mathbf{I} + \Delta t\ \mathbf{A}(t_0)]\det(\mathbf{Z}(t_0)) \\ \mathcal{W}(t) &= \det[\mathbf{I} + \Delta t\ \mathbf{A}(t_0)]\,\mathcal{W}(t_0)\end{aligned}$$

An identity of use at this point is the series expansion of a general determinant of the form encountered above, i.e. $\det(\mathbf{I} + \epsilon\mathbf{C}) = 1 + \epsilon\mathrm{Tr}(\mathbf{C}) + \mathcal{O}(\epsilon^2)$. This result follows from there being a term in the determinant which is a product of the diagonal entries and the zeroth and first order in ϵ contributions come from it. Applying this to the expression for the Wronskian gives

$$\mathcal{W}(t) = \mathcal{W}(t_0)\,[1 + \Delta t\ \mathrm{Tr}(\mathbf{A}(t_0))]$$

This may be compared to the Taylor series expansion of $\mathcal{W}(t)$ upto first order in Δt and reading off the first order coefficients from this gives the following differential

equation for $\mathcal{W}(t)$

$$\dot{\mathcal{W}}(t) = \mathcal{W}(t)\mathrm{Tr}\left(\mathbf{A}(t)\right)$$

where, the t_0 dependence of the equation has been generalized to all times t as there have been no assumptions made regarding any fixed choice of t_0. The solution to the above equation given by

$$\mathcal{W}(t) = \mathcal{W}(t_0)\exp\left(\int_{t_0}^{t} \mathrm{Tr}\left(\mathbf{A}(t')\right) dt'\right) \tag{B.5}$$

is a useful relation that will help to prove the identity in eq.(B.2). Soon we shall need this result to obtain a condition on the quasienergies that is dependent on the time average of the trace of the periodic time dependent Hamiltonian.

So far we have not made use of the periodicity property of the system of differential equations in determining the behaviour of their solutions. It is natural from the discussion so far, that if $\mathbf{Z}(t)$ is a solution matrix for the system then $\mathbf{Z}(t+T)$ must also be one. Since this too satisfies the matrix differential equation defined for the system in eq.(B.1). This is easily shown by translating the matrix differential equation, $\dot{\mathbf{Z}}(t) = \mathbf{A}(t)\mathbf{Z}(t)$, by the period T and using the periodicity of $\mathbf{A}(t)$. The question that arises then is how are these two fundamental matrices related to one another.

To understand this let us define $\mathbf{Y}(t) = \mathbf{Z}(t+T)$ and assume a non-singular $\mathbf{C}(t)$ such that $\mathbf{C}(t) = \mathbf{Z}^{-1}(t)\mathbf{Y}(t)$. Now, since

$$\begin{aligned}\mathbf{Y}(t) &= \mathbf{Z}(t)\mathbf{Z}^{-1}(t)\mathbf{Y}(t)\\ &= \mathbf{Z}(t)\mathbf{C}(t)\end{aligned}$$

one can write $\mathbf{Y}(t_0) = \mathbf{Z}(t_0)\mathbf{C}(t_0)$ where we may denote $\mathbf{C}(t_0) = \mathbf{C}_0$. If we choose to

write $\mathbf{Y}_0(t) = \mathbf{Z}(t)\mathbf{C}_0$, which as we know from the property of a fundamental matrix when multiplied by a constant non-singular matrix is also a fundamental matrix, it results in $\mathbf{Y}_0(t)$ also being a solution matrix. At $t = t_0$, $\mathbf{Y}(t_0) = \mathbf{Y}_0(t_0)$ and from the theory of linear ordinary differential equations it is known that they possess a unique solution for a given set of bounadary conditions, therefore it must hold that $\mathbf{Y}_0(t) = \mathbf{Y}(t)$ at all times. Equivalently, $\mathbf{C}(t) = \mathbf{C}_0$ i.e. a constant for all times hence time independent. Thus we arrive at an important property for the solution matrix while applying Floquet theory to a periodic system,

$$\begin{aligned} \mathbf{Y}(t) &= \mathbf{Z}(t)\mathbf{C}_0 \\ \Rightarrow \mathbf{Z}(t+T) &= \mathbf{Z}(t)\mathbf{C}_0. \end{aligned} \tag{B.6}$$

Here, we note that the solution matrices for the system which are seperated in time by a period are related through a transformation by a constant matrix. This result is significant as it is an important step towards obtaining some time independent component from the time dependent equations. The constant matrix $\mathbf{C}_0$ is unique to the given system whose solutions over an interval of period duration are related by it and it will be shown that its eigenvalues will define the quasienergies for the time periodic quantum problem. For the periodic-in-time Schrödinger equation the physical implications of this result stem from, as we shall see, the intimate relation between the unitary evolution operator over a period and the constant matrix $\mathbf{C}_0$.

The periodicity of the Wronskian may be used to show how the result in eq.(B.5) may be extended to the non-singular constant matrix $\mathbf{C}_0$, as follows

$$\begin{aligned} \mathcal{W}(t+T) &= \mathcal{W}(t_0)\exp\left(\int_{t_0}^{t} \mathrm{Tr}\left(\mathbf{A}(t')\right)dt' + \int_{t}^{t+T} \mathrm{Tr}\left(\mathbf{A}(t')\right)dt'\right) \\ \Rightarrow \mathcal{W}(t+T) &= \mathcal{W}(t)\exp\left(\int_{t}^{t+T} \mathrm{Tr}\left(\mathbf{A}(t')\right)dt'\right) \end{aligned}$$

$$\Rightarrow \mathcal{W}(t+T) = \mathcal{W}(t)\exp\left(\int_0^T \mathrm{Tr}\left(\mathbf{A}(t')\right)dt'\right)$$

The last step above makes use of the time translation symmetry of the integral over the trace by equating the integral over any interval of a period's length to that over the interval $(0, T)$. From eq.(B.6) it is apparent that taking the determinant of the expression on either side leads us to

$$\det(\mathbf{Z}(t+T)) = \det(\mathbf{Z}(t))\det(\mathbf{C}_0)$$
$$\mathcal{W}(t+T) = \mathcal{W}(t)\det(\mathbf{C}_0)$$

Comparing the two expressions for $\mathcal{W}(t)$ obtained above, one finds

$$\det(\mathbf{C}_0) = \exp\left(\int_0^T \mathrm{Tr}\left(\mathbf{A}(t')\right)dt'\right) \tag{B.7}$$

The time independence of $\mathbf{C}_0$ allows it to be determined by setting $t = 0$ in its definition as $\mathbf{C}_0 = \mathbf{Z}^{-1}(0)\mathbf{Y}(0) = \mathbf{Z}^{-1}(0)\mathbf{Z}(T)$. We see that for a boundary condition of the form $\mathbf{Z}(0) = \mathbf{I}$, in which case $\mathbf{Z}(t)$ is a principal fundamental matrix, $\mathbf{C}_0 = \mathbf{Z}(T)$. In mathematical parlance $\mathbf{C}_0$ is referred to as the monodromy matrix for the system of linear differential equations, obtained by evaluating the fundamental matrix at the period of the system.

The properties of the constant matrix $\mathbf{C}_0$ are of interest as it provides a form of invariant for the discrete time translation invariance of the system represented by $\dot{\mathbf{Z}}(t) = \mathbf{A}(t)\mathbf{Z}(t)$. The eigenvalues of this matrix are called the characteristic multipliers, denoted by $b_1, b_2, \ldots, b_N$, for the system. By definition, a set of exponents $q_1, q_2, \ldots, q_N$ that satisfies

$$b_1 = e^{q_1 T} \quad b_2 = e^{q_2 T} \quad \cdots b_N = e^{q_N T} \tag{B.8}$$

are termed as the characteristic exponents or Floquet exponents and they turn out to be the best effective static description of the energies of 'quasi'-stationary states that might be had for a time periodic quantum system. These exponents could in general be complex valued. We shall see, that for the case of quantal evolution, there are restrictions of unitarity and hermiticity that constrain these values to be purely imaginary. From eq.(B.7) the product of the characteristic multipliers which is nothing but $\det(\mathbf{C}_0)$ is established. Another feature of these multipliers is that they are not uniquely defined as $b_\alpha = e^{q_\alpha T}$ and $b_\alpha = e^{(q_\alpha + \frac{2\pi m}{T})T}$ are both valid multipliers for a given α and $m \in \mathbb{Z}$, the set of integers. They are fundamentally associated to the system of periodic differential equations used to derive them and are independent of the choice of fundamental matrix. This can be shown as the following sequence of steps, let $\acute{\mathbf{Z}}(t)$ be another fundamental matrix with $\acute{\mathbf{Z}}(t+T) = \acute{\mathbf{Z}}(t)\acute{\mathbf{C}}_0$ where by definition one is allowed to write $\acute{\mathbf{Z}}(t) = \mathbf{Z}(t)\mathbf{B}$,$\acute{\mathbf{C}}_0$ and $\mathbf{B}$ being constant non-singular matrices, then

$$\begin{aligned}
\acute{\mathbf{Z}}(t+T) &= \mathbf{Z}(t+T)\mathbf{B} \\
(\acute{\mathbf{Z}}(t)\acute{\mathbf{C}}_0) &= (\mathbf{Z}(t)\mathbf{C}_0)\,\mathbf{B} \\
\mathbf{Z}(t)\mathbf{B}\acute{\mathbf{C}}_0 &= \mathbf{Z}(t)\mathbf{C}_0\mathbf{B} \\
\mathbf{B}\acute{\mathbf{C}}_0 &= \mathbf{C}_0\mathbf{B} \\
\mathbf{B}\acute{\mathbf{C}}_0\mathbf{B}^{-1} &= \mathbf{C}_0
\end{aligned} \tag{B.9}$$

Thus, the eigenvalues of $\acute{\mathbf{C}}_0$ are the same as those of $\mathbf{C}$, which shows that the characteristic multipliers are unique for a given system of differential equations. It is useful to note that the final expression above has the form of a similarity transformation which allows one the freedom to choose a $\mathbf{B}$ such that it diagonalizes $\acute{\mathbf{C}}_0$ to $\mathbf{C}_0$.

Now we come to deriving the properties of the individual solutions $\mathbf{z}(t)$, the

column entries of the fundamental matrix $\mathbf{Z}(t)$, from our understanding of Floquet systems so far. Consider some characteristic multiplier b of the system with the corresponding exponent given by q as in $b = e^{qT}$. If $\mathbf{c}$ represents an eigenvector of $\mathbf{C}_0$ corresponding to the eigenvalue b, then one may write a solution of the form $\mathbf{z}(t) = \mathbf{Z}(t)\mathbf{c}$. This is nothing but another solution vector formed out of a linear superposition of the column vectors of $\mathbf{Z}(t)$ weighted by the components of the vector $\mathbf{c}$. Naturally, such a $\mathbf{z}(t)$ satisfies the differential equation $\dot{\mathbf{z}} = \mathbf{A}\mathbf{z}$. It would be useful to note here that as one can see from the property of the fundamental matrix $\mathbf{Z}(t)$ in eq.(B.6), there is an implicit choice of a particular column vector in defining $\mathbf{z}(t)$ of the form chosen here. Since this would dictate the particular characteristic multiplier choice from a diagonalized $\mathbf{C}_0$ and the corresponding choice of $\mathbf{c}$. We would like to see how this vector translated in time by a period relates to its initial form. This may be known from the following, where we use results derived previously,

$$\mathbf{z}(t+T) = \mathbf{Z}(t+T)\mathbf{c} = (\mathbf{Z}(t)\mathbf{C}_0)\,\mathbf{c} = b\mathbf{Z}(t)\mathbf{c} = b\mathbf{z}(t) \tag{B.10}$$

One obtains $\mathbf{z}(t+T) = b\mathbf{z}(t)$ which shows that solutions seperated in time by a period are related by the characteristic multipliers. Another important property has to do with the form of the solution i.e $\mathbf{z}(t)$, as was postulated at the beginning of this section, of the kind $e^{qt}\mathbf{p}(t)$ with $\mathbf{p}(t)$ being periodic with T . Let there be a $\mathbf{p}(t)$ such that $\mathbf{p}(t) = \mathbf{z}(t)e^{-qt}$. We wish to show that this has the periodicity of the system of differential equations as follows

$$\mathbf{p}(t+T) = \mathbf{z}(t+T)e^{-q(t+T)} = b\mathbf{z}(t)e^{-q(t+T)} = \mathbf{z}(t)e^{-qt} = \mathbf{p}(t) \tag{B.11}$$

where we have made use of the earlier assertion that b is a characteristic multiplier of the form e^{qT} hence, $be^{-qT} = 1$. Thus, a solution exists of the form $\mathbf{z}(t) = e^{qt}\mathbf{p}(t)$,

with $\mathbf{p}$ being T-periodic. Note that, as mentioned earlier, a column choice is implicit in $\mathbf{z}(t)$ so the multiplier b and the exponent q are correspondingly fixed and this attributes the same column index to $\mathbf{p}(t)$. This enables one to write in a complete matrix formulation the fundamental matrix $\mathbf{Z}(t)$ as

$$\mathbf{Z}(t) = e^{\mathbf{Q}t}\mathbf{P}(t) \tag{B.12}$$

where, $\mathbf{Q}$ is the $N \times N$ matrix with its diagonal entries as the characteristic exponents $q_1, q_2, \ldots, q_N$ and $\mathbf{P}(t)$ is the matrix, of the same dimensions, with column entries being the vectors $\mathbf{p}(t)$.

There are some general properties of the solutions which are determined by the nature of the characteristic multipliers. Since these multipliers are most generally complex, they can fall into three categories based on their magnitude. These are $|b| < 1$, $|b| = 1$ and $|b| > 1$. In the first and the last case the solutions are exponentially decaying and rising respectively. However, for the second case, the $\mathrm{Re}(q) = 0$ and the solutions are pseudo-periodic and in case $b = \pm 1$ the solutions are exactly periodic with period T. This is the case that we shall be interested in throughout the discussions in this appendix and the study of Floquet quantum systems in general. This concludes our outline of the basic notions of Floquet theory that form the mathematical framework for the following discussion.

B.3 Schrödinger equation with a periodic Hamiltonian and the Floquet Hamiltonian

The content of this section is adapted from the discussion in Chapter 6 of J.H. Shirley's thesis [329]. This provides, by far, the best treatment known to us of the application of the fundamentals of Floquet theory to periodic quantum systems. It

is reproduced here for the purposes of clarity and continuity. Here we treat the special case of the Schrödinger equation with a periodic in time Hamiltonian using the formalism developed so far. The periodic time dependent Schrödinger equation is given by

$$i\hbar\dot{\Psi}(t) = \mathcal{H}(t)\Psi(t) \tag{B.13}$$

where, $\mathcal{H}(t+T) = \mathcal{H}(t)$ is the T-periodic, $N \times N$ dimensional Hamiltonian of the periodic system and $\Psi(t)$ is the $N \times 1$ dimensional column vector representing the the time dependent state of the quantum system. We deviate slightly from our chosen notational convention here, of designating vectors with lower case bold face Roman letters, by denoting the state vector with a greek symbol. This and the fact that we do not use bold face notation for the time dependent Hamiltonian and later, the Floquet Hamiltoniain, are the only exceptions made. The N independent solutions of eq.(B.13) may be represented as the columns of the $N \times N$ matrix $\mathbf{\Psi}(t)$, which happens to be the fundamental matrix for the given system of equations just like $\mathbf{Z}(t)$ in the previous section.

From the properties of fundamental matrices that have been discussed, it is possible to define a fundamental matrix $\mathbf{\Psi}(t)\mathbf{\Psi}^{-1}(t_0)$, where $\mathbf{\Psi}^{-1}(t_0)$ is a constant non-singular matrix, denoted by $\mathbf{U}(t;t_0)$. This is a construction of the kind used to define $\mathbf{Y}'(t)$ earlier with the additional feature that at $t = t_0$, $\mathbf{U}(t_0;t_0) = \mathbf{I}$. Thus making it a principal fundamental matrix under the given initial conditions. This matrix is is of particular interest since it gives the time evolution of the solutions to the system in eq.(B.13) as

$$\Psi(t) = \mathbf{U}(t;t_0)\Psi(t_0) \tag{B.14}$$

The elements of this evolution matrix can be directly interpreted as the transition probability amplitudes for going between the states of the system. So the element $U_{\beta\alpha}(t;t_0)$ represents such a probability amplitude for an intial state α, at time t_0,

going to βat time t. The requirement that the total probability adds up to one is fulfilled by the hermiticity of $\mathcal{H}$ from which it follows that $\Psi^\dagger(t)\Psi(t)$ and hence, more generally $\mathbf{\Psi}^\dagger(t)\mathbf{\Psi}(t)$, is constant and allows for normalization. In the specific case of $\mathbf{U}$ this constant is unity as evaluated for the given initial condition. This makes $\mathbf{U}$ unitary for all times. This unitary property imposes its own conditions on the results derived from the application of Floquet theory and hence enables a quantum mechanical interpretation of the characteristic quantities as a sort of stationary state picture of the system.

Now, the application of the techniques of Floquet theory discussed in the previous section, to the system in eq.(B.13) allows us to write, as in eq.(B.6)

$$\mathbf{\Psi}(t+T) = \mathbf{\Psi}(t)\mathbf{C}_0. \tag{B.15}$$

One can diagonalize $\mathbf{C}_0$ above, using the freedom from the uniqueness of characteristic multipliers shown in eq.(B.9), usually with a constant unitary matrix say $\mathbf{B}$ such that $\mathbf{B}^{-1}\mathbf{C}_0\mathbf{B} = e^{-i\mathbf{Q}'T}$. This exponential matrix is just like the one in eq.(B.12) and its diagonal entries are again the characteristic exponents $q'_1, q'_2, \ldots, q'_N$ related to those of the previous section as $q_\alpha = -iq'_\alpha$. We have seperated out the i in an attempt to make explicit the purely imaginary nature of the q 's which followed from the requirement for the multipliers that $|b| = 1$ and $b = \pm 1$ for periodic solutions, as discussed in the last section. That the q' 's are real will be shortly shown via the unitarity of $\mathbf{U}$ just discussed. Coming back to the above equation this diagonalization can be performed and we have

$$\begin{aligned} \mathbf{\Psi}(t+T) &= \mathbf{\Psi}(t)\mathbf{B}e^{-i\mathbf{Q}'T}\mathbf{B}^{-1} \\ \mathbf{\Psi}(t+T)\mathbf{B}e^{i\mathbf{Q}'(t+T)} &= \mathbf{\Psi}(t)\mathbf{B}e^{i\mathbf{Q}'t} \end{aligned}$$

The second step involves multiplying $\mathbf{B}e^{i\mathbf{Q}'(t+T)}$ on either side of the first. Looking at

the RHS of the second expression one notes that from the property of fundamental matrices, $\mathbf{\Psi}(t)\mathbf{B}$ is also a solution matrix. If this RHS is denoted by $\mathbf{P}'(t)$ then $\mathbf{P}'(t+T) = \mathbf{P}'(t)$ i.e. periodic and the solution $\mathbf{\Psi}(t)\mathbf{B}$ can be expressed in terms of it as $\mathbf{P}'(t)e^{-i\mathbf{Q}'t}$. We may recall that $\mathbf{P}'$ here is nothing but an analog of the $\mathbf{P}(t)$ matrix of the previous section. Thus, we have shown that, for the time dependent Schrödinger equation with a periodic Hamiltonian, the matrix form of the solution has the general form of the Floquet theory solution. The components of the solution are given by $P'_{\alpha\beta}(t)e^{-iq'_\beta t}$.

The choice of $\mathbf{\Psi}(t)$ above is arbitrary and one could as easily have chosen the matrix of linearly independent unitary solutions, $\mathbf{U}$, for this purpose. This would require that the corresponding $\mathbf{C}_0$ be a constant unitary matrix also and basically turns out to be the evolution matrix over a period i.e. $\mathbf{U}(t_0+T;t_0)$. As by definition, it has the property of taking a matrix of solutions at some instant t_0 to one a period apart at t_0+T. The composition property of the time evolution operator, well known from quantum mechanics, can be used to illustrate this. We can write $\mathbf{U}(t+T;t_0) = \mathbf{U}(t+T;t)\mathbf{U}(t;t_0)$ and map to the notation of the previous section as $\mathbf{Z}(t) = \mathbf{U}(t;t_0)$, $\mathbf{Y}(t) = \mathbf{U}(t+T;t_0)$ and $\mathbf{C}(t) = \mathbf{U}^{-1}(t;t_0)\mathbf{U}(t+T;t_0)$. Then, following the same sequence of steps that lead up to eq.(B.6), we can show the correspondence $\mathbf{C}_0 = \mathbf{U}(t_0+T;t_0)$. The diagonalizing transformation $\mathbf{B}$ in this case can also be chosen to be unitary as a result imparting the same property to the matrix $e^{-i\mathbf{Q}'T}$, thereby making $\mathbf{Q}'$ hermitian. From this it follows that the eigenvalues of $\mathbf{Q}'$ must be real making q'_α 's real. A feature that is consistent with the previous statements regarding the nature of the characteristic exponents for periodic systems. Thus, here we see that the eigenvalues of the unitary evolution matrix over a period are the characteristic multipliers. Since $\mathbf{\Psi}(t) = \mathbf{U}(t;t_0)$, $\mathbf{B}$ and $e^{-i\mathbf{Q}'t}$ are all unitary it can be reasoned that $\mathbf{P}'(t)$ is also unitary. With this it is possible to write a general unitary solution for the matrix Schrödinger equation

$i\hbar\dot{\mathbf{\Psi}}(t) = \mathcal{H}\mathbf{\Psi}(t)$ of the form $\mathbf{\Phi}(t) = \mathbf{P}'(t)e^{-i\mathbf{Q}'t}$. This may then be used to express the special solution $\mathbf{U}$ as

$$\mathbf{U}(t;t_0) = \mathbf{\Phi}(t)\mathbf{\Phi}^{-1}(t_0) = \mathbf{P}'(t)e^{-i\mathbf{Q}'(t-t_0)}\mathbf{P}'^{-1}(t_0) \tag{B.16}$$

The above equation is an important result and offers a useful decomposition of the time evolution matrix or operator. The exponential term $e^{-i\mathbf{Q}'(t-t_0)}$ has a hermitian time independent $\mathbf{Q}'$ which provides the motivation for developing a time independent description of time-periodic quantum systems. This matrix or operator may be thought of as giving the time evolution of the system as in a stationary quantum system. Therefore lending the interpretation of stationary quasi-energies for the characteristic exponents. While this operator evolves the system over any given duration, the time dependence of the evolution is accounted for by the periodic, time dependent unitary operators $\mathbf{P}'(t)$ and $\mathbf{P}'(t_0)$, at the terminal points of the interval of evolution. This formulation forms the basis of much of the discussion in future sections.

A property that we can apply here from our general discussion on Floquet theory is the one derived in eq.(B.5) where from the condition that the Wronskian of the linearly independent solutions is identical to the determinant of the fundamental matrix, one can write the determinant of the evolution operator as

$$\begin{aligned}\det(\mathbf{U}(t;t_0)) &= \det(\mathbf{U}(t_0;t_0))\exp\left(-i\int_{t_0}^{t}\mathrm{Tr}\left(\mathcal{H}(t')\right)dt'\right)\\ &= \exp\left(-i\int_{t_0}^{t}\mathrm{Tr}\left(\mathcal{H}(t')\right)dt'\right)\end{aligned} \tag{B.17}$$

From what we have in eq.(B.7), and the correpondence between the $\mathbf{C}_0$ there and

$\mathbf{U}(t_0+T;t_0)$ which has just been discussed, one can write

$$\begin{aligned}\det(\mathbf{C}_0) = \det(\mathbf{U}(t_0+T;t_0)) &= \exp\left(-i\int_{t_0}^{t_0+T}\mathrm{Tr}\left(\mathcal{H}(t')\right)dt'\right) \\ &= \prod_\alpha e^{-iq'_\alpha T} = \exp\left(-iT\sum_\alpha q'_\alpha\right) \end{aligned} \tag{B.18}$$

where we have used the fact that $\det(\mathbf{C}_0)$ can be written as a product of eigenvalues i.e the characteristic multipliers. Comparing the terms in the exponent of both the expressions gives an important constraint on the characteristic multipliers or the quasienergies

$$\sum_\alpha q'_\alpha = \frac{1}{T}\int_{t_0}^{t_0+T}\mathrm{Tr}\left(\mathcal{H}(t')\right)dt' \tag{B.19}$$

with their sum (upto some integral multiple of the driving frequency $\omega = 2\pi/T$) being equal to the time average of the trace of the Hamiltonian over a period. Since the determination of the characteristic exponents forms the central problem while applying Floquet theory to periodic quantum systems, any condition that helps to restrict the number of such independent unknowns is of great help. The above condition is one such identity. The trace of the Hamiltonian , as it so happens, is of no particular physical significance and hence can be fixed to suit our convenience. In fact this is effectively like fixing a reference for measuring the energies. This feature combined with the above identity helps to reduce the number of independent multiplier values.

It is possible to gain a more insightful understanding of the unitary solution $\mathbf{\Phi}(t)$ by means of Fourier analysis, where it shall become apparent that a complete description of the periodic quantum problem in a time independent picture requires one to deal with inifinite dimensional matrices. Let us begin by writing $\mathbf{\Phi}(t)$ in its component form

$$\Phi_{\alpha\beta}(t) = P'_{\alpha\beta}(t)e^{-iq'_\beta t} \tag{B.20}$$

The periodicity of $P'_{\alpha\beta}(t)$ allows for it to be expanded in an infinite Fourier series, with the coefficients represented by $\Phi^n_{\alpha\beta}$, where lower case Roman letters are used to denote the Fourier indices,

$$\Phi_{\alpha\beta}(t) = \sum_n \Phi^n_{\alpha\beta} e^{i(n\omega - q'_\beta)t} \tag{B.21}$$

Similarly one can write for the elements of the periodic $\mathcal{H}$

$$\mathcal{H}_{\alpha\beta}(t) = \sum_n \mathcal{H}^n_{\alpha\beta} e^{in\omega t} \tag{B.22}$$

The summations all range over $-\infty$ to ∞. Substituting these expansions in the Schrödinger equation $i\hbar\dot{\mathbf{\Phi}} = \mathcal{H}\mathbf{\Phi}$ gives

$$\begin{aligned}
i\hbar\frac{\partial}{\partial t}\Phi_{\alpha\beta}(t) = (\mathcal{H}\Phi)_{\alpha\beta} &= \sum_\gamma \mathcal{H}_{\alpha\gamma}(t)\Phi_{\gamma\beta}(t) \\
i\hbar\frac{\partial}{\partial t}\sum_n \Phi^n_{\alpha\beta} e^{i(n\omega - q'_\beta)t} &= \sum_\gamma \sum_n \mathcal{H}^n_{\alpha\gamma} e^{in\omega t} \sum_m \Phi^m_{\gamma\beta} e^{i(m\omega - q'_\beta)t} \\
i\hbar\sum_n \Phi^n_{\alpha\beta} i(n\omega - q'_\beta) e^{i(n\omega - q'_\beta)t} &= \sum_\gamma \sum_n \sum_m \mathcal{H}^n_{\alpha\gamma}\Phi^m_{\gamma\beta} e^{i((n+m)\omega - q'_\beta)t}
\end{aligned}$$

where introducing a shift in the summation indices by replacing n in terms of $n' = n + m$, and then relabelling n' by n again in what results, we get

$$\begin{aligned}
\sum_\gamma \sum_n \sum_m \mathcal{H}^{n-m}_{\alpha\gamma}\Phi^m_{\gamma\beta} e^{i(n\omega - q'_\beta)t} &= \sum_n \Phi^n_{\alpha\beta}(-\hbar n\omega + \hbar q'_\beta) e^{i(n\omega - q'_\beta)t} \\
\sum_{\gamma m} \mathcal{H}^{n-m}_{\alpha\gamma}\Phi^m_{\gamma\beta} + \hbar n\omega \Phi^n_{\alpha\beta} &= \hbar q'_\beta \Phi^n_{\alpha\beta} \\
\sum_{\gamma m} \left[\mathcal{H}^{n-m}_{\alpha\gamma} + \hbar\delta_{\alpha\gamma}\delta_{nm} n\omega\right] \Phi^m_{\gamma\beta} &= \hbar q'_\beta \Phi^n_{\alpha\beta}
\end{aligned} \tag{B.23}$$

Here one could choose to work in units of $\hbar$ and drop it from the eigenvalue equation in the final step above. In interpreting this as an eigenvalue equation one is led

to recognize q'_β as an eigenvalue and $\Phi^n_{\alpha\beta}$ as the corresponding eigenstate. It is important to note that the equation has both greek and roman indices denoting the system states and the Fourier components respectively. The description of the eigenstate here requires both of these and for a given α i.e. system state there are infinitely many possibilities for n i.e. a Fourier component. Thus a state vector as a column or row requires two indices to be described uniquely much like two quantum numbers are needed in several examples of quantum systems. This is also revelaed in the structure of the eigenvalue equation where the summation extends over a pair of greek and Roman indices i.e. γ and m respectively,thus indicating that both together represent the components of a column vector for the state $\Phi^m_{\gamma\beta}$. Thus form the RHS it is apparent that a tuple of the form (α, n) indexes the elements of a column and hence for a particular value labels a row. While reading the the operating matrix or operator from this eigenvalue equation the (α, n) lables the rows and (γ, m) labels the columns. This operator is referred to as the Floquet Hamiltonian for the corresponding time dependent $\mathcal{H}$, and may be denoted $\mathcal{H}_F$. By virtue of the Fourier components this is an infinite matrix. It can be ensured while writing the Floquet Hamiltonian and the state vectors that the components are so ordered that they cycle through all the system states before a change in the Fourier index occurs.

From the above discussion it appears natural to turn to the Dirac bra-ket notation to denote the vectors that form an orthonormal basis for representing the eigenvalue equation in (B.23). Thus one may write $|\alpha n\rangle$ to denote an infinite column vector with a possible representation involving all zero entries except for a 1 at the particular choice of (α, n) values. With such a choice of basis the components of the Floquet Hamiltoniain $\mathcal{H}_F$ become $\langle \alpha n|\mathcal{H}_F|\gamma m\rangle = \mathcal{H}^{n-m}_{\alpha\gamma} + \delta_{\alpha\gamma}\delta_{nm}n\omega$. In a more formal sense these basis vectors may be thought of as spanning an extended Hilbert space or Sambe space [91], $\mathbb{F} = \mathbb{H} \otimes \mathbb{T}$, which is a direct product of the Hilbert

space of quantum states of the system and the space of square integrable functions periodic with period T. The Fourier basis $e^{in\omega t}$ is a natural orthonormal basis in $\mathbb{T}$. In explicit terms one may express $|\alpha n\rangle = |\alpha\rangle e^{in\omega t}$. Thus, $\mathcal{H}_F$ is an operator in such an extended Floquet Hilbert space and its eigenvectors are also vectors in this space, as is $\mathbf{\Phi}$ in the discussion above. These states in Sambe space are not physical states of the periodic quantum system in any sense but exhibit similar traits.

Since $\mathcal{H}$ is hermitian it follows that so is $\mathcal{H}_F$, thus it must admit an orthonormal system of eigenstates and real eigenvalues. The eigenstate $\Phi^n_{\alpha\beta}$ in (B.23) is essentially the column $\beta$of the periodic part of the unitary solution $\mathbf{\Phi}(t)$, i.e. $\mathbf{P}\ '(t)$, but now represented in the extended Floquet Hilbert space. These columns of $\mathbf{P}'(t)$ shall henceforth be called the Floquet modes and the elements $\Phi^n_{\alpha\beta}$ stand for the components of the 'β-vector of this set or the βFloquet mode, as represented in the basis, $|\alpha n\rangle$, of the Floquet Hilbert space. So although in the space $\mathbb{H}$ the columnns of $\mathbf{\Phi}(t)$ are linearly independent vectors with a definite normalization, this may no longer be true once one moves to $\mathbb{F}$ by including the Fourier indices. Moreover the state vector given by the components $\Phi^n_{\alpha\beta}$ in the $|\alpha n\rangle$ basis does not generally give an exactly diagonal representation of $\mathcal{H}_F$, as the non-zero Fourier components $\mathcal{H}^{n-m}_{\alpha\gamma}$ contribute to off-daigonal terms. So let us then define a normalized basis for $\mathcal{H}_F$ in $\mathbb{F}$ denoted by the kets $|\tau_{\not k}\rangle$ and corresponding eigenvalues by $\epsilon_{\not k}$. Thus satisfying the eigenvalue relation

$$\mathcal{H}_F|\tau_{\not k}\rangle = \epsilon_{\not k}\ |\tau_{\not k}\rangle \tag{B.24}$$

Introducing the completeness of states $\sum_{\gamma m}|\gamma m\rangle\langle\gamma m| = \mathbf{I}$ in the LHS of the above equation and taking the inner product with $\langle\alpha n|$ on both sides gives

$$\sum_{\gamma m}\langle\alpha n|\mathcal{H}_F|\gamma m\rangle\langle\gamma m|\tau_{\not k}\rangle = \epsilon_{\not k}\ \langle\alpha n|\tau_{\not k}\rangle \tag{B.25}$$

The above eigenvalue equation may be compared to eq.(B.23) to get a better un-

derstanding of the structure of the matrix $\mathcal{H}_F$ and its eigenstates, since now it is possible to interpret components of column vectors in $\mathbf{\Phi}$ as the projections $\langle \alpha n | \tau_{\not{R}} \rangle$. Before exploring the representation of the eigenstates it is important to understand the construction of $\mathcal{H}_F$. An element of this matrix has the form $\langle \alpha n | \mathcal{H}_F | \gamma m \rangle = \mathcal{H}_{\alpha\gamma}^{n-m} + \delta_{\alpha\gamma}\delta_{nm} n\omega$, where as we know (αn) denotes a row and (γm) a column and for given values of n and m all the entries for the finite set of α and γ values are grouped together and ordered. This gives rise to a structure where any pair of (n, m) values corresponds to a block of $N \times N$ dimensions i.e. equivalent to those of $\mathcal{H}$. The blocks are laid out such that the one corresponding to $n = m = n - m = 0$ lies at the centre of the infinite matrix occupying the middle of the diagonal. Its neighbours, from the chosen row and column convention, are the blocks $n = 0, m = 1$ to the right and $n = 0, m = -1$ to the left, $n = 1, m = 0$ up top and $n = -1, m = 0$ down below, and along the left and right diagonals ($n = 1, m = -1$; $n = -1, m = 1$) and ($n = 1, m = 1$;$n = -1, m = -1$) respectively. This scheme extends in all these directions infinitely. The matrix element of $\mathcal{H}_F$ also tells us that the factor $n\omega$ gets added to all the diagonal elements of the block in the n-th 'block' row lying on the main diagonal of $\mathcal{H}_F$. The blocks with $n - m = 0$ lie along the main diagonal of the matrix and these blocks are identical except that between any two blocks the corresponding diagonal elements differ by some integer multiple of ω. This sort of periodicity can be expressed as

$$\langle \alpha n + s | \mathcal{H}_F | \gamma m + s \rangle = \langle \alpha n | \mathcal{H}_F | \gamma m \rangle + s\omega\delta_{\alpha\gamma}\delta_{nm} \tag{B.26}$$

for some integer s. The effect of this property on the eigenvalues and eigenvectors of the matrix merits some attention. If one looks at the matrix elements of $\mathcal{H}_F$, one sees the property that one could add or subtract an infinite diagonal matrix with $s\omega$ as the diagonal entries for some integer s and the matrix remains unchanged with a shift of the diagonal entries which is ultimately indistinguishable. Very much

like the translation symmetry of an infinite lattice in its lattice vectors the Floquet Hamiltonian shows this symmetry in translations by multiples of ω atleast for its diagonal. The eigenvalues reflect this freedom as is apparent from the eigenvalue equation in (B.23) where any number of ω s may be adjusted with the q'_β by a shift in the Roman summation index and so if ϵ is an eigenvalue then so is $\epsilon + s\omega$. Thus it is possible to interpret an eigenvalue as $\epsilon_{\alpha n} = \epsilon_{\alpha 0} + n\omega$ which highlights the fact that as far as the Floquet quasienergies, $\epsilon_{\alpha 0} = q'_\alpha$ are concerned, the truly distinct eigenvalues are finite and indexed, as written here, by α and all others are related to this set by multiples of ω. Therefore the quasienergies can be thought of as belonging to a sort of Brillouin zone wich can be folded to form a circle in a reduced zone scheme for the spectrum. The q'_α or $\epsilon_{\alpha 0}$ represents the eigenvalue with the lowest magnitude in the set containing it and the various energies related to it by all possible integer multiples of ω.

Similarly we can analyse the effect this periodicity property has on the components $\langle \alpha n | \tau_{\not{k}} \rangle$ of the eigenvector for the eigenvalue $\epsilon_{\not{k}}$. Let us see the effect of ω-translation on the eigenstates i.e. to find out how are $|\tau_{\not{k}} \rangle$ and $|\tau_{\not{k}+s} \rangle$ related given that we now know $\epsilon_{\not{k}+s} = \epsilon_{\not{k}} + s\omega$. Writing the eigenvalue equation in eq.(B.24) for the shifted state $|\tau_{\not{k}+s} \rangle$ one gets

$$\mathcal{H}_F |\tau_{\not{k}+s} \rangle = \epsilon_{\not{k}+s} \, |\tau_{\not{k}+s} \rangle.$$

Adopting manipulations similar to the ones used in obtaining eq.(B.25) we have

$$\sum_{\gamma m} \langle \alpha n + s | \mathcal{H}_F | \gamma m + s \rangle \langle \gamma m + s | \tau_{\not{k}+s} \rangle = \epsilon_{\not{k}+s} \, \langle \alpha n + s | \tau_{\not{k}+s} \rangle$$

Using our knowledge of the matrix element on the LHS from eq.(B.26) and the

periodic relation for ϵ_{k+s} the above equation becomes

$$\sum_{\gamma m} \left[\langle \alpha n|\mathcal{H}_F|\gamma m\rangle + s\omega\delta_{\alpha\gamma}\delta_{nm}\right] \langle \gamma m + s|\tau_{k+s}\rangle = (\epsilon_k + s\omega)\langle \alpha n + s|\tau_{k+s}\rangle$$

$$\sum_{\gamma m} \langle \alpha n|\mathcal{H}_F|\gamma m\rangle \langle \gamma m + s|\tau_{k+s}\rangle = \epsilon_k \langle \alpha n + s|\tau_{k+s}\rangle$$

The second step follows from the first after cancelling $s\omega$ from both sides of the first equation. Thus we see that the components $\langle \alpha n + s|\tau_{k+s}\rangle$ satisfy the same set of homogeneous equations as those satisfied by the $\langle \alpha n|\tau_k\rangle$ in eq.(B.25). They are both normalized by definition and could be assigned arbitrary relative phase based on how we choose, so it follows that we can write

$$\langle \alpha n + s|\tau_{k+s}\rangle = \langle \alpha n|\tau_k\rangle \tag{B.27}$$

Hence the components of the eigenvectors show a periodicity similar to what is observed in the case of the eigenvalues. It shows that the same eigenvector holds for all the eigenvalues which are related by some integer multiple of ω. One can therefore define, just like for the quasienergies, a set of distinct, unique eigenvectors for $\mathcal{H}_F$ that correspond in a one is to one fashion to the these quasienergies in the reduced Brillouin zone.

We may now proceed to analyse the relationship between $\Phi^n_{\alpha\beta}$ and $\langle \alpha n|\tau_k\rangle$ both of which denote components of the eigenstates of $\mathcal{H}_F$. There are differences in the choice of representation of the eigenvectors in both cases and more importantly in the nature of their respective normalizations. However one expects a close correlation between the two given the fact that one is attempting to preserve unitarity and that the eigenvalue to which they both correspond is the same, i.e. $q'_\beta = \epsilon_\beta$. So it is

possible to write as an ansatz the following relation

$$\Phi^n_{\alpha\beta} = R_\beta \langle \alpha n | \tau_{\not\beta} \rangle \tag{B.28}$$

where R_β is a scalar, may be real or complex, which needs to be determined. The significance of the above equation lies in the opportunity that it offers to solve the periodic time dependent problem using a time independent formalism. Since we are required to obtain the unitary solution $\Phi^n_{\alpha\beta}$ or more generally the columns of $\mathbf{\Phi}(t)$ for a complete solution of the problem, the above equation helps to transform this search into one of computing the eigenstates, $|\tau_{\not\beta} \rangle$ of the time independent, infinite dimensional $\mathcal{H}_F$.

To determine R_β in the above we use the unitarity of $\mathbf{\Phi}$ i.e. $\mathbf{\Phi}^\dagger \mathbf{\Phi} = \mathbf{I}$, which in component form can be expressed as

$$\sum_\gamma \Phi^*_{\gamma\alpha}(t) \Phi_{\gamma\beta}(t) = \delta_{\alpha\beta}$$

then,

$$\sum_\gamma \left(\sum_m (\Phi^m_{\gamma\alpha})^* e^{-im\omega t} e^{iq'_\alpha t} \right) \left(\sum_n \Phi^n_{\gamma\beta} e^{in\omega t} e^{-iq'_\beta t} \right) = \delta_{\alpha\beta}$$

Since the RHS dictates that the LHS has to be a diagonal matrix with all 1 s along the diagonal, it is required that $\alpha = \beta$be imposed on the elements of the LHS to get the non-zero values. Thus $e^{i(q'_\alpha - q'_\beta)t}$ may be set to unity and it also helps to modify the summation index m to l with $l = n - m$,

$$\sum_\gamma \sum_l \sum_n (\Phi^{n-l}_{\gamma\alpha})^* \Phi^n_{\gamma\beta} e^{il\omega t} = \delta_{\alpha\beta}$$

$$\sum_\gamma \sum_n (\Phi^{n-l}_{\gamma\alpha})^* \Phi^n_{\gamma\beta} = \delta_{\alpha\beta} \delta_{l0}$$

The second step follows from the fact that as the RHS is time independent the LHS should be too, and is ensured by putting l to 0. The final expression above can be rewritten using the component form in eq.(B.28) as

$$\sum_{\gamma}\sum_{n}\langle\tau_{\alpha 0}|\gamma n-l\rangle R^{*}_{\alpha}R_{\beta}\langle\gamma n|\tau_{\beta}\rangle=\delta_{\alpha\beta}\delta_{l0}$$

where we can make use of the complex conjugate of eq.(B.27) to write $\langle\tau_{\alpha 0}|\gamma n-l\rangle=\langle\tau_{\alpha l}|\gamma n\rangle$, and putting this back gives

$$\begin{aligned}\sum_{\gamma}\sum_{n}\langle\tau_{\alpha l}|\gamma n\rangle\langle\gamma n|\tau_{\beta}\rangle|R_{\beta}|^{2}&=\delta_{\alpha\beta}\delta_{l0}\\ \langle\tau_{\alpha l}|\tau_{\beta}\rangle|R_{\beta}|^{2}&=\delta_{\alpha\beta}\delta_{l0}\\ |R_{\beta}|^{2}&=1\end{aligned}\tag{B.29}$$

In the above we make use of the completeness of the basis states $|\gamma n\rangle$ and the orthonormality of the eigenstates $|\tau_{\beta}\rangle$ of $\mathcal{H}_F$. From the above R_β is determined to be a unit complex number in general, where it basically represents a phase and can be taken to be 1. Thus the relation in eq.(B.28) becomes

$$\Phi^{n}_{\alpha\beta}=\langle\alpha n|\tau_{\beta}\rangle\tag{B.30}$$

and we have acheived our stated objective of converting the problem of finding time dependent solutions to the periodic in time Schrödinger equation to one of finding the eigenstates of the time independent $\mathcal{H}_F$.

It is instructive also to look at the structure of the time evolution operator $\mathbf{U}(t;t_0)=\mathbf{\Phi}(t)\mathbf{\Phi}^{-1}(t_0)$ in this formalism of the eigenstates of $\mathcal{H}_F$. In this basis the

components of the evolution operator become

$$U_{\alpha\beta}(t;t_0) = \sum_{\gamma}\sum_{k}\langle\beta k|\tau_{\gamma 0}\rangle e^{ik\omega t}e^{-iq'_{\gamma}t}\sum_{l}\langle\tau_{\gamma 0}|\alpha - l\rangle e^{il\omega t_0}e^{iq'_{\gamma}t_0}$$

in which the second sum is conducted by transforming the summation variable $l \to -l$. Next is to eliminate the variable k by using a new variable $n = k + l$ and use eq.(B.27) of translating the eigenvectors in the Roman index, in this case $n - l$ to n, to project onto the same vector $|\tau_{\gamma l}\rangle$ as follows

$$\begin{aligned} U_{\alpha\beta}(t;t_0) &= \sum_{n}\sum_{\gamma l}\langle\beta n|\tau_{\gamma l}\rangle e^{-i(q'_{\gamma}+l\omega)(t-t_0)}\langle\tau_{\gamma l}|\alpha 0\rangle e^{i\omega nt} \\ &= \sum_{n}\sum_{\gamma l}\langle\beta n|\tau_{\gamma l}\rangle e^{-i\epsilon_{\gamma l}(t-t_0)}\langle\tau_{\gamma l}|\alpha 0\rangle e^{i\omega nt} \end{aligned}$$

Note that the portion $|\tau_{\gamma l}\rangle e^{-i\epsilon_{\gamma l}(t-t_0)}\langle\tau_{\gamma l}|$ in the above expression with the summation running over γl is nothing but writing the exponentiated matrix $e^{-i\mathcal{H}_F(t-t_0)}$ in its own eigenbasis formed by the $|\tau_{\gamma l}\rangle$ and hence diagonal with the eigenvalues $\epsilon_{\gamma l}$. With this we can write the elements of the unitary evolution operator as

$$U_{\alpha\beta}(t;t_0) = \sum_{n}\langle\beta n|e^{-i\mathcal{H}_F(t-t_0)}|\alpha 0\rangle e^{i\omega nt} \tag{B.31}$$

Looking at the equation above, describing the components of the special, unitary, matrix solution to the Schrödinger equation that governs the time evolution of the state vectors for a given initial condition, we observe the similarity in structure to eq.(B.16). Except that there one was writing in the time dependent notation and within the space $\mathbb{H}$ of the system's time dependent quantum states. Here, on the other hand, the same quantum evolution is described in the extended Floquet Hilbert space $\mathbb{F}$. The states which are now used to represent the operator $\mathbf{U}$ are the orthonormal set $|\alpha n\rangle$. It can be gathered from the manner of expressing the

matrix elements in the above equation that they represent states that are evolved by the time independent $\mathcal{H}_F$ through the Schrödinger equation. Essentially $\mathcal{H}_F$ can be thought to connect states $|a_{t_0}\rangle$ at time t_0 and $|a_t\rangle$ at t via $i\hbar\frac{d}{dt}|a_t\rangle = \mathcal{H}_F|a_t\rangle$. Where, it may be noted that $|a_{t_0}\rangle = |\alpha 0\rangle$ and more interestingly, $|a_t\rangle = \sum_n |\beta n\rangle e^{-in\omega t}$. So, while earlier $U_{\alpha\beta}(t;t_0)$ represented the transition probability of the system going from the single physical state $|\alpha\rangle$ at time t_0 to another one $|\beta\rangle$ at time t, a sightly more elaborate picture emerges when the Fourier indices are made explicit and one attempts a description of the time dependent quantum processes in a time independent picture. In this manner of viewing the system dynamics, as is apparent from the above expression, the transition probability connects states in $\mathbb{F}$ such that the system beginning in the state $|\alpha 0\rangle$ has the option of transitioning to a multiplicity of states $|\beta n\rangle$, indexed by n, and then one defines the transition amplitude as the sum of the amplitudes corresponding to all these possibilities weighted by the factor $e^{i\omega nt}$. Though we have no qualms about transitions between the physical states $|\alpha\rangle$ and $|\beta\rangle$ of the system, the present scenario confronts us with the proper interpretation of the states in $\mathbb{F}$. One could regard the Floquet picture as merely a calculational tool without any physical significance and the finally computed transition probabilities correspond to observed values irrespective of this choice. There is however the some what physical interpretation of the periodic system as a static system interacting with a classical oscillating field and the Floquet states being the quantized states of this field. If indeed this is the actual nature of the system , which happens to be the case in most physical problems, then the application of Floquet theory acheives a quantization of the interaction of the static system with the field in a manner similar to quantum field theoretic approaches. This has led to the introduction of terminology which reflects this, with the Fourier indices being called the photon number of the Floquet space state and the multiple transition possibilities in this formalism now portraying multi-photon processes. Thus getting from one physical

quantum state to another involves several paths through the absorption and emission of various number of photons, which, in the Floquet Hamiltonian $\mathcal{H}_F$ as well as its eigensvalues (quasienergies) and eigenstates, is incorporated in the freedom of translating by integer multiples of ω while keeping physical quantities unchanged. In those situations where the physical picture does not exacty contain an oscillating field and the periodicity has alternative origins, the multi-photon processes stand in for other time dependent dynamics the system might exhibit. For instance, in the case of periodically driven lattice systems this dynamics may take the form of hopping to far off neigbours where only nearest neighbour hoppings were considered in the static lattice Hamiltonian for the Bloch electron. In a more general sense the Floquet conception of the time evolution operator may be analogized to the propogator in the path integral approach to quantum mechanics. Where, instead of summing transition amplitudes over all possible paths or histories, the sum is over all possible photon processes that connect the two end states at the begining and end of the evolution. There is also the exponential weight factor associated with each of these possibilities just like the exponential of the classical action in path integrals.

The discussion so far prepares a sound base for understanding the terminology and techniques of Floquet theory in quantum mechanics by clarifying the the nature of $\mathcal{H}_F$ and the Floquet Hilbert space $\mathbb{F}$. We also saw the role of the orthonormal basis in $\mathbb{F}$ and its connection with the eigenstates of $\mathcal{H}_F$ as well as the periodicity of the eigenstates and eigenvalues of the Floquet Hamiltonian. Since the final shape the problem takes is that of diagonalizing an infinite matrix, the following section(s) shall focus on how to acheive this in the most computationally efficient manner. We shall also shift to more contemporary notation and terms to denote various, by now, familiar quantities, to enable greater correlation with present usage in the literature.

B.4 Diagonalizing the Floquet Hamiltonian: Effective Hamiltonians, Micromotion and Perturbative Expansions

Before getting into the business of diagonalizing the Floquet Hamiltonian, it would be useful to collate the major ideas that have thus far emerged and to cast them in terminology and notation that brings them semantically closer to familiar concepts from time independent quantum mechanics. Our previous discussions have brought to light the significance of the time evolution operator over a period, $\mathbf{U}(t_0+T;t_0)$, in determining certain time independent characteristics of periodic quantum systems which allow their effective static description. We saw that the eigenvalues of this operator could be used to determine the quasienergies of the periodic time dependent system from these characteristic multipliers which are independent of the choice of initial conditions i.e t_0. This independence can be shown by the same reasoning as that used to demonstrate their uniqueness in eq.(B.9). If there one were to make the set of correspondences of the form, $\mathbf{Z}(t) = \mathbf{U}(t;t_0)$, $\mathbf{Z}'(t) = \mathbf{U}(t;t_0')$, $\mathbf{C}_0 = \mathbf{U}(t_0+T;t_0)$ and $\mathbf{C}_0' = \mathbf{U}(t_0'+T;t_0')$, then it is possible to show that the evolution operators over a period for two distinct starting times, t_0 and t_0' are related by a similarity transformation using a constant unitary matrix as

$$\mathbf{U}(t_0'+T;t_0') = \mathbf{U}^{-1}(t_0;t_0')\mathbf{U}(t_0+T;t_0)\mathbf{U}(t_0;t_0') \tag{B.32}$$

An additional useful property of this operator relates to its eigenstates. From the arguments leading up to eq.(B.16), in the previous section, we can write

$$\mathbf{U}(t;t_0)\mathbf{\Phi}(t_0) = \mathbf{\Phi}(t) \tag{B.33}$$

where we have already shown that Floquet theory dictates $\mathbf{\Phi}(t) = \mathbf{P}'(t)e^{-i\mathbf{Q}'t}$. In the above, on making the substitution $t \to t_0 + T$ we see,

$$\begin{aligned}\mathbf{U}(t_0+T;t_0)\mathbf{\Phi}(t_0) &= \mathbf{\Phi}(t_0+T) \\ &= \mathbf{P}'(t_0+T)e^{-i\mathbf{Q}'(t_0+T)} = e^{-i\mathbf{Q}'T}\mathbf{P}'(t_0)e^{-i\mathbf{Q}'t_0} = e^{-i\mathbf{Q}'T}\mathbf{\Phi}(t_0)\end{aligned}$$

Thus $\mathbf{\Phi}(t_0)$ is a matrix of eigenstates of $\mathbf{U}(t_0+T;t_0)$ with the eigenvalue matrix given by $e^{-i\mathbf{Q}'T}$. Since these steps are independent of the choice of t_0 the matrix eigenvalue equation observed above can be said to hold at all times. Thereby making the columns of $\mathbf{\Phi}(t)$, denoted from here on as $|\boldsymbol{\phi}_\beta(t)\rangle$, the eigenstates of the general $\mathbf{U}(t+T;t)$, with the corresponding eigenvalues given by the characteristic multipliers $e^{-iq'_\beta T}$. The $|\boldsymbol{\phi}_\beta(t)\rangle$ are henceforth referred to as the Floquet states or the complete, time dependent solutions to the periodic problem, expressed in Dirac notation as

$$|\boldsymbol{\phi}_\beta(t)\rangle = |\mathbf{p}'_\beta(t)\rangle e^{-iq'_\beta t}. \tag{B.34}$$

Here the $|\mathbf{p}'_\beta(t)\rangle$ denotes a column of the unitary periodic matrix $\mathbf{P}'(t)$, hence is itself periodic, and will be called a Floquet mode. This terminology is borrowed from recent usage in the literature [82]. The development in [82] also motivates the structure of the discussion in this section.

The Floquet states form a complete orthonormal set since they are eigenvectors of a unitary operator. In terms of these states the general time evolution operator connecting two instants t_i and t_f can be written as

$$\mathbf{U}(t_f;t_i) = \sum_\beta |\mathbf{p}'_\beta(t_f)\rangle e^{-iq'_\beta(t_f-t_i)}\langle \mathbf{p}'_\beta(t_i)| \tag{B.35}$$

which harks back to the form of the operator in eq.(B.16), being made more explicit here. Using these properties of Floquet states one may write for the time evolution

of any arbitrary state vector $|\boldsymbol{\psi}(t)\rangle$

$$|\boldsymbol{\psi}(t)\rangle = \mathbf{U}(t;t_0)|\boldsymbol{\psi}(t_0)\rangle = \sum_{\beta} c_{\beta} e^{-iq'_{\beta}(t-t_0)}|\mathbf{p}'_{\beta}(t)\rangle \tag{B.36}$$

with $c_{\beta} = \langle \mathbf{p}'_{\beta}(t)|\boldsymbol{\psi}(t_0)\rangle$. We note that being the eigenstates of the evolution operator, the time evolution of pure Floquet states is fairly trivial and is almost completely determined (upto the global phase $e^{-iq'_{\beta}t}$) by the corresponding Floquet mode and is consequently periodic. However for a state that is initially made up of several Floquet states, as in the equation above, the time evolution is much more involved and usually not periodic. There are two factors whose interplay will determine the nature of the temporal evolution in such a case. One is the periodicity of the the Floquet modes and the contribution coming from these is termed as the 'micromotion'. The other are the phases that accompany these modes, the $e^{-iq'_{\beta}t}$, which could interfere in a manner that detrimentally affects the periodicity. The quasienergies , q'_{β}, impart the same complex exponential contribution to the evolution of the time dependent system state as the eigen-energies of a time independent Hamiltonian do for its stationary states.

Between eqs.(B.15) and (B.16) we had established $\mathbf{C}_0 = \mathbf{U}(t_0 + T; t_0)$ and that $\mathbf{C}_0$ and hence $\mathbf{U}(t_0 + T; t_0)$ could be diagonalized using constant unitary matrices to give $e^{-i\mathbf{Q}'T}$. Thus we have

$$\mathbf{U}(t_0 + T; t_0) \equiv e^{-i\mathbf{Q}'T} \tag{B.37}$$

where the hermitian matrix $\mathbf{Q}'$ may be regarded as the generator of unitary evolution over a period and hence a time independent Hamiltonian for the system over the duration of a period with the initial time at t_0. This choice of initial instant is subjective and though the characteristic multipliers are independent of this, the expanded zone spectrum of quasienergies has multiple values that apply to a given

multiplier (as was seen for the $\epsilon_{\beta n}$ in the previous section) and hence the representation of the operator is sensitive to it. So one could make this sensitivity explicit by denoting this Hamiltonian as $\mathbf{Q}'_{t_0}$. From eq.(B.35) one can write

$$\mathbf{Q}'_{t_0} = \sum_{\beta} q'_{\beta} |\mathbf{p}'_{\beta}(t_0)\rangle\langle\mathbf{p}'_{\beta}(t_0)| \tag{B.38}$$

It is clear from the above that a diagonal representation follows from the choice of Floquet modes, at the intial instant t_0, as basis to represent the operator. Due to the periodicity of these modes the $\mathbf{Q}'_{t_0}$ are periodic in the initial time parameter t_0 as $\mathbf{Q}'_{t_0+T} = \mathbf{Q}'_{t_0}$. The operators $\mathbf{Q}'_{t_0}$ therefore, can be distinct upto the instants lying within a period and, as this stems from the non-trivial relation between Floquet modes defined at different instants within a given period, it follows that this is a property from the micromotion. These operators at different initial times may be related by the same transformation which was used in eq.(B.32) as, $\mathbf{Q}'_{t'_0} = \mathbf{U}^{-1}(t_0;t'_0)\mathbf{Q}'_{t_0}\mathbf{U}(t_0;t'_0)$ .Since the micromotion is the part of the evolution with periodicity originating in the Floquet modes, it may be quantified as the following unitary operator by isolating it from the general form of $\mathbf{U}(t_f;t_i)$ in eq.(B.35) as

$$\mathbf{M}(t_f,t_i) = \sum_{\beta} |\mathbf{p}'_{\beta}(t_f)\rangle\langle\mathbf{p}'_{\beta}(t_i)| \tag{B.39}$$

The operator $\mathbf{Q}'_{t_0}$ may be called the stroboscopic Floquet Hamiltonian as it describes the system for a period of the evolution and is like looking at the system after intervals of T-length and hence stroboscopic. Its diagonalization gives the quasienergies just like the infinite dimensional $\mathcal{H}_F$ of the previous section but one overlooks the effects of the micromotion here, whereas $\mathcal{H}_F$ accounted for that as well. This operator is of interest when the system behaviour is looked at over durations much larger than the period T and the micromotion can be ignored. Often times, as in [82] itself, $\mathbf{Q}'_{t_0}$ is referred to as the Floquet Hamiltonian though

we refrain from this here to avoid confusion with $\mathcal{H}_F$. As we saw earlier, $\mathcal{H}_F$ offers the most complete time independent description of the periodic system yet it involves diagonalizing an infinite matrix. We do always have the option of calculating the time evolution operator for a period and then from it obtaining the quasienergies and the Floquet modes. This knowledge may be used to write down the operators $\mathbf{Q}'_{t_0}$ and $\mathbf{M}(t_f, t_i)$ also. However the true advantage offered by seperating the evolution into the stroboscopic part and the micromotion lies in the possibility of computing these operators using certain perturbative approximation schemes which need no prior knowledge of the quasienergies or Floquet modes. This forms the central approach in most of the 'Floquet Engineering' applications in the literature and is the main theme of the discussion to follow.

In fact in most cases where Floquet theory is used this is the method of choice and once $\mathbf{Q}'_{t_0}$ and $\mathbf{M}(t_f, t_i)$ have been computed, in an effective approximate manner using convergent expansions, they may be used to write the time evolution operator as

$$\mathbf{U}(t_f; t_i) = e^{-i(t_f - t_i)\mathbf{Q}'_{t_f}} \mathbf{M}(t_f, t_i) = \mathbf{M}(t_f, t_i) e^{-i(t_f - t_i)\mathbf{Q}'_{t_i}} \tag{B.40}$$

and the quasienergies and Floquet modes may be obtained by solving the eigenvalue equation

$$\mathbf{Q}'_{t_0} |\mathbf{p}'_\beta(t_0)\rangle = q'_\beta |\mathbf{p}'_\beta(t_0)\rangle \tag{B.41}$$

Where a Floquet mode at any arbitrary instant may be obtained from the one at t_0 by $|\mathbf{p}'_\beta(t)\rangle = \mathbf{M}(t, t_0)|\mathbf{p}'_\beta(t_0)\rangle$.

B.4.1 Effective Hamiltonian

At present we have two means of reaching the solution of any time periodic quantum problem. One is via the direct diagonalization of the Floquet Hamiltonian or operator $\mathcal{H}_F$ which, in the space of time dependent states $\mathbb{H}$, is denoted by

$\widehat{\mathcal{H}}_F(t) = \mathcal{H}(t) - i\frac{d}{dt}$. This operator may be called the quasienergy operator, a term borrowed from [82], as it has the action $\widehat{\mathcal{H}}_F(t)|\mathbf{p}'_{\beta k}\ (t)\rangle = \epsilon_{\beta k}\ |\mathbf{p}'_{\beta k}\ (t)\rangle$. Where the $\epsilon_{\beta k}$ are the eigenenergies of $\mathcal{H}_F$ itself and hence have the quasienergies in the expanded scheme which goes beyond a period. The states $|\mathbf{p}'_{\beta k}\ (t)\rangle$ are the $\mathbb{H}$ couterparts of the vectors of components $\langle \alpha n|\tau_{\beta k}\ \rangle$ in $\mathbb{F}$. They are related by $|\mathbf{p}'_{\beta k}\ (t)\rangle = \langle \alpha n|\tau_{\beta\ \ }\rangle|\alpha\rangle e^{in\omega t}$. The other approach is using the stroboscopic $\mathbf{Q}'_{t_0}$ and the micromotion $\mathbf{M}(t_f, t_i)$. But each of these is not without its own limitations or difficulties be it the infinite dimensional nature of $\mathcal{H}_F$ or the parametric dependence on the initial instant in $\mathbf{Q}'_{t_0}$.

We may yet refine our attempts at a time independent description of the periodic system by introducing the notion of an effective Hamiltonian, H_{eff}, which is time independent and related to $\mathcal{H}_F$ and $\mathbf{Q}'_{t_0}$ by suitable unitary transformations, as we shall see. In this section we shall motivate the existence and usefulness of this operator before proceeding in the next to discuss perturbative methods that allow a direct, to various orders approximate, calculation of this operator under certain assumptions.

Going back to the representation of $\mathcal{H}_F$ in the Floquet Hilbert space $\mathbb{F}$ that made use of the basis $|\alpha n\rangle$ of orthonormal states in $\mathbb{F}$ with $|\alpha n\rangle = |\alpha\rangle e^{in\omega t}$, and using the relationship from Fourier analysis that helps to compute the Fourier components from their time dependent counterparts, we may show the relation between the operators $\mathcal{H}_F$ and $\widehat{\mathcal{H}}_F(t)$ as follows

$$\begin{aligned}
\langle \alpha n|\mathcal{H}_F|\gamma m\rangle &= \mathcal{H}^{n-m}_{\alpha\gamma} + \delta_{\alpha\gamma}\delta_{nm} m\omega \\
\mathcal{H}^k &= \frac{1}{T}\int_0^T e^{-ik\omega t}\mathcal{H}(t)dt \\
\mathcal{H}^{n-m} &= \frac{1}{T}\int_0^T e^{-i(n-m)\omega t}\mathcal{H}(t)dt \\
\mathcal{H}^{n-m}_{\alpha\gamma} &= \langle \alpha|\mathcal{H}^{n-m}|\gamma\rangle = \frac{1}{T}\int_0^T e^{-i(n-m)\omega t}\langle \alpha|\mathcal{H}(t)|\gamma\rangle dt
\end{aligned}$$

Similarly it may be shown that

$$\langle \alpha n|m\omega|\gamma m\rangle = \delta_{_{\alpha\gamma}}\delta_{_{nm}} m\omega = \frac{1}{T}\int_0^T e^{-in\omega t}\langle\alpha|-i\frac{d}{dt}|\gamma\rangle e^{im\omega t}dt \tag{B.42}$$

It is now possible to write down

$$\begin{aligned}\langle \alpha n|\mathcal{H}_F|\gamma m\rangle &= \frac{1}{T}\int_0^T e^{-in\omega t}\langle\alpha|\mathcal{H}(t) - i\frac{d}{dt}|\gamma\rangle e^{im\omega t}dt \\ &= \frac{1}{T}\int_0^T e^{-in\omega t}\langle\alpha|\widehat{\mathcal{H}}_F(t)|\gamma\rangle e^{im\omega t}dt \end{aligned}\tag{B.43}$$

A few remarks are in order looking at the above relationship between the Floquet Hamiltonian in $\mathbb{F}$ and the quasienergy operator in $\mathbb{H}$. We see that the matrix elements $\langle\alpha|\mathcal{H}^{n-m}|\gamma\rangle$ of the $\mathbb{H}$-space operator $\mathcal{H}^{n-m}$, itself determined from the integral giving the Fourier components of the $\mathbb{H}$-space operator $\mathcal{H}$, depend on the difference $n-m$ in the photon number index and hence $\mathcal{H}_F$ in $\mathbb{F}$ is invariant under translations in photon number. This is a general property of the $\mathbb{F}$-space counterparts of T-periodic operators in $\mathbb{H}$ which have a purely functional dependence on time instantaneously and are hence called 'time-local' [82]. Which means to say that they do not have any differential or integral operators with respect to time. This, as seen above, is not the case with the $\mathbb{H}$-space operator $-i\frac{d}{dt}$ which is a part of $\widehat{\mathcal{H}}_F(t)$ and from its matrix elements in Floquet space, see eq.(B.42), it is clear that its $\mathbb{F}$-space version is not translationally invariant in the photon number. It is a natural consequence of the Fourier relations that Hermitian or unitary time dependent operators in $\mathbb{H}$ retain these characteristics in going over to their corresponding opertors in $\mathbb{F}$.

We can now outline the broad approach to diagonalize or block diagonalize $\mathcal{H}_F$ using unitary operators $\mathbf{U}$ in $\mathbb{F}$ which are translationally invariant in the photon index such that $\langle\alpha n|\mathbf{U}|\gamma m\rangle = \langle\alpha|\mathbf{U}^{n-m}|\gamma\rangle$. $\mathbf{U}^{n-m}$ are operators in $\mathbb{H}$ which can be related, using a Fourier series, to the T-periodic unitary operator $\widehat{\mathbf{U}}(t) = \sum_k e^{ik\omega t}\mathbf{U}^k$. Applying this transformation on the Floquet Hamiltonian $\mathcal{H}_F$ and on any arbitrary

state in $\mathbb{F}$ would imply

$$\mathcal{H}_F \rightarrow \mathcal{H}'_F = \mathbf{U}^\dagger \mathcal{H}_F \mathbf{U}$$
$$|u_{\alpha n}\rangle \rightarrow |u'_{\alpha n}\rangle = \mathbf{U}^\dagger |u_{\alpha n}\rangle$$

This, in the time dependent picture of $\mathbb{H}$, translates into a time dependent gauge transformation for the periodic Hamiltonian $\mathcal{H}(t)$, under $\widehat{\mathbf{U}}(t)$, as can be seen by feeding the transformed operator written explicitly in terms of the untransformed one into the Schrödinger equation as follows

$$\mathcal{H}(t) \rightarrow \mathcal{H}'(t) = \widehat{\mathbf{U}}^\dagger(t)\mathcal{H}(t)\widehat{\mathbf{U}}(t) - i\widehat{\mathbf{U}}^\dagger(t)\left(\frac{d}{dt}\widehat{\mathbf{U}}(t)\right)$$
$$|\boldsymbol{\psi}(t)\rangle \rightarrow |\boldsymbol{\psi}'(t)\rangle = \widehat{\mathbf{U}}^\dagger(t)|\boldsymbol{\psi}(t)\rangle$$

Thus, one can write the matrix elements of the transformed Floquet Hamiltonian, $\mathcal{H}'_F$ as

$$\langle \alpha n|\mathcal{H}'_F|\gamma m\rangle = \langle \alpha|\mathcal{H}'^{n-m}|\gamma\rangle + \delta_{\alpha\gamma}\delta_{nm} m\omega \tag{B.44}$$

where $\mathcal{H}'^{k} = \frac{1}{T}\int_0^T dt\mathcal{H}'(t)e^{-ik\omega t}$ i.e. the operators $\mathcal{H}'^{n-m}$ are Fourier components of $\mathcal{H}'(t)$, the gauge transformed periodic Hamiltonian.

With this knowledge of the effects of unitary transformations on the operators in $\mathbb{H}$ and $\mathbb{F}$ and how the relationship between the representations of an operator, in the two spaces, is preserved by such transformations, we may define a unitary operator $\mathcal{U}$ in $\mathbb{F}$ such that it diagonalizes the Floquet Hamiltonian with reference to the $|\alpha n\rangle$ basis,

$$\langle \alpha n|\mathcal{U}^\dagger \mathcal{H}_F \mathcal{U}|\gamma m\rangle = (\langle \alpha|\mathcal{H}_F^{\mathrm{D}}|\gamma\rangle + m\omega)\delta_{\alpha\gamma}\delta_{nm}$$

in such a manner so as to make $\mathcal{H}_F^{\mathrm{D}}$ time independent. Where $\mathcal{H}_F^{\mathrm{D}}$, of course, satisfies the gauge transformation relation

$$\mathcal{H}_F^{\mathrm{D}} = \widehat{\mathcal{U}}^\dagger(t)\mathcal{H}(t)\widehat{\mathcal{U}}(t) - i\widehat{\mathcal{U}}^\dagger(t)\left(\frac{d}{dt}\widehat{\mathcal{U}}(t)\right) \tag{B.45}$$

and is diagonal in the basis $|\alpha\rangle$ of the time independent part in $\mathcal{H}(t)$

$$\langle\alpha|\mathcal{H}_F^{\mathrm{D}}|\gamma\rangle = \delta_{\alpha\gamma}q'_\alpha \tag{B.46}$$

It is interesting to note that we may relate the stroboscopic time independent Hamiltoniain $\mathbf{Q}'_{t_0}$ to the $\mathcal{H}_F^{\mathrm{D}}$ above, again by the unitary transformation, but now a time independent one, specific to the instant when one begins to observe the stroboscopic evolution,

$$\mathbf{Q}'_{t_0} = \widehat{\mathcal{U}}(t_0)\mathcal{H}_F^{\mathrm{D}}\widehat{\mathcal{U}}^\dagger(t_0) \tag{B.47}$$

The Floquet Hamiltonian eigenstate $|\tau_{\alpha n}\rangle = \mathcal{U}|\alpha n\rangle$ with eigenenergy $\epsilon_{\alpha n} = q'_\alpha + n\omega$ has the corresponding Floquet mode $|\mathbf{p}'_{\alpha n}(t)\rangle = \widehat{\mathcal{U}}(t)|\alpha\rangle e^{in\omega t}$ and so the micromotion in the transformed picture becomes

$$\mathbf{M}(t,t') = \widehat{\mathcal{U}}(t)\widehat{\mathcal{U}}^\dagger(t') \tag{B.48}$$

With the machinery of gauge transformations put in place so far, and its use in the diagonalization of $\mathcal{H}_F$, we have a route to obtain the stroboscopic Floquet Hamiltonian and the micromotion, as sketched in eqs.(B.47) amd (B.48), without the need for the quasienergies and Floquet modes. The exact diagonalization of $\mathcal{H}_F$ is, however, not necessary and it suffices to obtain a transformation that block diagonalizes it in the photon number index. This works because, referring to our earlier discussion on the structure of $\mathcal{H}_F$ in the previous section, what such a block diagonalization does is to make the $n-m \neq 0$ blocks of $\mathcal{H}_F$ zero which is equivalent

to transforming the transition amplitudes from the higher Fourier coefficients of $\mathcal{H}(t)$, the $\mathcal{H}^{n-m}_{\alpha\gamma}$, into the time independent digonal blocks. The corresponding operator in $\mathbb{H}$, which is naturally time independent, is called the effective Hamiltonian, and we choose to denote it as H_{eff}.

A unitary operator $\mathbf{U}_F$ may be introduced that block diagonalizes $\mathcal{H}_F$ in the following way

$$\langle \alpha n|\mathbf{U}_F^{\dagger}\mathcal{H}_F\mathbf{U}_F|\gamma m\rangle = \delta_{nm}(\langle \alpha|H_{\text{eff}}|\gamma\rangle + \delta_{\alpha\gamma}m\omega) \tag{B.49}$$

with the time independent H_{eff} acting on the system Hilbert space $\mathbb{H}$ and satisfying the gauge transformation of the kind in eq.(B.45). The time periodic unitary operator, that affects this transformation, in this case being, $\widehat{\mathbf{U}}_F(t)$. These transformations, $\mathbf{U}_F$ and $\widehat{\mathbf{U}}_F$ for that matter, are not unique in that their multiplication by constant unitary operators from the right leads to an intermixing of elements in the diagonal blocks while preserving the block diagonal form of $\mathbf{U}_F^{\dagger}\mathcal{H}_F\mathbf{U}_F$.

Each of the diagonal blocks of $\mathbf{U}_F^{\dagger}\mathcal{H}_F\mathbf{U}_F$, which are essentially the matrix H_{eff} with different integer multiples of ω being added to the diagonal elements of the block, depending on its position along the diagonal, is a possible candidate for the stroboscopic Floquet Hamiltonian. This becomes apparent by writing $\mathcal{H}_F$ in its eigenbasis as $\mathcal{H}_F = \sum_{n=-\infty}^{\infty}\sum_{\beta}|\tau_{\beta n}\rangle(q'_{\beta} + n\omega)\langle\tau_{\beta n}|$, and comparing this with the structure of the $\mathbf{Q}'_{t_0}$ matrix in eq.(B.38). Let us consider the basis of states, in $\mathbb{F}$, in which $\mathcal{H}_F$ is block diagonal to be denoted by $|\alpha n\rangle' \equiv \mathbf{U}_F|\alpha n\rangle$, i.e. a transformed basis. In the explicit time way of writing where $|\alpha n\rangle_t = |\alpha\rangle e^{in\omega t}$, the new basis allows, $|\alpha n\rangle'_t \equiv \mathbf{U}_F|\alpha n\rangle_t = \widehat{\mathbf{U}}_F(t)|\alpha\rangle e^{in\omega t}$. This for $t = t_0$ and zero photon number yeilds $|\alpha 0\rangle'_{t_0} = |\alpha\rangle'_{t_0} = \widehat{\mathbf{U}}_F(t_0)|\alpha\rangle$. Expressing $\mathbf{Q}'_{t_0}$ as the $n = m = 0$ block of $\mathbf{U}_F^{\dagger}\mathcal{H}_F\mathbf{U}_F$, which may be called the zero photon sector, onto which we are projecting using states that span this subspace, is equivalent to the following representation in

the new basis

$$\begin{aligned}
\mathbf{Q}'_{t_0} &= \sum_{\alpha\gamma} |\alpha 0\rangle'_{t_0} \left(\langle \alpha 0|\mathcal{H}_F|\gamma 0\rangle'\right)_{t_0} \langle \gamma 0| \\
&= \sum_{\alpha\gamma} \mathbf{U}_F|\alpha 0\rangle\langle\alpha 0|\mathbf{U}_F^\dagger \mathcal{H}_F \mathbf{U}_F|\gamma 0\rangle\langle\gamma 0|\mathbf{U}_F^\dagger \\
&= \sum_{\alpha\gamma} \widehat{\mathbf{U}}_F(t_0)|\alpha 0\rangle\langle\alpha 0|\mathbf{U}_F^\dagger \mathcal{H}_F \mathbf{U}_F|\gamma 0\rangle\langle\gamma 0|\widehat{\mathbf{U}}_F^\dagger(t_0) \\
&= \widehat{\mathbf{U}}_F(t_0)\left(\sum_{\alpha\gamma}|\alpha 0\rangle\langle\alpha|H_{\text{eff}}|\gamma\rangle\langle\gamma 0|\right)\widehat{\mathbf{U}}_F^\dagger(t_0) \\
&= \widehat{\mathbf{U}}_F(t_0) H_{\text{eff}} \widehat{\mathbf{U}}_F^\dagger(t_0)
\end{aligned} \tag{B.50}$$

Where in the final stages we have used eq.(B.49), thus we see that the stroboscopic and the effective Hamiltonians are related by a unitary transformation. The micromotion operator in this case becomes

$$\mathbf{M}_F(t,t') = \widehat{\mathbf{U}}_F(t)\widehat{\mathbf{U}}_F^\dagger(t') \tag{B.51}$$

From eqs.(B.50) and (B.51), the time evolution operator can be calculated using the expression in (B.40). In fact the time evolution operator can be directly written using the effective Hamiltonian as follows

$$\mathbf{U}(t_2;t_1) = \widehat{\mathbf{U}}_F(t_2) e^{-i(t_2-t_1)H_{\text{eff}}} \widehat{\mathbf{U}}_F^\dagger(t_1) \tag{B.52}$$

The above manner of computing the evolution operator may be compared to the one presented in eq.(B.40) to illustrate the relative merits and demerits of the two techniques. The above method clearly constructs the evolution operator as a product of three operators instead of just the two required in eq.(B.40). However the micromotion in the formulation here is just dependent on single time instants i.e. $\widehat{\mathbf{U}}_F(t)$, unlike the micromotion operator $\mathbf{M}(t,t')$. Most imporantly the use of the

effective Hamiltonian, H_{eff}, gets rid of the initial time sensitivity that was encountered with the stroboscopic $\mathbf{Q}'_{t_0}$. A key property of the micromotion, that shall be useful in the perturbative expansion methods to be discussed shortly, is that being a unitary operator it may be expressed as the exponential of a hermitian operator, $\widehat{F}(t)$, as

$$\widehat{\mathbf{U}}_F(t) = e^{i\widehat{F}(t)} \tag{B.53}$$

This $\widehat{F}(t)$ has, of late, acquired the moniker 'kick operator' in the literature [80].

It is worth noting here that we can compute the Floquet modes and quasienergies by diagonalizing H_{eff} which essentially means diagonalizing with respect to the states $|\alpha\rangle$ of the time independent part in $\mathcal{H}(t)$. Then one may write down the eigenvalue equation for H_{eff},

$$H_{\text{eff}}|a_\beta\rangle = q'_\beta|a_\beta\rangle$$

from which the Floquet modes and extended quasienergies can be computed

$$\begin{aligned}
|\mathbf{p}'_{\beta n}(t)\rangle &= \widehat{\mathbf{U}}_F(t)|a_\beta\rangle e^{in\omega t} \\
\epsilon_{\beta n} &= q'_\beta + n\omega \\
|\mathbf{p}'_\beta(t)\rangle &\equiv |\mathbf{p}'_{\beta 0}(t)\rangle \\
|\mathbf{p}'_\beta(t)\rangle &= \sum_\alpha \Phi^0_{\alpha\beta}|\alpha\rangle'_t
\end{aligned}$$

where it holds that

$$|\alpha\rangle'_t = \widehat{\mathbf{U}}_F(t)|\alpha 0\rangle = \widehat{\mathbf{U}}_F(t)|\alpha\rangle$$

and

$$\Phi^0_{\alpha\beta} = \langle\alpha|a_\beta\rangle = \langle\alpha 0|a_\beta\rangle = \langle\alpha 0|\tau_{\beta 0}\rangle$$

Here we make the association to the eigenstates $|\tau_{\alpha}\rangle$ of the Floquet Hamiltonian $\mathcal{H}_F$ which were discussed in the previous section. We note, it is in fact true that the eigenstates of H_{eff}, the $|a_\beta\rangle$, are nothing but the finite N-tuple vectors $|\tau_{\beta}\rangle$ which span the N-dimensional zero photon subspace of the infinite dimensional Floquet Hilbert space $\mathbb{F}$. This follows from the fact that diagonalizing H_{eff} must take one to the same basis as that in which $\mathcal{H}_F$ is diagonal in its zero photon sector. Since $\mathbf{U}_F^\dagger \mathcal{H}_F \mathbf{U}_F$ is also translationally invariant in the photon index the same transformation diagonalizes the entire $\mathcal{H}_F$ as the one that does so for the zero photon subspace. Also we see above that as $\widehat{\mathbf{U}}_F(t)$ is the operator that defines the micromotion, it plays a role in evolving the Floquet modes and also completely accounts for the initial time dependence while transforming from the effective Hamiltonian to the stroboscopic one.

In the process of obtaining H_{eff}, using photon number translation invariant $\mathbf{U}_F$ and T-periodic $\widehat{\mathbf{U}}_F(t)$, operators which block diagonalize $\mathcal{H}_F$ assimilated the contributions arising from the Fourier coefficients of the higher order harmonics and hence are concerned with changes occuring within the duration of a period. They acheive the equivalent of a phase factoring/rotating frame coordinate transformation to seperate out the effects of short term dynamics. Thus the micromotion which is determined by these operators is also of significance over intervals of evolution $t_f - t_i < T$. This is one part of the periodic evolution problem. Once H_{eff} has been obtained it may be used as an effective static system that describes the evolution over durations $t_f - t_i \gg T$, such that the system states are stationary states given by the eigenstates of H_{eff} and the evolution is of the trivial unitary phase kind. This is the long term dynamics which is granted by the diagonalization of H_{eff}. The choice of the zero photon sector projection to express $\mathbf{Q}'_{t_0}$ in eq.(B.50) ensures that the evolution is observed over just one period. Observing the evolution in multiples of the fundamental period still renders the system periodic but then one is bound to

consider the blocks of $\mathcal{H}_F$ with the quasienergies lifted by multiples of ω. The evolution operator as segregated in eq.(B.52) addresses both the long term and short term dynamical components using the effective Hamiltonian to give a stationary state description which is more dominant at long times. The 'kicks' due to $\widehat{\mathbf{U}}_F(t)$ at the ends of the evolution, help to adjust for the portions that remain after the integer multiple of the period T nearest to the duration under consideration has been subtracted from it, hence the short term dynamics.

We shall now proceed to a discussion of certain perturbative expansions which can be used to compute the effective Hamiltonian in the limit of the driving frequency becoming very large, in principle, infinity. These are a useful tool which may be used to compute the effective Hamiltonian atleast to a suitable approximation. In cases where other means of solving the periodic problem are not analytically accessible, these techniques come to the rescue by allowing an infinite frequency limit of the problem to be obtained in an approxiamte analytic manner.

B.4.2 High Frequency Expansions

In this section we shall look at two high frequency expansion schemes, both of which approximate the effective Hamiltonian, and the micromotion or a quantity analogous to it. Both of these use the inverse powers of the frequency as the vanishing parameter in the expansions. The first scheme we look at is the Van Vleck like expansion for the effective Hamiltonian as discussed in [80, 86, 87]. The other makes use of the Brillouin-Wigner method of perturbation theory as developed in [92]. The following contains only prescriptions on how these schemes may be applied to a given periodic time dependent Hamiltonian and we make no attempt to compare the accuracy of these schemes or explore the relation between the effective Hamiltonians obtained from each of them.

B.4.2.1 Van Vleck Expansion for H_{eff} and $\widehat{F}$

Let us consider

$$\mathcal{H}(t) = \widehat{H}_0 + \widehat{V}(t)$$

where $\widehat{H}_0$ is the time independent part of the Hamiltonian and $\widehat{V}(t) = \widehat{V}(t+T)$ is the periodic time dependent potential that makes the Hamiltonian periodic. We know from the previous section that the effective Hamiltonian H_{eff} must be related to $\mathcal{H}(t)$ by a time dependent gauge transformation of the kind in eq.(B.45), hence

$$H_{\text{eff}} = e^{i\widehat{F}(t)}\mathcal{H}e^{-i\widehat{F}(t)} + i\frac{\partial}{\partial t}\left(e^{i\widehat{F}(t)}\right)e^{-i\widehat{F}(t)} \tag{B.54}$$

where we have used $\widehat{\mathbf{U}}_F(t) = e^{i\widehat{F}(t)}$ from eq.(B.53) in the previous section.

From eq.(B.52) we have seen that the entire solution is divided into

a. Initial Kick $(e^{i\widehat{F}(t_i)})$

b. Evolution under a time-independent Hamiltonian $H_{\text{eff}}(e^{-iH_{\text{eff}}(t_f - ti)})$

c. Final Kick $(e^{-i\widehat{F}(t_f)})$

We assume the period T to be small and $\omega = \frac{2\pi}{T}$ to be large and make the following perturbation ansatz.

$$\begin{aligned} H_{\text{eff}} &= \sum_{0\leq n<\infty} \frac{1}{\omega^n}\widehat{H}^{(n)} \\ \widehat{F} &= \sum_{1\leq n<\infty} \frac{1}{\omega^n}\widehat{F}^{(n)} \end{aligned} \tag{B.55}$$

Convergence of these expansions is not guaranteed.

The prescription is as follows:

a. Write eq.(B.54) for H_{eff} as an expanded perturbation series in $(\frac{1}{\omega})$.

b. At each order of perturbation, which corresponds to a specific power of $(\frac{1}{\omega})$ retain the time-independent average in H_{eff} and adjust $\widehat{F}$ to annhilate any time dependence.

c. Repeat the procedure at each order in perturbation.

Except for special cases H_{eff} cannot be obtained from (B.54) in a closed form. We use the following identities:

$$e^{i\widehat{F}}\mathcal{H}e^{-i\widehat{F}} = \mathcal{H} + i[\widehat{F},\mathcal{H}] - \frac{1}{2}\left[\widehat{F},[\widehat{F},\mathcal{H}]\right] - \frac{i}{6}\left[\widehat{F},\left[\widehat{F},[\widehat{F},\mathcal{H}]\right]\right] + ...$$

and

$$\left(\frac{\partial}{\partial t}e^{\widehat{F}}\right)e^{-i\widehat{F}} = i\frac{\partial\widehat{F}}{\partial t} - \frac{1}{2}[\widehat{F},\frac{\partial\widehat{F}}{\partial t}] - \frac{i}{6}\left[\widehat{F},[\widehat{F},\frac{\partial\widehat{F}}{\partial t}]\right] + ...$$

Substituting $H_{\text{eff}} = \sum_{0\leq n<\infty}\frac{1}{\omega^n}\widehat{H}^{(n)}$ and $\widehat{F} = \sum_{1\leq n<\infty}\frac{1}{\omega^n}\widehat{F}^{(n)}$ in eqn.(5) and only retaining upto $\mathcal{O}\left(\frac{1}{\omega^2}\right)$ we have

$$\begin{aligned}H_{\text{eff}} = \widehat{H}_0 + \widehat{V}(t) + i\left[\frac{\widehat{F}^{(1)}}{\omega},\mathcal{H}\right] + i\left[\frac{\widehat{F}^{(2)}}{\omega^2},\mathcal{H}\right] - \frac{1}{2}\left[\frac{\widehat{F}^{(1)}}{\omega},\left[\frac{\widehat{F}^{(1)}}{\omega},\mathcal{H}\right]\right] - \frac{1}{\omega}\frac{\partial\widehat{F}^{(1)}}{\partial t} - \frac{1}{\omega^2}\frac{\partial\widehat{F}^{(2)}}{\partial t} \\ -\frac{1}{\omega^3}\frac{\partial\widehat{F}^{(2)}}{\partial t} - \frac{i}{2}\left[\frac{\widehat{F}^{(1)}}{\omega} + \frac{\widehat{F}^{(2)}}{\omega^2},\frac{1}{\omega}\frac{\partial\widehat{F}^{(1)}}{\partial t} + \frac{1}{\omega^2}\frac{\partial\widehat{F}^{(2)}}{\partial t}\right] + \frac{1}{6}\left[\frac{\widehat{F}^{(1)}}{\omega},\left[\frac{\widehat{F}^{(1)}}{\omega},\frac{1}{\omega}\frac{\partial\widehat{F}^{(1)}}{\partial t}\right]\right]\end{aligned} \tag{B.56}$$

The operator $\widehat{F}$ is periodic with period T and has zero mean.

$$\Rightarrow \frac{1}{T}\int_0^T \widehat{F}dt = 0$$

. $\Rightarrow \widehat{F}^{(n)}$ are all periodic and have zero mean or

$$\langle \widehat{F}^{(n)} \rangle = 0 \qquad \widehat{F}^{(n)}(t+T) = \widehat{F}^{(n)}(t)$$

At each order in perturbation, the time independent average is retained in H_{eff} and $\widehat{F}$ is used to nullify the time dependent part.

ORDER ω^0 :

$$\widehat{H}_0 + \widehat{V}(t) - \frac{1}{\omega}\frac{\partial \widehat{F}^{(1)}}{\partial t}$$

$$\widehat{H}^{(0)} = \left\langle \widehat{H}_0 + \widehat{V}(t) - \frac{1}{\omega}\frac{\partial \widehat{F}^{(1)}}{\partial t} \right\rangle$$

$$= \langle \widehat{H}_0 \rangle + \langle \widehat{V}(t) \rangle - \frac{1}{\omega}\left\langle \frac{\partial \widehat{F}^{(1)}}{\partial t} \right\rangle$$

$$= \frac{\widehat{H}_0}{T}\int_0^T dt + \frac{1}{T}\int_0^T \widehat{V}(t)dt - \frac{1}{\omega T}\int_0^T \frac{\partial \widehat{F}^{(1)}}{\partial t}dt$$

$$\widehat{V}(t) = \widehat{V}(t+T)$$

$\widehat{V}(t)$ may be expanded in a Fourier series as

$$\widehat{V}(t) = \widehat{V}_0 + \sum_{1 \le n < \infty} \widehat{V}_n e^{in\omega t} + \sum_{1 \le n < \infty} \widehat{V}_{-n} e^{-in\omega t}$$

$\widehat{F}^{(1)}$ can be expanded similarly but $\widehat{F}^{(1)}$ has zero mean. So $\frac{\partial \widehat{F}^{(1)}}{\partial t}$ also has zero mean.

$$\widehat{H}^{(0)} = \widehat{H}_0 + \widehat{V}_0 \qquad \widehat{V}_0 = \frac{1}{T}\int_{0 \le t \le T} \widehat{V}(t)dt$$

The time dependent part is

$$\widehat{H}_0 + \widehat{V}(t) - \frac{1}{\omega}\frac{\partial \widehat{F}^{(1)}}{\partial t} - \left\langle \widehat{H}_0 + \widehat{V}(t) - \frac{1}{\omega}\frac{\partial \widehat{F}^{(1)}}{\partial t} \right\rangle$$

$$\Rightarrow \widehat{V}(t) - \widehat{V}_0 - \frac{1}{\omega}\frac{\partial \widehat{F}^{(1)}}{\partial t}$$

(equating this to zero)

or

$$\sum_{1\leq n<\infty} \widehat{V}_n e^{in\omega t} + \sum_{1\leq n<\infty} \widehat{V}_{-n} e^{-in\omega t} = \frac{1}{\omega}\frac{\partial \widehat{F}^{(1)}}{\partial t}$$

$$\Rightarrow \widehat{F}^{(1)} = \omega \int_0^t \left(\sum_{1\leq n<\infty} \widehat{V}_n e^{in\omega \acute{t}} + \sum_{1\leq n<\infty} \widehat{V}_{-n} e^{-in\omega \acute{t}} \right) d\acute{t}$$

$$\Rightarrow \frac{1}{i} \sum_{1\leq n<\infty} \frac{1}{n} \left(\widehat{V}_n e^{in\omega t} - \widehat{V}_{-n} e^{-in\omega t} \right)$$

or at order ω_0

$$\widehat{H}^{(0)} = \widehat{H}_0 + \widehat{V}_0$$

$$\widehat{F}^{(1)} = \frac{1}{i} \sum_n \frac{1}{n} \left(\widehat{V}_n e^{in\omega t} - \widehat{V}_{-n} e^{-in\omega t} \right)$$

ORDER ω^{-1}

$$i \left[\frac{\widehat{F}^{(1)}}{\omega}, \mathcal{H} \right] - \frac{1}{\omega^2}\frac{\partial \widehat{F}^{(2)}}{\partial t} - \frac{i}{2} \left[\frac{\widehat{F}^{(1)}}{\omega}, \frac{1}{\omega}\frac{\partial \widehat{F}^{(1)}}{\partial t} \right]$$

$$\widehat{H}^{(1)} = \left\langle i \left[\frac{\widehat{F}^{(1)}}{\omega}, \mathcal{H} \right] \right\rangle - \left\langle \frac{1}{\omega^2}\frac{\partial \widehat{F}^{(2)}}{\partial t} \right\rangle - \frac{i}{2} \left\langle \left[\frac{\widehat{F}^{(1)}}{\omega}, \frac{1}{\omega}\frac{\partial \widehat{F}^{(1)}}{\partial t} \right] \right\rangle$$

The second bracket in the above expression is put to zero. Hence,

$$\widehat{H}^{(1)} = i\left\langle\left[\frac{\widehat{F}^{(1)}}{\omega}, \mathcal{H}\right]\right\rangle - \frac{i}{2}\left\langle\left[\frac{\widehat{F}^{(1)}}{\omega}, \frac{1}{\omega}\frac{\partial\widehat{F}^{(1)}}{\partial t}\right]\right\rangle$$

$$= i\left\langle\left[\frac{\widehat{F}^{(1)}}{\omega}, (\widehat{V}(t) - \widehat{V}_0)\right]\right\rangle - \frac{i}{2}\left\langle\left[\frac{\widehat{F}^{(1)}}{\omega}, (\widehat{V}(t) - \widehat{V}_0)\right]\right\rangle$$

$$= \frac{i}{2}\left\langle\left[\frac{\widehat{F}^{(1)}}{\omega}, (\widehat{V}(t) - \widehat{V}_0)\right]\right\rangle$$

$$\widehat{V}(t) - \widehat{V}_0 = \sum_n \frac{1}{n}\left(\widehat{V}_n e^{in\omega t} - \sum_n \widehat{V}_{-n} e^{-in\omega t}\right)$$

$$\widehat{F}^{(1)} = \int^t (\widehat{V}(\acute{t}) - \widehat{V}_0) d\acute{t}$$

$$\frac{\widehat{F}^{(1)}}{\omega} = \sum_n \left(\frac{\widehat{V}_n e^{in\omega t}}{in\omega} - \frac{\widehat{V}_{-n} e^{-in\omega t}}{in\omega}\right)$$

$$\left\langle\frac{\widehat{F}^{(1)}}{\omega}(\widehat{V}(t) - \widehat{V}_0)\right\rangle = \frac{1}{T}\int_0^t \sum_{n,m}\left(\frac{\widehat{V}_n e^{in\omega\acute{t}}}{in\omega} - \frac{\widehat{V}_{-n} e^{-in\omega\acute{t}}}{in\omega}\right)\left(\widehat{V}_m e^{im\omega\acute{t}} + \widehat{V}_{-m} e^{-im\omega\acute{t}}\right)$$

$$= \frac{1}{T}\int_0^T d\acute{t} \sum_{m,n} \frac{\widehat{V}_n\widehat{V}_m}{in\omega} e^{i(n+m)\omega\acute{t}} + \frac{\widehat{V}_n\widehat{V}_{-m}}{in\omega} e^{i(n-m)\omega\acute{t}} - \frac{\widehat{V}_{-n}\widehat{V}_m}{in\omega} e^{-i(n-m)\omega\acute{t}} - \frac{\widehat{V}_{-n}\widehat{V}_{-m}}{in\omega} e^{-i(n+m)\omega\acute{t}}$$

$$= \sum_n \frac{\widehat{V}_n\widehat{V}_{-n}}{in\omega} - \frac{\widehat{V}_{-n}\widehat{V}_n}{in\omega} \tag{B.57}$$

$$\left\langle (\widehat{V}(t) - \widehat{V}_0)\frac{\widehat{F}^{(1)}}{\omega} \right\rangle = \sum_n \frac{\widehat{V}_{-n}\widehat{V}_n}{in\omega} - \frac{\widehat{V}_n\widehat{V}_{-n}}{in\omega} \tag{B.58}$$

Subtracting (B.58) from (B.57) we get,

$$\Rightarrow \sum_n \frac{2}{in\omega}[\widehat{V}_n, \widehat{V}_{-n}]$$

or

$$\widehat{H}^{(1)} = \frac{i}{2}\sum_n \frac{2}{in\omega}[\widehat{V}_n, \widehat{V}_{-n}]$$

$$= \sum_n \frac{1}{n\omega}[\widehat{V}_n, \widehat{V}_{-n}]$$

$$i\left[\frac{\widehat{F}^{(1)}}{\omega}, \mathcal{H}\right] - \frac{1}{\omega^2}\frac{\partial \widehat{F}^{(2)}}{\partial t} - \frac{i}{2}\left[\widehat{F}^{(1)}, \frac{\partial \widehat{F}^{(1)}}{\partial t}\right] - \sum_n \frac{1}{n\omega}[\widehat{V}_n, \widehat{V}_{-n}] = 0$$

$$\Rightarrow \widehat{F}^{(2)} = \frac{1}{i}\sum_n \frac{1}{n^2}\left([\widehat{V}_n, \widehat{H}_0 + \widehat{V}_0]e^{in\omega t} - h.c.\right) + \frac{1}{2i}\sum_{n,m=1}^{\infty} \frac{1}{n(n+m)}\left([\widehat{V}_n, \widehat{V}_m]e^{i(n+m)\omega t} + h.c.\right)$$

$$+ \frac{1}{2i}\sum_{n\neq m=1}^{\infty} \frac{1}{n(n+m)}\left([\widehat{V}_n, \widehat{V}_{-m}]e^{i(n-m)\omega t} + h.c.\right)$$

Finally, we have in the same manner

$$\begin{aligned} H_{\text{eff}} = \widehat{H}_0 + \widehat{V}_0 + \frac{1}{\omega}\sum_{n=1}^{\infty}\frac{1}{n}[\widehat{V}_n, \widehat{V}_{-n}] + \frac{1}{2\omega^2}\sum_{n=1}^{\infty}\frac{1}{n^2}\left(\left[[\widehat{V}_n, \widehat{H}_0], \widehat{V}_{-n}\right] + h.c.\right) \\ + \frac{1}{3\omega^2}\sum_{n,m=1}^{\infty}\frac{1}{nm}\left(\left[\widehat{V}_n, [\widehat{V}_m, \widehat{V}_{-(n+m)}]\right] - 2\left[\widehat{V}_n, [\widehat{V}_{-n}, \widehat{V}_{(n-m)}]\right] + h.c.\right)\ldots \end{aligned} \tag{B.59}$$

and

$$\widehat{F}(t) = \frac{1}{i\omega}\sum_{n=1}^{\infty}\frac{1}{n}\left(\widehat{V}_n e^{in\omega t} - \widehat{V}_{-n}e^{-in\omega t}\right) + \frac{1}{i\omega^2}\sum_{n=1}^{\infty}\frac{1}{n^2}\left([\widehat{V}_n, \widehat{H}_0 + \widehat{V}_0]e^{in\omega t} - h.c.\right)$$
$$+ \frac{1}{2i\omega^2}\sum_{n,m=1}^{\infty}\frac{1}{n(n+m)}\left([\widehat{V}_n, \widehat{V}_m]e^{i(n+m)\omega t} - h.c.\right)$$
$$+ \frac{1}{2i\omega^2}\sum_{n\neq m=1}^{\infty}\frac{1}{n(n-m)}\left([\widehat{V}_n, \widehat{V}_{-m}]e^{i(n-m)\omega t} - h.c.\right)\ldots \tag{B.60}$$

Thus, in this way we obtain the series expansions for the effective Hamiltonian H_{eff} and the kick operator $\widehat{F}(t)$ from which the micromotion can be calculated. In the high frequency limit one can expect convergence to be fast enough and then one may treat it as a regular perturbation series with finite order corrections.

B.4.2.2 The Brillouin-Wigner Method

First we provide a general outline of this perturbation theory method as it is used in time independent quantum mechanics. Given a Hamiltonian $\hat{H} = \hat{H}_0 + \hat{V}$ where $\hat{H}_0$ is exactly solvable and $\hat{V}$ is the perturbation term, and the eigendecomposition of $\hat{H}_0$ —

$$\hat{H}_0|\alpha\rangle = \epsilon_\alpha|\alpha\rangle$$
$$\langle\beta|\alpha\rangle = \delta_{\beta\alpha}$$
$$\sum_\beta |\beta\rangle\langle\beta| = \mathbf{I}$$

using Brillouin-Wigner (BW) perturbation theory, we try to obtain $\{|\psi_\alpha\rangle, \ldots\}$ and $\{E_\alpha, \ldots\}$, such that $\hat{H}|\psi_\alpha\rangle = E_\alpha|\psi_\alpha\rangle$, in terms of $\hat{V}$ and $\{|\alpha\rangle, \ldots\}$.

To obtain the BW perturbative expansion, we begin with the eigenvalue equation.

$$\hat{H}|\psi_\alpha\rangle = (\hat{H}_0 + \hat{V})|\psi_\alpha\rangle = E_\alpha|\psi_\alpha\rangle$$

The wavefunctions $|\psi_\alpha\rangle$ are normalized as $\langle\alpha|\psi_\alpha\rangle = 1$. On contracting with $\langle\alpha|$,

$$\begin{aligned}
\langle\alpha|(\hat{H}_0 + \hat{V})|\psi_\alpha\rangle &= E_\alpha\langle\alpha|\psi_\alpha\rangle \\
\epsilon_\alpha\langle\alpha|\psi_\alpha\rangle + \langle\alpha|\hat{V}|\psi_\alpha\rangle &= E_\alpha\langle\alpha|\psi_\alpha\rangle \\
E_\alpha &= \epsilon_\alpha + \langle\alpha|\hat{V}|\psi_\alpha\rangle
\end{aligned} \tag{B.61}$$

Rewriting the eigenvalue equation as

$$\begin{aligned}
(E_\alpha - \hat{H}_0)\,|\psi_\alpha\rangle &= \hat{V}\,|\psi_\alpha\rangle \\
&= \mathbf{I}\,\hat{V}\,|\psi_\alpha\rangle \\
&= \sum_m |m\rangle\,\langle m|\,\hat{V}\,|\psi_\alpha\rangle \\
&= |\alpha\rangle\,\langle\alpha|\hat{V}|\psi_\alpha\rangle + (\mathbf{I} - |\alpha\rangle\,\langle\alpha|)\hat{V}\,|\psi_\alpha\rangle
\end{aligned} \tag{B.62}$$

Using eq. (B.61),

$$\begin{aligned}
&= (E_\alpha - \hat{H}_0)\,|\alpha\rangle + (\mathbf{I} - |\alpha\rangle\,\langle\alpha|)\hat{V}\,|\psi_\alpha\rangle \\
(E_\alpha - \hat{H}_0)(|\psi_\alpha\rangle - |\alpha\rangle) &= (\mathbf{I} - |\alpha\rangle\,\langle\alpha|)\hat{V}\,|\psi_\alpha\rangle \\
|\psi_\alpha\rangle &= |\alpha\rangle + (E_\alpha - \hat{H}_0)^{-1}(\mathbf{I} - |\alpha\rangle\,\langle\alpha|)\hat{V}\,|\psi_\alpha\rangle
\end{aligned}$$

Defining the resolvent operator as $\hat{R}_\alpha = (E_\alpha - \hat{H}_0)^{-1} = \sum_\alpha |\alpha\rangle\,(E_\alpha - \epsilon_\alpha)^{-1}\,\langle\alpha|$,

$$|\psi_\alpha\rangle = |\alpha\rangle + \hat{R}_\alpha(\mathbf{I} - |\alpha\rangle\,\langle\alpha|)\hat{V}\,|\psi_\alpha\rangle \tag{B.63}$$

The above equation is the main result of BW perturbation theory. Peculiarity of the above equation is that it depends on the undertermined parameter E_α, and this is unlike the Rayleigh-Schrödinger perturbation theory. Solving Eq. (B.63) self-consistently with Eq. (B.61), solutions to the eigenvalue equation are obtained. Using the equation, we obtain an iterative solution to the Schrödinger equation. In each iteration, we obtain a new estimate of $|\psi_\alpha\rangle$ by substituting the old estimate of $|\psi_\alpha\rangle$ on the righthand side of Eq. (B.63)

$$
\begin{aligned}
|\psi_\alpha^{(j)}\rangle &= |\alpha\rangle + \hat{R}(E_\alpha)\,(\mathbf{I} - |\alpha\rangle\langle\alpha|)\hat{V}\,|\psi_\alpha^{(j-1)}\rangle \\
|\psi_\alpha^{(0)}\rangle &= |\alpha\rangle \\
\lim_{j\to\infty} |\psi_\alpha^{(j)}\rangle &= |\psi_\alpha\rangle
\end{aligned}
\tag{B.64}
$$

No approximation has been used until this point, and exact solution can be obtained if iterated infinitely. In practice, approximate solution is obtained by truncating the iteration.

Further, eq. (B.63) can be simplified by expanding the recurrence relation

$$
\begin{aligned}
|\psi_\alpha\rangle &= |\alpha\rangle + \hat{R}_\alpha\hat{Q}_\alpha\hat{V}\,|\psi_\alpha\rangle \\
\text{where } \hat{Q}_\alpha = \mathbf{I} - |\alpha\rangle\langle\alpha|\,, \quad & \\
&= |\alpha\rangle + \hat{R}_\alpha\hat{Q}_\alpha\hat{V}\,|\alpha\rangle + \hat{R}_\alpha\hat{Q}_\alpha\hat{V}\hat{R}_\alpha\hat{Q}_\alpha\hat{V}\,|\alpha\rangle + \ldots \\
&= \sum_{k=0}^{\infty} \{\hat{R}_\alpha\hat{Q}_\alpha\hat{V}\}^k\,|\alpha\rangle \\
&= (\mathbf{I} - \{\hat{R}_\alpha\hat{Q}_\alpha\hat{V}\})^{-1}\,|\alpha\rangle
\end{aligned}
$$

When higher order term contributions are diminishingly small, truncating the series produces approximate solutions to the problem. The operator $\hat{Q}_\alpha$ appearing in the series is essentially a projection operator onto the eigenstates of $\hat{H}_0$ that are orthogonal to $|\alpha\rangle$. This motivates the idea that the BW scheme can be formulated in terms

of projection operators which also leads to the notion of an effective Hamiltonian in BW perturbation theory. In the following we shall develop this notion and apply it to the solution of the eigenvalue problem of the infinite dimensional $\mathcal{H}_F$.

Also known as the model space approach, in this way of looking at the perturbation problem, the eigenbasis of the uperturbed $\hat{H}_0$ is chosen as an orthonormal basis for the Hilbert space of the problem. The idea is to regard one of the states of this basis as the model space and the rest of the basis as constituting the orthogonal space. One is free to choose multiple basis states for the model space in which case it is multidimensional. Here, for the time being, we restrict to a single state as the model space to derive the essential results regarding the effective Hamiltonian.

Let $\mathrm{R} \equiv \{|\phi_\alpha\rangle \dots\}$ is the set of reference states, $|\phi_0\rangle \in \mathrm{R}$ is the model state, then $P = |\phi_0\rangle \langle\phi_0|$ is the corresponding projection operator of the model space and $Q = 1 - P$ is the projection operator corresponding to orthogonal space. A state $|\psi\rangle$ in the Hilbert space can be projected onto the model space using operator P, $|\phi\rangle = P|\psi\rangle$ and a wavefunction $|\phi\rangle$ in model space can be reconstructed in Hilbert space using the wave operator Ω as $|\psi\rangle = \Omega|\phi\rangle$.

Some useful relationships between operators P, Q and Ω are

a. $P + Q = 1$ (by definition)

b. $P^2 = P$ and $Q^2 = Q$ (property of projection operators)

c. $PQ = QP = 0$ (using Property 1)

d. $\Omega^2|\phi\rangle = \Omega|\phi\rangle$ (by definition)

e. $\Omega P|\phi\rangle = \Omega|\phi\rangle$ and $P\Omega|\psi\rangle = P|\psi\rangle$ (by definition)

Provided the eigenvalue equation $\hat{H}|\psi\rangle = E|\psi\rangle$, then $|\phi\rangle = P|\psi\rangle$ satisfies the equation $\hat{H}_{eff}|\phi\rangle = E|\phi\rangle$, where

$$\hat{H}_{eff} = P\hat{H}\Omega P \tag{B.65}$$

$$\begin{aligned}
\hat{H}_{eff}\,|\phi\rangle &= P\hat{H}\Omega P\,|\phi\rangle \\
&= P\hat{H}\Omega PP\,|\psi\rangle \\
&= P\hat{H}\,|\psi\rangle \\
&= E\,P\,|\psi\rangle \\
&= E\,|\phi\rangle
\end{aligned}$$

The derivation of $\hat{H}_{eff}$ can be illustrated via the following sequence of steps. We begin with the complete eigenvalue equation of the problem, for an eigenstate $|\psi\rangle$ and eigenvalue E, and apply a series of manipulations as shown

$$\begin{aligned}
\hat{H}\,|\psi\rangle &= E\,|\psi\rangle \\
\hat{H}(P+Q)\,|\psi\rangle &= E(P+Q)\,|\psi\rangle \\
Q\hat{H}(P+Q)\,|\psi\rangle &= QE(P+Q)\,|\psi\rangle \\
Q\hat{H}(P+Q)\,|\psi\rangle &= EQ\,|\psi\rangle \\
Q\hat{H}P\,|\psi\rangle + Q\hat{H}Q\,|\psi\rangle &= EQ\,|\psi\rangle \\
Q\hat{H}P\,|\psi\rangle + Q\hat{H}QQ\,|\psi\rangle &= EQ\,|\psi\rangle \\
(E - Q\hat{H}Q)Q\,|\psi\rangle &= Q\hat{H}P\,|\psi\rangle \\
Q\,|\psi\rangle &= (E - Q\hat{H}Q)^{-1}Q\hat{H}P\,|\psi\rangle
\end{aligned} \tag{B.66}$$

where we have used the properties of the projection operators mentioned earlier. We also have,

$$\begin{aligned}
\hat{H}\,|\psi\rangle &= E\,|\psi\rangle \\
\hat{H}(P+Q)\,|\psi\rangle &= E(P+Q)\,|\psi\rangle \\
P\hat{H}(P+Q)\,|\psi\rangle &= PE(P+Q)\,|\psi\rangle \\
P\hat{H}(P+Q)\,|\psi\rangle &= EP\,|\psi\rangle
\end{aligned}$$

$$P\hat{H}P\,|\psi\rangle + P\hat{H}Q\,|\psi\rangle = EP\,|\psi\rangle$$
$$P\hat{H}P + P\hat{H}(E - Q\hat{H}Q)^{-1}Q\hat{H}P\,|\psi\rangle = EP\,|\psi\rangle \tag{B.67}$$

In the last step above we use eq.(B.66), and we may now define the effective Hamiltonian as

$$\hat{H}_{eff} = P\hat{H}P + P\hat{H}(E - Q\hat{H}Q)^{-1}Q\hat{H} \tag{B.68}$$

and so we get the already defined eigenvalue equation $\hat{H}_{eff}\,|\phi\rangle = E\,|\phi\rangle \Rightarrow \hat{H}_{eff}P\,|\psi\rangle = EP\,|\psi\rangle$, and $P\,|\psi\rangle$ is naturally an eigenstate of $\hat{H}_{eff}$. Interestingly, with the eigenvalue E which is the eigenenergy of $\hat{H}$ for the state $|\psi\rangle$ and thus the effective Hamiltonian has the same eigenvalues as those of $\hat{H}$ but for the corresponding eigenstates projected onto the model space.

From the property of the wave operator , $|\psi\rangle = \Omega P\,|\psi\rangle$, we can write $\hat{H}\Omega P\,|\psi\rangle = E\Omega P\,|\psi\rangle$ and similarly for the $\hat{H}_{eff}$

$$\Omega\hat{H}_{eff}P\,|\psi\rangle = E\Omega P\,|\psi\rangle$$

By acting with P from the left on both sides of we have $\hat{H}\Omega P\,|\psi\rangle = E\Omega P\,|\psi\rangle$

$$P\hat{H}\Omega P\,|\psi\rangle = EP\Omega P\,|\psi\rangle = EP\,|\psi\rangle$$

Now, eq.(B.67) is nothing but

$$P\hat{H}[P + \hat{H}(E - Q\hat{H}Q)^{-1}Q\hat{H}]P\,|\psi\rangle = EP\,|\psi\rangle \tag{B.69}$$

and comparing with the previous equation we can identify the wave operator Ω as

$$\Omega = [\mathbf{I} + (E - Q\hat{H}Q)^{-1}Q\hat{H}]P \tag{B.70}$$

The inverse operation in the wave operator can be expanded to obtain the perturbative expansion.

Usually, the effective Hamiltonian is parameterized by energy. To obtain the solutions, we must diagonalize the effective Hamiltonian by treating E as a free parameter to obtain the eigenvalue expressions $E_i (i = 1 \ldots \dim(\hat{H}))$, and solve the equations $E = E_i$ to obtain the numerical values of energy eigenvalues.

We now apply the above formalism of the effective Hamiltonian and the wave operator to the Floquet Hamiltonian and its eigenvalue equation to treat it as perturbation problem in the limit of large frequencies. The approach outlined here is adopted from [**?**] which the reader may refer to for details regarding the application of this technique to various periodic/driven quantum systems.

We begin by considering the Floquet space eigenvalue equation of (B.23), where we introduce ket notation from the Floquet modes to denote $\Phi^n_{\alpha\beta}$ as $|\mathbf{p}'_\beta\rangle$, the photon number index being suppressed and the implicit assumption that one is working in the $|\alpha n\rangle$ basis of $\mathbb{F}$, we may write

$$(\overline{\mathcal{H}}_F - \mathcal{M}\omega)\,|\mathbf{p}'_\beta\rangle = \epsilon_\beta\,|\mathbf{p}'_\beta\rangle \tag{B.71}$$

$$\mathcal{H}^{m-n} = \frac{1}{T}\int_0^T \mathcal{H}(t)e^{i(m-n)\omega t}dt = \mathcal{H}_{m,n} \tag{B.72}$$

$$\mathcal{M}^{mn} = m\delta_{mn} \tag{B.73}$$

where $\overline{\mathcal{H}}_F$ is used to denote the matrix operator whose elements are the Fourier coefficients of $\mathcal{H}(t)$.

The seperation into the model space and orthogonal space is done with the operator $\mathcal{P}^{mn} = \delta_{mn}\delta_{m0}$, which essentially maps the eigenfunctions into a space devoid of the micromotion information, or simply the $n = m = 0$ photon subspace. As a result, we may define $\mathcal{Q}^{mn} = 1 - \mathcal{P}^{mn} = \delta_{mn}(1 - \delta_{m0})$, with the resulting properties, $(\mathcal{PM})^{mn} = k\delta_{mk}\delta_{m0}\delta_{kn} = 0$ and $(\mathcal{QM})^{mn} = k\delta_{mk}(1 - \delta_{m0})\delta_{kn} = m\delta_{mk}\delta_{kn}(1 - \delta_{k0}) =$

$(\mathcal{M}\mathcal{Q})^{mn}$. The operators $\mathcal{P}$ and $\mathcal{Q}$ are the projection operators of the kind P and Q discussed earlier, and act in the extended Floquet Hilbert space. The BW effective Hamiltonian, from what we already know, is defined as

$$H_{eff} = \mathcal{P}(\overline{\mathcal{H}}_F - \mathcal{M}\omega)\Omega\mathcal{P} \tag{B.74}$$

We determine the Ω wave operator as follows, acting with $\mathcal{Q}$ from the left on eq.(B.71) and using the properties of the projectors,

$$\begin{aligned}
\mathcal{Q}(\overline{\mathcal{H}}_F - \mathcal{M}\omega)\left|\mathbf{p}'_\beta\right\rangle &= \epsilon_\beta \mathcal{Q}\left|\mathbf{p}'_\beta\right\rangle \\
\mathcal{Q}\overline{\mathcal{H}}_F\left|\mathbf{p}'_\beta\right\rangle &= \mathcal{Q}\mathcal{M}\omega\left|\mathbf{p}'_\beta\right\rangle + \epsilon_\beta \mathcal{Q}\left|\mathbf{p}'_\beta\right\rangle \\
\mathcal{Q}\overline{\mathcal{H}}_F\left|\mathbf{p}'_\beta\right\rangle &= \mathcal{M}\omega\mathcal{Q}\left|\mathbf{p}'_\beta\right\rangle + \epsilon_\beta \mathcal{Q}\left|\mathbf{p}'_\beta\right\rangle \\
(\epsilon_\beta + \mathcal{M}\omega)\mathcal{Q}\left|\mathbf{p}'_\beta\right\rangle &= \mathcal{Q}\overline{\mathcal{H}}_F\left|\mathbf{p}'_\beta\right\rangle \\
\mathcal{Q}\left|\mathbf{p}'_\beta\right\rangle &= \frac{\mathcal{Q}}{\epsilon_\beta + \mathcal{M}\omega}\overline{\mathcal{H}}_F\left|\mathbf{p}'_\beta\right\rangle
\end{aligned} \tag{B.75}$$

and

$$\begin{aligned}
\left|\mathbf{p}'_\beta\right\rangle &= \mathcal{P}\left|\mathbf{p}'_\beta\right\rangle + \mathcal{Q}\left|\mathbf{p}'_\beta\right\rangle \\
&= \mathcal{P}\left|\mathbf{p}'_\beta\right\rangle + \frac{\mathcal{Q}}{\epsilon_\beta + \mathcal{M}\omega}\overline{\mathcal{H}}_F\left|\mathbf{p}'_\beta\right\rangle \\
\mathcal{P}\left|\mathbf{p}'_\beta\right\rangle &= \left|\mathbf{p}'_\beta\right\rangle - \frac{\mathcal{Q}}{\epsilon_\beta + \mathcal{M}\omega}\overline{\mathcal{H}}_F\left|\mathbf{p}'_\beta\right\rangle \\
\left|\mathbf{p}'_\beta\right\rangle &= \left(1 - \frac{\mathcal{Q}}{\epsilon_\beta + \mathcal{M}\omega}\overline{\mathcal{H}}_F\right)^{-1}\mathcal{P}\left|\mathbf{p}'_\beta\right\rangle
\end{aligned} \tag{B.76}$$

We recognize the wave operator from the above expression as

$$\Omega(\epsilon) = \left(1 - \frac{\mathcal{Q}}{\epsilon + \mathcal{M}\omega}\overline{\mathcal{H}}_F\right)^{-1} \tag{B.77}$$

and consequently the effective Hamiltonian as

$$\begin{aligned} H_{eff}(\epsilon) &= \mathcal{P}(\overline{\mathcal{H}}_F - \mathcal{M}\omega)\left(1 - \frac{\mathcal{Q}}{\epsilon + \mathcal{M}\omega}\overline{\mathcal{H}}_F\right)^{-1}\mathcal{P} \\ &= \mathcal{P}\overline{\mathcal{H}}_F\left(1 - \frac{\mathcal{Q}}{\epsilon + \mathcal{M}\omega}\overline{\mathcal{H}}_F\right)^{-1}\mathcal{P} - \omega\mathcal{P}\mathcal{M}\left(1 - \frac{\mathcal{Q}}{\epsilon + \mathcal{M}\omega}\overline{\mathcal{H}}_F\right)^{-1}\mathcal{P} \\ &= \mathcal{P}\overline{\mathcal{H}}_F\left(1 - \frac{\mathcal{Q}}{\epsilon + \mathcal{M}\omega}\overline{\mathcal{H}}_F\right)^{-1}\mathcal{P} \end{aligned} \tag{B.78}$$

We look to extend this theory by defining an ϵ-independent effective Hamiltonian.

$$\begin{aligned} \Omega(\epsilon) = \Omega(\epsilon)\mathcal{P} &= \left(1 - \frac{\mathcal{Q}}{\epsilon + \mathcal{M}\omega}\overline{\mathcal{H}}_F\right)^{-1}\mathcal{P} \\ \left(1 - \frac{\mathcal{Q}}{\epsilon + \mathcal{M}\omega}\overline{\mathcal{H}}_F\right)\Omega(\epsilon) &= \mathcal{P} \\ \Omega(\epsilon) - \frac{\mathcal{Q}}{\epsilon + \mathcal{M}\omega}\overline{\mathcal{H}}_F\Omega(\epsilon) &= \mathcal{P} \\ (\epsilon + \mathcal{M}\omega)\Omega(\epsilon) - \mathcal{Q}\overline{\mathcal{H}}_F\Omega(\epsilon) &= \epsilon\mathcal{P} + \mathcal{M}\omega\mathcal{P} \\ \Omega(\epsilon)\epsilon - \mathcal{P}\epsilon + \mathcal{M}\omega\Omega(\epsilon) - \mathcal{Q}\overline{\mathcal{H}}_F\Omega(\epsilon) &= \mathcal{M}\omega\mathcal{P} \\ \Omega(\epsilon)\epsilon - \mathcal{P}\Omega(\epsilon)\epsilon + \mathcal{M}\omega\Omega(\epsilon) - \mathcal{Q}\overline{\mathcal{H}}_F\Omega(\epsilon) &= \mathcal{M}\omega\mathcal{P} \\ (1 - \mathcal{P})\Omega(\epsilon)\epsilon + \mathcal{M}\omega\Omega(\epsilon) - \mathcal{Q}\overline{\mathcal{H}}_F\Omega(\epsilon) &= \mathcal{M}\omega\mathcal{P} \\ \mathcal{Q}\Omega(\epsilon)\epsilon + \mathcal{M}\omega\Omega(\epsilon) - \mathcal{Q}\overline{\mathcal{H}}_F\Omega(\epsilon) &= \mathcal{M}\omega\mathcal{P} \\ \mathcal{M}\omega\mathcal{P} + \mathcal{Q}\overline{\mathcal{H}}_F\Omega(\epsilon) - \mathcal{Q}\Omega(\epsilon)\epsilon &= \mathcal{M}\omega\Omega(\epsilon) \end{aligned}$$

$$\Omega(\epsilon) = \mathcal{P} + \frac{\mathcal{Q}}{\mathcal{M}\omega}\overline{\mathcal{H}}_F\Omega(\epsilon) - \frac{\mathcal{Q}}{\mathcal{M}\omega}\Omega(\epsilon)\epsilon \tag{B.79}$$

We can replace the ϵ in the above equation with H_{eff}.

$$\Omega(\epsilon) = \mathcal{P} + \frac{\mathcal{Q}}{\mathcal{M}\omega}\overline{\mathcal{H}}_F\Omega(\epsilon) - \frac{\mathcal{Q}}{\mathcal{M}\omega}\Omega(\epsilon)\mathcal{P}\overline{\mathcal{H}}_F\Omega(\epsilon)\mathcal{P}$$

We omit the $\mathcal{P}$ in the last term, as it Ω is anyway acted on $\mathcal{P}\,|\mathbf{p}'_\beta\rangle$.

ϵ independent wave operator is defined by the recursive relation

$$\Omega(\epsilon) = \mathcal{P} + \frac{\mathcal{Q}}{\mathcal{M}\omega}\overline{\mathcal{H}}_F\Omega(\epsilon) - \frac{\mathcal{Q}}{\mathcal{M}\omega}\Omega(\epsilon)\mathcal{P}\overline{\mathcal{H}}_F\Omega(\epsilon) \tag{B.80}$$

and the ϵ independent effective Hamiltonian is obtained from the solution Ω_{BW}, of the preceding equation.

$$H_{BW} = \mathcal{P}\overline{\mathcal{H}}_F\Omega_{BW}\mathcal{P} \tag{B.81}$$

Ω_{BW} is obtained by substitution of the $1/\omega$ series,

$$\Omega_{BW} = \sum_{N=0}^{\infty}\Omega_{BW}^{(N)} \tag{B.82}$$

where $\Omega_{BW}^{(N)}$ corresponds to order $1/\omega^N$ coefficient in the iterative solution to Ω_{BW}, in the eq.(B.80). Similarly, the effective Hamiltonian is also expanded in a series

$$H_{BW} = \sum_{N=0}^{\infty}H_{BW}^{(N)}$$

and $H_{BW}^{(N)} = \mathcal{P}\overline{\mathcal{H}}_F\Omega_{BW}^{(N)}\mathcal{P}$.

This prescription may be implemented as follows. Substituting the series in eq.(B.82) in the iterative solution for the wave operator in eq.(B.80) one gets

$$\sum_{N=0}^{\infty}\Omega_{BW}^{(N)} = \mathcal{P} + \sum_{N=0}^{\infty}\frac{\mathcal{Q}}{\mathcal{M}\omega}\overline{\mathcal{H}}_F\Omega_{BW}^{(N)} + \sum_{N=0}^{\infty}\sum_{M=0}^{\infty}\frac{\mathcal{Q}}{\mathcal{M}\omega}\Omega_{BW}^{(N)}\mathcal{P}\overline{\mathcal{H}}_F\Omega_{BW}^{(M)} \tag{B.83}$$

Equating terms from both sides of the same order $\mathcal{O}(1/\omega^N)$

$$\begin{aligned}
\Omega_{BW}^{(0)} &= \mathcal{P} \\
\Omega_{BW}^{(1)} &= \frac{\mathcal{Q}}{\mathcal{M}\omega}\overline{\mathcal{H}}_F\mathcal{P} \\
\Omega_{BW}^{(N+1)} &= \frac{\mathcal{Q}}{\mathcal{M}\omega}\overline{\mathcal{H}}_F\Omega_{BW}^{(N)} - \sum_{M=0}^{N}\frac{\mathcal{Q}}{\mathcal{M}\omega}\Omega_{BW}^{(M)}\mathcal{P}\overline{\mathcal{H}}_F\Omega_{BW}^{(N-M)}
\end{aligned}$$

Using $H_{BW} = \mathcal{P}\overline{\mathcal{H}}_F\Omega_{BW}\mathcal{P}$, we obtain

$$
\begin{aligned}
H_{BW}^{(0)} &= \mathcal{P}\overline{\mathcal{H}}_F\mathcal{P}\mathcal{P} = \mathcal{H}_{0,0} \\
H_{BW}^{(1)} &= \mathcal{P}\overline{\mathcal{H}}_F\frac{\mathcal{Q}}{\mathcal{M}\omega}\overline{\mathcal{H}}_F\mathcal{P}\mathcal{P} = \sum_{n_1\neq 0}\frac{\mathcal{H}_{0,n_1}\mathcal{H}_{n_1,0}}{n\omega} \\
H_{BW}^{(2)} &= \mathcal{P}\overline{\mathcal{H}}_F\Omega_{BW}^{(2)}\mathcal{P} = \sum_{n_1\neq 0,n_2\neq 0}\frac{\mathcal{H}_{0,n_1}\mathcal{H}_{n_1,n_2}\mathcal{H}_{n_2,0}}{n_1n_2\omega^2} - \frac{\mathcal{H}_{0,n_1}\mathcal{H}_{n_1,0}\mathcal{H}_{0,0}}{n_1^2\omega^2} \\
H_{BW}^{(N)} &= \mathcal{P}\overline{\mathcal{H}}_F\Omega_{BW}^{(N)}\mathcal{P}
\end{aligned}
$$

The higher order terms in the above sequence may be found in [92] and we see that using the above expansion coefficients we may expand the effective Hamiltonian to various orders in ω^{-1}. Thus under the high frequency limit $\omega \to \infty$, the operators tend to their $0th$ order terms, $\Omega_{BW} \to \mathcal{P}$ and $H_{BW} \to H_{0,0}$. This guarantees that the eigenvalues of H_{BW} are in the first brillouin zone, as the contributions from higher order terms in the series is very small to transport the eigenvalues to the higher photon number sectors.

This concludes our discussion of the high frequency expansion schemes that may be used to approximate the Floquet eigenvalue problem such that one reduces the dimensionality of the operational Hilbert space to the finite ones of the time dependent problem yet retaining the eigenvalues of the original problem.

Appendix C

Geometric Phase and Topological Invariants

In this appendix we shall present the ideas associated with the Berry Phase [79], or Pancharatnam phase [330], in a generalized framework, originally worked out by Mukunda and Simon [20, 275, 276], which is a culmination of the efforts of several predecessors [305, 331] to bring out the fundamental nature of the phase by freeing it of the originally imposed constraints of cyclicity, adiabaticity and even unitarity. Mukunda and Simon's work, key aspects of which are essentially summarized here, is a kinematical take on the geometric phase, as the quantity is deservedly named. Besides exposing the fundamental, and hence, universal qualities of the phase we shall see that one may trace a path from this framework to the calculation of toplogical invariants for quantum systems.

A major portion of this appendix is a cogent summarization and amalgamation of portions of two key references, [20] and lecture notes, very generously provided by Prof. N. Mukunda, of the series of talks delivered by him at IMSc Chennai. Similarities in tone and notation were not entirely avoidable due to the axiomatic nature of the discussion.

C.1 Formalism

Let us begin by considering an N-level quantum system, where N in principle could be infinite, in the complex Hilbert space $\mathbb{H}$ of pure quantum states. It follows that such a Hilbert space has N complex dimensions or $2N$ real dimensions. The states being complex valued vectors with real and imaginary parts. These vectors are represented by Greek letters $\phi, \psi, \cdots$. Using the notion of an inner product on this complex space we may define, two subsets of $\mathbb{H}$, the space of non-zero vectors $\mathcal{N}$ and the space of unit vectors $\mathcal{B}$ as follows

$$\begin{aligned} \mathcal{N} &= \{\psi \neq 0 | \psi \in \mathbb{H}\} \subset \mathbb{H} \\ \mathcal{B} &= \{\langle\psi|\psi\rangle = 1 | \psi \in \mathbb{H}\} \subset \mathbb{H} \end{aligned} \tag{C.1}$$

Thus $\mathcal{B}$ can be thought of as the set of points on a unit $(2N-1)$-sphere in $\mathbb{H}$. The normalization constraint reduces the dimensionality of the representative space for the states by 1. $\mathcal{B}$ though a subset of $\mathbb{H}$, is not a subspace. These subsets obey $\mathcal{B} \subset \mathcal{N} \subset \mathbb{H}$.

Consider the fact that the action of the unitary, single parameter group, $U(1)$, on $\mathbb{H}$ and $\mathcal{B}$ leaves them invariant. So,

$$\psi \in \mathcal{B} \longrightarrow \psi' = e^{i\alpha}\psi \in \mathcal{B} \quad 0 \leq \alpha \leq 2\pi \tag{C.2}$$

With this it is possible to define an equivalence class of all state vectors which are related by a $U(1)$ transformation of the above sort and differ upto a phase. The set of all such equivalence classes is a space in itself and is called a ray space or projective space in general. It is customary to denote the operation of grouping elements into equivalence classes as taking the quotient of the set in question with the group used to define the equivalence relation. So if the ray space is denoted by

$\boldsymbol{\mathcal{R}}$, then

$$\boldsymbol{\mathcal{R}} = \frac{\mathcal{B}}{U(1)} = \{\rho_\psi = |\psi\rangle\langle\psi| \quad \text{or} \quad \psi\psi^\dagger \; | \psi \in \mathcal{B}\} \tag{C.3}$$

Where we denote the points in $\boldsymbol{\mathcal{R}}$ as the pure state density matrices, ρ_ψ, which represent the set of all ψ' related to ψ by a phase. The density matrix representation works here as these are $U(1)$ invariant quantities themselves and the ray space is so called as it is the space of true physical states of the system, or rays, as they are also known. At every point in ray space one can conceive an entire $U(1)$ worth of states along an infinitely extended mathematical object called a fibre which is based at that point in $\boldsymbol{\mathcal{R}}$. Thus the differential geometric structure is that of a $U(1)$ principal fibre bundle, and $\mathcal{B}$ is such a fibre bundle over ray space. We define a projection map using a projection operator which takes any point in $\mathcal{B}$ along a given fibre to its corresponding base point in $\boldsymbol{\mathcal{R}}$ as follows

$$\pi : \mathcal{B} \longrightarrow \boldsymbol{\mathcal{R}} : \quad \psi \in \mathcal{B} \longrightarrow \rho_\psi = \psi\psi^\dagger \in \boldsymbol{\mathcal{R}} \tag{C.4}$$

Similarly one may define the inverse of the projection operation which naturally is a one to many map that takes the ray space point to the members (in $\mathcal{B}$) of the equivalence class that it dentoes, being related by phase differences to one another,

$$\rho_\psi \longrightarrow \pi^{-1}(\rho_\psi) = \{\psi' = e^{i\alpha}\psi \in \mathcal{B} | \text{ for fixed } \psi, 0 \leq \alpha < 2\pi\} \subset \mathcal{B} \tag{C.5}$$

The ray space is not a linear vector space and it has $2(N-1)$ real dimensions. As a complex space it is $N-1$ dimensional and is technically denoted as CP^{N-1} i.e. complex projective space of $N-1$ dimensions. Intutively, the ray space is one complex dimension lower than $\mathcal{B}$ due to the projection of an entire fibre of states onto a single point.

We now introduce the notion of Bargmann invariants which is central to the Mukunda-Simon formulation of the geometric phase.

C.2 Bargmann invariants

From our introduction of density matrices and appeal to $U(1)$ invariant quantities it is apparent that invariants under unitary transformations in general, especially since we are interested in invariance on the set $\mathcal{B}$, are of interest to us. One such class of invariants was introduced by V. Bargmann in proving Wigner's theorem on the representation of symmetry operations in quantum mechanics [332], and are hence called Bargmann invariants.

A simple invariant making use of only two state vectors ψ_1 and ψ_2 is the norm of their inner product

$$|\langle\psi_1|\psi_2\rangle| = \sqrt{\langle\psi_1|\psi_2\rangle\langle\psi_2|\psi_1\rangle} \tag{C.6}$$

which remains unchanged if one were to make the transformations, $\psi_1 \to \psi_1' = e^{i\alpha_1}\psi_1$ and $\psi_2 \to \psi_2' = e^{i\alpha_2}\psi_2$ where α_1 and α_2 are real scalars. Thus this is a $U(1) \times U(1)$ real valued invariant. The one which can be created with the least number of states and happens to be the only real valued invariant constructed out of pure states. Bargmann's idea was to generalize to higher order invariants with more number of states which could even be made infinite. The simplest example of this is the 3-state or 3-point invariant of the form

$$\Omega_3(\psi_1, \psi_2, \psi_3) = \langle\psi_1|\psi_2\rangle\langle\psi_2|\psi_3\rangle\langle\psi_3|\psi_1\rangle \tag{C.7}$$

Important to note here is that these invariants are now complex valued, the above being the simplest example of one and happens to be invariant under transformations of the group $U(1) \times U(1) \times U(1)$. Similarly one could define a general N-point invariant Ω_N which would be invariant under $U(1) \times U(1) \times U(1) \cdots N\text{times}$. We shall see the use of these invariants in defining the geometric phase later on in this appendix. For now we proceed with the definiton of gauge and reparametrization invariant quantities in $\mathcal{B}$ and $\boldsymbol{\mathcal{R}}$ and pay heed to the fact that with the kind of

discrete invariant described above only algebraic approaches are avialble. In order to perform analytical and infinitesimal calculations ideas of the continuum have to be brought in their definition and application. This we do in the following section.

C.3 Gauge and reparametrization invariance

Let us consider $\mathfrak{C}$ to denote the set of all vectors $\psi(s)$, parametrized by a real continuous variable s, that lie on a smooth (i.e. continuous and sufficiently differentiable) curve in $\mathcal{B}$,

$$\mathfrak{C} = \{\psi(s) \in \mathcal{B} | s_1 \leq s \leq s_2\} \subset \mathcal{B} \tag{C.8}$$

No assumptions are made as to wether the curve is closed or open and it may extend even beyond the specified range of s. Since the $\psi(s)$ are normalized to unity for all s we have

$$\begin{aligned} &\mathrm{Re}\{\langle\psi(s)|\dot{\psi}(s)\rangle\} = 0 \\ &\Rightarrow \langle\psi(s)|\dot{\psi}(s)\rangle = i\mathrm{Im}\{\langle\psi(s)|\dot{\psi}(s)\rangle\} \end{aligned} \tag{C.9}$$

where the dot is used to donate derivative w.r.t s i.e. $\dot{\psi}(s) = \frac{d\psi(s)}{ds}$. Like we saw for the case of the Bargmann invariants where we defined discrete N-point invariants, we would like to do the same here but for a continuous set of points such as the $\psi(s) \in \mathcal{B}$ at each value of s. This set of independent unitary transformations at each point along the curve in the set of unit vectors is a form of gauge transformation performed using the real function $\alpha(s)$. It takes every point on $\mathfrak{C}$ to points on a $\mathfrak{C}' \subset \mathcal{B}$

$$\mathfrak{C}' = \{\psi'(s) = e^{i\alpha(s)}\psi(s) | \psi(s) \in \mathfrak{C}, s_1 \leq s \leq s_2\} \subset \mathcal{B} \tag{C.10}$$

Such a transformation affects the term identified in eq.(C.9) as follows

$$\mathrm{Im}\{\langle\psi'(s)|\dot{\psi}'(s)\rangle\} = \mathrm{Im}\{\langle\psi(s)|\dot{\psi}(s)\rangle\} + \dot{\alpha}(s) \tag{C.11}$$

This allows us to construct a functional of $\mathfrak{C}$ which obeys gauge invariance such that it has the same value for both the curves $\mathfrak{C}$ and $\mathfrak{C}'$. The following is such a quantity

$$\begin{aligned}
&\arg\{\langle\psi'(s_1)|\psi'(s_2)\rangle\} - \mathrm{Im}\int_{s_1}^{s_2} ds\,\langle\psi'(s)|\dot{\psi}'(s)\rangle \\
&= \arg\{\langle\psi'(s_1)|\psi'(s_2)\rangle\} - \mathrm{Im}\int_{s_1}^{s_2} ds\,\langle\psi(s)|\dot{\psi}(s)\rangle - \int_{s_1}^{s_2}\dot{\alpha}(s)ds \\
&= \arg\{\langle\psi(s_1)|\psi(s_2)\rangle\} + \alpha(s_2) - \alpha(s_1) - \mathrm{Im}\int_{s_1}^{s_2} ds\,\langle\psi(s)|\dot{\psi}(s)\rangle - (\alpha(s_2) - \alpha(s_1)) \\
&= \arg\{\langle\psi(s_1)|\psi(s_2)\rangle\} - \mathrm{Im}\int_{s_1}^{s_2} ds\,\langle\psi(s)|\dot{\psi}(s)\rangle
\end{aligned} \tag{C.12}$$

and as can be seen from the steps performed it does indeed exhibit such invariance. Where the $\arg\{\langle\psi'(s_1)|\psi'(s_2)\rangle\}$ represents the phase difference between the vectors at the two ends of the curve. To understand the fundamental nature of this quantity it shall be useful also to look at it from a ray space perspective. So far we have been looking at curves in $\mathcal{B}$ however, by virtue of the projection operator defined earlier, we may project any such curve onto its image curve $C \in \mathfrak{R}$, such as

$$C = \pi[\mathfrak{C}] = \{\rho_{\psi(s)} = |\psi(s)\rangle\langle\psi(s)| = \psi(s)\psi^{\dagger}(s) \in \mathfrak{R} | s_1 \leq s \leq s_2\} \subset \mathfrak{R} \tag{C.13}$$

C itself is a smooth curve in $\mathfrak{R}$ and allows for a continuous parametrization. We may note that given the definition of points in $\mathfrak{R}$, any curve $\mathfrak{C}'$ obtained by gauge transforming $\mathfrak{C}$ also projects to the same $C \in \mathfrak{R}$. Thus we have $C = \pi[\mathfrak{C}] = \pi[\mathfrak{C}']$ and $\mathfrak{C}$ and $\mathfrak{C}'$ are called different *lifts* of $C \in \mathfrak{R}$. The quantity defined in eq.(C.12) therefore, is in a true sense a functional on the ray space curve C.

Another important property of this gauge invariant functional is its invariance

under reparametrization. A fact that may not seem altogether surprising given the linear dependence on the velocity i.e. the tangent $\dot{\psi}(s)$ in the integrand within eq.(C.12). It is possible to prove this by replacing s in the previous expressions by s' which, again a real valued parameter, has a monotonically increasing dependence on s. Under this transformation $s \in [s_1, s_2] \rightarrow s' \in [s'_1, s'_2]$ and $\mathfrak{C} \rightarrow \bar{\mathfrak{C}}$ with,

$$\bar{\mathfrak{C}} = \{\psi'(s') \in \mathcal{B} | s'_1 \leq s' \leq s'_2\}$$
$$\psi'(s'(s)) = \psi(s)$$
$$\psi'(s'_1) = \psi(s_1) \quad \psi'(s'_2) = \psi(s_2)$$

In this manner it becomes apparent that both $\mathfrak{C}$ and $\bar{\mathfrak{C}}$ traverse the same set of points in $\mathcal{B}$ the difference being only in the rate at which this curve is traversed in the two cases. By implication the same holds for the ray space curves C and $\bar{C}$ which are related to the $\mathfrak{C}$ and $\bar{\mathfrak{C}}$ as $C = \pi[\mathfrak{C}]$, $\bar{C} = \pi[\bar{\mathfrak{C}}]$. Once again we see an invariance of the functional in eq.(C.12) as below

$$\begin{aligned} \arg\{\langle\psi'(s'_1)|\psi'(s'_2)\rangle\} - \mathrm{Im}\int_{s'_1}^{s'_2} ds\, \langle\psi'(s')|\dot{\psi}'(s')\rangle & \\ = \arg\{\langle\psi(s_1)|\psi(s_2)\rangle\} - \mathrm{Im}\int_{s_1}^{s_2} ds\, \langle\psi(s)|\dot{\psi}(s)\rangle & \end{aligned} \tag{C.14}$$

Thus we obtain a functional of ray space curves which is invariant under both gauge and reparametrization transformations and we denote it by Θ_g,

$$\Theta_g[C] = \arg\{\langle\psi(s_1)|\psi(s_2)\rangle\} - \mathrm{Im}\int_{s_1}^{s_2} ds\, \langle\psi(s)|\dot{\psi}(s)\rangle \tag{C.15}$$

This happens to be the geometric phase that is acquired on traversing the smooth curve $C \in \mathfrak{R}$. The gauge invariance property makes this phase a ray space quantity and associates it with a C in ray space i.e. the space of density matrices. The geometric character of the phase is a consequence of its reparametrization invariance,

since it becomes a fundamental property of the curve irrespective of how fast or slow it is travelled. The right hand side of the functional involves operations with states from $\mathcal{B}$ belonging to some $\mathfrak{C} \in \mathcal{B}$, given the invariances just discussed it is possible to calculate the functional using any such lift $\mathfrak{C}$ of the ray space curve C. Also due to the nature of the functional this lift could be performed under any monotonic parametrization of C which gets lifted to some $\mathfrak{C}$, which is itself parametrized suitably.

A few properties of the geometric phase become apparent from the form of the functional in eq.(C.15). Firstly, the fact that it is defined only modulo 2π which follows from the first term on the right hand side. Then there is the restriction that the states at the end points $\psi(s_1)$ and $\psi(s_2)$ should not be orthogonal to each other as in this case both $\arg\{\langle\psi(s_1)|\psi(s_2)\rangle\}$ and $\Theta_g[C]$ are undefined. All such cases are excluded from consideration. This acts as a condition on the terminal points of the curve C. A distinguishing feature of curves in $\mathcal{B}$ and $\mathfrak{R}$ is that they are defined completely by specifying a choice of parametrization, as far as $\Theta_g[C]$ is concerned. Since, although $\Theta_g[C]$ is independent of any pair of choices related monotonically to each other, there are still the cases of multiple traversala around closed loops, path crossings and overlaps which affect the value of the phase and require the parametrization to be specified clearly.

Focusing on the RHS in eq.(C.15) the two terms appearing may be designated as follows

$$\begin{aligned} \arg\{\langle\psi(s_1)|\psi(s_2)\rangle\} &= \Theta_{\text{tot}}[C] = \text{total phase} \\ \text{Im}\int_{s_1}^{s_2} ds\,\langle\psi(s)|\dot{\psi}(s)\rangle &= \Theta_{\text{dyn}}[C] = \text{dynamical phase} \end{aligned} \tag{C.16}$$

Θ_{tot} is by definition non-local as it depends on the end points of the choice of $\mathfrak{C}$ used to calculate it and its value ofcourse comes out to be modulo 2π. Θ_{dyn} on the

other hand is an integral of a locally defined quantity, independently evaluated at each point along the curve, which under the integral accumulates additively along the path. Both of these components depend on the particular choice $\boldsymbol{\mathcal{C}} \in \mathcal{B}$ but their difference does not and is purely a property of $C = \pi[\boldsymbol{\mathcal{C}}] \in \boldsymbol{\mathcal{R}}$. We can thus write

$$\Theta_g[C] = \Theta_{\text{tot}}[C] - \Theta_{\text{dyn}}[C] \tag{C.17}$$

Having the freedom to choose between different lifts $\boldsymbol{\mathcal{C}} \in \mathcal{B}$ for a given curve $C \in \boldsymbol{\mathcal{R}}$ as a consequence of the infinite gauge degree of freedom permitted by $\Theta_g[C]$, one has the option of making any one of the terms in the above expression vanish. So it is possible to choose a lift where $\Theta_{\text{tot}}[C] = 0$ i.e. $\Theta_g[C] = -\Theta_{\text{dyn}}[C]$(a case known as the states at the ends of the path being Pancharatnam in-phase with each other) i.e. $\psi(s_1)$ and $\psi(s_2)$ are in phase with their inner product being real and positive. The only thing to be kept in mind while selecting such a lift is that while performing the gauge transformation, $\alpha(s)$ has the same value for both s_1 and s_2, and it is easy to notice that there still remains infinite gauge freedom in the choice of lift.

Another possibility involves choosing a lift that makes $\Theta_{\text{dyn}}[C] = 0$ which implies $\Theta_g[C] = \Theta_{\text{tot}}[C]$. Such a lift $\boldsymbol{\mathcal{C}'}$ in $\mathcal{B}$ of a C in $\boldsymbol{\mathcal{R}}$ is called a *horizontal lift* and states along it satisfy

$$\boldsymbol{\mathcal{C}'} \text{ horizontal} \Leftrightarrow \text{Im}\{\langle\psi(s)|\dot{\psi}(s)\rangle\} = 0$$
$$\langle\psi(s)|\dot{\psi}(s)\rangle = 0$$

In order to find out the gauge freedom available in the above case one would require a condition on the continuous gauge parameter $\alpha(s)$. This we may find by regarding the lift $\boldsymbol{\mathcal{C}'}$ to be the result of a gauge transformation on some arbitrary lift $\boldsymbol{\mathcal{C}}$ and

combining the above condition with the one obtained in eq.(C.11), we get

$$\begin{aligned}\dot{\alpha}(s) &= -\mathrm{Im}\{\langle\psi(s)|\dot{\psi}(s)\rangle\} \\ \alpha(s) &= \alpha(s_1) - \mathrm{Im}\int_{s_1}^{s} ds'\,\langle\psi(s')|\dot{\psi}(s')\rangle\end{aligned} \tag{C.18}$$

The above expression specifies the condition on the gauge transformation or the allowed transformations for which the resultant curve is a horizontal lift. If we were to impose the additional requirement that $\mathfrak{C}'$ and $\mathfrak{C}$ have the same starting points at s_1, the transformation is completely determined as

$$\alpha(s) = -\mathrm{Im}\int_{s_1}^{s} ds'\,\langle\psi(s')|\dot{\psi}(s')\rangle \tag{C.19}$$

With this it is clear that having chosen a $\mathfrak{C}' \in \mathcal{B}$ satisfying the above requirement and starting at a state $\psi(s_1)$ which projects onto the starting point of C, there is no further gauge freedom available and the said choice of horizontal lift is a unique one for $C \in \boldsymbol{\mathcal{R}}$.

The dynamic phase $\Theta_{\mathrm{dyn}}[C]$ allows an interpretation in terms of differntial geometric objects. The idea is to consider a *one form* A on $\mathcal{B}$ which is defined as a real-valued functional on tangent vectors at each $\psi \in \mathcal{B}$. This allows us to define those vectors in $\mathbb{H}$ at $\psi \in \mathcal{B}$ as horizontal for which A becomes zero. Prior to exactly defining the one form we would need the idea of a tangent space $T_\psi\mathcal{B}$ to $\mathcal{B}$ at ψ which may be defined as the collection of those vectors in $\mathbb{H}$ which are tangent to any curve $\psi(s) \in \mathcal{B}$ at the point ψ where $\psi(s)$ passes through ψ at $s = 0$. Thus

$$\psi \in \mathcal{B} : T_\psi\mathcal{B} = \{\phi \in \mathbb{H} \mid \mathrm{Re}\{\langle\psi|\phi\rangle\} = 0 \text{ or } \langle\psi|\phi\rangle = \text{ purely imaginary}\} \subset \mathbb{H} \tag{C.20}$$

The purely imaginary condition follows from the fact that along any curve in $\mathcal{B}$ it must be true that $\langle\psi(s)|\psi(s)\rangle = 1$ and differentiating this condition gives the general

relation between vectors in $\mathcal{B}$ and vectors in tangent space. Further the tangent space is a real linear space since any vector $\phi' = \phi_1 + i\phi_2$, where $\phi_1, \phi_2 \in T_\psi\mathcal{B}$, has an inner product with $\psi \in \mathcal{B}$ with a non-zero real part and therefore does not belong to the tangent space at ψ. So the multiplying scalar field on which the vector space is defined has to be real. We can use the $U(1)$ group action to define the vertical subspace, $V_\psi\mathcal{B}$, to the tangent space, which is nothing but the fibre of $U(1)$ -transformation related equivalent states in $\mathcal{B}$ projecting to a fixed $\pi(\psi) \in \mathfrak{R}$ and the action of the group is to *push* states along the fibre. We can define

$$\psi \in \mathcal{B} : V_\psi\mathcal{B} = \{ia\psi \mid a \text{ being real}\} \subset T_\psi\mathcal{B} \tag{C.21}$$

This again is a real linear space. It can be thought of as the inifitesimal limit of a being very small in a transformation of the kind $\psi \to \psi' = e^{ia}\psi$ such that one may approximate to first order as $\psi' = \psi + ia\psi$, thus giving the element of the vertical subspace. Another important element of the tangent space is its horizontal subspace, $H_\psi\mathcal{B}$. This is basically what remains after removing the vertical subspace from the complete tangent space. It follows from the need for a *connection* over the principal fibre bundle of $U(1)$ fibres over $\mathfrak{R}$ to establish notions of continuity and differentiability in the orthogonal complement to the fibres. It satisfies the following requirements:

- $T_\psi\mathcal{B} = V_\psi\mathcal{B} \oplus H_\psi\mathcal{B}$
- $H_\psi\mathcal{B}$ has a one to one projection map onto the tangent space to $\mathfrak{R}$ at $\pi(\psi)$.
- $e^{i\alpha} \in U(1),\ \phi \in H_\psi\mathcal{B} \Rightarrow e^{i\alpha}\phi \in H_{e^{i\alpha}\phi}\mathcal{B}$. This is known as the push forward of the horizontal space under the group action. It applies here because $U(1)$ is an abelian group and the horizontal

Thus with these properties the horizontal subspace $H_\psi\mathcal{B}$ at any ψ is defined as

$$\psi \in \mathcal{B} : H_\psi\mathcal{B} = \{\phi \in T_\psi\mathcal{B} \mid \langle\psi|\phi\rangle = 0\} \subset T_\psi\mathcal{B} \tag{C.22}$$

and it is a complex linear space since any vector which is a complex linear combination of vectors in $H_\psi\mathcal{B}$ also lies in it. Such as a vector $\phi' = \phi_1 + i\phi_2$, where $\phi_1, \phi_2 \in H_\psi\mathcal{B}$, has an inner product with $\psi \in \mathcal{B}$ which is zero and therefore belongs to $H_\psi\mathcal{B}$.

The one form A_ψ at ψ, introduced earlier, acts on vectors in $T_\psi\mathcal{B}$ and can be defined as

$$\psi \in \mathcal{B},\ \phi \in T_\psi\mathcal{B} : A_\psi(\phi) = \mathrm{Im}\{\langle\psi|\phi\rangle\} = -i\,\langle\psi|\phi\rangle \text{ belongs to reals} \tag{C.23}$$

We can now use this one form to redefine the horizontal subspace of eq.(C.22) as

$$H_\psi\mathcal{B} = \{\phi \in T_\psi\mathcal{B} \mid A_\psi(\phi) = 0\} \tag{C.24}$$

and the horizontal subspace can be said to constitute all those tangent vectors that are mapped to zero by the action of the one form. Even the condition for the horizontal lift obtained from the case $\Theta_{\mathrm{dyn}}[C] = 0$ implies that the tangent vectors $\dot{\psi}(s)$ along the curve are elements of the horizontal subspace. So using the present definitions it is possible to characterize a horizontal lift as the curve whose tangent space at every point is the horizontal subspace and hence the curve of which the tangent space when acted on by the one form gives a null result everywhere along it. In fact the dynamical phase can be entirely formulated using the above defined one form as

$$\Theta_{\mathrm{dyn}}[C] = \int_C ds A_{\psi(s)}(\dot{\psi}(s))$$

$$= \int_C A_\psi(d\psi) \tag{C.25}$$

In the second step above, the one form is expressed in a parameter independent form. A general remark regarding lifts of curves $C \in \mathfrak{R}$ in $\mathcal{B}$ may be worth making. An arbitrary lift of a closed C, in which case $\Theta_{\text{tot}}[C] = 0$, may be closed or it could be open. However, for a horizontal lift there is no such ambiguity and the lift is closed if $\Theta_{\text{tot}}[C] = 0$, i.e. a closed c and open if $\Theta_{\text{tot}}[C] \neq 0$, i.e. an open C.

Next we consider the idea of geodesics in ray space, which we shall be needing to make the connection between the Bargmann invariants and the geometric phase. In order to define geodesics it is first necessary to define a functional for the length of curves $C \in \mathfrak{R}$, denoted by $L[C]$ which itself should be gauge and reparametrization invariant. Begin by considering how the tangent vector $\dot{\psi}(s)$ transforms under a gauge transformation, precisely what was used to derive the relation in eq.(C.11). Thus if the transformed $\dot{\psi}(s)$ is denoted by $\dot{\psi}'(s) = u(s)$, and $\psi'(s)$ denotes the gauge transformed curve as usual, we may write

$$u(s) = e^{i\alpha(s)}(\dot{\psi}(s) + i\dot{\alpha}(s)\psi(s)) \tag{C.26}$$

which is a linear but inhomogeneous transformation. In order to get a simpler transformation rule under the gauge transformation it is advisable to consider the projection of $\dot{\psi}(s)$ orthogonal to $\psi(s)$, dentoted by $\dot{\psi}_\perp(s)$, and write its transformation law, as

$$\begin{aligned} \dot{\psi}_\perp(s) &= \dot{\psi}(s) - \psi(s)\,\langle\psi(s)|\dot{\psi}(s)\rangle \\ u_\perp(s) = \dot{\psi}'_\perp(s) &= u(s) - \psi'(s)\,\langle\psi'(s)|u(s)\rangle = e^{i\alpha(s)}u_\perp(s) \end{aligned} \tag{C.27}$$

With this we may write down the length of curve functional $L[C]$ for any C in ray

space as

$$L[C] = \int_{s_1}^{s_2} ds(\langle u_\perp(s)|u_\perp(s)\rangle)^{1/2}$$
$$= \int_{s_1}^{s_2} ds(\langle \dot{\psi}(s)|\dot{\psi}(s)\rangle - \langle \psi(s)|\dot{\psi}(s)\rangle \langle \dot{\psi}(s)|\psi(s)\rangle)^{1/2} \tag{C.28}$$

This functional is a ray space quantity as it is gauge and reparametrization invariant. Hence any lift of C in $\mathcal{B}$ may be used to evaluate it for the path joining the states $\psi(s_1)$ and $\psi(s_2)$ which project to the end points of $C \in \mathfrak{R}$. Geodesics are curves in $\mathfrak{R}$ for which $L[C]$ is minimum given two end points. All lifts of any geodesic curve in ray space are also geodesics in $\mathcal{B}$. The reader is recommended the references [20] and [331] for details on obtaining the expressions for such curves as various special lifts and discussions regarding their properties. For us, the central result concerning geodesics, of use, was derived by Samuel and Bhandari [331] in trying to generalize the notion of geometric phase to non-cyclic evolutions and defining it for such a Schrödinger equation dictated evolution under a hermitian Hamiltonian. They found that for a general lift $\mathfrak{C}_\mathbf{0}$ of a geodesic C_0

$$\int_C A_\psi d\psi = \text{Im} \int_0^\theta ds\, \langle \psi(s)|u(s)\rangle = \text{Im} \int_0^\theta ds\, \langle \psi_0(s)|\dot{\psi}_0(s) + i\dot{\alpha}(s)\psi_0(s)\rangle = \alpha(\theta) - \alpha(0)$$
$$\Rightarrow \arg\{\langle \psi(0)|\psi(\theta)\rangle\} = \int_C A_\psi d\psi \tag{C.29}$$

The $\psi_0(s)$ here correspond to states on a special geodesic lift $\mathfrak{C}'_\mathbf{0}$ of C_0 (see [20]) for which the end points of C_0, $\rho_{\psi_0(s_1)}$ and $\rho_{\psi_0(s_2)}$, have inverses, $\psi_0(s_1)$ and $\psi_0(s_2)$, under the projection map π such that they satisfy the condition $\langle \psi_0(s_1)|\psi_0(s_2)\rangle = \cos\theta$ where, $0 < \theta < \pi/2$. A choice that gauge freedom permits. It can be shown that this special lift has the property that $L[\pi[\mathfrak{C}'_\mathbf{0}]] = \theta$ and hence we may mark off points along the geodesic with θ as a parameter starting from 0. In the calculation of the dynamic phase above, using the notion of the one form, such a parametrization is

used to evaluate the integral and the lift chosen is a general one, denoted by its states $\psi(s)$, obtained by gauge transforming $\mathfrak{C}'_{\mathbf{0}}$. Such that $\psi(s) = e^{i\alpha(s)}\psi_0(s)$ and $u(s) = \dot{\psi}(s)$ in the above. This generalization of the lift ensures that the result holds generally for all lifts of a geodesic C_0. The essential content of the very significant result above, as can be seen from the definiton of the geometric phase, is that for geodesics,

$$\Theta_{\text{dyn}}[C_0] = \Theta_{\text{tot}}[C_0] \Rightarrow \Theta_g[C_0] = 0. \tag{C.30}$$

Samuel and Bhandari ingeniously used this property to define the geometric phase for open paths of quantal Schrödinger evolution. Let $\psi(t)$ be the set of solution states, for the Schrödinger equation at each instant in $t_i \leq t \leq t_f$, which form an open curve in $\mathcal{B}$ connecting $\psi(t_i)$ and $\psi(t_f)$. One may think of closing this curve using a geodesic going from $\psi(t_f)$ back to $\psi(t_i)$ to use the, at the time, prevalent cyclic definition of the phase. In which case the geometric phase of the closed path is nothing but Θ_g[open path Schrödinger evolution] + Θ_g[closing geodesic]. From the property of geodesics just discussed the second part vanishes and since the curve is closed the $\Theta_{\text{tot}} = 0$, thus leaving

$$\Theta_g[\text{open path Schrödinger evolution}] = \int_{\text{closed path}} d\psi A_\psi \tag{C.31}$$

This was the central result of their work on generalizing the geometric phase to non-cyclic quantal evolution. We shall use the property of the geometric phase vanishing for geodesics to establish the link between Bargmann invariants and the geometric phase. This shall form the basis for calculating various important differential geometric quantities of ray space that finally relate to topological ideas. It is worth noting that the import of Mukunda and Simon's work is the purely kinematical development of ideas related to the geometric phase which makes no special reference to the Schrödinger equation or any particular choice of Hamiltonian.

C.4 Bargmann Invariants and Geometric Phase

From the introduction to Bargmann invariants in Sec.C.2 we may conclude that the inner products used to construct the invariants might very well be expressed in the Von Neumann density matrix formulation as the trace operation on the product of pure state density matrices for the two states involved in writing the inner product. In this notation the simplest i.e. the 3-point Bargmann invariant can be written as

$$\Omega_3(\psi_1,\psi_2,\psi_3) = \langle\psi_1|\psi_2\rangle\,\langle\psi_2|\psi_3\rangle\,\langle\psi_3|\psi_1\rangle = \mathrm{Tr}(\rho_{\psi_1}\rho_{\psi_2}\rho_{\psi_3}) \tag{C.32}$$

This makes manifest the fact that the invariant is a ray space quantity. Let us connect the ray space points ρ_{ψ_1}, ρ_{ψ_2} and ρ_{ψ_3} by geodesics in $\boldsymbol{\mathcal{R}}$ such that C_{12} joins ρ_{ψ_1} and ρ_{ψ_2}, C_{23} joins ρ_{ψ_2} and ρ_{ψ_3}, and C_{31} joins ρ_{ψ_3} and ρ_{ψ_1}. Also a general lift of these curves in $\mathcal{B}$ could be chosen, with $\boldsymbol{\mathcal{C}_{12}}$ connecting ψ_1 and ψ_2, $\boldsymbol{\mathcal{C}_{23}}$ connecting ψ_2 and ψ_3 and $\boldsymbol{\mathcal{C}_{31}}$ connecting ψ_3 and ψ_1. With this we have the closed curves $C_{12}\cup C_{23}\cup C_{31}$ in $\boldsymbol{\mathcal{R}}$ and $\boldsymbol{\mathcal{C}_{12}}\cup\boldsymbol{\mathcal{C}_{23}}\cup\boldsymbol{\mathcal{C}_{31}}$ in $\mathcal{B}$. Using the property of geodesics mentioned in eq.(C.30) it can be shown

$$\begin{aligned}\arg\{\Omega_3(\psi_1,\psi_2,\psi_3)\} &= \arg\{\langle\psi_1|\psi_2\rangle\} + \arg\{\langle\psi_2|\psi_3\rangle\} + \arg\{\langle\psi_3|\psi_1\rangle\}\\ &= \Theta_{\mathrm{dyn}}[C_{12}] + \Theta_{\mathrm{dyn}}[C_{23}] + \Theta_{\mathrm{dyn}}[C_{31}]\\ &= \Theta_{\mathrm{dyn}}[C_{12}\cup C_{23}\cup C_{31}] = -\Theta_g[C_{12}\cup C_{23}\cup C_{31}]\end{aligned} \tag{C.33}$$

This gives the relation that the phase of a 3-point Bargmann invariant is the negative of the geometric phase of a geodesic triangle in $\boldsymbol{\mathcal{R}}$. One could just as easily go ahead and show this result for an N-point Bargmann invariant and an N-sided geodesic polygon. This generalization allows us to write, for $\psi_j \in \mathcal{B}, j = 1,2,\ldots,N$ such

that $\langle\psi_j|\psi_{j+1}\rangle \neq 0$,

$$\Omega_N(\psi_1,\psi_2,\ldots,\psi_N) = \langle\psi_1|\psi_2\rangle\,\langle\psi_2|\psi_3\rangle\ldots\langle\psi_{N-1}|\psi_N\rangle\,\langle\psi_N|\psi_1\rangle$$
$$\arg\{\Omega_N(\psi_1,\psi_2,\ldots,\psi_N)\} = -\Theta_g[C \equiv \text{ N-sided geodesic polygon with vertices } \rho_{\psi_1},\rho_{\psi_2},\ldots,\rho_{\psi_N}] \tag{C.34}$$

Armed with this general connection between the phase and Bargmann invariants we may now proceed to exploit the density matrix formalism to compute expressions for differential geomatric quantities such as the metric and curvature 2-form in ray space and illustrate the relation to toplogical invariants.

C.5 Ray space metric, Berry curvature and Topology

The notion of distance and hence a metric in ray space can be defined using the inner product for a pair of non-orthogonal states, ψ_1 and ψ_2 belonging to $\mathcal{B}$, in the following way

$$ds^2(\psi_1,\psi_2) = 1 - |\langle\psi_1|\psi_2\rangle|^2 = 1 - \langle\psi_1|\psi_2\rangle\,\langle\psi_2|\psi_1\rangle = 1 - \mathrm{Tr}(\rho_{\psi_1}\rho_{\psi_2}) \tag{C.35}$$

It is apparent that this distance is a ray space quantity given its $U(1)$ invariance and it qualifies as a distance function as it satisfies the general properties required of any distance function in a metric space. We also introduce a coordinate system in ray space with each point being denoted by the tuple $\mathbf{x} = (x^1, x^2, \ldots, x^{2(N-1)})$ given that $\boldsymbol{\mathcal{R}}$ is of $2(N-1)$-dimensions for an N-level quantum system. Using this we may shift to a continuous description of ray space in terms of the density matrices by making them functions of the coordinates as $\rho(\mathbf{x})$. Thus we drop the subscript

notation of explicitly writing the state and instead denote a density matrix operator field over $\mathfrak{R}$ which is defined at each point. This allows an easier route to introduce the differential and infinitesimal notions required to obtain the differential geometric quantities. With this it is possible to write the distance between two infinitesimally seperated points $\mathbf{x}$ and $\mathbf{x}+\delta\mathbf{x}$, as

$$ds^2(\mathbf{x}, \mathbf{x}+\delta\mathbf{x}) = 1 - \mathrm{Tr}(\rho(\mathbf{x})\rho(\mathbf{x}+\delta\mathbf{x})) \tag{C.36}$$

The expression inside the trace on the right hand side may be expanded by using a Taylor series to write $\rho(\mathbf{x}+\delta\mathbf{x})$ as

$$\mathrm{Tr}(\rho(\mathbf{x})\rho(\mathbf{x}+\delta\mathbf{x})) = \mathrm{Tr}(\rho(\mathbf{x})[\rho(\mathbf{x}) + \frac{\partial\rho}{\partial x^a}\delta x^a + \frac{1}{2}\frac{\partial^2\rho}{\partial x^a \partial x^b}\delta x^a \delta x^b + \dots] \tag{C.37}$$

where we go upto only the quadratic order to retain the bilinear terms that are significant to define the metric tensor for a Riemannian manifold. The Einstein summation convention is assumed here of regarding implicit sums over repeated indices such as a and b which run over the ray space dimensions. When the trace operation is applied on the expanded series upto the considered order, and using the general properties of density matrices along with the following ones,

$$\begin{aligned}
&\mathrm{Tr}(\rho^2) = 1 \\
&\mathrm{Tr}(\rho\frac{\partial\rho}{\partial x^a}) = 0 \\
&\mathrm{Tr}(\frac{\partial\rho}{\partial x^b}\frac{\partial\rho}{\partial x^a}) + Tr(\rho\frac{\partial^2\rho}{\partial x^a \partial x^b}) = 0
\end{aligned}$$

the metric can, after simplifications, be written as

$$ds^2(\mathbf{x}, \mathbf{x}+\delta\mathbf{x}) = \frac{1}{2}\mathrm{Tr}\frac{\partial\rho}{\partial x^a}\frac{\partial\rho}{\partial x^b}\delta x^a \delta x^b = g_{ab}\delta x^a \delta x^b \tag{C.38}$$

Here,

$$g_{ab} = \frac{1}{2}\mathrm{Tr}\partial_a\rho\partial_b\rho \tag{C.39}$$

denotes the symmetric metric tensor for the ray space manifold. We may make an observation regarding 2-level systems such as a spin-$\frac{1}{2}$ particle in a magnetic field in the above context. For such a system the Hilbert space is two dimensional in complex dimensions, the set of unit vectors $\mathcal{B} \simeq S^3$ i.e. the 3-sphere and the ray space $\boldsymbol{\mathcal{R}} \simeq S^2$ i.e. a Poincaré sphere. The ray space in such a case may be 'coordinatized' by the angular variables (θ, ϕ) and from the spin-$\frac{1}{2}$ analogy this is nothing but the Bloch sphere. The density matrix in this case is known to be $\rho(\theta,\phi) = (1 + \boldsymbol{\sigma}\cdot\mathbf{n}(\theta,\phi))/2$ where $\boldsymbol{\sigma}$ is the vector of Pauli matrices and $\mathbf{n}(\theta,\phi) = (\sin\theta\cos\phi, \sin\theta\sin\phi, \cos\theta)$ denotes the unit normal vector to the states on the Bloch sphere. Then the application of eq.(C.39) to this density matrix gives the metric on the Bloch sphere which is also known as the Fubini-Study metric.

The other important ray space quantity of interest is its curvature tensor or 2-form which we shall see has deep connections to the geometric phase. First we consider a geodesic triangle in ray space, as shown in fig.(C.1),

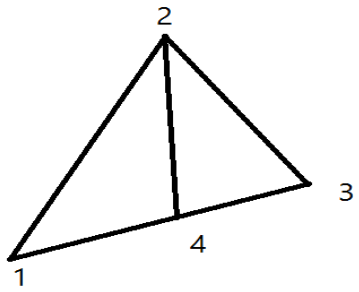

Figure C.1: A partitioned geodesic triangle in ray space.

whose lift is cornered at the states ψ_1 at 1 , ψ_2 at 2 and ψ_3 at 3 respectively. We also consider a partitioning of this triangle again by a geodesic connecting 1 to the state ψ_4 at 4 on the opposite side. The ray space geodesics between the various points are C_{12}, C_{23}, C_{31} and C_{14} respectively. Now it is easily seen that one may

relate the argument of the Bargmann invariant of corners of the 123-triangle with that of the 124 and 423 triangles as

$$\arg\{\Omega_3(\psi_1,\psi_2,\psi_3)\} = \arg\{\Omega_3(\psi_1,\psi_2,\psi_4)\} + \arg\{\Omega_3(\psi_4,\psi_2,\psi_3)\} \tag{C.40}$$

And now using the relation derived in eq.(C.33) between the phase of Bargmann invariants and geometric phases for geodesic triangles we may write from the above equation

$$\Theta_g[C_{12}\cup C_{23}\cup C_{31}] = \Theta_g[C_{12}\cup C_{24}\cup C_{41}] + \Theta_g[C_{42}\cup C_{23}\cup C_{34}] \tag{C.41}$$

The above result could be easily generalized to N-sided polygons. This gives us a very useful result that for any geodesic polygon which is subdivided into smaller geodesic polygons, the geometric phase going around the larger polygon is the sum of the geometric phases for going around each of the constituent ones. This allows a Stokes' Theorem like interpretation where the curl of a vector field around a path can be transformed to the integral of its flux over the enclosed surface by regarding the total curl to be the sum of the curl around infinitesimal tiles in an infinite tesselation of the enclosed area. Here too, one may consider the geometric phase for an infinitesimal geodesic triangle and then the phase over a curve enclosing any finite region of ray space may be obtained by an integration of the phases of all such triangles that fill up the said region.

We employ the continuum density matrix formulation, introduced earlier to derive the metric, to express the Bargmann invariant for an infinitesimal geodesic triangle cornered at $\mathbf{x}$, $\mathbf{x}+\delta\mathbf{x_1}$ and $\mathbf{x}$, $\mathbf{x}+\delta\mathbf{x_2}$. Thus the corners in ray space for such a triangle are given by $\rho(\mathbf{x})$, $\rho(\mathbf{x}+\delta\mathbf{x_1})$ and $\rho(\mathbf{x}+\delta\mathbf{x_2})$. If we consider the large triangle in fig.(C.1) for reference, with the same corner states of the lift taken before ,we may write the Bargmann invariant for the states at the corners in clockwise and

anti-clockwise fashion as follows

$$\begin{aligned}\Omega_3(\psi_1,\psi_2,\psi_3) &= e^{i\theta_{123}} = \mathrm{Tr}(\rho(\mathbf{x})\rho(\mathbf{x}+\delta\mathbf{x_1})\rho(\mathbf{x}+\delta\mathbf{x_2}))\\ \Omega_3(\psi_1,\psi_3,\psi_2) &= e^{i\theta_{132}} = \mathrm{Tr}(\rho(\mathbf{x})\rho(\mathbf{x}+\delta\mathbf{x_2})\rho(\mathbf{x}+\delta\mathbf{x_1}))\end{aligned} \tag{C.42}$$

Note that here we have regarded the normalized versions of the invariants and thus they are just phases of unit modulus. Clearly the phases θ_{123} and θ_{132} are just geometric phases for the two paths $C_{12} \cup C_{23} \cup C_{31}$ and $C_{13} \cup C_{32} \cup C_{21}$ and are related by $\theta_{123} = -\theta_{132}$ This is clear if one thinks of the two paths differing in the ordering of the limits for the dynamic phase integrals along each of the component geodesics. Thus being related by a change of sign. Thus we may now write the ratio of the clockwise and anti-clockwise Bargmann invariants as

$$\frac{\Omega_3(\psi_1,\psi_2,\psi_3)}{\Omega_3(\psi_1,\psi_3,\psi_2)} = e^{i2\theta_{123}} \tag{C.43}$$

Now since the triangle is considered infinitesimal one expects the phase θ_{123} to be small also and hence one can expand the RHS above to first order and get

$$\begin{aligned}e^{i2\theta_{123}} &\approx 1 + i2\theta_{123} = 1 + i\theta_{123} - (1 - i\theta_{123}) = 1 + i\theta_{123} - (1 + i\theta_{132})\\ &\approx e^{i\theta_{123}} - e^{i\theta_{132}} = \Omega_3(\psi_1,\psi_2,\psi_3) - \Omega_3(\psi_1,\psi_3,\psi_2)\end{aligned}$$

Where we see that the phase may be related to the difference of the Bargmann invariants in the infinitesimal case. This difference may be written in the continuously parametrized density matrix formulation as follows

$$\begin{aligned}\Omega_3(\psi_1,\psi_2,\psi_3) - \Omega_3(\psi_1,\psi_3,\psi_2) &= \mathrm{Tr}(\rho(\mathbf{x})\rho(\mathbf{x}+\delta\mathbf{x_1})\rho(\mathbf{x}+\delta\mathbf{x_2}))\\ &\quad - \mathrm{Tr}(\rho(\mathbf{x})\rho(\mathbf{x}+\delta\mathbf{x_2})\rho(x+\delta\mathbf{x_1}))\\ \implies \Omega_3(\psi_1,\psi_2,\psi_3) - \Omega_3(\psi_1,\psi_3,\psi_2) &= \mathrm{Tr}(\rho(\mathbf{x})\left[\rho(\mathbf{x}+\delta\mathbf{x_1}),\rho(\mathbf{x}+\delta\mathbf{x_2})\right])\end{aligned} \tag{C.44}$$

where the [,] denotes a commutator bracket. We proceed to expand the density matrices $\rho(\mathbf{x}+\delta\mathbf{x_1})$ and $\rho(\mathbf{x}+\delta\mathbf{x_2})$ in Taylor expansions as follows,

$$\begin{aligned}\rho(\mathbf{x}+\delta\mathbf{x_1}) &= \rho(\mathbf{x}) + \frac{\partial\rho}{\partial x_1^a}\delta x_1^a + \frac{1}{2}\frac{\partial^2\rho}{\partial x_1^a \partial x_1^b}\delta x_1^a \delta x_1^b + .. \\ \rho(\mathbf{x}+\delta\mathbf{x_2}) &= \rho(\mathbf{x}) + \frac{\partial\rho}{\partial x_2^a}\delta x_2^a + \frac{1}{2}\frac{\partial^2\rho}{\partial x_2^a \partial x_2^b}\delta x_2^a \delta x_2^b + ..\end{aligned} \tag{C.45}$$

These may be now fed into the commutator in eq.(C.44) and on expanding the action of the trace across the commutator bracket, where we use the properties of the density matrix expressions under trace as mentioned while deriving the metric tensor with an additional property $\mathrm{Tr}(\rho[\rho,\partial\rho]) = \mathrm{Tr}(\rho^2\partial_a\rho - \rho\partial_a\rho\rho) = 0$, we obtain

$$\begin{aligned}2i\theta_{123} &= \mathrm{Tr}(\rho(\mathbf{x})\,[\rho(\mathbf{x}+\delta\mathbf{x_1}),\rho(\mathbf{x}+\delta\mathbf{x_2})]) \\ &= \mathrm{Tr}\left(\rho\left(\frac{\partial\rho}{\partial x_1^a}\frac{\partial\rho}{\partial x_2^b}\delta x_1^a\delta x_2^b - \frac{\partial\rho}{\partial x_2^b}\frac{\partial\rho}{\partial x_1^a}\delta x_2^b\delta x_1^a\right)\right)\end{aligned} \tag{C.46}$$

In the expanded expression of the RHS above, the term inside the trace that is multiplied with ρ may be written in a fully antisymmetrized form by adding to it the following term which is essentially zero

$$\frac{\partial\rho}{\partial x_2^b}\frac{\partial\rho}{\partial x_1^a}\delta x_1^b\delta x_2^a - \frac{\partial\rho}{\partial x_1^a}\frac{\partial\rho}{\partial x_2^b}\delta x_1^b\delta x_2^a$$

This then gives us the following expression inside the trace

$$\rho\left\{\left(\frac{\partial\rho}{\partial x_1^a}\frac{\partial\rho}{\partial x_2^b} - \frac{\partial\rho}{\partial x_2^b}\frac{\partial\rho}{\partial x_1^a}\right)(\delta x_1^a\delta x_2^b - \delta x_2^b\delta x_1^a)\right\} \tag{C.47}$$

We consider this expression in two parts. Let us take the term $(\delta x_1^a\delta x_2^b - \delta x_2^b\delta x_1^a)$ which is antisymmetric like a cross product of coordinate vectors and we may transform the infinitesimal displacements therein to a new set of coordinates or parameters, chosen as $\mathbf{x}(s_1,s_2)$ along the geodesics to the vertices $\mathbf{x}+\delta\mathbf{x_1}$ and $\mathbf{x}+\delta\mathbf{x_2}$, as

$\delta x_1^a = \frac{\partial x^a}{\partial s_1} ds_1$ and $\delta x_2^a = \frac{\partial x^a}{\partial s_2} ds_2$. This allows us to write the term in a cross product form with a set of complete differentials

$$\left(\frac{\partial x^a}{\partial s_1} \frac{\partial x^b}{\partial s_2} - \frac{\partial x^b}{\partial s_1} \frac{\partial x^a}{\partial s_2} \right) ds_1 ds_2 = dx^a \wedge dx^b$$

which takes the form of a wedge product where the term in brackets on the left is the Jacobian of the transformation. The remaining part of the expression for the phase is the antisymmetric tensor or curvature 2-form

$$\begin{aligned} \mathcal{F}_{ab} &= \mathrm{Tr} \left(\rho \left(\frac{\partial \rho}{\partial x_1^a} \frac{\partial \rho}{\partial x_2^b} - \frac{\partial \rho}{\partial x_2^b} \frac{\partial \rho}{\partial x_1^a} \right) \right) \\ &= \mathrm{Tr} \rho [\partial_a \rho, \partial_b \rho] \end{aligned} \tag{C.48}$$

where the [,] again dentoes commutator brackets. The expression for the infinitesimal geometric phase can therefore be written as

$$\theta_{123} = \frac{1}{2i} \mathcal{F}_{ab} dx^a \wedge dx^b \tag{C.49}$$

We could assume the $1/2i$ factor to be implicit within the definition of the tensor $\mathcal{F}_{ab}$ and then the geometric phase over a curve enclosing any finite region of ray space, given by say $\mathcal{S}$, is the integral of this 2-form over this area as follows

$$\Theta_g = \int_{\mathcal{S}} \mathcal{F}_{ab} dx^a \wedge dx^b \tag{C.50}$$

$\mathcal{F}_{ab}$ it so happens, is the Berry field or curvature derived by Sir M.V. Berry [79] while considering the geometric phase in the parameter space of an adiabatically time dependent, cyclic Hamiltonian. The link to topology follows from the fact that the above expression is the integral of a curvature over a manifold and can be analogized to the integral of the Gauss-Bonnet curvature giving the genus of a manifold which

is a topological invariant. Similarly the above integral over a compact ray space manifold, say a Bloch sphere for the case of spin-$\frac{1}{2}$ systems, evaluates to an integer (in multiples of the solid angle 4π) for whole coverings of the sphere by any 2×2 Hamiltonian which is mapped to such a system using the $SU(2)$ representation with Pauli matrices. For systems invarant under discrete translations such as periodic lattice systems, the ray space is defined as the space of the density matrices of Bloch functions that exist over the first Brillouin zone which is a torus. In case of say Graphene where the reciprocal space Hamiltonian is 2-dimensional the problem gets mapped from the torus to the Bloch sphere. In this case the evaluation of the above integral for the wave vector varying over the torus and the corresponding density matrices constructed of Bloch states of a given band, yields the integer topological invariant called the Chern number for the band. Thus the topological invariant of Thouless et. al. [15] popularly known as the TKNN invariant can be obtained from the formalism discussed here. In this manner the general kinematical notions of Bargmann invariants can be applied to the calculation of topological quantities for quantum systems.

References

[1] T. Ando, A. B. Fowler, and F. Stern, Rev. Mod. Phys. **54**, 437 (1982).

[2] S. M. Reimann and M. Manninen, Rev. Mod. Phys. **74**, 1283 (2002).

[3] R. C. Ashoori, Nature **379**, 413 (1996).

[4] A. H. Castro Neto, F. Guinea, N. M. R. Peres, K. S. Novoselov, and A. K. Geim, Rev. Mod. Phys. **81**, 109 (2009).

[5] M. A. Reed, J. N. Randall, R. J. Aggarwal, R. J. Matyi, and T. M. Moore, Physical Review Letters **60**, 535 (1988).

[6] J. Cibert *et al.*, Applied Physics Letters **49**, 1275 (1986), http://dx.doi.org/10.1063/1.97384.

[7] D. S. L. Abergel, V. Apalkov, J. Berashevich, K. Ziegler, and T. Chakraborty, Advances in Physics **59**, 261 (2010), 1003.0391.

[8] A. C. Neto, F. Guinea, and N. M. Peres, Physics World **19**, 33 (2006).

[9] F. A. Buot, Physics Reports **234**, 73 (1993).

[10] R. C. Ashoori *et al.*, Phys. Rev. Lett. **68**, 3088 (1992).

[11] C. Sikorski and U. Merkt, Phys. Rev. Lett. **62**, 2164 (1989).

[12] K. v. Klitzing, G. Dorda, and M. Pepper, Phys. Rev. Lett. **45**, 494 (1980).

[13] S. Das Sarma, S. Adam, E. H. Hwang, and E. Rossi, Rev. Mod. Phys. **83**, 407 (2011).

[14] M. O. Goerbig, Rev. Mod. Phys. **83**, 1193 (2011).

[15] D. J. Thouless, M. Kohmoto, M. P. Nightingale, and M. den Nijs, Phys. Rev. Lett. **49**, 405 (1982).

[16] B. I. Halperin, Phys. Rev. B **25**, 2185 (1982).

[17] J. E. Avron, R. Seiler, and B. Simon, Phys. Rev. Lett. **51**, 51 (1983).

[18] Q. Niu, D. J. Thouless, and Y.-S. Wu, Phys. Rev. B **31**, 3372 (1985).

[19] Y. Hatsugai, Phys. Rev. Lett. **71**, 3697 (1993).

[20] N. Mukunda and R. Simon, Annals of Physics **228**, 205 (1993).

[21] P. G. Harper, Proceedings of the Physical Society A **68**, 874 (1955).

[22] J. Avron and B. Simon, Annals of Physics **110**, 85 (1978).

[23] J. Bellissard and B. Simon, Journal of functional analysis **48**, 408 (1982).

[24] S. Y. Jitomirskaya, Annals of Mathematics **150**, 1159 (1999).

[25] S. Aubry and G. André, Ann. Israel Phys. Soc **3**, 18 (1980).

[26] P. W. Anderson, Phys. Rev. **109**, 1492 (1958).

[27] E. Abrahams, P. W. Anderson, D. C. Licciardello, and T. V. Ramakrishnan, Phys. Rev. Lett. **42**, 673 (1979).

[28] T. Oka and L. Bucciantini, Phys. Rev. B **94**, 155133 (2016).

[29] D. Raventós, T. Graß, B. Juliá-Díaz, L. Santos, and M. Lewenstein, Phys. Rev. A **93**, 033605 (2016).

[30] L. Landau, Z. Phys **45**, 430 (1927).

[31] J. K. Jain, *Composite Fermions* (Cambridge, UK: Cambridge University Press, 2007).

[32] C. G. Darwin, Proceedings of the Cambridge Philosophical Society **27**, 86 (1931).

[33] C. Furtado, B. G. C. da Cunha, F. Moraes, E. R. B. de Mello, and V. B. Bezzerra, Physics Letters A **195**, 90 (1994).

[34] E. R. Bezerra de Mello and V. B. Bezerra, Journal of Mathematical Physics **36**, 5297 (1995).

[35] C. Furtado and F. Moraes, EPL (Europhysics Letters) **45**, 279 (1999).

[36] G. d. A. Marques, C. Furtado, V. B. Bezerra, and F. Moraes, Journal of Physics A Mathematical General **34**, 5945 (2001), quant-ph/0012146.

[37] K. S. Novoselov *et al.*, Science **306**, 666 (2004), cond-mat/0410550.

[38] M. Wilson, Physics Today **59**, 21 (2006), http://dx.doi.org/10.1063/1.2180163.

[39] G. W. Semenoff, Phys. Rev. Lett. **53**, 2449 (1984).

[40] M. I. Katsnelson, K. S. Novoselov, and A. K. Geim, Nature Physics **2**, 620 (2006), cond-mat/0604323.

[41] A. Iorio and G. Lambiase, Physics Letters B **716**, 334 (2012), 1108.2340.

[42] J. González, F. Guinea, and M. A. H. Vozmediano, Phys. Rev. Lett. **69**, 172 (1992).

[43] M. A. H. Vozmediano, M. I. Katsnelson, and F. Guinea, Physics Reports **496**, 109 (2010), 1003.5179.

[44] F. de Juan, J. L. Mañes, and M. A. H. Vozmediano, Phys. Rev. B **87**, 165131 (2013).

[45] J. L. Mañes, F. de Juan, M. Sturla, and M. A. H. Vozmediano, Phys. Rev. B **88**, 155405 (2013).

[46] F. Guinea, M. I. Katsnelson, and A. K. Geim, Nature Physics **6**, 30 (2010), 0909.1787.

[47] P. San-Jose, J. González, and F. Guinea, Phys. Rev. Lett. **108**, 216802 (2012).

[48] F. de Juan, A. Cortijo, and M. A. H. Vozmediano, Phys. Rev. B **76**, 165409 (2007).

[49] A. Cortijo, F. Guinea, and M. A. H. Vozmediano, Journal of Physics A: Mathematical and Theoretical **45**, 383001 (2012).

[50] A. Iorio, Annals of Physics **326**, 1334 (2011), 1007.5012.

[51] A. Cortijo and M. A. H. Vozmediano, European Physical Journal Special Topics **148**, 83 (2007), cond-mat/0612623.

[52] A. Cortijo and M. A. H. Vozmediano, EPL (Europhysics Letters) **77**, 47002 (2007), cond-mat/0603717.

[53] A. Cortijo and M. A. H. Vozmediano, Nuclear Physics B **763**, 293 (2007), cond-mat/0612374.

[54] A. Cortijo and M. A. H. Vozmediano, Phys. Rev. B **79**, 184205 (2009).

[55] F. Guinea, M. I. Katsnelson, and M. A. H. Vozmediano, Phys. Rev. B **77**, 075422 (2008).

[56] S.-L. Zhu, B. Wang, and L.-M. Duan, Phys. Rev. Lett. **98**, 260402 (2007).

[57] K. L. Lee, B. Grémaud, R. Han, B.-G. Englert, and C. Miniatura, Phys. Rev. A **80**, 043411 (2009).

[58] J.-M. Hou, W.-X. Yang, and X.-J. Liu, Phys. Rev. A **79**, 043621 (2009).

[59] G. Juzeliūnas, J. Ruseckas, M. Lindberg, L. Santos, and P. Öhberg, Phys. Rev. A **77**, 011802 (2008).

[60] B. Wunsch, F. Guinea, and F. Sols, New Journal of Physics **10**, 103027 (2008), 0807.4245.

[61] R. Shen, L. B. Shao, B. Wang, and D. Y. Xing, Phys. Rev. B **81**, 041410 (2010).

[62] K. Asano and C. Hotta, Phys. Rev. B **83**, 245125 (2011).

[63] M. Polini, F. Guinea, M. Lewenstein, H. C. Manoharan, and V. Pellegrini, Nature Nanotechnology **8**, 625 (2013), 1304.0750.

[64] L. Tarruell, D. Greif, T. Uehlinger, G. Jotzu, and T. Esslinger, Nature **483**, 302 (2012).

[65] G. Jotzu *et al.*, Nature **515**, 237 (2014).

[66] F. D. M. Haldane, Phys. Rev. Lett. **61**, 2015 (1988).

[67] Y. Hatsugai, T. Fukui, and H. Aoki, Phys. Rev. B **74**, 205414 (2006).

[68] B. A. Bernevig and S.-C. Zhang, Phys. Rev. Lett. **96**, 106802 (2006).

[69] B. A. Bernevig, T. L. Hughes, and S.-C. Zhang, Science **314**, 1757 (2006), http://science.sciencemag.org/content/314/5806/1757.full.pdf.

[70] C. L. Kane and E. J. Mele, Phys. Rev. Lett. **95**, 226801 (2005).

[71] C. Kane and E. Mele, Phys. Rev. Lett. **95**, 146802 (2005).

[72] P. Delplace, D. Ullmo, and G. Montambaux, Phys. Rev. B **84**, 195452 (2011).

[73] Y. Zhang, Y.-W. Tan, H. L. Stormer, and P. Kim, Nature **438**, 201 (2005).

[74] S. Koghee, L.-K. Lim, M. O. Goerbig, and C. M. Smith, Phys. Rev. A **85**, 023637 (2012).

[75] M. C. Rechtsman *et al.*, Phys. Rev. Lett. **111**, 103901 (2013).

[76] I. F. Herbut, Phys. Rev. B **78**, 205433 (2008).

[77] S. Zhu *et al.*, Phys. Rev. B **90**, 075426 (2014).

[78] J. L. Mañes, F. Guinea, and M. A. H. Vozmediano, Phys. Rev. B **75**, 155424 (2007).

[79] M. V. Berry, Proceedings of the Royal Society of London A: Mathematical, Physical and Engineering Sciences **392**, 45 (1984), http://rspa.royalsocietypublishing.org/content/392/1802/45.full.pdf.

[80] N. Goldman and J. Dalibard, Phys. Rev. X **4**, 031027 (2014).

[81] M. Bukov, L. D'Alessio, and A. Polkovnikov, Advances in Physics **64**, 139 (2015), 1407.4803.

[82] A. Eckardt and E. Anisimovas, New Journal of Physics **17**, 093039 (2015).

[83] L. Landau and E. Lifshitz, New York , 93 (1976).

[84] I. C. Percival and D. Richards, *Introduction to Dynamics* (Cambridge University Press, UK, 1983).

[85] A. Nauts and R. E. Wyatt, Phys. Rev. A **30**, 872 (1984).

[86] T. P. Grozdanov and M. J. Raković, Phys. Rev. A **38**, 1739 (1988).

[87] S. Rahav, I. Gilary, and S. Fishman, Phys. Rev. A **68**, 013820 (2003).

[88] M. M. Maricq, Phys. Rev. B **25**, 6622 (1982).

[89] Avan, P., Cohen-Tannoudji, C., Dupont-Roc, J., and Fabre, C., J. Phys. France **37**, 993 (1976).

[90] J. H. Shirley, Phys. Rev. **138**, B979 (1965).

[91] H. Sambe, Phys. Rev. A **7**, 2203 (1973).

[92] T. Mikami *et al.*, Phys. Rev. B **93**, 144307 (2016).

[93] F. Casas, J. A. Oteo, and J. Ros, Journal of Physics A: Mathematical and General **34**, 3379 (2001).

[94] I. Bloch, Nature Physics **1**, 23 (2005).

[95] I. Bloch, J. Dalibard, and W. Zwerger, Rev. Mod. Phys. **80**, 885 (2008).

[96] A. S. Sørensen, E. Demler, and M. D. Lukin, Phys. Rev. Lett. **94**, 086803 (2005).

[97] L.-K. Lim, C. M. Smith, and A. Hemmerich, Phys. Rev. Lett. **100**, 130402 (2008).

[98] A. Hemmerich, Phys. Rev. A **81**, 063626 (2010).

[99] C. E. Creffield and F. Sols, Phys. Rev. A **84**, 023630 (2011).

[100] A. Bermudez, T. Schaetz, and D. Porras, Phys. Rev. Lett. **107**, 150501 (2011).

[101] J. Struck *et al.*, Phys. Rev. Lett. **108**, 225304 (2012).

[102] P. Hauke *et al.*, Phys. Rev. Lett. **109**, 145301 (2012).

[103] B. M. Anderson, I. B. Spielman, and G. Juzeliūnas, Phys. Rev. Lett. **111**, 125301 (2013).

[104] I. I. Satija, D. C. Dakin, J. Y. Vaishnav, and C. W. Clark, Phys. Rev. A **77**, 043410 (2008).

[105] D. Jaksch and P. Zoller, New Journal of Physics **5**, 56 (2003), quant-ph/0304038.

[106] G. Juzeliūnas, J. Ruseckas, P. Öhberg, and M. Fleischhauer, Phys. Rev. A **73**, 025602 (2006).

[107] K. J. Günter, M. Cheneau, T. Yefsah, S. P. Rath, and J. Dalibard, Phys. Rev. A **79**, 011604 (2009).

[108] N. Goldman, A. Kubasiak, P. Gaspard, and M. Lewenstein, Phys. Rev. A **79**, 023624 (2009).

[109] J. Ruseckas, G. Juzeliūnas, P. Öhberg, and M. Fleischhauer, Phys. Rev. Lett. **95**, 010404 (2005).

[110] N. Goldman *et al.*, Phys. Rev. Lett. **103**, 035301 (2009).

[111] J. Dalibard, F. Gerbier, G. Juzeliūnas, and P. Öhberg, Rev. Mod. Phys. **83**, 1523 (2011).

[112] P. Soltan-Panahi *et al.*, Nature Physics **7**, 434 (2011), 1005.1276.

[113] H. Miyake, G. A. Siviloglou, C. J. Kennedy, W. C. Burton, and W. Ketterle, Phys. Rev. Lett. **111**, 185302 (2013).

[114] M. Aidelsburger *et al.*, Phys. Rev. Lett. **111**, 185301 (2013).

[115] J. Struck *et al.*, Science **333**, 996 (2011), 1103.5944.

[116] J. Struck *et al.*, Nature Physics **9**, 738 (2013), 1304.5520.

[117] Y. T. Katan and D. Podolsky, Phys. Rev. Lett. **110**, 016802 (2013).

[118] Y. Wang, H. Steinberg, P. Jarillo-Herrero, and N. Gedik, Science **342**, 453 (2013).

[119] Q.-J. Tong, J.-H. An, J. Gong, H.-G. Luo, and C. H. Oh, Phys. Rev. B **87**, 201109 (2013).

[120] D. Y. H. Ho and J. Gong, Phys. Rev. B **90**, 195419 (2014).

[121] A. G. Grushin, A. Gómez-León, and T. Neupert, Phys. Rev. Lett. **112**, 156801 (2014).

[122] Z. Zhou, I. I. Satija, and E. Zhao, Phys. Rev. B **90**, 205108 (2014).

[123] C. He and Z. Zhang, Physics Letters A **378**, 3200 (2014).

[124] L. Zhou, H. Wang, D. Y. Ho, and J. Gong, The European Physical Journal B **87**, 204 (2014).

[125] Z. bo Wang, H. Jiang, H. Liu, and X. Xie, Solid State Communications **215216**, 18 (2015).

[126] E. Anisimovas, G. Žlabys, B. M. Anderson, G. Juzeliūnas, and A. Eckardt, Phys. Rev. B **91**, 245135 (2015).

[127] M. Benito and G. Platero, Physica E: Low-dimensional Systems and Nanostructures **74**, 608 (2015).

[128] A. Farrell and T. Pereg-Barnea, Phys. Rev. B **93**, 045121 (2016).

[129] L. Zhou, C. Chen, and J. Gong, Phys. Rev. B **94**, 075443 (2016).

[130] T.-S. Xiong, J. Gong, and J.-H. An, Phys. Rev. B **93**, 184306 (2016).

[131] K. Saha, Phys. Rev. B **94**, 081103 (2016).

[132] J.-i. Inoue and A. Tanaka, Phys. Rev. Lett. **105**, 017401 (2010).

[133] B. Dóra, J. Cayssol, F. Simon, and R. Moessner, Phys. Rev. Lett. **108**, 056602 (2012).

[134] N. H. Lindner, D. L. Bergman, G. Refael, and V. Galitski, Phys. Rev. B **87**, 235131 (2013).

[135] A. Kundu, H. A. Fertig, and B. Seradjeh, Phys. Rev. Lett. **113**, 236803 (2014).

[136] D. Y. H. Ho and J. Gong, Phys. Rev. Lett. **109**, 010601 (2012).

[137] H. Dehghani, T. Oka, and A. Mitra, Phys. Rev. B **90**, 195429 (2014).

[138] V. Dal Lago, M. Atala, and L. E. F. Foa Torres, Phys. Rev. A **92**, 023624 (2015).

[139] P. Titum, E. Berg, M. S. Rudner, G. Refael, and N. H. Lindner, Phys. Rev. X **6**, 021013 (2016).

[140] T. Oka and H. Aoki, Phys. Rev. B **79**, 081406 (2009).

[141] T. Kitagawa, T. Oka, A. Brataas, L. Fu, and E. Demler, Phys. Rev. B **84**, 235108 (2011).

[142] Z. Gu, H. A. Fertig, D. P. Arovas, and A. Auerbach, Phys. Rev. Lett. **107**, 216601 (2011).

[143] E. Suárez Morell and L. E. F. Foa Torres, Phys. Rev. B **86**, 125449 (2012).

[144] T. Iadecola *et al.*, Phys. Rev. Lett. **110**, 176603 (2013).

[145] P. Delplace, A. Gómez-León, and G. Platero, Phys. Rev. B **88**, 245422 (2013).

[146] P. M. Perez-Piskunow, G. Usaj, C. A. Balseiro, and L. E. F. F. Torres, Phys. Rev. B **89**, 121401 (2014).

[147] G. Usaj, P. M. Perez-Piskunow, L. E. F. Foa Torres, and C. A. Balseiro, Phys. Rev. B **90**, 115423 (2014).

[148] P. M. Perez-Piskunow, L. E. F. Foa Torres, and G. Usaj, Phys. Rev. A **91**, 043625 (2015).

[149] M. Sentef *et al.*, Nature communications **6** (2015).

[150] M. C. Rechtsman *et al.*, Nature **496**, 196 (2013), Letter.

[151] W. Zheng and H. Zhai, Phys. Rev. A **89**, 061603 (2014).

[152] M. D. Reichl and E. J. Mueller, Phys. Rev. A **89**, 063628 (2014).

[153] F. Mei *et al.*, Phys. Rev. A **90**, 063638 (2014).

[154] L. Yuan and S. Fan, Phys. Rev. A **92**, 053822 (2015).

[155] Z. Yan, B. Li, X. Yang, and S. Wan, Scientific Reports **5**, 16197 EP (2015), Article.

[156] A. Verdeny and F. Mintert, Phys. Rev. A **92**, 063615 (2015).

[157] D. Leykam, M. C. Rechtsman, and Y. D. Chong, Phys. Rev. Lett. **117**, 013902 (2016).

[158] M. Račiūnas, G. Žlabys, A. Eckardt, and E. Anisimovas, Phys. Rev. A **93**, 043618 (2016).

[159] P. Leboeuf, J. Kurchan, M. Feingold, and D. P. Arovas, Phys. Rev. Lett. **65**, 3076 (1990).

[160] I. Dana, Phys. Rev. E **52**, 466 (1995).

[161] E. P. L. van Nieuwenburg, J. M. Edge, J. P. Dahlhaus, J. Tworzydło, and C. W. J. Beenakker, Phys. Rev. B **85**, 165131 (2012).

[162] R. W. Bomantara, G. N. Raghava, L. Zhou, and J. Gong, Phys. Rev. E **93**, 022209 (2016).

[163] M. Lababidi, I. I. Satija, and E. Zhao, Phys. Rev. Lett. **112**, 026805 (2014).

[164] H. Wang, D. Y. H. Ho, W. Lawton, J. Wang, and J. Gong, Phys. Rev. E **88**, 052920 (2013).

[165] M. Thakurathi, A. A. Patel, D. Sen, and A. Dutta, Phys. Rev. B **88**, 155133 (2013).

[166] D. Babajanov, D. U. Matrasulov, and R. Egger, The European Physical Journal B **87**, 258 (2014).

[167] S. Dasgupta, U. Bhattacharya, and A. Dutta, Phys. Rev. E **91**, 052129 (2015).

[168] A. Agarwala, U. Bhattacharya, A. Dutta, and D. Sen, Phys. Rev. B **93**, 174301 (2016).

[169] A. Altland and M. R. Zirnbauer, Phys. Rev. B **55**, 1142 (1997).

[170] A. P. Schnyder, S. Ryu, A. Furusaki, and A. W. W. Ludwig, Phys. Rev. B **78**, 195125 (2008).

[171] A. Kitaev, Periodic table for topological insulators and superconductors, in *AIP Conference Proceedings* Vol. 1134, 2009.

[172] T. Kitagawa, E. Berg, M. Rudner, and E. Demler, Phys. Rev. B **82**, 235114 (2010).

[173] A. Gómez-León and G. Platero, Phys. Rev. Lett. **110**, 200403 (2013).

[174] M. S. Rudner, N. H. Lindner, E. Berg, and M. Levin, Phys. Rev. X **3**, 031005 (2013).

[175] J. K. Asbóth, B. Tarasinski, and P. Delplace, Phys. Rev. B **90**, 125143 (2014).

[176] D. Carpentier, P. Delplace, M. Fruchart, and K. Gawedzki, Phys. Rev. Lett. **114**, 106806 (2015).

[177] F. Nathan and M. S. Rudner, New Journal of Physics **17**, 125014 (2015).

[178] I. C. Fulga and M. Maksymenko, Phys. Rev. B **93**, 075405 (2016).

[179] M. Fruchart, Phys. Rev. B **93**, 115429 (2016).

[180] R. Roy and F. Harper, ArXiv e-prints (2016), 1603.06944.

[181] T. Chakraborty, *Quantum Dots: A survey of the properties of artificial atoms* (Elsevier, 1999).

[182] K. Kash, A. Scherer, J. M. Worlock, H. G. Craighead, and M. C. Tamargo, Applied Physics Letters **49**, 1043 (1986), http://dx.doi.org/10.1063/1.97466.

[183] H. Temkin, G. J. Dolan, M. B. Panish, and S. N. G. Chu, Applied Physics Letters **50**, 413

(1987), http://dx.doi.org/10.1063/1.98159.

[184] O. Makarovsky *et al.*, Phys. Rev. Lett. **101**, 226807 (2008).

[185] T. P. Smith, K. Y. Lee, C. M. Knoedler, J. M. Hong, and D. P. Kern, Phys. Rev. B **38**, 2172 (1988).

[186] R. C. Ashoori *et al.*, Phys. Rev. Lett. **71**, 613 (1993).

[187] W. Hansen *et al.*, Phys. Rev. Lett. **62**, 2168 (1989).

[188] T. Demel, D. Heitmann, P. Grambow, and K. Ploog, Phys. Rev. Lett. **64**, 788 (1990).

[189] B. Boyacioglu and A. Chatterjee, Journal of Applied Physics **112**, 083514 (2012), http://dx.doi.org/10.1063/1.4759350.

[190] P. A. Maksym and T. Chakraborty, Phys. Rev. Lett. **65**, 108 (1990).

[191] N. Mermin, Rev. Mod. Phys. **51**, 591.

[192] E. Kröner *et al.*, Physics of defects **35**, 217 (1981).

[193] M. Kleman, Liquid Crystals, Magnetic Systems and Various Ordered Media. J. Wiley, New York (1983).

[194] V. A. Osipov, Physics Letters A **164**, 327 (1992).

[195] J. Kumar, P. A. Sreeram, and S. Dattagupta, Phys. Rev. E **79**, 021130 (2009).

[196] J. Kumar and E. Kamil, ArXiv e-prints (2010), 1010.1205.

[197] S. Dattagupta, J. Kumar, S. Sinha, and P. A. Sreeram, Phys. Rev. E **81**, 031136 (2010).

[198] V. Volterra, Sur l'équilibre des corps élastiques multiplement connexes, in *Annales scientifiques de l'École normale supérieure* Vol. 24, pp. 401–517, 1907.

[199] A. Vilenkin, Phys. Rev. D **23**, 852 (1981).

[200] A. Kumar, S. E. Laux, and F. Stern, Phys. Rev. B **42**, 5166 (1990).

[201] F. Evers and A. D. Mirlin, Rev. Mod. Phys. **80**, 1355 (2008).

[202] D. R. Grempel, S. Fishman, and R. E. Prange, Phys. Rev. Lett. **49**, 833 (1982).

[203] S. Ostlund, R. Pandit, D. Rand, H. J. Schellnhuber, and E. D. Siggia, Phys. Rev. Lett. **50**, 1873 (1983).

[204] M. Kohmoto, Phys. Rev. Lett. **51**, 1198 (1983).

[205] H. Hiramoto and M. Kohmoto, Phys. Rev. Lett. **62**, 2714 (1989).

[206] D. J. Thouless, Phys. Rev. Lett. **61**, 2141 (1988).

[207] S. Das Sarma, S. He, and X. C. Xie, Phys. Rev. Lett. **61**, 2144 (1988).

[208] S. Das Sarma, S. He, and X. C. Xie, Phys. Rev. B **41**, 5544 (1990).

[209] Y. Hashimoto, K. Niizeki, and Y. Okabe, Journal of Physics A Mathematical General **25**, 5211 (1992).

[210] B. Simon, Advances in Applied Mathematics **3**, 463 (1982).

[211] J. Biddle, B. Wang, D. J. Priour, and S. Das Sarma, Phys. Rev. A **80**, 021603 (2009).

[212] J. Biddle and S. Das Sarma, Phys. Rev. Lett. **104**, 070601 (2010).

[213] J. Biddle, D. J. Priour, B. Wang, and S. Das Sarma, Phys. Rev. B **83**, 075105 (2011).

[214] S. Ganeshan, J. H. Pixley, and S. Das Sarma, Phys. Rev. Lett. **114**, 146601 (2015).

[215] J. Billy *et al.*, Nature **453**, 891 (2008), 0804.1621.

[216] G. Roati *et al.*, Nature **453**, 895 (2008).

[217] K. Drese and M. Holthaus, Phys. Rev. Lett. **78**, 2932 (1997).

[218] Y. Lahini *et al.*, Phys. Rev. Lett. **103**, 013901 (2009).

[219] G. Roux *et al.*, Phys. Rev. A **78**, 023628 (2008).

[220] R. Roth and K. Burnett, Phys. Rev. A **68**, 023604 (2003).

[221] J. E. Lye *et al.*, Phys. Rev. A **75**, 061603 (2007).

[222] R. B. Diener, G. A. Georgakis, J. Zhong, M. Raizen, and Q. Niu, Phys. Rev. A **64**, 033416 (2001).

[223] M. Modugno, New Journal of Physics **11**, 033023 (2009), 0901.0210.

[224] B. Damski, J. Zakrzewski, L. Santos, P. Zoller, and M. Lewenstein, Phys. Rev. Lett. **91**, 080403 (2003).

[225] V. Guarrera, L. Fallani, J. E. Lye, C. Fort, and M. Inguscio, New Journal of Physics **9**, 107 (2007).

[226] G. Ritt, C. Geckeler, T. Salger, G. Cennini, and M. Weitz, Phys. Rev. A **74**, 063622 (2006).

[227] L. Fallani, J. E. Lye, V. Guarrera, C. Fort, and M. Inguscio, Phys. Rev. Lett. **98**, 130404 (2007).

[228] H. Yamada and K. S. Ikeda, Phys. Rev. E **59**, 5214 (1999).

[229] D. F. Martinez and R. A. Molina, Phys. Rev. B **73**, 073104 (2006).

[230] R. Lima and D. Shepelyansky, Phys. Rev. Lett. **67**, 1377 (1991).

[231] L. Hufnagel *et al.*, Phys. Rev. B **62**, 15348 (2000).

[232] A. R. Kolovsky and G. Mantica, Phys. Rev. B **86**, 054306 (2012).

[233] E. Arimondo, D. Ciampini, A. Eckardt, M. Holthaus, and O. Morsch, arXiv preprint arXiv:1203.1259 (2012).

[234] T. Mishra, T. Guha Sarkar, and J. N. Bandyopadhyay, European Physical Journal B **88**, 231 (2015), 1411.1423.

[235] L. Morales-Molina, E. Doerner, C. Danieli, and S. Flach, Phys. Rev. A **90**, 043630 (2014).

[236] P. Qin, C. Yin, and S. Chen, Phys. Rev. B **90**, 054303 (2014).

[237] C. Aulbach, A. Wobst, G.-L. Ingold, P. Hänggi, and I. Varga, New Journal of Physics **6**, 70 (2004).

[238] G.-L. Ingold, A. Wobst, C. Aulbach, and P. Hänggi, The European Physical Journal B - Condensed Matter and Complex Systems **30**, 175 (2002).

[239] A. Wobst, G.-L. Ingold, P. Hänggi, and D. Weinmann, European Physical Journal B **27**, 11 (2002), cond-mat/0110028.

[240] Y.-J. Lin *et al.*, Phys. Rev. Lett. **102**, 130401 (2009).

[241] Y.-J. Lin *et al.*, Nature Physics **7**, 531 (2011), 1008.4864.

[242] D. R. Hofstadter, Phys. Rev. B **14**, 2239 (1976).

[243] M. Abramowitz *et al.*, Applied Mathematics Series **55**, 39 (1966).

[244] F. H. Claro and G. H. Wannier, Phys. Rev. B **19**, 6068 (1979).

[245] Y. Hatsugai and M. Kohmoto, Phys. Rev. B **42**, 8282 (1990).

[246] D. J. Thouless, Phys. Rev. B **28**, 4272 (1983).

[247] J. H. Han, D. J. Thouless, H. Hiramoto, and M. Kohmoto, Phys. Rev. B **50**, 11365 (1994).

[248] D. J. Thouless, Physics Reports **13**, 93 (1974).

[249] J. T. Edwards and D. J. Thouless, Journal of Physics C Solid State Physics **5**, 807 (1972).

[250] R. Bell and P. Dean, Discussions of the Faraday society **50**, 55 (1970).

[251] F. Liu, S. Ghosh, and Y. D. Chong, Phys. Rev. B **91**, 014108 (2015).

[252] J. B. Sokoloff, Physics Reports **126**, 189 (1985).

[253] A. Janner and T. Janssen, Phys. Rev. B **15**, 643 (1977).

[254] R. B. Laughlin, Phys. Rev. B **23**, 5632 (1981).

[255] L. Fu, C. L. Kane, and E. J. Mele, Phys. Rev. Lett. **98**, 106803 (2007).

[256] J. E. Moore, Nature **464**, 194 (2010).

[257] Y. Chen *et al.*, Science **325**, 178 (2009).

[258] M. Z. Hasan, S.-Y. Xu, D. Hsieh, L. A. Wray, and Y. Xia, arXiv preprint arXiv:1401.0848 (2014).

[259] M. Z. Hasan and C. L. Kane, Rev. Mod. Phys. **82**, 3045 (2010).

[260] X.-L. Qi and S.-C. Zhang, Rev. Mod. Phys. **83**, 1057 (2011).

[261] J. Cayssol, B. Dóra, F. Simon, and R. Moessner, physica status solidi (RRL) Rapid Research Letters **7**, 101 (2013).

[262] U. Bhattacharya, S. Dasgupta, and A. Dutta, The European Physical Journal B **89**, 216 (2016).

[263] K. Plekhanov, G. Roux, and K. Le Hur, Phys. Rev. B **95**, 045102 (2017).

[264] A. R. Wright, Scientific Reports **3**, 2736 (2013), 1211.6519.

[265] A. M. Cook and A. Paramekanti, Phys. Rev. Lett. **113**, 077203 (2014).

[266] A. M. Cook, Phys. Rev. B **94**, 205135 (2016).

[267] T. Li and O. P. Sushkov, Phys. Rev. B **94**, 155311 (2016).

[268] J. Jung, A. M. DaSilva, A. H. MacDonald, and S. Adam, Nature Communications **6**, 6308 EP (2015), Article.

[269] C. Ortix, L. Yang, and J. van den Brink, Phys. Rev. B **86**, 081405 (2012).

[270] M. Weinberg, C. Staarmann, C. lschlger, J. Simonet, and K. Sengstock, 2D Materials **3**, 024005 (2016).

[271] Y.-X. Wang, F.-X. Li, and Y.-M. Wu, EPL (Europhysics Letters) **99**, 47007 (2012).

[272] T. Thonhauser and D. Vanderbilt, Phys. Rev. B **74**, 235111 (2006).

[273] A. A. Soluyanov and D. Vanderbilt, Phys. Rev. B **83**, 035108 (2011).

[274] M. Kohmoto, Annals of Physics **160**, 343 (1985).

[275] N. Mukunda and R. Simon, Annals of Physics **228**, 269 (1993).

[276] E. M. Rabei, Arvind, N. Mukunda, and R. Simon, Phys. Rev. A **60**, 3397 (1999).

[277] U. Bhattacharya and A. Dutta, Phys. Rev. B **95**, 184307 (2017).

[278] M. Greiner, O. Mandel, T. Esslinger, T. W. Hänsch, and I. Bloch, Nature **415**, 39 (2002).

[279] Z. Hadzibabic, P. Krüger, M. Cheneau, B. Battelier, and J. Dalibard, Nature **441**, 1118 (2006), cond-mat/0605291.

[280] M. Grifoni and P. Hänggi, Physics Reports **304**, 229 (1998).

[281] J. N. Bandyopadhyay and T. Guha Sarkar, Phys. Rev. E **91**, 032923 (2015).

[282] S. Y. Zhou *et al.*, Nature Materials **6**, 916 (2007), 0709.1706.

[283] S. E. Savel'ev, W. Häusler, and P. Hänggi, European Physical Journal B **86**, 433 (2013).

[284] S. E. Savel'ev, W. Häusler, and P. Hänggi, Phys. Rev. Lett. **109**, 226602 (2012).

[285] O. Boada, A. Celi, J. I. Latorre, and M. Lewenstein, New Journal of Physics **13**, 035002 (2011), 1010.1716.

[286] M. Pollock, Acta Physica Polonica B **41** (2010).

[287] Y. Sucu and N. Ünal, Journal of Mathematical Physics **48**, 052503 (2007).

[288] V. R. Khalilov and C.-L. Ho, Modern Physics Letters A **13**, 615 (1998), hep-th/9801012.

[289] V. R. Khalilov and C.-L. Ho, Chinese Journal of Physics **47**, 294 (2009).

[290] C.-L. Ho and V. R. Khalilov, Phys. Rev. A **61**, 032104 (2000).

[291] S. P. Gavrilov, D. M. Gitman, and A. A. Smirnov, European Physical Journal C **32**, 119 (2004), hep-th/0210312.

[292] S. P. Gavrilov and D. M. Gitman, Phys. Rev. D **53**, 7162 (1996).

[293] P. Das Gupta, S. Raj, and D. Chaudhuri, ArXiv e-prints (2010), 1012.0976.

[294] L. Menculini, O. Panella, and P. Roy, Phys. Rev. D **87**, 065017 (2013).

[295] D. R. Brill and J. A. Wheeler, Rev. Mod. Phys. **29**, 465 (1957).

[296] S. Weinberg, *Gravitation and Cosmology: Principles and Applications of the General Theory of Relativity* (John Wiley & Sons, Inc., 1972).

[297] A. Bácsi and A. Virosztek, Phys. Rev. B **82**, 193405 (2010).

[298] G. Gui, J. Li, and J. Zhong, Phys. Rev. B **78**, 075435 (2008).

[299] M. Y. Han, B. Özyilmaz, Y. Zhang, and P. Kim, Phys. Rev. Lett. **98**, 206805 (2007).

[300] I. Snyman, Phys. Rev. B **80**, 054303 (2009).

[301] R. P. Tiwari and D. Stroud, Phys. Rev. B **79**, 205435 (2009).

[302] C. Coletti *et al.*, Phys. Rev. B **81**, 235401 (2010).

[303] K. K. Gomes, W. Mar, W. Ko, F. Guinea, and H. C. Manoharan, Nature **483**, 306 (2012).

[304] R. de Gail, J.-N. Fuchs, M. O. Goerbig, F. Piéchon, and G. Montambaux, Physica B Condensed Matter **407**, 1948 (2012), 1203.1262.

[305] Y. Aharonov and J. Anandan, Phys. Rev. Lett. **58**, 1593 (1987).

[306] J. Struck, J. Simonet, and K. Sengstock, Phys. Rev. A **90**, 031601 (2014).

[307] R. Peierls, *On the Theory of the Diamagnetism of Conduction Electrons* (World Scientific Publishing Co, 1997), pp. 97–120.

[308] G. H. Wannier, Phys. Rev. **117**, 432 (1960).

[309] J. M. Luttinger, Phys. Rev. **84**, 814 (1951).

[310] W. Kohn, Phys. Rev. **115**, 1460 (1959).

[311] G. H. Wannier, Rev. Mod. Phys. **34**, 645 (1962).

[312] T. Kjeldaas and W. Kohn, Phys. Rev. **105**, 806 (1957).

[313] G. H. Wannier, Physica Status Solidi B Basic Research **88**, 757 (1978).

[314] G. M. Obermair and G. H. Wannier, Physica Status Solidi B Basic Research **76**, 217 (1976).

[315] M. Y. Azbel, Sov. Phys. JETP **19**, 634 (1964).

[316] G. Zil'Berman, Sov. Phys. JETP **5**, 208 (1957).

[317] S. Janecek, M. Aichinger, and E. R. Hernández, Phys. Rev. B **87**, 235429 (2013).

[318] G. H. Wannier, Physica Status Solidi B Basic Research **70**, 727 (1975).

[319] J. Zak, Physics Letters A **117**, 367 (1986).

[320] Y. Hasegawa, P. Lederer, T. M. Rice, and P. B. Wiegmann, Phys. Rev. Lett. **63**, 907 (1989).

[321] H. J. Schellnhuber and G. M. Obermair, Phys. Rev. Lett. **45**, 276 (1980).

[322] A. H. MacDonald, Phys. Rev. B **28**, 6713 (1983).

[323] H. J. Stöckmann, *Quantum Chaos : An Introduction* (Cambridge University Press, UK, 2007).

[324] J. C. Slater, Phys. Rev. **76**, 1592 (1949).

[325] G. H. Wannier, Phys. Rev. **52**, 191 (1937).

[326] M. Kohmoto, Phys. Rev. B **39**, 11943 (1989).

[327] J. Zak, Phys. Rev. **134**, A1602 (1964).

[328] W. R. Salzman, Phys. Rev. A **10**, 461 (1974).

[329] J. H. Shirley, *Ph.D. Thesis : Interaction of a quantum system with a strong oscillating field* (California Institute of Technology, CaltechTHESIS Collection (unpublished), 1963).

[330] S. Pancharatnam, Proceedings of the Indian Academy of Sciences - Section A **44**, 247 (1956).

[331] J. Samuel and R. Bhandari, Phys. Rev. Lett. **60**, 2339 (1988).

[332] V. Bargmann, Journal of Mathematical Physics **5**, 862 (1964), http://dx.doi.org/10.1063/1.1704188.

List of Publications and Presentations

Peer reviewed International Journals:

- *"Thermal properties of a particle confined to a parabolic quantum well in two-dimensional space with conical disclination"*

  Tridev Mishra, Tapomoy Guha Sarkar and Jayendra N. Bandyopadhyay, Phys. Rev. E **89**, 012103 (2014).

- *"Floquet analysis of pulsed Dirac systems: a way to simulate rippled graphene"*

  Tridev Mishra, Tapomoy Guha Sarkar and Jayendra N. Bandyopadhyay, The European Physical Journal B **88**, 231 (2015).

- *"Phase transition in an Aubry-André system with a rapidly oscillating magnetic field"*

  Tridev Mishra, Rajath Shashidhara, Tapomoy Guha Sarkar and Jayendra N. Bandyopadhyay, Phys. Rev. A **94**, 053612 (2016).

- *"Floquet topological phase transitions in a kicked Haldane-Chern insulator"*

  Tridev Mishra, Anurag Pallaprolu, Tapomoy Guha Sarkar and Jayendra N. Bandyopadhyay, (under review) arXiv: 1709.08354 (2017).

List of conferences/schools attended/participated:

- *"Current Trends in Condensed Matter Physics"*,
  February 19-22, 2015, NISER **Bhubaneswar, INDIA**.
- *"SERC School on Topology and Condensed Matter Physics"*,
  November 23- December 12, 2015, SNBNCBS (organised by RKMVU), **Kolkata, INDIA**.
- *"School on Current Frontiers in Condensed Matter Research"*,
  June 20-29, 2016, ICTS, **Bangalore, INDIA.**
- *"Conference on Interactions and Topology in Dirac Systems"*,
  August 3-9, 2016, ICTP, **Trieste, Italy.**

Brief Biography of the Supervisor

Dr. Tapomoy Guha Sarkar is an Assistant Professor in the Department of Physics at Birla Institute of Technology & Science Pilani, Pilani Campus. He received his Ph.D. degree from IIT Kharagpur, in 2011. He joined the Physics Department of BITS Pilani, Pilani Campus in June, 2012 after an year's post doctoral stint at HRI, Allahabad. He has published several highly cited papers in reputed international journals. His research interests are in theoretical cosmology, specializing in the study of the diffuse intergalactic medium through the Lyman alpha forest spectra and redshifted 21-cm signal. Recently he has forayed into the domain of driven systems in condensed matter physics.

Brief Biography of the Co-Supervisor

Dr. Jayendra Nath Bandyopadhyay is an Assistant Professor in the Department of Physics at Birla Institute of Technology & Science Pilani, Pilani Campus. He received his Ph.D. degree from Physical Research Laboratory (PRL), Ahmedabad, in 2004. This was followed by post-doctoral research work for an year at PRL, two and a half years at Max Planck Institute for Complex Systems, Dresden, Germany and close to 4 years at National University Singapore most of which was at their Centre for Quantum Technologies. He joined the Physics Department of BITS Pilani, Pilani Campus in July, 2012. He has several highly cited papers in reputed international journals. His research interests are in the areas of quantum chaos, quantum information, quantum disordered systems, dynamics in kicked quantum systems and Quantum Biology.

Brief Biography of the Student

Mr. Tridev Mishra obtained his Bachelors degree in Electronics and Communication engineering from Netaji Subhas Institute of Technology, New Delhi in 2012. He cleared his CSIR-UGC NET exam in 2012 and he joined the Department of Physics, BITS Pilani as a research scholar in July, 2012, working as a JRF and then as a SRF. He is currently pursuing a Ph.D. in the area of theoretical condensed matter physics. His research interests are in the areas of low dimensional systems and periodically driven quantum systems, specifically looking at phenomena of topological origin and localization-delocalization transitions. He has published some papers in international journals and few are under review. In addition to this, he has participated in and presented his work at some national and international conferences of high repute.

Chapter 6

Conclusions and Future Scope

We are now prepared to summarize the essential results of the various studies undertaken in the different chapters of this thesis. We shall list some broad inferences from these and sketch the possible avenues of further inquiry into the systems studied here. In Chapter 2 we looked at a charged particle in a Landau-Fock-Darwin environment with conical disclination defect in the background metric. Besides the splitting expected due to Fock Darwin confinement, the spectrum showed the imprint of the defect by manifesting a modification of the energy eigenvalues by an amount quantified by the defect parameter. We observe an interplay between the magnetic field and temperature in the study of thermodynamic variables and quantities like the entropy and specific heat indicate the defect as having modified the temperature scale in the system. In the presence of a defect that has a local presence in the background the properties of the Landau levels problem are seen to be modified in a non-local manner. This provides the general rationale behind studying the problem in novel geometries.

Chapter 3 looked at the modifications to the metal-insulator transition in a 1-D bosonic optical lattice realization of the Aubry-André-Harper Hamiltonian which is driven by a high frequency oscillating magnetic field. Here we observe that the effective time independent Hamiltonian for the driven system has a nearest neighbor,

tight binding form upto $\mathcal{O}(\omega^{-2})$ corrections and exhibits a mobility edge along with slight modifications to the transition. The duality of the AAH model is lost as the driven model couples far off sites in reciprocal space. The driving is seen to impart properties commonly attributed to a disordered system. A key feature, though not the focus of attention in the chapter, that appears is the large critical region of wavefunctions in the phase plot of the inverse participation ratio in the plane of energies and lattice modulation strength. This highlights the role of periodic driving in the generation of critical/multifractal wavefunctions in Fibonacci and quasicrystalline 1-D structures. Though in this study we used the effective Hamiltonian derived in [80], we propose as a future work the use of the Brillouin-Wigner method of calculating the effective Hamiltonian [92], discussed in appendix B, to study the Floquet topological properties of the AAH Hamiltonian driven by the application of linearly and circuarly polarized light. A more difficult problem would be to consider the topological features of the AAH Hamiltonian for a magnetic field induced driving. The present formalism used to derive the spectrum and topological aspects of the AAH model would be woefully inadequate for this purpose.

In chapter 4 we considered topological properties of the periodically δ-kicked Haldane model. The kicking was chosen such that it modified the inversion breaking parameter of the model by the action of a time dependent, periodic, staggered sub-lattice potential. It was seen that the effect of the kicking was to shift the topological phase diagram of the driven model about its undriven position, linearly with respect to the driving amplitude, for a given choice of driving frequency. The resulting driven model was also seen to be a Chern insulator similar to the Haldane model. This allowed for the possibility of driving a topological choice of Haldane model parameters to a topologically trivial region by adiabatically changing the driving amplitude. A freedom that could be exploited to study Floquet topological phase transitions in a simple non-interacting model. This allows a controllable pa-

rameter that can be used to tune across the normal to Chern insulator boundary of the phase diagram. Another application of this feature could be in the study of dynamical quantum or topological phase transitions wherein the kicking amplitude may be used as the linear quenching parameter to go across the quantum critical point. An extension of this scheme could be made to the Quantum Spin Hall Hamiltonian for Graphene, where the effects of kicking on the Kane-Mele model could be examined. This is proposed as a future study to be undertaken, with the objective of studying the effects of kicking on the Z_2 topological index. Chapter 5 discussed a possible Floquet engineering technique to simulate curved Graphene in a cold atom optical lattice setup. A general pulsing sequence was identified that could be used to generate any conformal geomerty for the simulated 2-D monolayer Graphene analogue. The method offers a scheme to study the behaviour of the massless Dirac fermion excitations in various curved spaces and hence contributes to the panoply of such lattice systems which may be used as table top experimental setups to study relativistic quantum electrodynamics in $(2+1)$-dimensions. The technnique could also be used to simulate various gauge fields in Graphene which are customarily introduced via strain engineering in actual samples. The behavior of curvature as an effective gauge potential could be used to simulate Graphene with strains and defects that would ordinarily be difficult to study using experimentally synthesized samples.

We have, in the different chapters of this thesis, explored the effects of periodic driving on the properties of low dimensional Hamiltonians and observed that driving offers an exceptional tool to modify various properties in a controlled and desired manner and is a highly flexible and promising instrument for this purpose. There are aspects associated with the non-equlibrium nature of the physics of such systems which we have not carved out in the discussions here as our suggested methods of realizing these systems were drawn from the existing literature which prescribed the

suitable parameter ranges where non-equilibrium quasistatic states were realized on suitable time scales. The reason being that the experimental details and theoretical modelling of dissipation mechanisms at play lay beyond the scope of our theoretical investigations at the time. Other physical features that were neglected in the models considered were the role of spin and interactions. It is hoped that in future work we can incorporate the effects of both and obtain non-trivial physics of the kind which is currently being observed in the many body localization and thermalization phenomena.